Purification of Human Aldosterone Synthase and 11β-Hydroxylase for Structural Studies

Alette Ramos Brinth
B.Sc.(Hons.)

Submitted in part fulfilment for the degree of Doctor of Philosophy

Institute of Cardiovascular and Medical Sciences

College of Medical, Veterinary and Life Sciences

University of Glasgow

2012

Author's declaration

This thesis has been written in accordance with the University of Glasgow's regulations and is less than 50,000 words in length. This thesis is an original contribution, which describes work performed entirely by myself unless otherwise cited or acknowledged. Its contents have not previously been submitted for any other degree. The research for this thesis was performed between October 2008 and September 2012.

Alette Brinth

28th September 2012

Abstract

Elevated arterial blood pressure, or hypertension, is a major modifiable risk factor for the development of cardiovascular disease, the largest known cause of mortality in the world today. While it is clear that lifestyle factors contribute to the risk of developing hypertension, there is a strong genetic component too. Clinical studies have shown that up to 15% of patients with essential hypertension have elevated plasma levels of aldosterone relative to renin. Aldosterone is the principal mineralocorticoid steroid hormone in man, and plays a key role in regulating body fluid balance. Aldosterone acts on the distal tubules and collecting ducts of the kidney nephron where it regulates sodium uptake, potassium excretion and water retention. Drugs that antagonise aldosterone action lower blood pressure. Unfortunately, many of the existing therapeutics have unfavourable side effects. An alternative approach for lowering plasma levels of aldosterone in people is to inhibit aldosterone synthase (CYP11B2) (the rate-limiting enzyme involved in aldosterone production). Aldosterone synthase is a cytochrome p450 enzyme that has ~93% sequence homology with 11β-Hydroxylase (CYP11B1) (which catalyses the final step in cortisol biosynthesis). Detailed three-dimensional structures of both enzymes will facilitate the development of specific small molecule inhibitors of aldosterone synthase for the treatment of hypertension. Structural studies and drug-screening experiments require large amounts of pure, active protein. Here, systems have been developed that allow milligram quantities of human aldosterone synthase and 11β-Hydroxylase to be routinely prepared along with their electron donors adrenodoxin and adrenodoxin reductase.

An in-house expression system specifically tailored for the recombinant expression, purification and immobilisation of human (membrane) proteins was created. The *Pichia pastoris* expression vector pPICZA was engineered to have a "3C protease recognition site - iLOV - biotin acceptor domain - His_{10}" (CLBH) tag immediately downstream of the target protein. The CLBH expression system was characterised using the cholesterol biosynthetic enzyme sterol isomerase, a highly stable human integral membrane protein. iLOV is a novel fluorescent reporter derived from the LOV2 domain of *Arabidopsis thaliana* phototropin 2.

Optimal wavelengths for selectively exciting as well as measuring fluorescence emission from iLOV were identified. Using these wavelengths, it was possible to monitor CLBH-tagged membrane proteins both *in vivo* (as a reporter of recombinant protein production) and *in vitro* (for assessing the aggregation status of membrane proteins by fluorescence size exclusion chromatography). Human rhinovirus 3C protease was purified, and its catalytic properties characterised using SI-CLBH as substrate. Using the CLBH tag, a simple protocol was developed that allowed recombinant (membrane) proteins to be purified to homogeneity in four easy steps (nickel-affinity purification, cleavage with human rhinovirus 3C protease, reverse nickel-affinity purification and gel filtration). Where necessary, however, a second affinity purification step could be introduced by biotinylating the CLBH tag *in vitro* with recombinant biotin ligase, and then applying the protein mixture to (strept)avidin beads. The ability to immobilise target (membrane) proteins on (strept)avidin-coated surfaces platforms using the CLBH tag opens up the possibility of studying the interaction of small molecules and proteins of interest by techniques such as surface-plasmon resonance.

Efforts to express adrenodoxin reductase using the *P. pastoris* CLBH system were abandoned, as the production levels of the recombinant protein were too low to allow its purification on a milligram scale. However, adrenodoxin and adrenodoxin reductase were successfully expressed in *E. coli* using a modified version of the pET21a expression vector which contained the CLBH tag. In this system, adrenodoxin and adrenodoxin reductase could both be purified to homogeneity in four steps. Thermostability assays were performed with pure adrenodoxin and adrenodoxin reductase to identify the optimal buffer conditions for use with both electron transfer proteins. This was particularly important for adrenodoxin reductase as it is very unstable. Analysis of sequence data from the 1000 genomes project revealed a substantial number of non-synonymous single-nucleotide polymorphisms in the adrenodoxin and adrenodoxin reductase genes. The contribution that these natural variants make to blood pressure regulation in people is not yet understood. However, as a first step towards expressing, characterising and understanding the properties of the naturally occurring variants of adrenodoxin and adrenodoxin reductase *in vitro*, a biophysical characterisation of the wild-type proteins was performed. Circular dichroism

spectra for both electron carriers were obtained in the far- and near-UV regions. Crystallisation trials with adrenodoxin and adrenodoxin reductase were attempted. As yet, however, no diffracting crystals have been obtained.

Aldosterone synthase and 11β-Hydroxylase are both monotopic membrane proteins and were, therefore, expected to be challenging to make in a heterologous host on a milligram-scale as well as purify in an active form. No expression of either aldosterone synthase or 11β-Hydroxylase was observed in *P. pastoris* using the CLBH system. However, both enzymes were successfully expressed in *E. coli* using the pET21a-CLBH vector. Optimal expression conditions for aldosterone synthase were identified. Furthermore, it was shown that aldosterone synthase is sensitive to proteolysis at its C-terminus by bacterial metalloproteases. This problem was overcome by adding EDTA to all of the purification buffers. A novel technique called ELISA size-exclusion chromatography (ESEC) was developed which allowed the simultaneous assessment of the aggregation state and the polar surface exposure of aldosterone synthase in a range of different detergents. Using ESEC, sodium cholate was identified as the optimal detergent for solubilising and purifying aldosterone synthase. Using pET21a-CYP11B1/B2-His_6 constructs, aldosterone synthase and 11β-Hydroxylase were both purified in a functional form by sequential nickel-affinity, ion-exchange and size-exclusion chromatographies. To ensure successful purification of both enzymes, it was essential to break the *E. coli* cells open by sonication in the presence of sodium cholate and Tween-20. Furthermore, the nickel-affinity step had to be performed using nickel sepharose beads and not a pre-packed column to ensure efficient binding of the recombinant protein. The identities of the purified proteins were determined by tandem mass spectroscopy. Reduced carbon monoxide difference spectra for pure aldosterone synthase and 11β-Hydroxylase both had a prominent absorption maximum at *ca.* 450 nm, which is characteristic of all members of the cytochrome p450 superfamily. Furthermore, the purified enzymes could be shifted from their low- to their high-spin state by adding substrate. These spectroscopic measurements showed that aldosterone synthase and 11β-Hydroxylase had retained their functionality throughout the purification process.

In summary, systems have been developed that allow human aldosterone synthase, 11β-Hydroxylase, adrenodoxin and adrenodoxin reductase to be purified on a milligram-scale in a functional form. This work provides a solid foundation for future efforts to solve the structures of aldosterone synthase and 11β-Hydroxylase to atomic resolution. Furthermore, using all four proteins, activity assays for both aldosterone synthase and 11β-Hydroxylase can now be established which will allow the identification of novel specific inhibitors of aldosterone synthase for the treatment of hypertension.

Dedication

I had the honour of working closely with Dr. Gordon Inglis, who had worked for many years trying to purify aldosterone synthase and 11β-Hydroxylase. Sadly, he passed away after a brave fight with pancreatic cancer. I would like to dedicate this thesis to his memory.

Acknowledgements

My sincerest debt of gratitude is due to my principal supervisor Dr. Niall Fraser, who fostered my interest in science and trained me to carefully observe, think and evaluate. Thank you for your guidance, support and enthusiasm.

The good advice and support of my second supervisor, Professor Eleanor Davies, has been invaluable both on an academic and a personal level, for which I am extremely grateful. Thank you also to members of the Blood Pressure Group for their help and friendship. In particular, I would like to thank Professor Robert Fraser for patiently helping me with this thesis.

I am indebted to Professor Richard Cogdell for his generous support, and would like to express my gratitude for his wise counsel and for the use of his laboratory equipment. I would like to extend this gratitude to all members of the Cogdell group (past and present) for their expert help and advice. In particular, I would like to thank Dr. Alistair Gardiner, Mrs. June Southall, Dr. Sarah Henry, Dr. Nicola Picken, Dr. Tatas Brotosudarmo, Dr. Olek Roszak and Dr. Anne-Marie Carey.

I would like to express my appreciation to the following people in connection with this thesis: Dr. Sharon Kelly (University of Glasgow) for help with CD measurements, Professor Jim Naismith (St. Andrews University) for collaborating on the crystallisation of Adx and AdxRed, Professor Kunai Mukai (Keio University, Japan) for the anti-aldosterone synthase and 11β-Hydroxylase antibodies, Professor John Christie (University of Glasgow) for the gift of iLOV, Professor Hugh Nimmo (University of Glasgow) for helpful discussions, and Miss Helen

Heathcote for assistance with the ELISA-SEC experiments. I would particularly like to thank Dr. Chris Tate (University of Cambridge) for his invaluable advice and expertise.

A special thanks to my fellow postgraduates at the University of Glasgow for promoting a stimulating academic and social environment. I have made many friends over the course of my Ph.D., and it would be impossible to thank everyone individually. In particular, I would like to thank Miss Rachel Mulvaney and Mr. Khuram Ashraf for their generosity, help and friendship, Dr. Gillian Young for showing me the ropes, and Dr. Emily Ord for the marathon training sessions. I would also like to take this opportunity to thank the staff at the Glasgow Biomedical Research Centre. I have been touched on many occasions by the generosity and care shown by my colleagues and superiors alike. I also owe a very big thank you to the technical staff for all their help over the years.

For instilling in me the desire to learn: thank you to my family. I would also like to express my gratitude to my extended family, the Hunt clan, for their care and support over the past many years. *Go raibh maith agaibh*. This journey would not have been possible without the patience and unfailing support of my partner, Eoin Hunt. My gratitude goes beyond words, so I will pick a simple phrase: *Tusinde tak skal du have!*

Finally, I would like to acknowledge The Hypertension Trust for funding the research that is presented in this thesis.

Table of contents

List of tables

List of figures

List of Abbreviations

The S.I. standard was used throughout this thesis. Common abbreviations are used for amino acids and DNA bases.

12-HETE	12-hydroxyeicosatetraenoic acid
231-chol	3α-hydroxy-7α,12α-bis[(β-D-maltopyranosyl)ethloxy]cholane
A2aR	Adenosine 2a receptor
Ab	Antibody
ACE	Angiotensin converting enzyme
ACTH	Adrenocorticotrophic hormone
Adx	Adrenodoxin
AdxRed	Adrenodoxin reductase
AIP	Aldosterone induced protein
AngI	Angiotensin I
AngII	Angiotensin II
ATF	Activating transcription factor
APA	Adrenal producing adenoma
ARB	Angiotensin II receptor blocker
AU	Arbitrary units
BirA	Biotin ligase
BMGY	Buffered glycerol complex medium
BMMY	Buffered methanol complex medium
CAH	Congenital adrenal hyperplasia
CaMK	Ca^{2+}-calmodulin dependent protein kinases
CD	Circular Dichroism
CHIF	Channel-inducing factor
CLBH	3C cleavage site-iLOV-biotinylation acceptor domain-His_{10} tag
CMC	Critical micelle concentration
CNS	Central nervous system
CPR	Cytochrome p450 reductase
CPM	7-Diethylamino-3-(4-maleimidophenyl)-4-methylcoumarin)

CREB	cAMP response element-binding protein
CRH	Corticotrophin releasing hormone
CYP11A1	Side-chain cleavage enzyme
CYP11B1	11β-hydroxylase
CYP11B2	Aldosterone synthase
CYP19A1	Aromatase
DAG	1,2-diacylglycerol
DHEA	Dehydroepiandrosterone
DM	Decyl-β-D-maltoside
DMSO	Dimethyl sulfoxide
DTT	Dithiothreitol
EDTA	Ethylenediaminetetraacetic acid
ELISA	Enzyme-linked Immunosorbent Assay
ENaC	Epithelial sodium channel
ESEC	ELISA size exclusion chromatography
ER	Endoplasmic reticulum
ERK	Extracellular signal regulated kinase
FMN	Flavin mononucleotide
FSEC	Fluorescence size exclusion chromatography
FU	Fluorescence units
GFP	Green fluorescent protein
GPCR	G-protein coupled receptor
GR	Glucocorticoid receptor
GRE	Glucorcorticoid response element
GRH	Glucocorticoid remediable hyperaldosteronism
GST	Glutathione-S-transferase
HSD	Hydroxysteroid dehydrogenases
HPA	Hypothalamic-pituitary-adrenal
HRE	Hormone responsive element
HRV 3C	Human rhinovirus 3C protease
iLOV	Improved Light-Oxygen-Voltage domain
IHA	Idiopathic hyperplasia
IC	Intronic conversion
IP_3	1,4,5 inositol triphosphate

IMAC	Immobilised metal affinity chromatography
IPTG	Isopropyl-β-D-1-thiogalactopyranoside
Ki-RasA	Kirsten Ras GTP-binding protein 2A
LB	Luria-Bertani broth
LD	Linkage disequilibrium
LDL	Low-density lipoprotein
LS-LB	Low-salt Luria Bertani broth
MAPK	Mitogen activated protein kinase
MBP	Maltose binding protein
MC2R	Melanocortin type 2 receptor
MIS	Membrane insertion site
MR	Mineralocorticoid receptor
NBRE-1	NGFI-B response element
Nedd4-2	Neuronal precursor cell expressed developmentally down-regulated protein 4-2
NGFI-B	Nerve growth factor induced clone B
NHE	Na^+/H^+ exchanger
Nurr1	Nuclear receptor related
OD	Optical density
p450	Cytochrome p450
PCR	Polymerase chain reaction
PDB	Protein data bank
PI3K	Phosphatidylinositol-3 kinase
PIP_2	Phosphatidyl-inositol 4,5-bisphosphate
PKA	cAMP-dependent protein kinase
PKC	Protein kinase C
PKD	Protein kinase D
PLC	Phospholipase C
PMSF	Phenylmethanesulfonylfluoride
POMC	Proopiomelanocortin
RAAS	Renin-angiotensin-aldosterone system
SDS-PAGE	Sodium dodecyl sulphate polyacrylamide gel electrophoresis
SEC	Size exclusion chromatography

SF-1	Steroidogenic factor-1
SGK-1	Serum and glucocorticoid-induced kinase 1
SI	Sterol isomerase
SCC	Side-chain cleavage enzyme
SNP	Single nucleotide polymorphism
StAR	Steroidogenic acute regulatory protein
SPR	Surface plasmon resonance
SRS	Substrate recognition site
TAE	Tris-Acetate EDTA
TASK	TWIK-related acid-sensitive K^+
TB	Terrific Broth
TINS	Target immobilized NMR screening
TEV	Tobacco Etch Virus
T_m	Melting temperature
TWIK	Inward-rectifying potassium channel proteins
X-gal	5-bromo-4-chloro-3-indolyl-β-D galactopyranoside
YPD	Yeast extract peptone dextrose media
ZF	Zona fasciculata
ZG	Zona glomerulosa

Chapter 1 - Introduction

1.1 Hypertension

Elevated arterial blood pressure, or hypertension, is an important modifiable risk factor for the development of cardiovascular disease, the most common cause of morbidity and early mortality worldwide (Chobanian *et al.*, 2003; Lawes *et al.*, 2008; Ruilope, 2012). Hypertension is a substantial global health problem, affecting over a quarter of the world's adult population (Kearney *et al.*, 2004). Although a considerable number of therapeutics have been developed to treat hypertension, what causes people to have high blood pressure is poorly understood. What is clear, however, is that blood pressure is affected by a wide variety of environmental and genetic factors (Kaplan and Opie, 2006).

Blood pressure is a highly variable quantitative trait making it difficult to define precisely parameters for diagnosing hypertension. For convenience, however, hypertension is defined as having a resting blood pressure measured consistently at values above 140/90 mmHg, in accordance with the JNC VII report[1] (Chobanian *et al.*, 2003).

1.1.1 Blood pressure regulation

The body employs a complex network of control mechanisms to maintain blood pressure in people at rest. Blood pressure increases in response to external stimuli such as exercise or stress and decreases when such demands cease (Guyton, 1991). Arterial blood pressure is a function of total peripheral resistance (the sum of resistance in the vasculature) and cardiac output (the volume of blood ejected from the heart), each of which are under independent control (Figure 1.1) (Cowley, 2006).

[1] The seventh report of the Joint National Committee on Prevention, Detection, Evaluation, and Treatment of High Blood Pressure

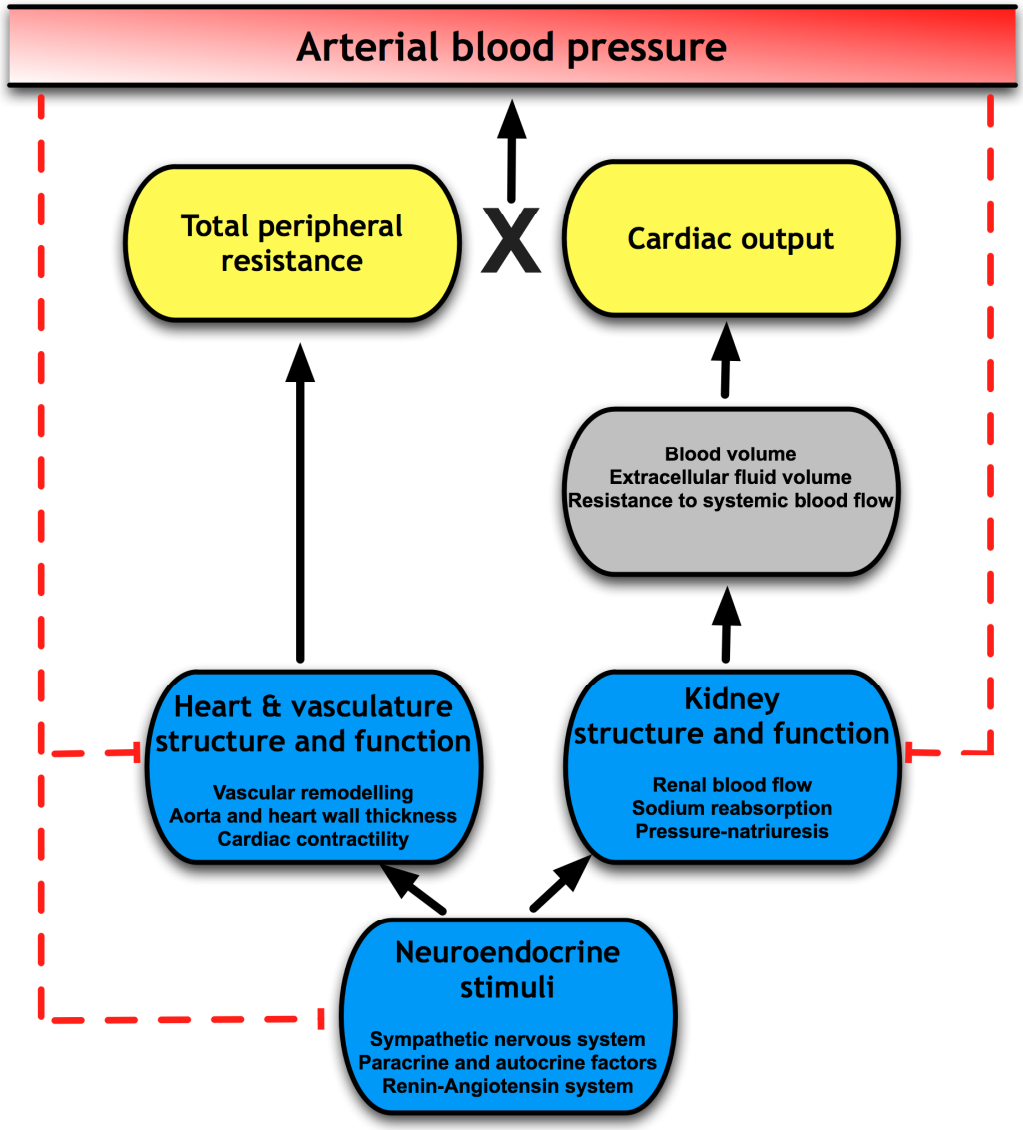

Figure 1.1 Mechanisms involved in the regulation of arterial blood pressure
Arterial blood pressure is the product of cardiac output and the total peripheral resistance. Total peripheral resistance is affected by changes in the structure and function of the vasculature and heart. Cardiac output is affected by the extracellular fluid volume, blood volume and resistance to systemic blood flow. The structure and function of the kidney plays a key role in regulating these factors. Neuroendocrine stimuli have an important influence on the function of both the kidneys and the vasculature through the actions of hormones such as aldosterone. Homeostatic feedback mechanisms (red dashed line) regulate arterial blood pressure through a variety of sensory mechanisms. Figure adapted from (Cowley, 2006).

1.1.2 Risk factors for the development of essential hypertension

Essential hypertension (where the cause of hypertension in an individual can not be identified) accounts for 95% of all people with high blood pressure (Cowley, 2006). Essential hypertension is a multifactorial disease that has both an environmental and genetic component. Investigative studies have shown that the development of hypertension can be influenced by environmental factors such as high salt intake (Stamler *et al.*, 1989), low potassium intake (Whelton *et al.*, 1997) and alcohol consumption (Puddey *et al.*, 1987). The development of essential hypertension also has a strong genetic component with multiple genes from many different physiological systems contributing. Research effort has been made worldwide to identify those genes that affect blood pressure. Only a few genes are known to cause hypertension through variations in their coding regions. However, it is striking that many of these monogenic causes of hypertension relate to aspects of corticosteroid biosynthesis and metabolism (Section 1.6.1). Further to this, several studies in recent years have shown that certain single-nucleotide polymorphisms in the promoters of genes encoding enzymes crucial to the synthesis of corticosteroids predispose an individual to the development of hypertension (Section 1.6.2).

The mineralocorticoid aldosterone plays a key role in regulating body fluid balance (Section 1.4), and elevated plasma aldosterone levels are known to cause high blood pressure (Connell *et al.*, 2008). Drugs that block aldosterone action through antagonising mineralocorticoid receptor function have been shown to lower blood pressure in hypertensive patients (Cranston and Jueljensen, 1962; Chapman *et al.*, 2007) as well as having a beneficial effect on patients with moderate to severe heart failure (Pitt *et al.*, 1999). Unfortunately, blocking mineralocorticoid receptor activity can lead to undesirable side effects such as gynecomastia and a lowered libido (Section 1.7.3). Aldosterone action *in vivo* can also be antagonised by blocking its production.

1.2 Corticosteroidogenesis in the adrenal gland

Corticosteroids are made in the adrenal gland cortex from cholesterol through a series of enzyme-catalysed reactions, and can be divided into two functional groups: the mineralocorticoids, essential in electrolyte and fluid balance, and the glucocorticoids, which primarily control intermediary metabolism. The principal mineralocorticoid and glucocorticoid hormones are aldosterone and cortisol, respectively (Connell *et al.*, 2001).

1.2.1 The adrenal gland cortex

The adrenal glands lie superior to each kidney. They comprise an inner medulla and a surrounding cortex. The adrenal gland cortex contains three histologically and enzymatically distinct zones (Figure 1.2). The outermost zone consists of the zona glomerulosa (ZG) where aldosterone is produced. This is followed by the zona fasciculata (ZF), which makes cortisol, and finally the zona reticularis (ZR), where the sex steroids are synthesised.

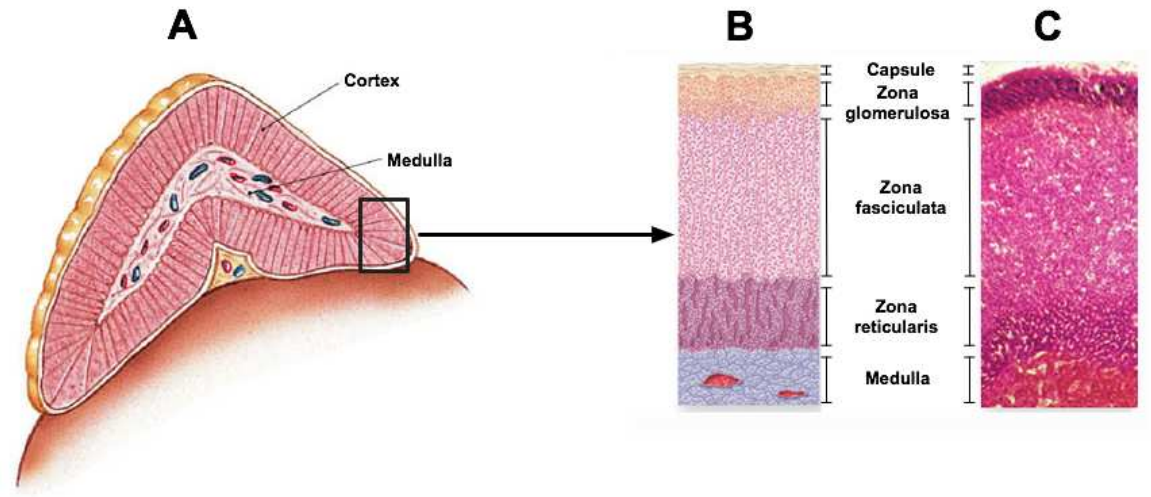

Figure 1.2 The histological zones of the adrenal gland
(A) The adrenal glands consist of an inner medulla and outer cortex surrounded by a fibrous capsule. The adrenal gland cortex consists of three histologically distinct zones presented (B) as a schematic diagram and (C) in a histological section. The zona glomerulosa produces and secretes aldosterone; cortisol is synthesised in the zona fasciculata. The sex steroids are made in the zona reticularis. Figure adapted from McGraw Hill online learning centre.

1.2.2 The human corticosteroid biosynthetic pathway

The corticosteroids are synthesised from cholesterol in a series of enzyme-catalysed reactions. Common names for the reaction intermediates are listed in Table 1.1 and their structures described in Figure 1.3.

Figure 1.3 The human corticosteroid biosynthetic pathway
The corticosteroids aldosterone and cortisol are synthesised from the common substrate cholesterol. Aldosterone and cortisol biosynthesis takes place in the zona glomerulosa (green dashed line) and the zona fasciculata (yellow dashed line) of the adrenal gland cortex, respectively. In total, five cytochrome p450 enzymes (side-chain cleavage enzyme, 17α-Hydroxylase, 21-Hydroxylase, 11β-Hydroxylase and aldosterone synthase) and one HSD (3β-HSDII) are required for aldosterone and cortisol biosynthesis. Chemical reactions that take place in the mitochondria and at the membrane of the smooth endoplasmic reticulum are denoted by red and blue arrows, respectively.

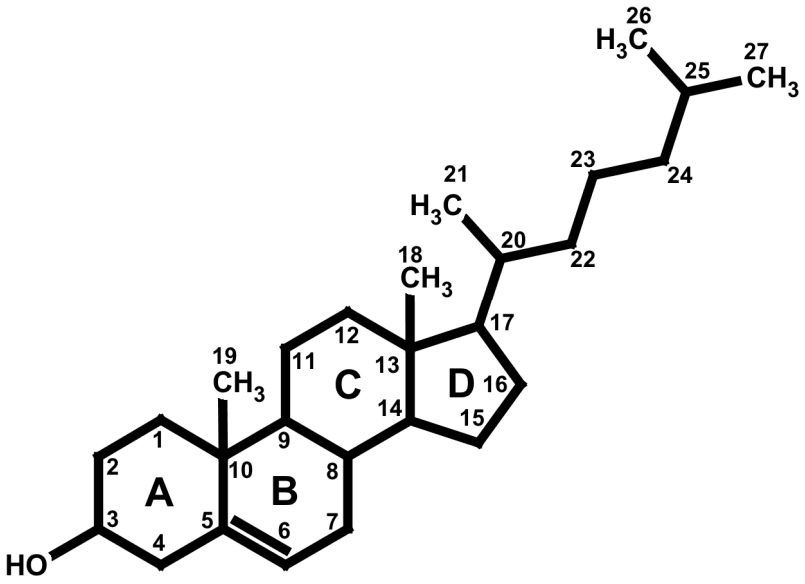

Figure 1.4 The chemical structure of cholesterol
Cholesterol has a four-ring structure (labelled A-D) with an aliphatic tail. In total, cholesterol has 27 carbon atoms. All steroid hormones contain the cyclopentanophenanthrene ring structure of cholesterol.

1.2.2.1 Cholesterol transfer into the mitochondria

Cholesterol is the precursor of all steroid hormones. The major sources of cholesterol for steroid biosynthesis are: (i) from dietary cholesterol incorporated into low-density lipoproteins (LDLs), (ii) the *de novo* synthesis of cholesterol from acetyl coenzyme A, and (iii) the hydrolysis of cholesterol esters stored in lipid droplets by cholesterol ester hydrolase (Ikonen, 2008; Hattangady *et al.*, 2012).

The first step in corticosteroidogenesis is the translocation of cholesterol from the outer to the inner mitochondrial membrane. This is facilitated by steroidogenic acute regulatory protein (StAR) (Stocco and Clark, 1996). Following import, cholesterol is converted to aldosterone and cortisol through a series of enzyme-catalysed steps. All steroid hormones have the cholesterol cyclopentanophenanthrene four-ring structure (Figure 1.4).

1.2.2.2 Corticosteroid biosynthesis

Cholesterol side-chain cleavage

In the first step of corticosteroid biosynthesis, cholesterol is converted to pregnenolone by side chain cleavage enzyme (SCC) (Figure 1.3). The conversion of cholesterol to pregnenolone requires three enzymatic reactions. Initially, side-chain cleavage enzyme stereospecifically hydroxylates cholesterol: first at C22 yielding 22(R) hydroxycholesterol, then at C20 giving 20(R),22(R) hydroxycholesterol. Finally, side-chain cleavage enzyme catalyses the oxidative scission of the C20-C22 bond to produce pregnenolone (Payne and Hales, 2004). Pregnenolone is the precursor for both aldosterone and cortisol biosynthesis.

Cortisol biosynthesis

Cortisol can be synthesised from pregnenolone in the zona fasciculata by one of two ways (Figure 1.3). In the first pathway, pregnenolone is converted to progesterone by 3β-HSD(II) in two steps: first, the C3-hydroxyl group is dehydrogenated to a keto group; second, the double bond in the B ring is isomerised to the A ring. Thereafter, 17α-Hydroxylase converts progesterone to 17α-OH-progesterone by 17α-hydroxylation. In the second pathway, this order of reactions is reversed: pregnenolone is first converted to 17-OH-pregnenolone by 17α-Hydroxylase, and thereafter to 17-OH progesterone by 3β-HSD(II). As 17α-Hydroxylase is only expressed in the zona fasciculata it is this enzyme that determines the site of cortisol synthesis (Narasaka *et al.*, 2001). Next, 17α-OH-progesterone is hydroxylated at the C21 position by 21-Hydroxylase to form 11-deoxycortisol (Figure 1.3). The final step in cortisol biosynthesis is catalysed by 11β-Hydroxylase, which is located on the matrix face of the inner mitochondrial membrane. 11β-Hydroxylase catalyses the 11β-hydroxylation of 11-deoxycortisol to form cortisol (Payne and Hales, 2004; Miller and Auchus, 2011)

Aldosterone biosynthesis

In aldosterone biosynthesis, pregnenolone is converted to 11-deoxycorticosterone by the sequential activity of 3β-HSDII and 21-Hydroxylase (Figure 1.3). The conversion of 11-deoxycorticosterone to aldosterone occurs via three consecutive reactions: (i) 11β-hydroxylation of 11-deoxycorticosterone

yielding corticosterone, (ii) 18-hydroxylation of corticosterone to give 18-hydroxycorticosterone, and finally (iii) 18-methyloxidation of 18-hydroxycorticosterone producing aldosterone. In humans, these three steps are all catalysed by aldosterone synthase, which is located on the matrix face of the inner mitochondrial membrane (Payne and Hales, 2004; Miller and Auchus, 2011). Aldosterone synthase is the rate-limiting enzyme in aldosterone biosynthesis and is, therefore, the best candidate protein for blocking aldosterone production *in vivo*.

1.2.3 Enzymes of the corticosteroid biosynthetic pathway

In total, five cytochrome p450 enzymes and one hydroxysteroid dehydrogenase are required to synthesise aldosterone and cortisol (Figure 1.3). Characteristics of both enzyme families will now be discussed.

1.2.3.1 Hydroxysteroid dehydrogenases

Hydroxysteroid dehydrogenases (HSDs) are non-metalloenzymes that catalyse the oxidoreduction of steroids. HSDs belong to two phylogenies: the short chain dehydrogenases and the aldo-keto reductase superfamily. HSDs have several isoforms and are expressed in various tissues including the placenta, adrenal gland, ovary and testis (Penning, 1997; Miller and Auchus, 2011). Within the adrenal gland cortex, the type II isoform of 3β-HSD plays an essential oxidative role in the synthesis of both mineralocorticoids and glucocorticoids. 3β-HSDII is a membrane-associated short-chain dehydrogenase and requires electrons from the co-factor NADH for activity (Simard *et al.*, 2005).

1.2.3.2 Cytochrome p450 enzymes

Corticosteroid synthesis requires the catalytic activity of five members of the cytochrome p450 superfamily (side-chain cleavage enzyme, 17α-Hydroxylase, 21-Hydroxylase, 11β-Hydroxylase and aldosterone synthase). Cytochrome p450 enzymes were first discovered by Tsuneo Omura and Ryo Sato in 1964 who observed an unusual cytochrome absorption in mammalian liver microsome samples that had an absorption maximum at 420 nm which shifted to 450 nm when complexed with carbon monoxide under reducing conditions (Omura and

Sato, 1964). From this observation, the term “pigment-450” or “p450” was coined, and all enzymes that have this property are known as “cytochrome p450” enzymes.

Cytochrome p450s (referred to hereafter as “p450s”) are widespread in nature occuring in plants, archea, microbes as well as mammals. The number of p450s in different species varies greatly (Werck-Reichhart and Feyereisen, 2000; Bernhardt, 2006). In the human genome, there are 57 genes encoding p450s[2]. p450s are monooxygenases capable of regio- and sterospecific oxygenation of a broad range of substrates. Consequently, p450s have a large number of biological functions including xenobiotic degradation, metabolism of chemical carcinogens and, of particular relevance to this thesis, the biosynthesis of physiologically important molecules such as steroid hormones (Sono *et al.*, 1996).

1.2.3.2.1 The catalytic cycle of cytochrome p450 enzymes

Cytochrome p450s use electrons provided by NADPH to hydroxylate substrates via the activation of molecular oxygen (Figure 1.5). The overall stoichiometry of this reaction is:

$$\mathbf{RH + O_2 + NADPH + H^+ \rightarrow ROH + H_2O + NADP^+}$$

The catalytic cycle of all p450s consists of five distinct steps (Figure 1.5). (1) The cycle is initiated by substrate binding. (2) The haem-iron is reduced from its ferric (Fe^{3+}) to its ferrous (Fe^{2+}) state. (3) The Fe^{2+} ion is able to bind molecular oxygen creating a stable dioxygen adduct. (4) The superoxide complex is reduced to a negatively charged iron-peroxo intermediate. (5) The distal oxygen atom is protonated and the O-O bond undergoes heterolytic cleavage causing the formation of a highly reactive iron-hydroxyperoxy species (compound I). Compound I reacts with the substrate incorporating the remaining oxygen atom to yield the hydroxylated substrate (Denisov *et al.*, 2005). Each p450 is highly specific for the orientation and location of the created hydroxyl group as well as the particular substrates that they bind.

[2] http://drnelson.uthsc.edu/CytochromeP450.html

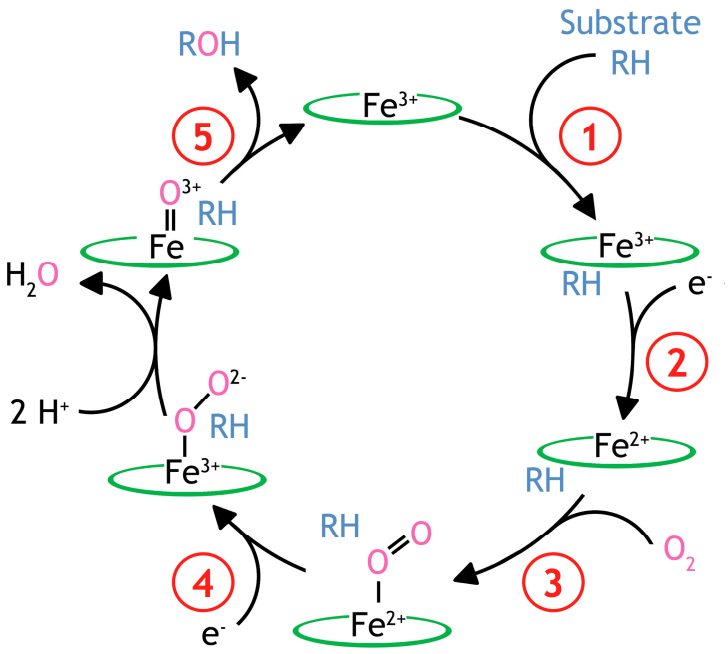

Figure 1.5 The catalytic cycle of cytochrome p450 enzymes
(1) Substrate binds to the p450 enzyme. (2) The haem iron is reduced to its ferrous (Fe^{2+}) state. (3) Oxygen binds to the Fe^{2+} ion creating a dioxygen adduct. (4) A second electron is transferred to the Fe^{2+} creating an iron-peroxo intermediate. (5) In the final step, the double bond between the oxygen atoms is cleaved. A highly reactive species named compound I is created, which reacts with the substrate resulting in its hydroxylation.

1.2.3.2.2 Redox partner interaction

Electrons required for the activity of p450s are provided by NADPH via an electron transfer chain. Mammalian p450s can be divided into two classes depending on their subcellular localisation and mode of electron transfer (Guengerich, 2004). Type I p450s are localised to the smooth endoplasmic reticulum (commonly referred to as 'microsomal p450s') and receive their electrons from a single electron transfer protein; type II p450s are located in mitochondria and receive their electrons from a two-component electron transfer chain.

Microsomal cytochrome p450 enzymes

Microsomal cytochrome p450s constitute by far the larger sub-group of p450s in higher eukaryotes. 50 of the 57 human cytochrome p450s are located at the

endoplasmic reticulum (Miller and Auchus, 2011). Microsomal p450s catalyse the breakdown of exogenous compounds and receive their electrons from cytochrome p450 reductase (CPR). They are anchored to the smooth endoplasmic reticulum through a single-spanning transmembrane domain.

Like the microsomal p450s to which it provides electrons, CPR is N-terminally anchored to the ER membrane giving both enzymes the correct spatial orientation for efficient electron transfer from the CPR to the p450. The C-terminal catalytic domain of CPR contains two prosthetic groups, FMN and FAD. CPR accepts a pair of electrons from NADPH and transfers these one at a time to the p450 enzyme (Wang *et al.*, 1997).

Mitochondrial cytochrome p450 enzymes

In humans, mitochondrial cytochrome p450s constitute the sub-families 11, 24 and 27; there are only 7 human mitochondrial p450s (Miller and Auchus, 2011). Unlike their microsomal counterparts, the mitochondrial enzymes are not anchored to a membrane by a transmembrane helix. Rather, following removal of their N-terminal mitochondrial targeting sequence, the mature enzyme becomes embedded within the inner mitochondrial membrane protruding into the matrix (Werck-Reichhart and Feyereisen, 2000).

Mitochondrial p450s receive their electrons via a two-component electron transfer chain. Electrons are transferred from NADPH to a [2Fe-2S] containing protein called adrenodoxin (Adx) via a FAD-containing protein called adrenodoxin reductase (AdxRed). Electrons are then transferred from the reduced form of Adx to p450 enzymes at two different points in the catalytic cycle (Hannemann *et al.*, 2007) (Figure 1.5). Three models have been proposed to describe the way that electrons are transferred from AdxRed to mitochondrial p450s via Adx (Figure 1.6). The “shuttle model” proposes that Adx acts as a mobile electron carrier moving between AdxRed and the p450 enzyme. The “ternary complex model” suggests that a AdxRed:Adx:p450 complex is formed with a 1:1:1 ratio. Finally, the “quarternary complex model” proposes a complex is formed between AdxRed, Adx and p450 with a ratio of 1:2:1 (Ewen *et al.*, 2011). The recent structure of a SCC-Adx complex showed that the region of Adx that interacts with AdxRed also interacts with side-chain cleavage enzyme,

suggesting that both the ternary and quaternary complex models are incorrect with electron transfer occurring via the "shuttle" mechanism (Strushkevich *et al.*, 2011).

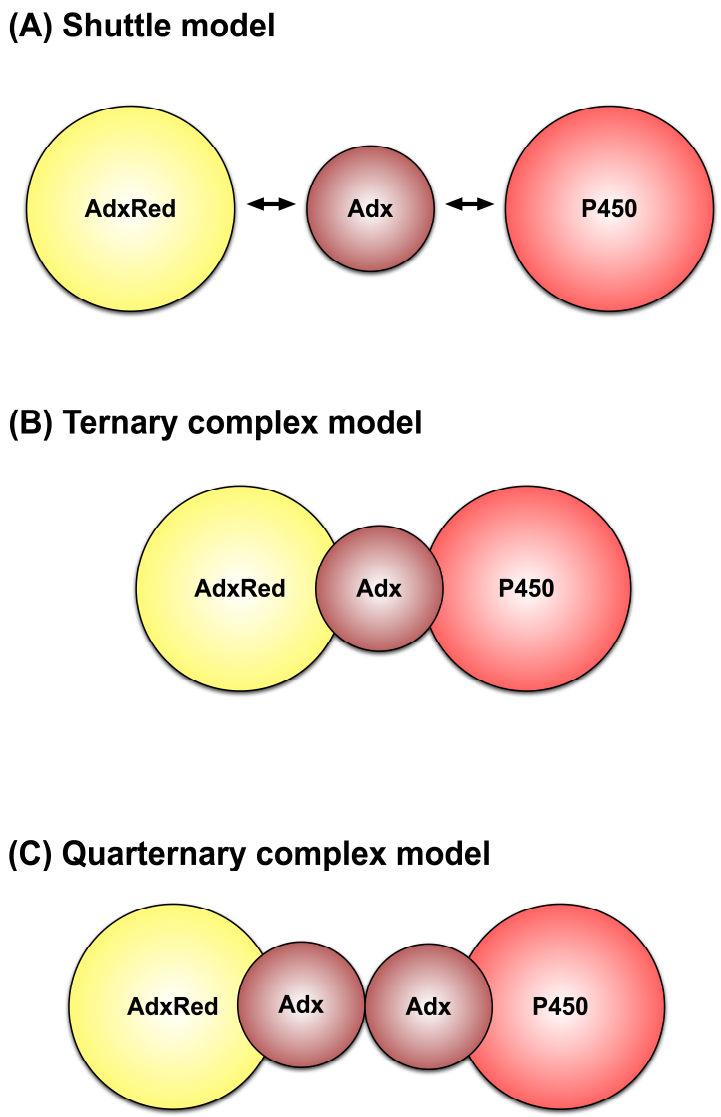

Figure 1.6 Models of electron transfer from adrenodoxin reductase to a p450 enzyme via adrenodoxin

The mechanism by which AdxRed transfers its electrons to mitochondrial p450 enzymes remains unclear. There are three possible ways by which this may happen. (A) The 'shuttle model', in which Adx acts as a molecular electron shuttle between AdxRed and the p450. (B) In the 'ternary model' Adx, AdxRed and a p450 are suggested to form a 1:1:1 complex. (C) In the 'quaternary model', two Adx proteins are thought to form a complex with AdxRed and a p450 enzyme.

1.3 Control of corticosteroid biosynthesis

Steroid secreting cells do not store steroid hormones following their synthesis. Therefore, the rate of steroid secretion by the adrenal glands is determined solely upon the rate of hormone synthesis. When required, corticosteroid synthesis can be upregulated in one of two ways. On a timescale of minutes, increased expression and phosphorylation of StAR results in increased transport of cholesterol into the mitochondria stimulating corticosteroid synthesis. Over the course of several hours, increased transcription of the *CYP11B1* and *CYP11B2* genes results in increased accumulation of 11β-Hydroxylase and aldosterone synthase, which causes increased production and secretion of cortisol and aldosterone, respectively.

Cortisol synthesis is regulated by adrenocorticotrophic hormone (ACTH), the main component of the hypothalamic-pituitary-adrenal (HPA) axis. Aldosterone synthesis is regulated by a range of factors, the principal of which are angiotensin II (AngII) and the extracellular potassium concentration ($[K^+]_e$). Under conditions of severe sodium (Na^+) or extracellular fluid loss, ACTH can also stimulate the production of aldosterone (Spät and Hunyady, 2004).

1.3.1 Angiotensin II and aldosterone production

Angiotensin II

AngII is a pressor octapeptide that causes an increase in blood pressure through: (i) vasoconstriction, (ii) stimulating an increase in sodium reabsorption at the distal convoluted tubules of the kidney, and (iii) promoting aldosterone release from the adrenal cortex. This last effect is mediated through the renin-angiotensin-aldosterone system (RAAS), of which AngII is the major effector peptide (Timmermans *et al.*, 1993).

The renin-angiotensin-aldosterone system

The RAAS becomes activated in response to a decreased intravascular volume or sodium (Na^+) concentration at the macula densa in the distal tubule of the kidney.

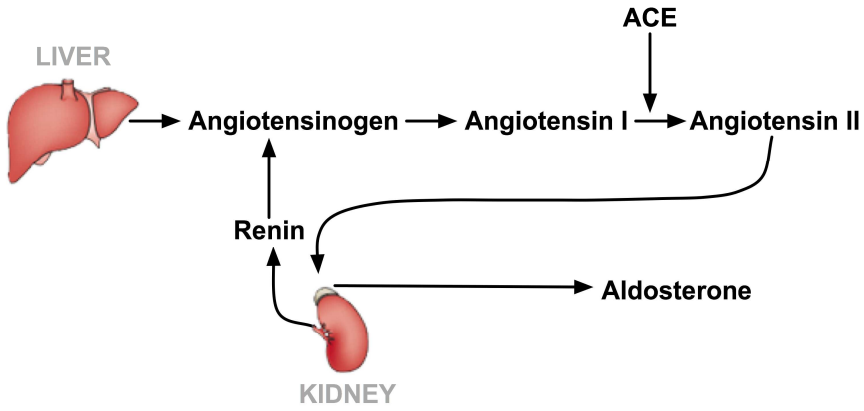

Figure 1.7 The Renin-Angiotensin-Aldosterone System
Angiotensinogen secreted by the liver is cleaved by renin, secreted by the kidney, to form angiotensin I (AngI). AngI is converted to angiotensin II (AngII) by angiotensin converting enzyme (ACE). AngII is the active component of the RAAS. Among other effects on blood pressure regulation, AngII stimulates aldosterone secretion by the adrenal gland cortex.

The initial step in the RAAS is the release of renin from the juxtaglomerular cells of the kidney. Renin is an aspartic protease that cleaves angiotensinogen (secreted by the liver) to form angiotensin I (AngI). AngI is a biologically inert decapeptide that is further cleaved by angiotensin converting enzyme (ACE) to form AngII (Tomaschitz *et al.*, 2010).

The RAAS plays a key role in fluid and electrolyte homeostasis and is, therefore, one of the principal blood pressure regulatory systems. Many treatments developed to lower hypertension have targeted the RAAS. These are further discussed in Section 1.7.

Acute effects of Angiotensin II

AngII stimulates short-term production of aldosterone through boosting StAR activity within the zona glomerulosa (Figure 1.8) (Hattangady *et al.*, 2012). Binding of AngII to the AT_1 receptor activates phospholipase C (PLC) which hydrolyses phosphatidylinositol 4,5-bisphosphate (PIP_2) to 1,4,5 inositol triphosphate (IP_3) and 1,2-diacyl glycerol (DAG) (both of which act as second messengers) (Neves *et al.*, 2002). Selective binding of IP_3 to its receptor on the endoplasmic reticulum causes stored Ca^{2+} to be released. The resultant rise in intracellular free calcium ($[Ca^{2+}]_i$) activates Ca^{2+}-calmodulin dependent protein kinases (CaMKs) which phosphorylate StAR.

This increases the rate of cholesterol uptake into mitochondria which increases flux through the aldosterone biosynthetic pathway. The CaMKs also phosphorylate the transcription factor cAMP response element-binding protein (CREB). Phosphorylated CREB binds to the promoter of the StAR gene, increasing its expression. Ultimately, elevated StAR production results in enhanced cholesterol import into the mitochondria. Two other signalling pathways downstream of the AT1 receptor activation converge on CREB phosphorylation/StAR transcription. DAG, released on PIP_2 hydrolysis, activates protein kinase D (PKD) which phosphorylates and activates CREB (Figure 1.8). 12-hydroxyeicosatetraenoic acid (12-HETE) (which is generated from DAG via arachidonic acid by the sequential activity of DAG lyase and 12-lipoxygenase) induces the phosphorylation (and activation) of CREB also (Figure 1.8).

Chronic effects of Angiotensin II

Prolonged stimulation of the zona glomerulosa with AngII causes increased aldosterone production through transcriptional regulation of the *CYP11B2* gene (Figure 1.9). CaMKs, activated following binding of AngII to the AT_1 receptor, phosphorylate selected transcription factors (including activating transcription factor (ATF) 1, ATF2, CREB, NURR1, NGF1B) that bind to specific DNA sequences (CRE, NBRE-1) in the promoter of the *CYP11B2* gene. Increased transcription of the *CYP11B2* gene results in more aldosterone synthase being made which leads, in turn, to an increase in the synthesis and subsequent release of aldosterone from the adrenal glands (Bassett *et al.*, 2004; Nogueira and Rainey, 2010).

1.3.2 The effects of potassium on aldosterone synthesis

Aldosterone production is extremely sensitive to small fluctuations in $[K^+]_e$. The zona glomerulosa membrane has a negative resting potential maintained by the TWIK-related acid-sensitive K^+ (TASK) channels. An increase in $[K^+]_e$ causes depolarisation of the plasma membrane, opening voltage-dependent transient (T)- and long lasting (L)-type Ca^{2+} channels on the cell surface. The inward movement of Ca^{2+} ions results in a rapid rise in the intracellular calcium concentration ($[Ca^{2+}]_i$). Subsequent CaMK activation stimulates StAR transcription and activity as well as increases *CYP11B2* gene transcription in the same way as AngII (Spät, 2004).

Figure 1.8 Acute regulation of aldosterone production
Binding of angiotensin II (AngII) to the angiotensin type I (AT_1) receptor activates phospholipase C which hydrolyses phosphatidylinositol 4,5-bisphosphate (PIP_2) to form the second messengers 1,4,5 inositol triphosphate (IP_3) and 1,2-diacyl glycerol (DAG). Selective binding of IP_3 to its receptor on the endoplasmic reticulum causes stored Ca^{2+} to be released. The resultant rise in intracellular free calcium ($[Ca^{2+}]_i$) activates Ca^{2+}-calmodulin dependent protein kinases (CaMKs) which phosphorylate steroidogenic acute regulatory protein (StAR). This increases the rate of cholesterol uptake into the mitochondria which increases the rate of aldosterone production. The CaMKs also phosphorylate the transcription factor cAMP response element-binding protein (CREB). Phosphorylated CREB binds to the promoter of the StAR gene, increasing its expression. Ultimately, elevated StAR production results in enhanced cholesterol import into the mitochondria. CREB can also be phosphorylated by protein kinase D (PKD) and/or downstream of 12-hydroxyeicosatetraenoic acid (12-HETE) generation from arachidonic acid (ARA) by 12-lipoxygenase (12-LO). Depolarisation of the plasma membrane can also result in a rapid rise in the intracellular calcium concentration through opening of voltage-dependent transient (T)- and long lasting (L)-type Ca^{2+} channels on the cell surface.

Figure 1.9 Chronic regulation of aldosterone synthesis
The actions of AngII and potassium on the zona glomerulosa both result in an increase in intracellular Ca^{2+} followed by Ca^{2+}-calmodulin dependent protein kinases (CaMK) activation. Phosphorylation of selected transcription factors (including activating transcription factors (ATF) ATF1 and ATF2, camp response element-binding protein (CREB), nuclear receptor related-1 (NURR1), nerve growth factor induced clone b (NGFIB)) by CaMK allows them to bind to specific cis-elements (such as NGFIB response element-1 (NBRE-1), and cAMP response element (CRE)) in the *CYP11B2* promoter region thereby stimulating transcription. Enhanced expression of the gene results in more aldosterone synthase being made which leads, in turn, to an increase in the synthesis and subsequent release of aldosterone from the adrenal glands.

1.3.3 Adrenocorticotrophic hormone and cortisol production

In response to stimuli such as stress, corticotrophin releasing hormone (CRH) is secreted by the hypothalamus (Figure 1.10). In turn, CRH (transported in the portal system to the anterior pituitary) stimulates the conversion of pro-opiomelanocortin (POMC) to ACTH by prohormone convertase. ACTH is secreted from the anterior pituitary gland, and binds to ACTH specific melanocortin type 2 receptors (MC2R) (a GPCR) in the adrenal cortex. Activated receptor stimulates adenylate cyclase to make cAMP which activates cAMP-dependent protein kinase (PKA). Phosphorylation of transcription factors such as SF-1 by PKA increases *CYP11B1* gene expression. ACTH secretion is subject to negative

feedback regulation which is mediated by cortisol binding to glucocorticoid receptors in the hypothalamus, switching off ACTH production (Mountjoy *et al.*, 1992; Waterman and Bischof, 1996). Although ACTH is the principal secretagogue of cortisol production, it has also been shown to exert a small effect on aldosterone synthesis through cAMP mediated phosphorylation of StAR (Betancourt-Calle *et al.*, 2001; Jo *et al.*, 2005).

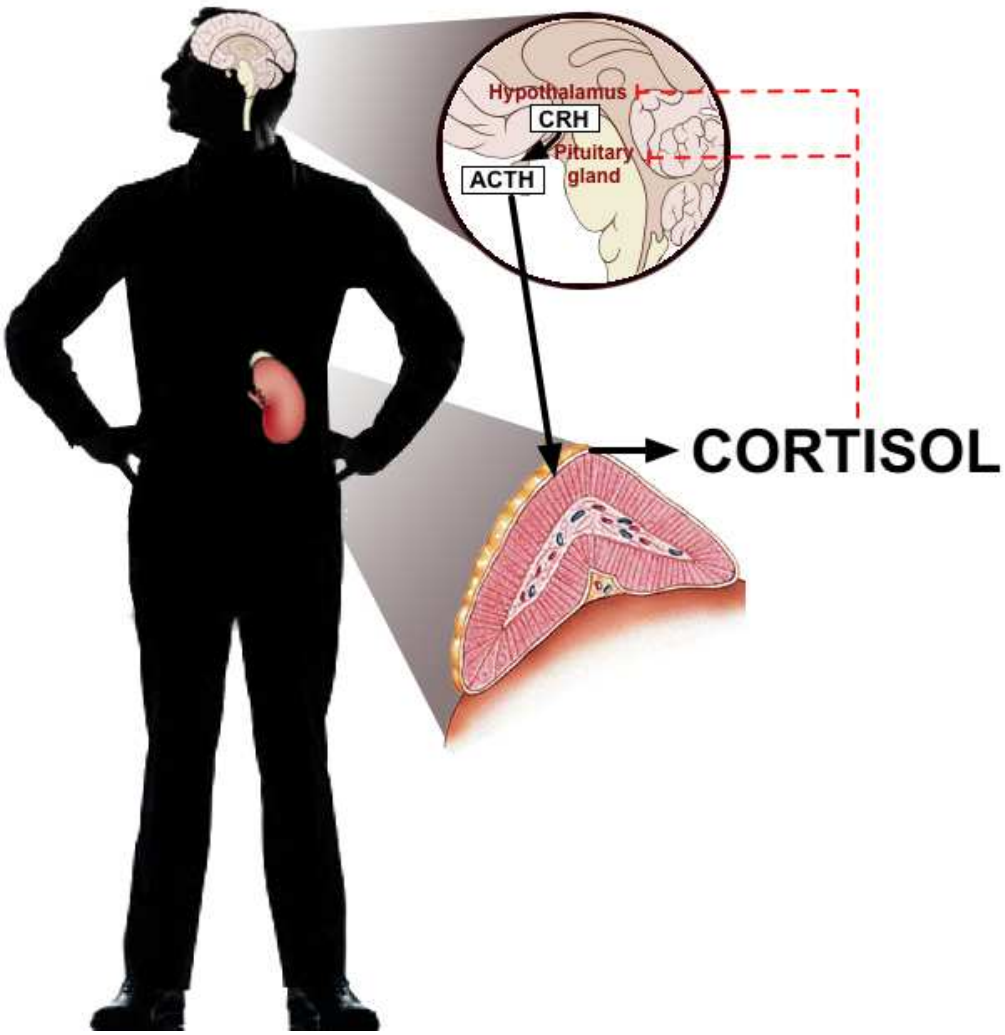

Figure 1.10 The Hypothalamic-Pituitary-Adrenal axis
Cortisol synthesis is regulated by the hypothalamic-pituitary-adrenal axis. In response to stimuli such as stress, corticotrophin hormone (CRH) is secreted by the hypothalamus. CRH stimulates the secretion of adrenocorticotrophic hormone (ACTH) from the pituitary gland. In turn, ACTH binds to MC2R receptors in the adrenal gland, activating a g-protein coupled receptor (GPCR) signalling cascade that causes increased synthesis and secretion of cortisol through increased transcription of the *CYP11B1* gene. ACTH secretion is subject to negative feedback regulation through cortisol binding to glucocorticoid receptors in the hypothalamus switching off ACTH production.

1.4 Physiological actions of aldosterone

Aldosterone mainly acts on the distal tubules and collecting ducts of the kidney nephron where it causes sodium conservation, potassium secretion and water retention. The overall effect of aldosterone action is to increase blood volume, which causes an increase in blood pressure. These classical effects of aldosterone action are known as its "genomic effects", and are mediated via mineralocorticoid receptors which regulate the transcription of specific target genes. In addition, aldosterone can also cause rapid effects within the body through the activation of, as yet, poorly-defined signalling cascades. These are termed its "non-genomic effects". Although aldosterone traditionally acts on epithelial cells, aldosterone has recently been shown to have effects elsewhere such as the vascular system, where it acts on the heart and blood vessels, as well as the central nervous system (CNS) where it regulates salt appetite and sympathetic tone (Spät and Hunyady, 2004).

1.4.1 Genomic actions of aldosterone

Aldosterone exerts its genomic actions through binding to mineralocorticoid receptors (MRs) located in the cytosol of target cells (Figure 1.11). The MRs belong to the nuclear receptor family of ligand-dependent transcription factors. In the absence of ligand, MRs are monomeric, transcriptionally inactive and bound by chaperone proteins. When aldosterone binds to the C-terminal tail of MRs, conformational changes occur which results in release of the receptors from their chaperones. The MRs then form dimers which translocate to the nucleus where they bind to hormone responsive elements (HRE) in the promoters of target genes altering transcription (Funder, 1997) (Figure 1.11).

MRs are unusual in that they have equal affinity for cortisol and aldosterone. This poses a conundrum: as cortisol circulates at concentrations of up to 1000x that of aldosterone, one would expected MRs to be primarily activated by cortisol. However, aldosterone is the main activator of MRs. This effect is mediated by 11β-HSDII, which converts cortisol to the inactive metabolite cortisone in mineralocorticoid target tissues, thereby conferring aldosterone-sensitivity on the MRs (Edwards *et al.*, 1988) (Figure 1.11).

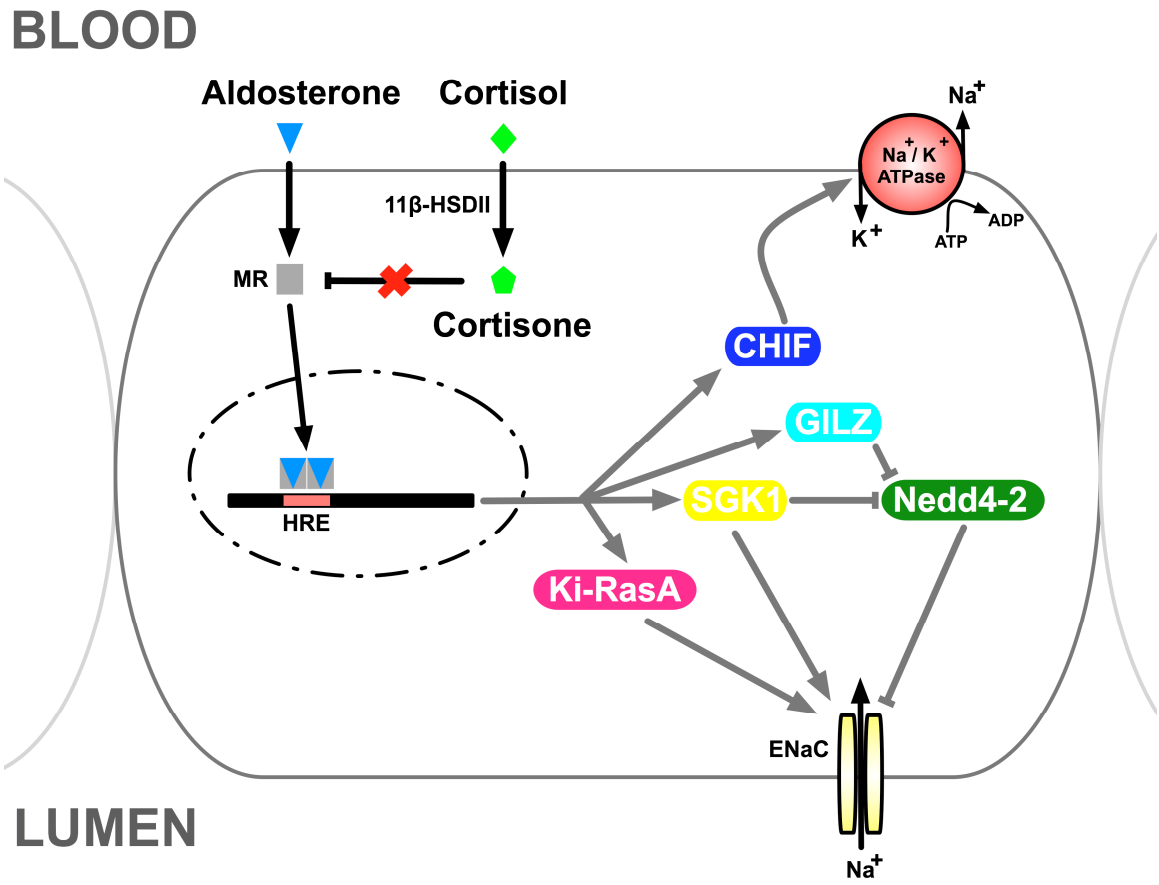

Figure 1.11 The genomic actions of aldosterone
Aldosterone binds to mineralocorticoid receptors (MRs) in the cytosol of target cells. Cortisol is converted to cortisone by 11β-HSDII, preventing it from binding to MRs. The MR-aldosterone complexes dimerise and translocate to the nucleus where they bind to hormone responsive elements (HRE) in the promoters of target genes. Aldosterone stimulates sodium reabsorption through the transcriptional regulation of the aldosterone-induced proteins SGK1 (serum and glucocorticoid-induced kinase 1), GILZ (glucocorticoid-induced leucine zipper protein), CHIF (channel-inducing factor) and Ki-RasA (Kirsten Ras GTP-binding protein 2A). Nedd4-2 (neuronal precursor cell expressed developmentally down-regulated protein 4-2) ubiquitinates ENaC (epithelial sodium channel), targeting it for degradation. SGK1 increases ENaC (epithelial sodium channel) activity by (i) phosphorylation of the channel, increasing the probability of channel opening, and (ii) phosphorylation of Nedd4-2, reducing its affinity for ENaC. Ki-RasA increases the probability of ENaC channel opening and GILZ regulates sodium reabsorption through decreasing Nedd4-2 affinity for ENaC. CHIF regulates Na^+/K^+-ATPase activity.

Aldosterone stimulates sodium reabsorption (and thereby water re-uptake) primarily by increasing epithelial sodium channel (ENaC) activity at the apical membrane of epithelial cells of the renal distal convoluted tubule and early collecting duct (Toddturla *et al.*, 1993). Aldosterone can increase the rate of Na^+ uptake in three different ways: (i) stimulating ENaC gene transcription, (ii) increasing trafficking of ENaC to the apical membrane, and (iii) post-translational modification of ENaC to increase the probability of channel opening (Horisberger, 1998; Butterworth *et al.*, 2009).

Aldosterone modulates ENaC activity indirectly through regulating the transcription of a wide-range of proteins collectively called aldosterone-induced proteins (AIPs) (Figure 1.11). The best characterised AIP is the serum and glucocorticoid-induced kinase 1 (SGK1). SGK1 is part of the phosphatidylinositol 3-kinase (PI3K) signalling pathway, and is activated by phosphorylation. SGK-1 can increase ENaC activity in one of two ways. First, phosphorylation of ENaC by SGK-1 increases the probability of channel opening. Second, the E3 ligase Nedd4-2 (neuronal precursor cell expressed developmentally down-regulated protein 4-2) ubiquitinates ENaC, targeting the channel for degradation. Phosphorylation of Nedd4-2 by SGK1 decreases it affinity for ENaC reducing the channel's turnover (Debonneville *et al.*, 2001; Pearce and Kleyman, 2007). The glucocorticoid-induced leucine zipper protein (GILZ) is another AIP, and regulates sodium reabsorption through decreasing Nedd4-2 affinity for ENaC reducing the amount of channel targeted for degradation (Bhalla *et al.*, 2006). Other less well-characterised AIPs include the channel-inducing factor (CHIF), which regulates Na^+/K^+-ATPase activity, and Kirsten Ras GTP-binding protein 2A (Ki-RasA), which increases the probability of ENaC channel opening (Stockand, 2002).

At the basolateral membrane of epithelial cells, sodium enters the bloodstream through active transport mediated by the Na^+/K^+-ATPase and Na^+/H^+ exchanger (NHE). Thus, aldosterone facilitates sodium (Na^+) reabsorption in exchange for potassium (K^+) and hydrogen (H^+) secretion. Through these changes in electrolyte balance, aldosterone regulates the extracellular fluid volume (and thereby blood pressure) while at the same time influencing K^+ distribution and acid-base balance.

1.4.2 Non-genomic actions of aldosterone

Aldosterone's genomic actions (often described as its "classic actions") are well-characterised and susceptible to transcription blockade by inhibitors such as Actinomycin D. However, physiological responses to aldosterone have also been observed in the nephron, distal colon and cardiovascular system that are independent of *de novo* protein synthesis and occur on a rapid time-scale (i.e. minutes).

The non-genomic activities of aldosterone are mediated via the generation of second messengers (e.g. Ca^{2+} and cAMP) and the activation of protein kinases (such as PKC and ERK). These signalling events modulate the activity of membrane proteins such as ENaC. The precise mechanism by which the rapid effects of aldosterone action occur remains under debate: it has been suggested that they may involve the MRs; others suspect binding to an as yet unidentified novel cell-surface receptor (Wehling, 1994; Dooley *et al.*, 2012).

1.4.3 Non-epithelial actions of aldosterone

Aldosterone has physiological effects in non-epithelial tissues, most notably the cardiovascular system and CNS. MRs are widely distributed in vascular (endothelial and smooth muscle), cardiac (fibroblast and cardiomyocytes) and neuronal tissues suggesting that aldosterone has widespread activities throughout the body (Odermatt and Atanasov, 2009). Curiously, however, with the exception of the vasculature, 11βHSDII is not expressed in the tissues where the MRs are found. This suggests the MRs are likely to be occupied by glucocorticoids such as cortisol rather than aldosterone. Despite this paradox, it is well established that excess aldosterone promotes cardiac remodeling, and causes both increased vascular resistance and vasoconstriction. These effects are aldosterone-induced, mediated via MRs, dependent on Na^{+} but independent of blood pressure (Brilla and Weber, 1992). It is possible that the ratio between glucocorticoid and mineralocorticoid occupied MR rather than the aldosterone level is responsible for the observed physiological effects. However, the precise mechanism by which aldosterone causes cardiovascular damage remains unclear.

1.5 The physiological roles of cortisol

Cortisol's biological activity is mediated through glucocorticoid receptors (GRs), which function in a similar way to MRs. Upon cortisol binding, GRs dimerise and the ligand bound receptor complex translocates to the nucleus where it binds to glucocorticoid response elements (GREs) in the promoter regions of target genes either inducing or repressing their expression (Funder, 1997).

In contrast to MRs, which are found in select target tissues only, GRs are ubiquitously expressed. This explains why cortisol is able to control a wide-range of physiological processes in humans including blood pressure regulation (Walker, 2007). Of particular relevance to this thesis, cortisol controls aspects of development and remodeling in vascular smooth muscle cells by modulating the production of nitric oxide and endothelin. The effects of excess cortisol secretion are apparent in conditions such as Cushing's syndrome where exaggerated cortisol activity leads to the development of obesity, insulin resistance and hypertension.

In order to further demonstrate the role that corticosteroids play in the regulation of blood pressure, diseases caused by aberrations in aldosterone and cortisol production will now be described.

1.6 The role of corticosteroids in hypertension

1.6.1 Corticosteroids and secondary hypertension

The cause of hypertension can only be identified in 5% of people with high blood pressure. These cases are termed secondary hypertension. In the general population, monogenic syndromes of hypertension caused by aberrations in corticosteroid synthesis are rather rare. However, these syndromes highlight the importance of corticosteroids in influencing blood pressure, and provide insights into the contribution that genetics plays in the development of hypertension (Vasan *et al.*, 2004). This Section summarises the types of secondary hypertension that have been identified in which corticosteroid production is altered.

1.6.1.1 Primary aldosteronism

The first case of primary aldosteronism (PA) was diagnosed by Dr. Jerome Conn in 1955. His patient was a 34 year old woman who had elevated blood pressure, weakness due to hypokalaemia and muscle spasms. During surgery, a right-sided adrenal tumour was discovered. When this was removed, the metabolic and clinical abnormalities were reversed (Conn, 1955). This clinical presentation was originally termed "primary aldosteronism" but has since been renamed an "adrenal producing adenoma" (APA). The term "primary aldosteronism" is now used to describe a group of related disorders characterised by high levels of aldosterone that occur independently of RAAS activity. Patients with PA have a higher risk of further development of cardiovascular diseases than age- and sex-matched patients with essential hypertension and the same degree of blood pressure elevation (Blumenfeld *et al.*, 1994; Milliez *et al.*, 2005).

There are five subtypes of PA of which the most prevalent forms are bilateral idiopathic hyperplasia (IHA) (*ca.* 60% of cases) and APA (35%). All patients with APA have small aldosterone-producing adenomas that produce aldosterone independent of AngII stimulation. Indeed, in these patients AngII is often suppressed to very low levels. In contrast, patients with IHA are hyper-responsive to AngII, which leads to expansion of the ZG. Less prevalent forms of PA include primary adrenal hyperplasia (*ca.* 2% of PA cases), familial hyperaldosteronism (<1%), pure aldosterone-producing adrenocortical carcinoma (<1%) and ectopic aldosterone producing adenoma or carcinoma (<0.1%) (Young, 2007).

1.6.1.2 Monogenic diseases of the corticosteroid biosynthetic pathway

Secondary hypertension can also be caused by mutations in genes encoding enzymes of the corticosteroid biosynthetic pathway. These are very rare, accounting for only approximately 1% of all hypertensive cases. Here, the monogenic forms of hypertension that arise from altered mineralocorticoid production are briefly described.

Glucocorticoid remediable hyperaldosteronism

Glucocorticoid remediable hyperaldosteronism (GRH) is caused by the formation of a chimeric gene composed of the 5' end of *CYP11B1* fused to the coding region of *CYP11B2*. The chimeric gene is expressed in the ZF and results in the production of aldosterone under the regulation of ACTH instead of AngII. GRH causes early-onset hypertension with the same biochemical features as primary aldosteronism. Upon treatment with glucocorticoids the phenotype is completely suppressed as a consequence of the removal of ACTH drive (Lifton *et al.*, 1992).

Apparent mineralocorticoid excess

Apparent mineralocorticoid excess is caused by mutations in the gene encoding 11β-HSDII which prevent the conversion of cortisol to cortisone. This results in the non-specific activation of MRs by cortisol, inducing a mineralocorticoid form of hypertension (Ulick *et al.*, 1979; Mune *et al.*, 1995; Stewart *et al.*, 1996).

Aldosterone synthase deficiency

Aldosterone synthase deficiency is caused by rare loss-of-function mutations in the *CYP11B2* gene which impede the final three steps of aldosterone synthesis. This condition is rare, and is characterised by salt-wasting, hyperkalaemia, increased plasma renin activity and hypotension (Ulick *et al.*, 1992). Aldosterone synthase deficiency can be divided into two subsets: corticosteroid methyloxidase types I and II. Both disorders have similar clinical features but the profile of mineralocorticoids present in individuals between types is different.

Congenital adrenal hyperplasia

Congenital adrenal hyperplasia (CAH) is caused by loss-of-function mutations in genes encoding enzymes involved in cortisol biosynthesis. Reduced cortisol production levels stimulate an increase in ACTH secretion which causes adrenal hyperplasia. This results in a build-up of corticosteroid intermediates to levels where they activate MRs. Symptoms of CAH vary according to which gene the causal mutations lie in (White *et al.*, 1987).

Inactivating mutations in 11β-Hydroxylase cause 11-deoxycorticosterone and 11-deoxycortisol to accumulate rather than cortisol. Under normal physiological

conditions, 11-deoxycorticosterone levels are insufficient to activate MRs. However, at the high levels found in people with CAH, 11-deoxycorticosterone can bind to MRs causing hypertension, hypokalaemia and low renin activity. CAH caused by 11β-Hydroxylase deficiency can be treated by glucocorticoid replacement therapy which normalises both the ACTH drive and increased blood pressure (White *et al.*, 1994).

CAH can also be caused by mutations in the gene encoding 17α-Hydroxylase. In these individuals, as well as having reduced cortisol levels, sex steroid production is also lowered due to inefficient conversion of 17-OH-pregnenolone to dehydroepiandrosterone (DHEA). This leads to the feminisation of males and the failure to develop secondary sex characteristics in females. All subjects have a mineralocorticoid-type hypertension caused by excessive 11-deoxycorticosterone production (Speiser and White, 2003).

Summary

What these rare hypertensive conditions have in common is that they are all caused by inappropriately high levels of mineralocorticoid activity resulting from either elevated aldosterone secretion, excess production of 11-deoxycorticosterone (a low-affinity MR agonist), or binding of cortisol to MRs.

1.6.2 Corticosteroids and essential hypertension

Although the role of corticosteroids in secondary hypertension is long-established, there is now compelling evidence that they are implicated in the aetiology of essential hypertension too. The *CYP11B1* and *CYP11B2* genes are located in tandem on human chromosome 8 only 40 kbp apart (Figure 1.12).

Polymorphic variations, including single nucleotide polymorphisms (SNPs), intron conversions and insertion/deletions, in the coding and regulatory regions of the *CYP11B* genes are strongly associated with the development of hypertension. One of the best studied SNPs is located at position -344 in the promoter of the *CYP11B2* gene. This polymorphism lies within a binding site for the steroidogenic factor (SF-1) transcription factor, and can be either a cytosine (C) or a thymine (T). Another well-studied variation is an intron conversion (IC) in which part of

the intron 2 sequence of the *CYP11B2* gene has been replaced with the corresponding portion of the *CYP11B1* gene (White and Slutsker, 1995). These two variants are in tight linkage disequilibrium (LD), meaning that there is a high likelihood of both alleles being inherited together.

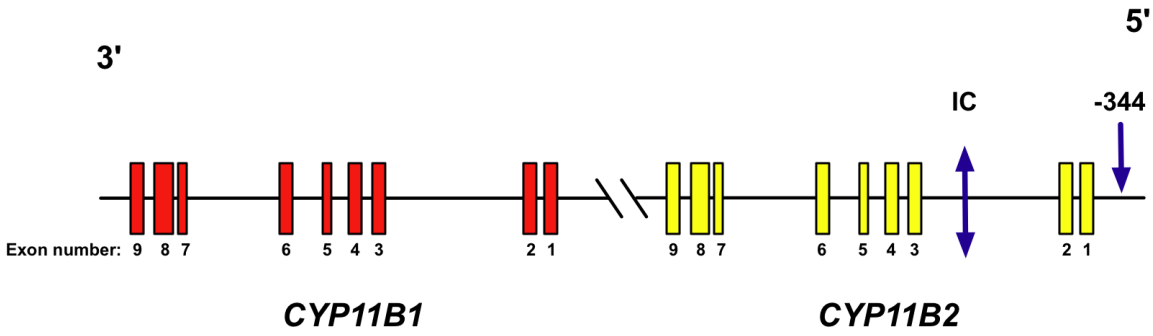

Figure 1.12 The exon and intron structure of the *CYP11B1* and *–B2* genes
The *CYP11B1* and *-B2* genes are located 40 kbp apart on chromosome 8. Each gene has 9 exons and 8 introns. The location of the -344 T/C SNP and the Intronic Conversion (IC) polymorphism are marked by arrows.

Several studies have shown that the -344T and IC polymorphisms are associated with hypertension. A case-control study led by Brand and colleagues found a positive association between high blood pressure and the -344T allele in a study of 280 hypertensive and 293 normotensive subjects (Brand *et al.*, 1998). In agreement with this finding, a study conducted by (Davies *et al.*, 1999) found that the -344T allele occurs with higher frequency in hypertensives than in age- and sex-matched normotensive subjects. Contrary to that observed by Brand, Davies discovered that significantly more people in the hypertensive group had the intron conversion compared to the WT allele. Additionally, in the North Glasgow MONItoring of CArdiovascular trends (MONICA) study, the -344T was associated with higher excretion rates of tetrahydroaldosterone than the C allele (Davies *et al.*, 1999). Plasma aldosterone levels were also found to be higher in subjects of -344T genotype. However, no significant differences were observed between subjects with different IC genotypes. Interestingly, a study of 27 well-characterised Conn's patients revealed a marked difference in the frequency of occurrence of the -344T/C and IC polymorphisms between patients with Conn's syndrome and controls, suggesting that there may be a causal link between the polymorphisms and the development of primary aldosteronism (Inglis *et al.*,

2001). However, other groups have reported findings contrary to these studies. Tsujita and colleagues did not find any association between the -344 SNP and hypertension in a case-control study of Japanese patients (Tsujita *et al.*, 2001), while Pojoga and co-workers have reported that the -344C allele is associated with increased plasma aldosterone levels in hypertensive patients (Pojoga *et al.*, 1998). A meta-analysis designed to address these conflicting results found that the -344T allele does indeed correlate with an increased risk of hypertension but not with the rate of aldosterone excretion (Sookoian *et al.*, 2007).

Despite the clinical importance of these polymorphisms, how they affect blood pressure is poorly understood. The -344 T/C SNP is located with a binding site for the steroidogenic factor-1 (SF-1) transcription factor, suggesting that this polymorphism may affect *CYP11B2* transcription. However, *in vitro* studies have shown that the polymorphism has no significant effect on gene transcription even though there is a 4-fold difference in binding affinity for SF-1 between alleles (Bassett *et al.*, 2002). It has also been proposed that the -344 and IC polymorphisms could be markers of a causal variant in nearby genes. Clinical studies have shown that there is a strong association between the -344T genotype and an increased ratio of 11-deoxycortisol to cortisol (or their metabolites), suggesting that altered 11β-Hydroxylase activity may be related to *CYP11B2* polymorphisms (Davies *et al.*, 2001). The *CYP11B1* gene is highly polymorphic, and most variations have been found to be in tight LD with those in the B2 locus. Two SNPs in the promoter region of the *CYP11B1* gene (-1899 G/T and -1859 A/G) were identified by Barr and colleagues in normotensive subjects homozygous for the -344T and IC polymorphisms in the *CYP11B2* locus (Barr *et al.*, 2007). When hypertensive patients from the British Genetics of Hypertension Study were genotyped for these polymorphisms, the -1899T and -1859G alleles were shown to associate with reduced levels of 11β-Hydroxylase activity *in vivo* (Barr *et al.*, 2007).

1.7 Aldosterone as a therapeutic target for treating hypertension and heart disease

Currently, there are several different therapeutic options for treating hypertension including ACE inhibitors, angiotensin receptor blockers, calcium blockers and diuretics. Despite the broad range of anti-hypertensive drugs that are available, however, there is still an urgent need to develop novel therapeutic agents for treating resistant hypertension (Paulis *et al.*, 2012).

1.7.1 Current anti-hypertensive treatment strategies

The multifactorial pathophysiology of hypertension necessitates therapeutic agents that have different mechanisms of action. Briefly, the clinical approach for lowering blood pressure regulation relies on either reducing the sensitivity of vascular smooth muscle to pressor agonists, or reducing intravascular volume by lowering the levels of exchangeable sodium. Often these approaches are combined to lower the blood pressure of hypertensive patients (Paulis and Unger, 2010).

Reduction of vascular smooth muscle tone can be obtained by blocking either the synthesis of AngII (through ACE inhibition) or its efficacy (through AngII receptor blockers (ARB)) (Zaman *et al.*, 2002), antagonising β-adrenergic receptor function (Che *et al.*, 2009) or blocking smooth muscle Ca^{2+} channels (Eisenberg *et al.*, 2004; Che *et al.*, 2009). Levels of exchangeable sodium in people can be lowered through dietary sodium restriction, the use of diuretics or aldosterone blockade. A summary of all these therapeutic approaches is given in Table 1.2.

Table 1.1 Major classes of pharmacological drugs for treating hypertension

Drug	Action	Side Effects/limitations	Types on market
ACE inhibitors	inhibits conversion of AngI to AngII	- dry cough, angiodema, dizziness, tiredness, headaches - not suitable if patient has a history of kidney/heart disease. - not effective in blacks or those over 55 - AngII escape	Rampipril, Lisinopril, Perindopril, Captopril, Cilazapril, Enalapril, Trandolapril
AngII receptor blockers	prevents activation of AT_1 receptors	- headaches, dizziness, diarrhoea, nasal congestion, back and leg pain - can not be used during pregnancy	Valsartan, Losartan, Eposartan, Irbesartan, Candesartan, Temisartan, EXP3174
β-Blockers	prevents activation of β-adrenergic receptors	- wide range of side effects including tiredness, cold hands and feet, slow heartbeat, diarrhoea, nausea, sleep disturbance, nightmares and impotence	Bisoprolol, Atenolol, Carvedilol, Propanolol, Metoprolol, Sotolol, Nevibolol
Calcium channel blockers	prevents opening of Calcium channels	- flushed face, headaches, swollen ankles, dizziness, tiredness and skin rashes. - not suitable for people with a history of heart disease, liver disease or circulation problems	Ditiazem, Verapamil, Amlodipine, Nifedipine
Diuretics	increases water excretion	- can raise potassium and blood sugar levels - can cause impotence - can not be used if you are pregnant or have gout	Amiloride, Bendrofluazide, Butanide, Chloradilone, Furosemide, Metolazone, Torasemide
Mineralocorticoid receptor blockers	prevents mineralocorticoid receptor activation	- gynecomastia - lowered libido	Spironolactone, Eplerenone

1.7.2 Inhibiting the renin-angiotensin-aldosterone system: angiotensin converting enzyme inhibitors and angiotensin receptor blockers

Currently, ACE inhibitors and ARBs are the first-line therapy in the treatment of hypertension. ACE inhibitors are effective therapeutic agents not just for treating hypertension (Ondetti and Cushman, 1977) but also substantially lower the risk of cardiovascular events such as stroke and heart failure (Heart Outcomes Prevention Evaluation (HOPE) Study Investigators, 2000). However, ACE inhibitors do have some side effects. Due to concomitant inhibition of bradykinin breakdown some patients prescribed ACE inhibitors experience a persistent dry cough. Additionally, a risk of angioedema has been reported (Zaman *et al.*, 2002). ARBs act by blocking AngII activation of the AT_1 receptor. ARBs have a similar effect on blood pressure as ACE inhibitors but they have a better tolerability profile and, therefore, enhanced patient compliance (Timmermans *et al.*, 1993; Dahlöf *et al.*, 2002; Julius *et al.*, 2006).

1.7.3 Mineralocorticoid receptor blockade: targeting aldosterone action

Prescription of the mineralocorticoid receptor blockers spironolactone or eplerenone in addition to triple-combination therapy (an ACE inhibitor or ARB supplemented with both a calcium channel blocker and a diuretic) significantly reduces blood pressure in patients with resistant hypertension, suggesting that this group of anti-hypertensives has great therapeutic potential (Nishizaka *et al.*, 2003; Chapman *et al.*, 2007).

Aldosterone is known to have deleterious effects on heart function independent of blood pressure. For example, several studies in rats have linked aldosterone excess to both vascular injury (Rocha *et al.*, 1998) and myocardial fibrosis (Brilla *et al.*, 1993). The usefulness of spironolactone and eplerenone to treat heart failure was probed in two milestone clinical studies conducted in 1999 and 2003 called RALES and EPHESUS, respectively. Both MR antagonists were found to reduce morbidity and mortality among patients with severe heart failure (RALES) as well as in individuals who had acute myocardial infarction complicated by left

ventricular dysfunction and heart failure (EPHESUS) (Pitt *et al.*, 1999; Pitt *et al.*, 2003).

Unfortunately, adverse side effects (such as gynecomastia and hypokalaemia) have been observed with spironolactone, which has limited its clinical use. These side effects are caused by non-specific interactions between the drug and the receptors for progesterone and androgen. Off-target effects have not been observed with eplerenone, which has greater specificity than spironolactone (Weinberger *et al.*, 2002).

1.7.4 Inhibiting aldosterone synthase

Over the last four years, substantial research effort has been made, both in academia and the pharmaceutical industry, to develop potent and specific aldosterone synthase inhibitors (Lucas *et al.*, 2008; Calhoun *et al.*, 2011; Lucas *et al.*, 2011). LCI699 (Novartis) was the first of these to be tested in a phase 2 clinical trial where its potential for treating essential hypertension was evaluated (Calhoun *et al.*, 2011). LCI699 was found to be well tolerated, rapidly absorbed following oral administration, and potent in suppressing both plasma and urinary aldosterone levels. However, *ca.* 20% of participants developed suppression of ACTH-stimulated cortisol release suggesting that LC1699 was partially inhibiting 11β-Hydroxylase too. Although disappointing, this was not a great surprise as 11β-Hydroxylase and aldosterone synthase have 93% amino acid sequence identity. Thus, while this study has provided proof-of-principle regarding the therapeutic potential of aldosterone synthase inhibitors, it has also served to underline the need for further work to identify new molecules that inhibit aldosterone synthase specifically.

1.8 Structural knowledge concerning p450 enzymes

Cytochrome p450s have a common structure comprising a small, N-terminal domain consisting of β-strands with a larger, α-helical C-terminal domain which contains the prosthetic haem group and enzyme active site. The p450 fold was first observed by Kraut and co-workers when they solved the structure of $p450_{cam}$ (Poulos *et al.*, 1985). Surprisingly, despite low (10-30%) primary sequence

homology among members of the cytochrome p450 superfamily, as the number of p450 structures that have been solved increases, it has been found the entire superfamily has the same overall fold.

1.8.1 $p450_{cam}$: a paradigm for cytochrome p450 structure

The first crystal structure of a cytochrome p450 to be elucidated was that of $p450_{cam}$ from the bacterium *Pseudomonas putida* which was solved to a resolution of 2.6 Å (Poulos *et al.*, 1985). $p450_{cam}$ is shaped like a triangular prism consisting of 12 α-helices (designated A-L) and 5 β-strands (designated β1-β5) (Figure 1.13).

Figure 1.13 The structure of $p450_{cam}$ from *Pseudomonas putida*
$p450_{cam}$ has a compact triangular shape with one side rich in β-sheet and the other consisting mainly of α-helices. The haem is located between helices I (yellow) and L (orange), and is positioned directly below the camphor (substrate) molecule (inset). $P450_{cam}$ is displayed in Chainbow ribbon representation (N-terminus blue; C-terminus red). PDB 2CPP (Poulos *et al.*, 1987).

Haem-binding region

The core of $p450_{cam}$ comprises a four-helix bundle, consisting of helices E, F, G and I. Helix I transcends the protein diagonally and lies parallel to helices L and D. This four-helical bundle is conserved between cytochrome p450 proteins. The prosthetic haem group, embedded between helices I and L, is surrounded by apolar residues and is co-ordinated by Cys357 (which is located at the N-terminal end of helix L). This cysteine is absolutely conserved across the entire cytochrome p450 superfamily and is part of the p450 signature amino acid sequence motif FxxGx(H/R)xCxG (Denisov *et al.*, 2005).

1.8.2 Substrate recognition sites

Despite the highly conserved fold possessed by all cytochrome p450s, there is a remarkable variation in the chemical structures of the substrates recognised by different members of the superfamily. While certain p450s are both highly regio- and stereo-specific in their oxygenation of substrate molecules, other enzymes can metabolise a large variety of substrates. Enzyme-specificity is determined by regions of variability distributed throughout the p450 primary sequence, termed substrate recognition sites (SRS).

SRS were first identified by Osamu Gotoh who performed a group-to-group alignment of mammalian CYP2 DNA sequences with those available from bacteria including that from *P. putida* (whose substrate-binding residues had been definitively identified by X-ray crystallography) (Gotoh, 1992). In doing this, 6 regions of variability (SRS1-6; Table 1.3) which had accumulated more amino-acid changing DNA substitutions than the rest of the sequence were identified. Gotoh predicted that these hypervariable regions were responsible for determining the substrate-specificity of individual cytochrome p450s.

Structures published subsequent to Gotoh's work have indeed confirmed his hypothesis that while the overall three-dimensional structure of cytochrome p450s is conserved, the substrate specificity of individual enzymes is determined by the 6 SRS.

Table 1.2 Substrate recognition sites (SRS) in $p450_{cam}$

SRS	Residues	Position in tertiary structure
1	103-162	Helix B' and flanking areas
2	209-216	Helix F (C-terminal end)
3	248-255	Helix G (N-terminal end)
4	302-320	Helix I (N-terminal end)
5	375-385	β3
6	485-493	β5 (middle)

1.8.3 Mammalian cytochrome p450 structure: CYP2C5

Rabbit microsomal p450 2C5 was the first mammalian cytochrome p450 to have its structure elucidated. 2C5 selectively hydroxylates the 21-methyl group on the 17β side chain of progesterone.

Unlike microbial cytochrome p450s (which are all water-soluble), all mammalian cytochrome p450s are membrane associated. Therefore, before the structure of any mammalian p450 could be obtained, a method had to be developed for working with these proteins in solution. Pioneering work by Eric Johnson's laboratory showed that when the N-terminal membrane anchor was removed from 2C5 and a further four amino acids substituted, the modified enzyme was soluble and monomeric in high salt containing buffers (Cosme and Johnson, 2000). The approach of Johnson was sufficient to enable the first purification and crystallisation of a mammalian cytochrome p450.

The structure of rabbit 2C5 was solved to a resolution of 3.0 Å by the groups of Johnson and Duncan McRee (Williams *et al.*, 2000). 2C5 has the same overall structure (Figure 1.14) as bacterial p450s, and provided the first evidence that the p450 fold discovered in prokaryotes was conserved in mammals also. In particular, the positions of helix I (where the Cys haem axial ligand is located) and the electron transfer site (formed by helix L and the β bulge) in 2C5 are

essentially superimposable with those from bacterial p450s. The structure of 2C5 revealed a broad hydrophobic patch on the surface of the enzyme which contributes to the monofacial binding of the protein to the membrane. This membrane-interaction surface occurs in close proximity to where the N-terminal transmembrane domain is thought to span the lipid bilayer. The two membrane interacting regions of 2C5 firmly anchor it to the ER membrane as well as determining the specific orientation of the enzyme's catalytic domain relative to the membrane surface. The entrance of the substrate access channel (formed between the F-G loop and the N-terminal β-sheet domain) is located within the bilayer thereby allowing hydrophobic substrates to enter the enzyme's active site directly from the membrane. In addition, the surface of 2C5 proximal to the haem group is perpendicular to the membrane, which facilitates contact with, and electron transfer from, CPR.

1.8.4 The structure of a mitochondrial CYP: 24-Hydroxylase

Johnson's genetic engineering approach for increasing mammalian p450 solubility has facilitated the structure determination of other microsomal enzymes including 2A6, 2B4, 2C8, 2C9, 2D6 and 3A4 (Otyepka *et al.*, 2007). The first structure of a mitochondrial p450, however, was not obtained until 2010, suggesting that this sub-set of the cytochrome p450 superfamily are more difficult to work with than their microsomal counterparts.

Mitochondrial p450s have an N-terminal leader sequence which targets them to mitochondria. Upon import, the leader sequence is cleaved from the p450 and the mature enzyme binds monotopically to the matrix side of the inner mitochondrial membrane. Unlike the microsomal enzymes, mitochondrial p450s do not have a transmembrane anchor. Rather, they are embedded in the membrane through insertion of surface hydrophobic patches into the core of the lipid bilayer. This Section describes how the groups of Eric Johnson and David Stout obtained the structure of rat vitamin D 24-Hydroxylase (CYP24A1) (Annalora *et al.*, 2010).

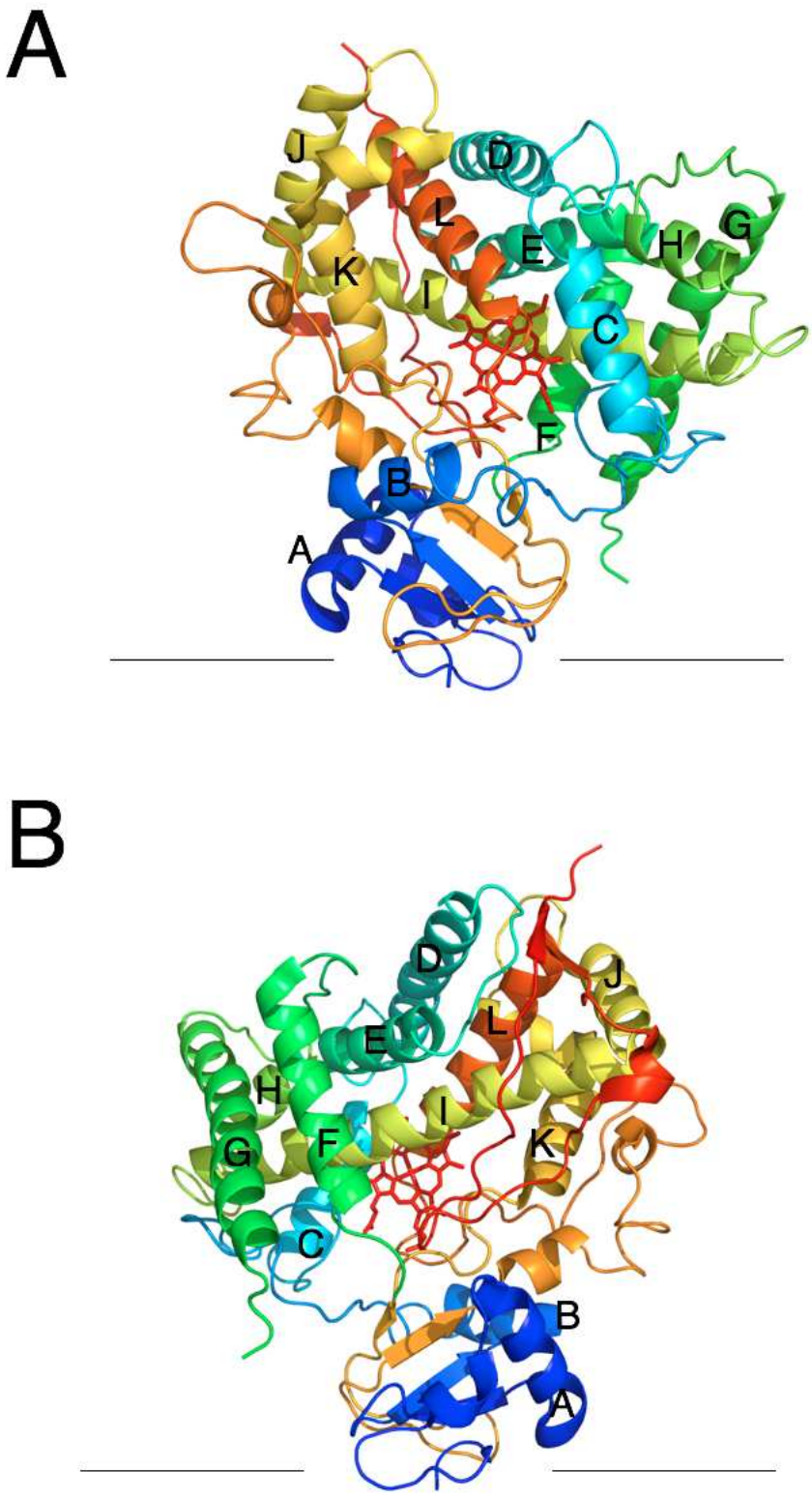

Figure 1.14 Two views of rabbit cytochrome p450 CYP2C5
The structure of the first mammalian p450, rabbit CYP2C5, was solved by Eric Johnson and colleagues in 2000. 2C5 is displayed in (A) front and (B) rear view. Electron density around the F-G loop was not clear and was, therefore, omitted from the final structure. The position of the membrane was derived from anti-peptide antibody experiments, and is represented by a line. 2C5 is displayed in ribbon representation with the chains coloured blue to red from the N- to the C-terminus. The haem is depicted in stick format and coloured red. PDB 10G2 (Williams *et al.*, 2000).

24-Hydroxylase expression optimisation

An engineered form of 24-Hydroxylase was expressed in *E. coli* with a production level of ~40-50 mg l^{-1} (Annalora *et al.*, 2004). The original construct was modified in several ways: (i) the N-terminal mitochondrial targeting sequence (Δ2-32) was removed; (ii) rare codons at positions three and four in the rat sequence were changed to ones that occur more commonly in *E. coli;* and (iii) a stabilising mutation S57D found previously to have no effect on catalytic function (Omdahl *et al.*, 2004) was introduced. Enhanced levels of 24-Hydroxylase were obtained by adding chloramphenicol (which stimulates *E. coli* to make cold-shock proteins) to the expression cultures along with IPTG (Annalora *et al.*, 2004).

Detergent optimisation: a critical step in obtaining diffracting crystals

Mammalian p450s can be extracted from their membrane environments using detergent. The optimal detergent for solubilising and purifying 24-Hydroxylase in a stable form was found to be Chaps (Annalora *et al.*, 2004). However, in this detergent alone no crystals were obtained. By exchanging 24-Hydroxylase into the detergent CYMAL-5 immediately prior to setting up crystallisation trays, crystals that diffracted to 3.0 Å resolution were obtained. Interestingly, when Chaps was used in combination with other common detergents such as CYMAL-5 and Fos Choline-12, protein crystals were obtained. The crystals which diffracted to highest resolution were obtained when Chaps was used in combination with the facial amphiphile 3α-hydroxy-7α,12α-bis[(β-D-maltopyranosyl)ethloxy]cholane (231-chol) to stabilise CYP24A1. Using this detergent combination, crystals were obtained that diffracted to 2.0 Å. The dramatic improvement in 24-Hydroxylase crystal quality that was obtained when facial amphiphiles were used has also been observed with two other p450 enzymes (CYP2B6 (Gay *et al.*, 2010) and CYP2B4 (Gay *et al.*, 2011)). Together, these results suggest that facial amphiphiles may prove to be particularly useful for crystallising mammalian p450s.

Understanding mitochondrial p450 function from the structure of 24-Hydroxylase

The structure of 24-Hydroxylase has provided the first insights into the way in which mitochondrial p450s insert into the membrane, bind substrate and interact with adrenodoxin.

24-Hydroxylase adopts the canonical p450 fold comprising 12 α helices and four β-strands (Figure 1.15). However, 24-Hydroxylase has additional helices (A', B' and G') on its distal surface with a further two (K' and K'') located between β2 and the conserved haem binding motif (Figure 1.15A). The substrate binding site is enclosed by the strands β1 and β4, the B-C loop as well as helices E, F, G, I and K. A membrane-directed substrate access channel is stabilised in an open conformation by a cluster of aromatic residues from helices B' (Trp134 and Tyr 137), F (Phe249) and G (His271, Trp275 and Phe279) (Figure 1.15B) as well as a salt bridge formed between Arg138 and Glu322 (Figure 1.15C). These eight residues are conserved in all mitochondrial p450s, suggesting a common mechanism of substrate access to the enzyme active site from the lipid bilayer.

The short helices A' and G', which flank the substrate access channel, anchor CYP24A1 to the inner mitochondrial membrane (Figure 1.15). The corresponding regions (sequence following the A helix and the F-G loop) in microsomal p450s are involved in membrane association also. Alignment of the CYP24A1 A' and G' amino acid sequences with those from other mitochondrial p450s identified each as a membrane insertion (MIS) domain. It is likely that all mitochondrial p450s are anchored to the inner membrane via their two MIS domains. Conserved surface features from helices K, K'' and L as well as the lysine-rich proximal loop of the meander region define the adrenodoxin binding site.

Figure 1.15 The crystal structure of 24-Hydroxylase
(A) CYP24A1 has the canonical p450 fold consisting of 12 α helices (labelled A-L) and four β-strands. CYP24A1 has two membrane insertion (MIS) domains comprising helices A' (MIS-1) and G' (MIS-2). The position of the membrane is represented by a line. A membrane-directed substrate access channel is stabilised in an open conformation by (B) a cluster of aromatic residues from helices B' (Trp134 and Tyr 137; blue), F (Phe249; pink) and G (His271, Trp275 and Phe279; yellow) as well as (C) a salt bridge formed between Arg138 and Glu322. PDB 3K9V (Annalora *et al.*, 2010).

1.8.5 Structures of p450 enzymes involved in steroidogenesis

In humans, there are six p450 enzymes that play a role in steroid biosynthesis (Miller and Auchus, 2011). These are side-chain cleavage enzyme, 11β-Hydroxylase, aldosterone synthase, 17α-Hydroxylase, aromatase and 21-Hydroxylase. In 2009, the 3-dimensional structure of aromatase was published (Ghosh *et al.*, 2009). Since then, structures of side-chain cleavage enzyme (Mast *et al.*, 2011; Strushkevich *et al.*, 2011), 17α- (DeVore and Scott, 2012) and 21-Hydroxylase (Zhao *et al.*, 2012) have also been obtained. This Section describes the structure of side-chain cleavage enzyme with substrate bound and in complex with adrenodoxin. An overview of the structures of aromatase, 17α- and 21-Hydroxylase is also presented. The remaining challenges in steroid p450 structural biology are considered.

1.8.5.1 The three dimensional structure of side-chain cleavage enzyme

Side-chain cleavage enzyme catalyses the conversion of cholesterol to pregnenolone, the first step in the synthesis of all steroid hormones. Side-chain cleavage enzyme catalyses three distinct reactions: (1) the conversion of cholesterol to 22-hydroxycholesterol (22-HC); (2) the 20-hydroxylation of 22-HC giving 20,22-dihydroxycholesterol (20,22-DHC); and finally (3) cleavage of the C20-C22 bond yielding pregnenolone. Although side-chain cleavage enzyme performs remarkable chemistry, without structural information little could be deduced about the way in which side-chain cleavage enzyme is able to carry out three sequential reactions in the same active site.

In 2011, two structures of side-chain cleavage enzyme were published. The first was of bovine side-chain cleavage enzyme co-crystallised with the first reaction intermediate 22-HC (Mast *et al.*, 2011). The second paper described the structure of human side-chain cleavage enzyme in complex with adrenodoxin (Strushkevich *et al.*, 2011). Structures were obtained for the side-chain cleavage enzyme-adrenodoxin fusion at all stages of the p450's catalytic cycle.

Substrate mobility in the active site

Cholesterol is transferred to the active site of side-chain cleavage enzyme directly from the inner mitochondrial membrane via a substrate access channel similar to that observed in the CYP24A1 structure (Annalora *et al.*, 2010). Cholesterol is bound in the active site with its side chain bent at positions C20 and C22 (Figure 1.16A) (Strushkevich *et al.*, 2011). The residues Leu101, Trp87, Phe202 and Ile461 position the side chain above the haem iron for subsequent hydroxylations (Figure 1.16A). There are extensive contacts between the cholesterol rings and amino acids located in the enzyme active site (Figure 1.16B-D). Leu450, Leu84 and Phe82 interact with the α-face of the sterol rings whereas Ser352, Val353, Thr354 and Gln356 contact the β-face. Phe482 and Arg81 interact with the edges of the cholesterol rings.

By co-crystallising side-chain cleavage enzyme with its reaction intermediates, it has been possible to gain insights into the way that this particular p450 works. For instance, the crystal structure of bovine side-chain cleavage enzyme with bound 22-HC showed that only two-thirds of the substrate cavity is occupied by the cholesterol-derivative (Mast *et al.*, 2011). The remaining space at the entrance to the active site is filled with ordered water molecules, some of which form H-bonds with the sterol's 3β-hydroxyl group. As there are no direct contacts between the 3β-hydroxyl and the protein, the substrate/reaction intermediates can make small movements while remaining bound to the protein. The shape of the active site is such that any substrate movement would have to be either away from or towards the haem. This translational freedom along with the torsional changes in the aliphatic tail results in correct positioning of the C20 or C22 atoms for stereospecific hydroxylation.

Interaction of side-chain cleavage enzyme with adrenodoxin

In order to elucidate how electrons are transferred from adrenodoxin (Adx) to side-chain cleavage enzyme (SCC), Park and colleagues solved the structure of a side-chain cleavage enzyme-adrenodoxin fusion protein capturing a static snapshot of a biologically transient reaction (Figure 1.17) (Strushkevich *et al.*, 2011).

Figure 1.16 Structure of the side-chain cleavage enzyme active site containing cholesterol
(A) The cholesterol molecule fits tightly into the side-chain cleavage enzyme active site, with its side chain bent at positions C20 and C22. Residues Leu101, Trp87, Phe202 and Ile461 position the side chain above the haem iron for subsequent hydroxylation reactions. There are extensive contacts between the sterol rings and active site amino acids: (B) Leu450, Ile84 and Phe82 interact with the α-face of cholesterol while (C) Phe482 and Arg81 make contacts with its edges. (D) Residues Ser352, Val353, Thr354 and Gln356 interact with the β-face of cholesterol. PDB 3N9Y (Strushkevich *et al.*, 2011).

Adrenodoxin binds at the proximal surface of side-chain cleavage enzyme. There are two main points of contact between side-chain cleavage enzyme and adrenodoxin: (i) the K helix of side-chain cleavage enzyme interacts with the F helix of adrenodoxin, and (ii) the haem-binding loop, C and L helices of side-chain cleavage enzyme form contacts with the loop surrounding the adrenodoxin [2Fe-2S] cluster. The complex is held together by a combination of hydrogen bonds (between $Lys109_{SCC}$ and $Ala45_{Adx}$; $Trp418_{SCC}$ and $Leu80_{Adx}$) and salt bridges (between $Lys339_{SCC}$ and $Asp72_{Adx}$; $Lys343_{SCC}$ and $Asp76_{Adx}$) (Figure 1.17). When adrenodoxin is bound to side-chain cleavage enzyme, the [2Fe-2S] cluster of adrenodoxin is positioned directly beneath the p450 haem group. From the co-crystal structure Park and colleagues suggested that electrons may be transferred from the adrenodoxin [2Fe-2S] cluster to the p450 haem via the amino acid residues $Cys52_{Adx}$, $Ala51_{Adx}$, $Gln422_{SCC}$ and $Cys423_{SCC}$, (Strushkevich *et al.*, 2011).

When the structure of adrenodoxin in complex with side-chain cleavage enzyme was compared with that between adrenodoxin and adrenodoxin reductase (Müller *et al.*, 2001), it was found that the adrenodoxin residues that interact with adrenodoxin reductase greatly overlap with those that form contacts with side-chain cleavage enzyme. This suggests that adrenodoxin can bind to either adrenodoxin reductase or a p450 enzyme but not both at the same time. This structural evidence suggests that electron transfer between adrenodoxin reductase and mitochondrial p450s can not occur via either the ternary or quaternary complex models (Section 1.2.3.2.2). Rather, if binding of adrenodoxin to adrenodoxin reductase and p450s is mutually exclusive, it would suggest that the "shuttle" mechanism of electron transfer between adrenodoxin reductase and mitochondrial p450 enzymes is correct.

1.8.5.2 Available structural data for other steroidogenic p450s

The first cytochrome p450 involved in steroid biosynthesis to have its structure solved was aromatase (Ghosh *et al.*, 2009). Aromatase is responsible for the biosynthesis of all oestrogens from androgens, and catalyses three distinct chemical reactions (two C19-methyl hydroxylations and an aromatisation of the steroid A ring). Unusually, the aromatase used for crystallisation trials had been purified from human placenta rather than obtained from a heterologous expression host. To date, aromatase is the only full-length cytochrome p450 where a structure has been obtained. Aromatase was crystallised in the presence of the steroid androstenedione, which was found to bind snugly in an androgen-specific cleft within the enzyme.

Recently, the structure of 17α-Hydroxylase has been solved by Emily Scott's laboratory (DeVore and Scott, 2012). 17α-Hydroxylase is required for the synthesis of many different human steroids including cortisol as well as the androgenic and oestrogenic sex hormones. Consequently, this enzyme is an important target in the treatment of breast and prostate cancer. X-ray crystal structures were obtained for 17α-Hydroxylase in the presence of two inhibitors (arbiraterone and TOK-001).

Figure 1.17 Interaction of side-chain cleavage enzyme with adrenodoxin
(A) The crystal structure of side-chain cleavage enzyme (teal) with cholesterol (yellow) bound in complex with Adx (dark pink). side-chain cleavage enzyme is anchored to the inner mitochondrial membrane (represented by a line) via its A' and G' helices. (B) When Adx is bound to side-chain cleavage enzyme, its [2Fe-2S] cluster (orange) is positioned directly beneath the p450 haem moiety (red). The crystal structure suggests that electrons are transferred from the Adx [2Fe-2S] cluster to the side-chain cleavage enzyme haem group via Cys52 and Ala51 of Adx, and Gln422 and Cys423 of side-chain cleavage enzyme. There are two main points of contact between side-chain cleavage enzyme and Adx: (i) the K helix of side-chain cleavage enzyme interacts with the F helix of Adx, and (ii) the haem-binding loop, C and L helices of side-chain cleavage enzyme form contacts with the loop surrounding the Adx [2Fe-2S] cluster. The side-chain cleavage enzyme -Adx complex is held together by a combination of (C) hydrogen bonds and (D) salt bridges side-chain cleavage enzyme residues are shown in green with the Adx ones in pink. PDB 3N9Y (Strushkevich *et al.*, 2011).

The overall structure has provided a rationale for many non-synonomous mutations known to cause steroidogenic disease. Features of the enzyme's active site also helped to explain its dual Hydroxylase and lyase activities.

Steroid 21-Hydroxylase deficiency accounts for *ca*. 95% of people with congenital adrenal hyperplasia (CAH) (which is characterised by impaired synthesis of aldosterone and cortisol with excessive androgen production). Mike Waterman's group has recently solved the structure of bovine 21-Hydroxylase with substrate (17-hydroxyprogesterone) bound to a resolution of 3 Å (Zhao *et al.*, 2012). This structure has given molecular insights into the genetic causes of CAH.

To date, there is no structural information available for either aldosterone synthase or 11β-Hydroxylase.

1.9 The structural biology of membrane proteins from humans

From a structural biology perspective, membrane proteins are regarded to be one of the most challenging classes of proteins to work with. Although ~30% of all proteins are located within lipid bilayers, the number of membrane proteins whose structures have been obtained and deposited in the protein data bank (PDB) is relatively small compared to the corresponding number for soluble proteins (Bill *et al.*, 2011). In recent years, however, there has been a substantial increase in the number of membrane protein structures that have been solved. This progress has been aided by the considerable technological advances that have been made in all aspects (expression, purification, stabilisation and crystallisation) of membrane protein structural biology (White, 2009).

The first membrane protein to have its structure solved to atomic resolution was the photosynthetic reaction centre from purple bacteria (Deisenhofer *et al.*, 1985). Since then, a further 350 unique membrane protein structures have been elucidated of which <20 are from humans[3]. These statistics suggest that obtaining the *de novo* structure of any human membrane protein is incredibly

[3] http://blanco.biomol.uci.edu/mpstruc/listAll/list

challenging. This Section outlines the main practical considerations when attempting to solve the crystal structure of a novel human membrane protein.

1.9.1 Recombinant production of human membrane proteins

There are only a few cases where membrane proteins have a sufficiently high natural abundance to allow their purification directly from native sources (e.g. bovine rhodopsin (Okada *et al.*, 1998). Therefore, the first step towards solving the structure of any membrane protein often involves establishing a robust recombinant expression system capable of making milligram quantities of functional protein for downstream processing. There are a variety of host systems available for producing human membrane proteins. These include bacteria, yeast, insect and mammalian cells. The usefulness of each of these host systems for making any given human membrane protein can only be assessed through experiment.

Bacterial expression hosts such as *E. coli* are popular hosts for making membrane proteins as the cells grow on cheap media with a short doubling time (*ca.* 20 min). Furthermore, a wide range of expression vectors and strains are commercially-available. Although *E. coli* is commonly used to make bacterial membrane proteins, its use with human membrane proteins is rather more restricted as bacteria are unable to perform many of the post-translational modifications required for correct folding and insertion of the protein into the membrane. Furthermore, there are substantial differences in the lipid content between lower and higher eukaryotes hindering efforts to make human membrane proteins in bacteria. However, where these limitations have been overcome, for example through protein engineering, bacteria have been successfully used to make milligram amounts of selected human membrane proteins for structural studies (Weiss and Grisshammer, 2002).

Yeasts such as *S. cerevisiae* and *P. pastoris* are a popular alternative to bacteria for making human membrane proteins (Andre *et al.*, 2006; Newstead *et al.*, 2007). Similar to bacteria, yeasts are cheap to grow. However, yeasts have the added benefit of being able to perform many of the post-translational modifications that occur in mammalian cells (including N-type glycosylation),

making them better suited for expressing human membrane proteins than bacteria. When expression has been obtained on a small scale, membrane protein production can be readily scaled up by growing the yeast in a fermenter. *P. pastoris* has been shown to be particularly useful for expressing milligram quantities of a wide range of human membrane proteins including G-protein coupled receptors (Weiss *et al.*, 1998; Andre *et al.*, 2006), transporters (Chloupkova *et al.*, 2007; Alisio and Mueckler, 2010), channels (Nyblom *et al.*, 2007; Lee *et al.*, 2009; Brohawn *et al.*, 2012) and membrane enzymes (Newton-Vinson *et al.*, 2000). The main advantage that *P. pastoris* has compared to *S. cerevisiae* is that it can grow to extremely high cell densities (10^9 cells/ml) in fermenter culture using methanol as a carbon source (Cereghino *et al.*, 2002). A limitation of using yeast cells for making human membrane proteins is that their membranes contain the fungal sterol ergosterol rather than the mammalian one cholesterol.

Insect cells infected with baculovirus are commonly used to make human membrane proteins. Indeed, all of the heterologously expressed G-protein coupled receptors that have had their structures solved to date have all been made in insect cells (Cherezov *et al.*, 2007). Insect cells grow to a density of 10^8 cells/ml and can perform most mammalian post-translational modifications. However, this expression system is considerably more expensive to use than either yeast or bacteria.

Mammalian cells (e.g. HEK293, CHO) can be considered the optimal hosts for making human membrane proteins as their cellular environment is essentially the same as that in which the heterologously expressed membrane proteins normally reside. However, the media used for growing mammalian cells is very expensive, the cells grow to low densities (10^6 – 10^7 cells/ml) even in bioreactors as well as having long doubling times (typically cell division occurs once every 24 h). For these reasons, mammalian cells tend only to be used for making human membrane proteins for structural studies when expression has not been possible in bacteria, yeast or insect cells.

1.9.2 Detergent solubilisation

Before a heterologously-expressed membrane protein can be purified, it must first be removed from the lipid bilayer using a detergent. All detergents are amphipathic molecules consisting of a hydrophilic headgroup (which interacts with the aqueous medium) and a hydrophobic tail (which associates with the hydrophobic regions of the protein that ordinarily reside within the core of the lipid bilayer).

There are a large number of biological detergents that can be used with membrane proteins. These can be classified into four groups according to the type of headgroup that the detergent possesses: zwitterionic, anionic, cationic and non-ionic. Ionic detergents (such as members of the Fos Choline family) are strong detergents and, therefore, excellent at solubilising membranes. However, they are harsh detergents and can often strip essential lipids required for functional activity from the surface of the target protein. In contrast, non-ionic detergents (such as the alkyl maltosides) are relatively mild, and, therefore, commonly used for membrane solubilisation.

The detergent concentration at which individual detergent molecules spontaneously form micelles is termed the critical micelle concentration (CMC). This concentration is different for each individual detergent. Proteins can be released from membranes by adding (a) detergent(s) at a concentration 5-200 fold greater than its/their CMC (Figure 1.18). Following membrane solubilisation, detergent must be included in all subsequent purification buffers to prevent the extracted proteins from aggregating. For integral membrane proteins, it is essential that the detergent concentration in the buffer solutions is greater than its CMC.

For membrane associated proteins, however, detergent concentrations less than the CMC can be used as only sufficient detergent requires to be added to the buffer to ensure that the hydrophobic patches exposed on the surface of the protein are “covered up”.

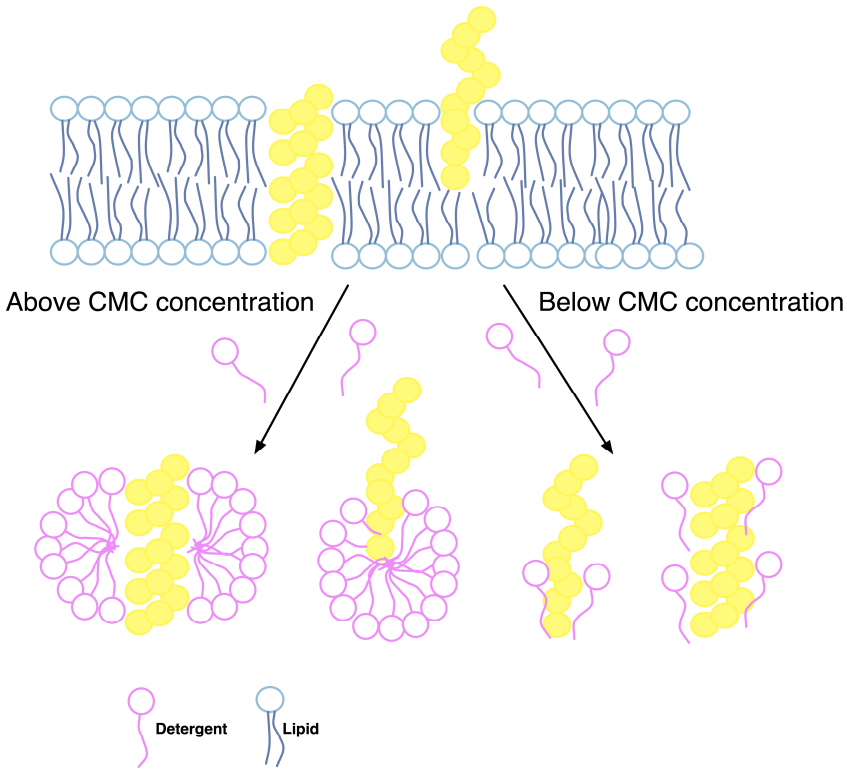

Figure 1.18 Membrane solubilisation
Membrane proteins can be removed from a lipid bilayer using amphipathic molecules termed detergents. The hydrophobic tail of the detergent associates with the parts of the protein buried within the membrane whereas the hydrophilic headgroup interacts with the surrounding aqueous environment. Above the critical micelle concentration (CMC), detergent molecules spontaneously form micelles. For integral membrane proteins, it is essential that the detergent concentration in solution is always greater than its CMC. For membrane associated proteins, however, detergent concentrations less than the CMC can be used as only sufficient detergent requires to be added to the buffer to ensure that the hydrophobic patches exposed on the surface of the protein are "covered up".

When working with membrane proteins, it is essential to identify a detergent that efficiently removes the target protein from the membrane but at the same time maintains it in a stable, active form (Carpenter *et al.*, 2008).

1.9.3 Purification of detergent-solubilised membrane proteins

Following successful expression and solubilisation of a target protein, it must be purified to homogeneity before structural trials can be commenced. Isolation protocols can be developed based on the protein's intrinsic properties. Methods include ion-exchange, where the protein is purified according to its overall net

charge, and size exclusion chromatography, where the protein is purified according to its size. However, the most common approach for purifying membrane proteins is that of affinity chromatography where the target protein is engineered to have an amino acid tag which can be pulled down with high-affinity using a specific resin (Lichty *et al.*, 2005; Waugh, 2005). Immobilised metal affinity chromatography (IMAC) can be used to purify recombinant proteins containing a polyhistidine (usually between 6 and 10 His) affinity tag (Hochuli *et al.*, 1988). The His tag is bound by a transition metal ion (usually Ni^{2+} but also Zn^{2+} and Co^{2+}) immobilised on a matrix (Terpe, 2003). Other commonly used affinity tags include glutathione-S-transferase (GST) and maltose-binding protein (MBP) which allow fusion proteins to be purified by binding to immobilised glutathione and amylose agarose, respectively. Recombinant proteins bound to an affinity resin by either a His, GST or MBP tag can be eluted using imidazole, glutathione or maltose, respectively. In contrast, immunoaffinity tags (such as FLAG and myc) bind irreversibly to antibody-coated resin. Consequently, these tags are primarily used for Western Blotting or pull-down experiments rather than purification purposes.

To simplify both the expression and purification of recombinant membrane proteins, it has become routine practice to fuse a fluorescent reporter to the C-terminus of the target protein (Drew *et al.*, 2001; Newstead *et al.*, 2007). The most commonly used reporter is green fluorescent protein (GFP) from the jellyfish *Aequoria victoria* (Chalfie *et al.*, 1994). GFP acquired its name from the strong green fluorescence it emits upon illumination with visible light. GFP comprises an 11-stranded β-barrel with the chromophore situated in a central α-helix (Figure 1.19) (Ormö *et al.*, 1996; Yang *et al.*, 1996). The chromophore is formed by the autocatalytic cyclisation of the tripeptide Ser65 – Tyr66 - Gly67 (Remington, 2006; Huang *et al.*, 2007; Malo *et al.*, 2007). As formation of the GFP chromophore is oxygen-dependent, GFP can not be used as a fluorescence reporter in anaerobic/hypoxic conditions (Drepper *et al.*, 2007). Remarkably, however, the GFP chromophore remains intact even upon treatment with SDS. This property means that GFP-fusion proteins can be readily visualised on SDS-PAGE following UV-illumination.

Christie and co-workers recently created the novel fluorescence reporter iLOV, derived from the LOV2 domain of phototropin 2 from *Arabidopsis thaliana*. iLOV has increased fluorescence quantum yield and reduced photobleaching compared to the wild-type protein (Chapman *et al.*, 2008). LOV domains non-covalently bind flavin mononucleotide (FMN) in a central cavity through hydrogen bonds and van der Waals interactions (Figure 1.19) (Christie *et al.*, 1998; Crosson and Moffat, 2001; Christie, 2007). LOV domains are yellow when viewed under natural light but emit a strong, green fluorescence when irradiated with UV light. iLOV has several advantages over GFP as a fluorescence reporter in that it is smaller than GFP (10 as compared to 25 kDa) and its fluorescence is not oxygen-dependent.

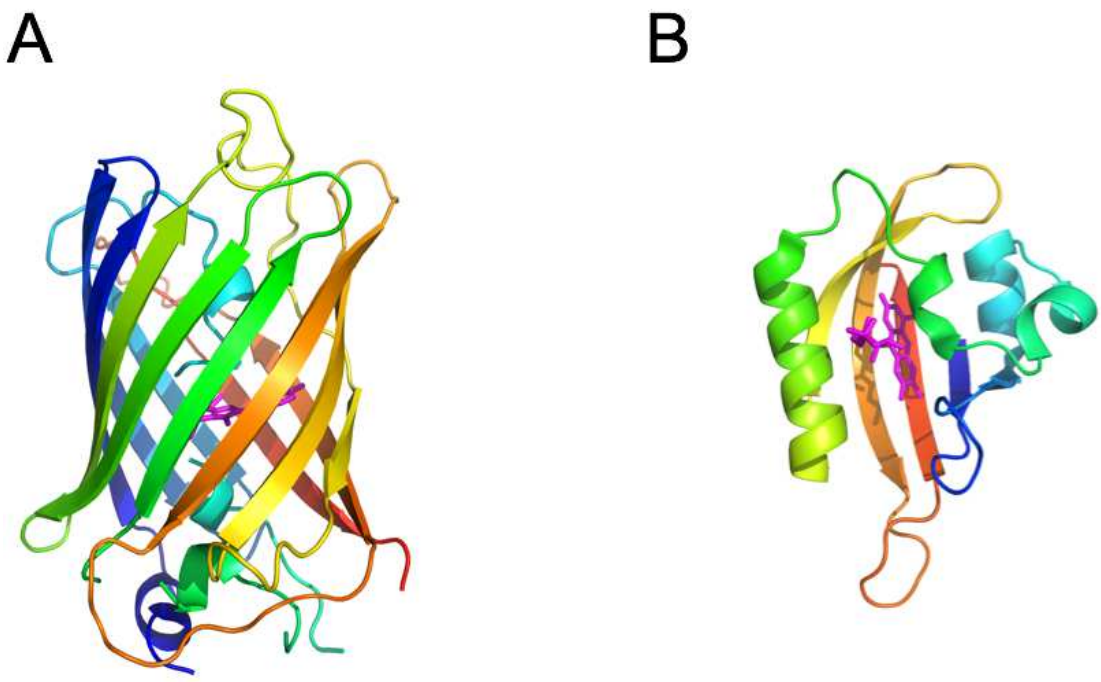

Figure 1.19 The three-dimensional structures of green fluorescent protein and light oxygen voltage domain 2
(A) Green fluorescent protein (GFP) is a commonly used fluorescence reporter with a molecular weight of 25 kDa. GFP comprises an 11-stranded β-barrel with the chromophore situated in a central α-helix. The novel fluorescent reporter improved light oxygen voltage (iLOV) is derived from (B) the light oxygen volage 2 (LOV2) domain of *Arabidopsis thaliana*. iLOV is smaller (10 kDa) than GFP and, in contrast to GFP, chromophore maturation is not oxygen-dependent. The structures of GFP (PDB 1GFL; (Yang *et al.*, 1996) and LOV2 (PDB 1G28; Crosson and Moffat, 2001) are depicted in the “chainbows” colouring scheme. Chromophores are coloured magenta.

1.9.4 Membrane protein stability in detergent solution

To a greater or lesser extent, all detergents are denaturants. Therefore, membrane proteins are often very unstable in detergent solution, giving them a propensity to unfold and aggregate. Human membrane proteins are particularly delicate, considerably more so than those of bacterial origin. Therefore, it is essential when working with human membrane proteins that sufficient time and effort is taken to identify buffers and detergents in which stable, monodisperse protein can be obtained.

1.9.4.1 Assessing membrane protein monodispersity in detergent solution

The aggregation state of a purified membrane protein can be assessed in several different ways including analytical ultracentrifugation (AUC) and size-exclusion chromatography (SEC). When a pure, stable and monodisperse protein is applied to a gel-filtration column the elution profile consists of a single, symmetrical Gaussian peak. Conversely, when a sample containing aggregated protein is applied to the same column the elution profile will contain multiple peaks, one of which will be in the void. Furthermore, the degree of symmetry as well as the broadness of the major elution peak is an useful indicator of the stability of the membrane protein being analysed in the detergent in which it has been purified (Sonoda *et al.*, 2010). However, as all proteins absorb at 280 nm, the target protein must be 100% pure before SEC can be used to evaluate its aggregation status. Moreover, analytical SEC requires milligram quantities of protein to give a measurable absorption with a good signal-to-noise ratio. Therefore, while analytical SEC is an easy-to-use technique for assessing membrane protein monodispersity, it is a time-consuming process that requires considerable resource. A further disadvantage of analytical SEC is that the stability of the target protein in the detergent used for its purification can not be assessed until the purification process has been completed.

To overcome these problems, Gouax and colleagues have developed a technique called fluorescence size exclusion chromatography (FSEC) which allows the aggregation status of a target membrane protein to be assessed even in the presence of other proteins (Kawate and Gouaux, 2006). By attaching a fluorescent tag to a membrane protein of interest, the aggregation status of the

target protein can be assessed at any stage of the solubilisation/purification procedure by applying it to a gel-filtration column and then measuring fluorescence (target-protein specific) rather than A_{280} (all proteins) in the elution fractions. The presence of a single, symmetric fluorescent peak in the elution profile indicates that the target protein is stable. Unlike analytical SEC, FSEC is a quick and efficient method for assessing the aggregation status of membrane proteins in detergent solution that only requires nanogram quantities of material.

1.9.4.2 Direct measurement of membrane protein thermostability

The stability of any protein can be measured in terms of its resistance to denaturation. Proteins that are unstable denature easily whereas stable proteins require harsher conditions (e.g. high temperatures, SDS) before they start to unfold. Protein unfolding can be followed using biophysical techniques such as circular dichroisim (CD) and nuclear-magnetic resonance (NMR). By measuring the changes in a spectroscopic signal from the target membrane protein (e.g. its far-UV CD spectrum) with temperature, a melting temperature (T_m) for the protein can be determined. A protein's T_m is a measure of its thermostability as T_m is defined as the temperature where 50% of the protein has become unfolded. Although melting temperatures can be determined in this way, the biophysical techniques used to follow the unfolding process have low sensitivity, require large quantities of protein and are not easily compatible with screening a range of conditions (e.g. buffers and salts).

To overcome this problem, Ray Stevens and co-workers have developed a sensitive, fluorescence-based (CPM) thermal stability assay that can be used with membrane proteins (Alexandrov *et al.*, 2008). In this assay, the solvent-exposed cysteine residues of the protein of interest are reacted with the thiol-specific fluorochrome N-[4-(7-diethylamino-4-methyl-3-coumarinyl)phenyl] maleimide (CPM) which results in the generation of a fluorescent signal. When a protein becomes denatured in the presence of CPM, as the cysteine residues located in the protein interior become solvent-exposed, there is an increase in CPM fluorescence intensity with time. By altering the assay conditions (e.g. different buffers - types and pH; salts - types and concentrations; addition of

specific ligands) those reagents that confer thermostability on the target protein can be identified. The CPM assay can be adapted for use with 96-well plates allowing numerous conditions to be screened at one time. Furthermore, as each CPM assay only consumes between 1-10 µg of protein considerably less pure protein is required to identify optimal conditions for protein thermostability compared to biophysical techniques such as CD.

1.9.5 Membrane protein crystallisation

Membrane protein crystals suitable for X-ray analysis can be obtained from highly concentrated (>10 mg/ml) solutions of pure protein. When precipitant is mixed with pure protein in a sealed environment, the precipitant drives the formation of nucleation sites. As the protein concentration within the drop increases due to water loss (by way of vapour diffusion to a reservoir containing a higher concentration of the precipitant), these nucleation sites can become protein crystals (Caffrey, 2003). The formation of well-ordered crystals requires slow, regulated crystal growth, and is highly influenced by the protein's concentration and solubility. As the range of possible precipitants is large, the process of identifying which will be best for crystal growth can be particularly time-consuming. However, the development and use of sparse matrix screens for initial crystallisation trials has greatly helped to overcome this rate-limiting step. Crystal hits are then optimised through a series of small variations to the original crystallisation condition with a view to obtaining good quality diffracting crystals (Caffrey, 2003; Kobilka and Schertler, 2008). Depending on the orientation of the individual proteins and the position of their lattice contacts, crystals of varied shape and symmetry can be formed (Nollert, 2005). Obtaining crystals of membrane proteins *in surfo* is considerably harder than that for soluble proteins as the detergent molecules often mask the extra-membranous regions of the protein, preventing the formation of crystal contacts (Mohanty *et al.*, 2003).

To increase the probability of obtaining crystals of a membrane protein in detergent solution, it is common to try and solve the structure of a target protein in complex with a soluble binding partner. The rationale for this approach is that the binding partner increases the polar surface area of the

membrane protein complex, thereby promoting the formation of crystal lattice contacts. For example, co-crystallisation with a F_{ab} fragment has been used to obtain the structures of the mitochondrial cytochrome bc_1 complex (Hunte *et al.*, 2000), a potassium channel (Zhou *et al.*, 2001) as well as the β2 adrenergic receptor (Rasmussen *et al.*, 2007). Using a similar strategy, the structure of the mitochondrial p450 human cholesterol side-chain cleavage enzyme has been obtained in complex with adrenodoxin as an engineered fusion protein (Strushkevich *et al.*, 2011).

1.10 Project context

In recent years, four of the six p450 enzymes involved in human steroid biosynthesis have had their structures solved (Ghosh *et al.*, 2009; Mast *et al.*, 2011; Strushkevich *et al.*, 2011; DeVore and Scott, 2012; Zhao *et al.*, 2012). As yet, however, there is no structural information available for either aldosterone synthase or 11β-Hydroxylase. As these two enzymes have 93% primary sequence identity, it has not yet been possible to design fully selective inhibitors of either aldosterone synthase or 11β-Hydroxylase. Detailed three-dimensional structures of both enzymes will facilitate the development of specific small molecule inhibitors of aldosterone synthase for the treatment of hypertension.

1.11 Aim

The main aim of my Ph.D. was to overexpress and purify aldosterone synthase and 11β-Hydroxylase as well as their associated electron transfer proteins, adrenodoxin and adrenodoxin reductase, for structural studies.

1.12 Objectives

i) develop a generic system for making, purifying and immobilising human proteins

ii) clone, express and purify adrenodoxin and adrenodoxin reductase

iii) clone, express and purify aldosterone synthase and 11β-Hydroxylase

iv) biophysically characterise pure adrenodoxin, adrenodoxin reductase, aldosterone synthase and 11β-Hydroxylase

Chapter 2 – Methods and Materials

2.1 Strains

Plasmids were maintained and propagated in *E. coli* strain DH5α (Invitrogen). All protein production in *E. coli* was performed in either BL21 (DE3) (Novagen) or C43 (DE3) (Lucigen) cells. Recombinant protein production in *P. pastoris* was performed in strain X33 (Invitrogen).

2.2 Media

E. coli was routinely grown on either Luria-Bertani (LB) (1% tryptone, 0.5% yeast extract and 1% NaCl) or Low-Salt LB (LS-LB) (1% tryptone, 0.5% yeast extract and 0.5% NaCl) media according to the antibiotic being used for selection. Bacteria containing ampicillin-resistant plasmids were grown on LB ([ampicillin] = 100 μg/ml), zeocin-resistant ones on LS-LB ([zeocin] = 25 μg/ml). Production of biotin ligase and 3C protease in *E. coli* was accomplished in LB media. Recombinant expression of Adx, AdxRed, aldosterone synthase and 11β-Hydroxylase was performed in Terrific Broth (TB) (1.2% tryptone, 2.4% yeast extract, 4% glycerol, 17 mM KH_2PO_4 and 72 mM K_2HPO_4).

P. pastoris was routinely cultured in YPD medium (1% yeast extract, 2% peptone and 2% glucose). For small-scale expression experiments, the yeast transformants were grown on Buffered-complex Glycerol (BMGY) medium (1% yeast extract, 2% peptone, 100 mM potassium phosphate, 1.34% yeast nitrogen base, $4x10^{-5}$% biotin and 1% glycerol, pH 6.0), and then induced using Buffered-complex Methanol (BMMY) medium (the same as BMGY except that it contains 0.5% methanol instead of 1% glycerol).

2.3 Expression plasmid construction

2.3.1 Sub-cloning strategies

Standard DNA manipulation techniques were used to construct the plasmids for recombinant protein expression (Sambrook *et al.*, 1989).

2.3.1.1 Polymerase chain reaction

DNA oligonucleotide primers were synthesised by Sigma Genosys (UK) or Eurofins MWG Operon (Germany). Primers were resuspended in sterile, distilled H_20 to a final concentration of 50 pmol/μl and stored at -20°C. All primers had at least 21 bases complimentary to the template DNA with a GC content of *ca.* 40%.

All polymerase chain reaction (PCR) amplifications were performed using KOD HotStart DNA polymerase (Merck Biosciences) using appropriate template and primer combinations. A typical PCR reaction consisted of an initial 2 min Polymerase activation step at 98°C followed by between 25-35 cycles, each consisting of a DNA denaturation step (98°C, 20 s), primer annealing (55°C, 10 s) and DNA extension (70°C, 20 s per Kb of DNA being amplified). After the last cycle, the PCR cocktail was incubated at 70°C for a further 10 min to ensure that all *de novo* DNA synthesis had been completed.

2.3.1.2 Agarose gel electrophoresis and gel-extraction

Following PCR amplification or restriction digestion, DNA fragments were resolved by electrophoresis through a 1% agarose gel in Tris-Acetate EDTA (TAE) buffer (1 mM EDTA in 40 mM Tris-Acetate pH 8.0). A 1kb DNA ladder (Promega) was used to estimate DNA fragment size. DNA was visualised using SYBR Safe DNA gel stain (Invitrogen). DNA fragments were extracted by cutting the band of interest out with a sterile blade, and then purified using a QIAGEN gel extraction kit according to the manufacturer's instructions.

2.3.1.3 Plasmid DNA purification

Plasmid DNA was isolated from small (5 ml) and large (100 ml) bacterial cultures using the QIAprep Spin MiniPrep and Maxi kits (both QIAGEN), respectively, according to the manufacturer's instructions. Plasmid DNA concentrations were determined using a NanoDrop 1000 (ThermoScientific).

2.3.1.4 Restriction digestion

Restriction enzymes were purchased from Roche Applied Science, Promega and New England Biolabs. Plasmid DNA was digested in the appropriate buffer according to the manufacturer's instructions.

2.3.1.5 DNA ligation

Unless stated otherwise, all DNA ligations were carried out using T4 DNA ligase (New England Biolabs) according to the manufacturer's instructions.

2.3.1.6 DNA sequencing

Recombinant plasmids were sequenced at the DNA Sequencing and Services Unit in the College of Life Sciences, University of Dundee using an Applied Biosystems model 3730 automated capillary DNA sequencer.

2.3.2 PCR amplification of human adrenodoxin, adrenodoxin reductase, aldosterone synthase and 11β-Hydroxylase

cDNAs encoding human Adx, AdxRed, aldosterone synthase and 11β-Hydroxylase were provided by Dr. Gordon Inglis (University of Glasgow).

A modified human Adx cDNA lacking the mitochondrial leader sequence was created by PCR using the primers GAATTCATGAGCAGCTCAGAAGATAAAATAACAG and GCGGCCGCTGGAGGTCTTGCCCACATCAATG that contained restriction sites (coloured red) for *Eco*RI and *Not*I, respectively. Similarly, a cDNA for human AdxRed without the mitochondrial leader sequence was generated using the primers GAATTCATGTCCACACAGGAGAAGACCCCCCAG and GCGGCCGCTGTGGCCC AGGAGGCGCAGCATCTC.

Modified human 11β-Hydroxylase and aldosterone synthase cDNAs were created by PCR amplification using a common forward primer CTTAATGAATTCATGGCCAC GAAGGCCGCCCGGG with different reverse primers (11β-Hydroxylase: CAGATTTT CAGCGGCCGCGTTGATGGCTCTGAAGGTGAGGAG; aldosterone synthase: CAGATTT TCAGCGGCCGCGTTAATCGCTCTGAAAGTGAGGAG). The sequence of the forward primer encoded the protein sequence MATKAAR instead of the mitochondrial targeting sequences found in the full-length proteins. The forward and reverse primers contained restriction sites for *Eco*RI and *Not*I, respectively.

The PCR fragments were cloned first into pGEM T-Easy (as described in Section 2.3.4) and then later transferred to either a yeast (Section 2.3.5) or bacterial expression vector (Section 2.3.6 and 2.3.7).

2.3.3 PCR amplification of the CLBH tag

The CLBH tag was amplified by PCR using primers GCGGCCGCTGTCCTATTCCAGG GCCCAACTAGTATAGAGAAGAATTTCGTC and GGATCCTCAGTGATGGTGATGGTGAT GGTGATGGTGATGCCCGAT using the pPICZA-SI-CLBH vector as template. The forward and reverse primers contained *Not*I and *Bam*HI restriction sites, respectively, for eventual cloning of the CLBH tag into pET21a. First, however, the PCR product was introduced into pGEM T-Easy (Section 2.3.4).

2.3.4 Cloning PCR products into pGEM T-Easy

PCR products were generated as described in Section 2.3.1.1, and then resolved on a 1% (w/v) agarose gel according to Section 2.3.1.2. The gel-purified PCR fragments were A-tailed by incubating the DNA fragment with Taq DNA polymerase (New England Biolabs) and 1 mM dATP at 70°C for 30 min. A-tailed PCR products were ligated into pGEM T-Easy (Promega) according to the manufacturer's instructions. The ligation mixture was transformed into competent DH5α cells by heat shock (Section 2.4.1.2). Transformed cells were plated onto LB-agar plates containing 100 μg/ml ampicillin (Sigma-Aldrich) and 100 μg/ml 5-bromo-4-chloro-3-indolyl-β-D galactopyranoside (X-gal) (Roche Applied Science), and then incubated for 16 h at 37°C. Colonies containing

recombinant plasmid were white whereas those that contained vector without an insert were blue.

Several putative white colonies for each pGEM construct were grown up in 5 ml of LB containing 100 μg/ml ampicillin overnight at 37°C in a shaking incubator. Plasmid DNA was isolated from cultures according to Section 2.3.1.3. Correct recombinant plasmids were identified first by restriction digestion (Section 2.3.1.4) and then by DNA sequencing (Section 2.3.1.6).

2.3.5 Sub-cloning cDNAs for adrenodoxin reductase, aldosterone synthase and 11β-Hydroxylase into the pPICZA-CLBH vector

The cDNAs for AdxRed, aldosterone synthase and 11β-Hydroxylase were released from pGEM T-Easy by digestion with *Eco*RI and *Not*I. Digests were resolved on an agarose gel. The cDNAs were purified by gel extraction (Section 2.3.1.2) and ligated to pPICZA-CLBH vector (which had also been digested with *Eco*RI and *Not*I). The ligation mixture was transformed into DH5α cells according to Section 2.4.1.2. Recombinant plasmids were identified first by restriction digestion (Section 2.3.1.4) and then DNA sequencing (Section 2.3.1.6). Later, the recombinant plasmids were transformed into *P. pastoris* strain X33 by electroporation (Section 2.4.2.2).

2.3.6 Engineering the pET21a-Adx(Red)-CLBH constructs

The cDNAs encoding Adx and AdxRed were released from pGEM T-Easy by digestion with *Nde*I (which cleaved a sequence located within the vector's multi-cloning site) and *Not*I. The –CLBH cDNA was released from pGEM T-Easy by digestion with *Not*I and *Bam*HI. The cDNAs were purified by gel extraction (Section 2.3.1.2). The –CLBH cDNA was ligated individually to the Adx and AdxRed cDNAs. Subsequently, the Adx-CLBH and AdxRed-CLBH fragments were cloned into pET21a (which had been previously digested with *Nde*I and *Bam*HI). The ligation mixture was transformed into *E. coli* strain DH5α (Section 2.4.1.2). Recombinant plasmids were identified by restriction digestion.

Later, pET21a-Adx-CLBH was transformed into the *E. coli* expression strain BL21(DE3). pET21a-AdxRed-CLBH was transformed into BL21(DE3) cells that contained the pGro7 plasmid (TaKaRa Bio). Glycerol stocks were prepared, snap-frozen with liquid nitrogen and stored at -80°C.

2.3.7 Assembling the pET21a - CYP11B1/B2 - CLBH constructs

The cDNAs encoding aldosterone synthase and 11β-Hydroxylase were excised from pGEM T-Easy using *Nde*I and *Not*I, and then purified according to Section 2.3.1.2. The enzyme cDNAs were ligated to the CLBH cDNA (which had been digested with *Not*I and *Bam*HI). CYP11B1- and CYP11B2-CLBH DNA fragments were ligated with pET21a (which had been digested with *Nde*I and *Bam*HI), and then transformed into *E. coli* strain DH5α (Section 2.4.1.2). Recombinant plasmids were identified by restriction digest (Section 2.3.1.4).

Later, the pET21a - CYP11B1/B2 - CLBH plasmids were transformed into *E. coli* expression strains BL21(DE3) and C43(DE3), in which the chaperone plasmid pGro7 (TaKaRa Bio) had been previously introduced. Glycerol stocks were prepared, snap-frozen with liquid nitrogen and stored at -80°C.

2.3.8 Making pET21a - CYP11B1/B2 - His6 expression constructs

Aldosterone synthase/11β-Hydroxylase cDNAs were released from pGEM T-Easy by digestion with *Nde*I and *Not*I. The DNA fragments were purified by gel extraction and then ligated to pET21a, which had been digested with *Nde*I and *Not*I also. Recombinant plasmids were identified by restriction digestion (Section 2.3.1.4), and then transformed into the *E. coli* expression strain C43(DE3), in which the pGro7 plasmid (TaKaRa Bio) had already been introduced. Glycerol stocks were prepared, snap-frozen with liquid nitrogen and stored at -80°C.

2.3.9 Constructing a pET15b-BirA expression plasmid

The biotin ligase (BirA) gene was amplified from *E. coli* 0157 genomic DNA (a gift from Dr. Mads Gabrielsen, University of Glasgow) by PCR using the primers TGAC CACATATGATGAAGGATAACACCGTGCCACTG and CGTAGAGGATCCTTATTTTTCTGC ACTACGCAGGGA. The forward and reverse primers contained *Nde*I and *Bam*HI

restriction sites, respectively, which were eventually used for cloning the BirA cDNA into pET15b. First, however, the PCR product was introduced into pGEM T-Easy according to Section 2.3.4. Recombinant plasmids were identified by restriction digestion (Section 2.3.1.4), and then sequenced (Section 2.3.1.6) to ensure that no mutations had been introduced during the PCR step. The BirA cDNA was sub-cloned into pET15b (Novagen Biosciences) between the *Nde*I and *Bam*HI restriction sites.

pET15b-BirA was transformed into *E. coli* strain BL21(DE3) for expression and purification purposes. Glycerol stocks were made and stored at -80°C.

2.4 DNA transformation

2.4.1 Transforming plasmid DNA into bacteria

2.4.1.1 Preparation of competent cells

DH5α cells used for cloning were purchased from Invitrogen. *E. coli* expression strain BL21(DE3) was purchased from Novagen Biosciences. C43(DE3) cells were a gift from Dr. Frank Kroner (University of Glasgow).

BL21(DE3) and C43(DE3) cells that had been transformed with the pGro7 plasmid (which encodes the molecular chaperones GroEL/ES) had to be made competent before any of the pET expression constructs could be introduced. The *E. coli* strain to be made competent was grown in 5 ml of Psi broth (0.5% yeast extract, 2% tryptone, 0.5% magnesium sulphate) overnight at 37°C in a shaking incubator.

The next morning, 1 ml of the starter culture was used to inoculate a further 500 ml of Psi broth in a 2000 ml unbaffled Erlenmeyer flask. The cells were grown to an optical density at 600 nm (OD_{600}) of 0.6, before they were incubated on ice for 15 min and harvested by centrifugation (4000g, 5 min, 4°C). Pelleted cells were resuspended in 400 ml of TfbI (30 mM potassium acetate, 100 mM rubidium chloride, 10 mM calcium chloride, 50 mM manganese chloride, 15% (v/v) glycerol, pH 5.8) and incubated on ice for 15 min. The cells were centrifuged again (4,000g, 5 min, 4°C), and the pellet resuspended in 40 ml of TfbII (75 mM calcium chloride, 15% (v/v) glycerol, 10 mM MOPS pH 6.5). The

cells, now competent, were split into aliquots, flash-frozen in liquid nitrogen and stored at -80°C.

2.4.1.2 Transformation of expression plasmids into *E. coli*

Plasmids were transformed into *E. coli* according to the method of Hanahan (1983). In short, 50 ng of DNA was mixed gently with 50 μl of competent *E. coli* cells, and the mixture incubated on ice for 15 min. The cells were subjected to heat-shock (42°C, 1 min), and then placed back on ice for a further 2 min. To allow the bacteria to recover, 450 μl of LB was added to the cells. The transformation mixture was then shaken at 37°C for 45 min before a 200 μl aliquot was spread on an (LS)-LB-agar plate containing the appropriate antibiotic(s) (100 μg/ml ampicillin, 20 μg/ml chloramphenicol, 25 μg/ml zeocin). [The pGEM T-Easy and pET expression vectors confer ampicillin resistance, pPICZA vector zeocin-resistance, and pGro7 chloramphenicol resistance]. Plates were incubated for 16 h at 37°C to allow selection of cells containing plasmid.

2.4.2 Transformation of expression plasmids into *P. pastoris*

2.4.2.1 Preparation of electrocompetent cells

5 ml of YPD broth was inoculated with *P. pastoris* strain X33 and grown for 16 h at 30°C in a shaking incubator. 500 μl of the overnight culture was used to inoculate 100 ml of YPD medium in a 500 ml flask, which was then shaken at 30°C for a further 16 h. Once the cells had reached an OD_{600} of between 1.3-1.5, they were harvested by centrifugation (1500g, 5 min, 4°C). The pellet was resuspended in 500 ml of sterile, ice-cold dH_20, before the cells were centrifuged again (1500g, 5 min, 4°C). This process was repeated a further three times, resuspending the cells first in 50 ml of ice-cold dH_20, then 4 ml and eventually 300 μl of ice-cold 1 M sorbitol. The cells were now competent, and used immediately for transformation.

2.4.2.2 Electroporation

10-50 μg of recombinant plasmid DNA in a volume of 20 μl was linearised by overnight digestion with *Pme*I, and then gently mixed gently with 80 μl of

competent X33 cells. The transformation mixture was incubated in a sterile 0.2 cm electroporation cuvette on ice for 5 min, and then pulsed (2 Kv, 5 ms) using an electroporator. 1 ml of 1 M sorbitol was added immediately to the yeast cells, which were then allowed to recover at 30°C for 2 h. The transformation mixture was then spread on a series of YPD plates containing 1M sorbitol and increasing concentrations of zeocin ranging from 0.2 to 2.0 mg/ml. The plates were incubated for 72 h. Colonies were re-streaked onto fresh YPD plates containing 0.5 mg/ml zeocin, and incubated for a further 24-72 h at 30°C. Colonies were then screened to identify the clone expressing the highest levels of recombinant protein (Section 2.5.1).

2.5 Protein expression in *P. pastoris*

2.5.1 1 ml cultures in 48-well plates

Yeast cells that had been transformed with a CLBH-tagged expression plasmid were screened to identify the clone which made the highest levels of recombinant protein by measuring whole cell iLOV fluorescence. Transformants were grown and induced on a 1 ml scale in a 48-well sterile plate. For each transformant, two 1 ml cultures were established in BMGY. Following inoculation, the deep-well blocks were shaken for 24 h at 30°C. The cells were pelleted by centrifugation (1,500g, 5 min, 4°C), and then resuspended in 1 ml of BMMY medium, to induce protein expression. The plate was returned to the shaking incubator for another 24 h but this time at 22°C. Cells were harvested by centrifugation as before, washed twice with and then resuspended in 1 ml of dH_20. Whole cell iLOV fluorescence levels were measured for each culture in a black 96-well plate (Corning) using a BMG LabTech Fluostar optima ($\lambda_{excitation}$ = 450 nm, $\lambda_{emission}$ = 520 nm). Glycerol stocks were prepared for the transformant found to have the highest expression level of the recombinant protein by mixing equal volumes of an overnight culture grown in YPD with 50% (v/v) glycerol in a sterile cryovial. The cultures were snap-frozen using liquid nitrogen and stored at -80°C.

2.5.2 Recombinant protein expression in fermenter culture

Large scale production of SI-, AdxRed- and CYP11B2-CLBH in *P. pastoris* was carried out using an Applikon 7L bioreactor and ADI 1025 bioreactor system. Dissolved oxygen (dO_2) was maintained above 25% using a combination of agitation (minimum 1000 rpm) and compressed air (0.8 litre min^{-1}). Oxygen (1 bar pressure) was automatically drawn in as required to maintain the dO_2 setpoint during growth at high cell densities. The culture was maintained at pH 5.0 through addition of 23% NH_4OH. 10% Antifoam A (Sigma-Aldrich) was added drop-wise when necessary to reduce foaming during culture growth.

4 litres of basal salts media (Table 2.1) was autoclaved within the bioreactor, and then 15 ml of PTM1 trace salts (Table 2.1) was added. The medium was inoculated with *ca.* 200 ml of yeast that had been grown up overnight in YPD so that the initial fermenter culture had an OD_{600} of 0.5-1.0. The yeast cells were grown in basal salts media for 18 h at 30°C. Following this, the culture was fed 50% glycerol (v/v) for 11 h at a rate of 1.09 ml/min. The yeasts were then starved for 1 h to ensure that all of the glycerol had been consumed before the culture was adapted for growth on methanol (4 h at 0.07 ml/min followed by 12 h at 0.09 ml/min). At this stage, the temperature of the culture was reduced to 22°C for recombinant protein production. Methanol feeding was continued for 12 h at 0.13 ml/min followed by 0.33 ml/min for another 36 h. Samples were taken at regular intervals to assess culture growth by measuring the wet cell weight per ml of culture. Recombinant protein expression levels were determined by measuring whole-cell iLOV fluorescence. Fermentations were stopped after 96 h, and the cells harvested by centrifugation (4,000g, 20 min, 4°C). Cell pellets were stored at -20°C, and used as they were required.

Table 2.1 Recipes for fermentation media and trace feed solution

4 litres of basal salts media was prepared and autoclaved immediately prior to beginning a fermentation. PTM_1 trace salt solution was prepared in advance, stored in 50 ml aliquots at 4°C and used as it was required.

	Components	Amount per litre
Basal salts medium	Phosphoric Acid (85%)	(26.7 ml)
	Calcium Sulphate	0.93 g
	Potassium Sulphate	18.2 g
	Magnesium Sulphate – $7H_20$	14.9 g
	Potassium Hydroxide	4.13 g
	Glycerol	40.0 g
	Water	to 1 litre
		Sterilised by autoclaving
PTM_1 trace salts	Cupric Sulphate - $5H_2O$	6.0 g
	Sodium Iodide	0.08 g
	Magnesium Sulphate - H_2O	3.0 g
	Sodium Molybdate - $2H_2O$	0.2 g
	Boric Acid	0.02 g
	Cobalt Chloride	0.5 g
	Zinc Chloride	20.0 g
	Ferrous Sulphate – $7H_2O$	65.0 g
	Biotin	0.2 g
	Sulphuric Acid	5.0 ml
	Water	to 1 litre
		Sterilised by filtration

2.6 Recombinant protein production in *E. coli*

2.6.1 Medium-scale (500 ml) expression cultures

2.6.1.1 Adrenodoxin production

BL21 cells containing the Adx-CLBH expression plasmid were grown up overnight from a glycerol stock (Section 2.3.6) in 5 ml of TB containing 100 μg/ml ampicillin at 37°C in a shaking incubator with shaking at 190 rpm. The next day, 1 ml of the starter culture was used to inoculate 500 ml of TB supplemented with 100 μg/ml ampicillin in a 2000 ml non-baffled Erlenmeyer flask. The culture was replaced in the shaking incubator at 37°C at a setting of 190 rpm. Cell growth was monitored at regular intervals by measuring the OD_{600} of the culture. At an OD_{600} of 0.6, Adx-CLBH expression was induced by adding 1 mM IPTG. The culture was shaken for a further 16 h at a temperature of 22°C before the cells were harvested by centrifugation (4,000g, 20 min, 4°C). Pellets were stored at -20°C, and used as required.

2.6.1.2 Production of adrenodoxin reductase, aldosterone synthase and 11β-Hydroxylase

AdxRed-CLBH (Section 2.3.6), CYP11B1/B2-CLBH (Section 2.3.7) and CYP11B1/B2-His_6 (Section 2.3.8) constructs were made in *E. coli* in the same way as for Adx-CLBH with the following exceptions. The cultures all contained 20 μg/ml chloramphenicol (to select for pGro7) as well as 100 μg/ml ampicillin (to select for the pET expression vector). 11β-Hydroxylase and aldosterone synthase expression was induced by adding 0.5 mM IPTG as well as 4 mg/ml arabinose (which switched on production of the GroEL/ES chaperones from the pGro7 plasmid). 1 mM δ-Aminolevulinic acid was also added to the media along with the chemical inducers to ensure that the bacteria had an abundance of haem to incorporate into the recombinant p450 enzymes. AdxRed expression was induced by adding 1 mM IPTG and 1 mg/ml arabinose. Aldosterone synthase/11β-Hydroxylase production was performed at a temperature of 27°C whereas AdxRed was expressed at 20°C. All cultures were induced for 16 h overnight.

2.6.1.3 Expression of human rhinovirus 3C protease and biotin ligase

The accessory proteins HRV 3C protease and biotin ligase were expressed in *E. coli* using the same protocol as that for Adx (Section 2.6.1.1) with the exception that LB was used for cell growth rather than TB.

2.6.2 Large-scale (15 litre) expression cultures

Large scale expression of adrenodoxin, adrenodoxin reductase, aldosterone synthase and 11β-Hydroxylase in *E. coli* was carried out using an Applikon 20l bioreactor and ADI 1025 bioreactor system. Dissolved oxygen (dO_2) was maintained above 30% using a combination of agitation (minimum 1000 rpm) and compressed air (0.8 litre min^{-1}). The culture was maintained at pH 7.0 through drop-wise addition of either 5 M NaOH or 100% HCl. Samples were withdrawn at regular intervals to monitor cell growth. Induction was carried out in the same way detailed for the shake-flask cultures (Sections 2.6.1.1 and 2.6.1.2).

2.7 Isolating membranes

Following expression of SI-CLBH in *P. pastoris* and CYP11B2-CLBH in *E. coli*, membranes containing the recombinant proteins were prepared as follows. Cell pellets were resuspended in Breaking Buffer (5 mM EDTA, 150 mM NaCl in 50 mM Tris HCl pH 7.4) and lysed by passing through a Constant Systems cell disrupter three times at a pressure of 20 kPsi for *E. coli* or 30 kPsi for *P. pastoris*. Following this, 10% glycerol (v/v) and protease inhibitors (phenylmethanesulphonylfluoride (PMSF) and benzamidine) were added to the cell lysate. A low speed spin (10,000g, 15 min, 4°C) was used to pellet cell debris and unbroken cells. The supernatant was retained and centrifuged at high speed (150,000g, 30 min, 4°C) to pellet the membranes. Membranes containing SI-CLBH were resuspended in 150 mM NaCl, 10% glycerol in 50 mM sodium phosphate pH 7.4 whereas those containing B2-CLBH were resuspended in 150 mM NaCl, 20% glycerol in 50 mM potassium phosphate pH 7.4. The protein concentration of the membrane samples was determined by BCA assay (Pierce) using BSA as a standard (Section 2.8.5). Membranes were diluted with the appropriate buffer to a final concentration of 20 mg/ml, and then stored at -20°C in 50 ml aliquots.

2.8 Protein purification

2.8.1 Purification of sterol isomerase

P. pastoris cell pellets containing SI-CLBH were resuspended in SI Buffer A (150 mM NaCl, 5 mM EDTA in 50 mM sodium phosphate pH 7.4). Cells were broken using a Constant Systems cell disrupter (Section 2.7). 1 mM PMSF, 1 mM benzamidine and 10% glycerol were added following cell lysis. Membranes were isolated (as described in Section 2.7), and resuspended in SI Buffer B (150 mM NaCl, 0.1 mM EDTA, 10% glycerol in 50 mM sodium phosphate pH 7.4) to a final concentration of 20 mg/ml. DM was added to the membranes from a 10% (w/v) stock solution to a final detergent concentration of 2.5%. The solubilisation mixture was stirred for 1 h. Unsolubilised material was removed by centrifugation (150,000g, 30 min, 4°C). The supernatant, containing solubilised SI-CLBH, was batch-loaded onto a 5 ml His-trap Ni^{2+} column (GE Healthcare) pre-equilibrated in SI Buffer B containing 0.15% DM. Following binding, the column was washed with 50 ml of SI Buffer C (500 mM NaCl, 75 mM imidazole, 0.1 mM EDTA, 10% glycerol in 50 mM sodium phosphate pH 7.4, 0.15% DM). SI-CLBH was eluted using SI Buffer D (150 mM NaCl, 300 mM imidazole, 0.1 mM EDTA, 10% glycerol in 50 mM sodium phosphate pH 7.4, 0.15% DM). Fluorescent fractions were pooled and desalted into SI Buffer B containing 0.15% DM using a PD-10 column (GE Healthcare) according to the manufacturer's instructions. The sample was incubated overnight at 4°C with 20 μg/ml 3C protease and 1 mM DTT. The cleaved sample was applied to a fresh Ni^{2+} column equilibrated in SI Buffer B containing 0.15% DM. The flow-through containing SI was retained and concentrated to a final volume of 1 ml using a 50 kDa MWCO centricon (Sartorious). Concentrated SI was applied to a Superose 6 gel filtration column, pre-equilibrated in SI Buffer B containing 0.15% DM. An ÄKTA prime plus system (GE Healthcare) was used to run the Superose 6 gel filtration column at a flow-rate of 0.3 ml/min, collecting 1 ml fractions. All purification steps were carried out at 4°C. The concentration of pure SI was determined using the extinction coefficient $\varepsilon 280 = 74160\ M^{-1}\ cm^{-1}$.

2.8.2 Purification of adrenodoxin

E. coli cell pellets containing Adx-CLBH were resuspended in Adx Buffer A (150mM NaCl, 0.1 mM EDTA in 50 mM Tris-HCl pH 7.4), and lysed using a Constant Systems cell disruptor (3x 20 kPsi). Following mechanical breakage, 1 mM PMSF, 1 mM benzamidine and 1x complete protease inhibitor tablet (Roche Applied Science) was added to the cell lysate to prevent proteolysis of the recombinant protein. Cell debris was removed by centrifugation (10,000g, 15 min, 4°C). The supernatant fraction containing Adx-CLBH was applied to a 5 ml HisTrap Ni^{2+} column (GE Healthcare) equilibrated with Adx Buffer B (50 mM imidazole, 300 mM NaCl, 0.1 mM EDTA in 50 mM Tris-HCl pH 7.4). Following binding, the column was washed with ten column volumes of Adx Buffer B. Adx-CLBH was eluted using Adx Buffer C (300 mM imidazole, 0.1 mM EDTA in 50 mM Tris-HCl pH 7.4), and then desalted into Adx cleavage buffer (1 mM DTT, 0.1 mM EDTA, 150 mM NaCl in 50 mM Tris-HCl pH 7.4). 20 μg of pure 3C protease per ml of sample was incubated with enriched Adx-CLBH overnight to ensure complete tag removal. Next morning, the cleavage mixture was passed over a fresh Ni^{2+} column equilibrated in Adx Buffer A. Brown-coloured fractions containing Adx were collected, pooled and concentrated using a 10 kDa MWCO centricon (Sartorious) to a volume of *ca.* 500 μl. Concentrated Adx was applied to a Superose 6 gel filtration column for a final, polishing purification step. The column was run at a flow-rate of 0.3 ml/min and 1 ml fractions were collected. Fractions containing pure Adx were identified using a Shimadzu UV-1700 Pharmaspec spectrophotometer, and pooled together. The concentration of the purified sample was determined using an extinction coefficient calculated from the primary sequence of the recombinant protein; Adx ε_{280} = 3230 $M^{-1}cm^{-1}$. All purification steps were carried out at 4°C.

Thermostability assays were performed on pure Adx (Section 4.6.2). Once optimal conditions had been identified, the purification buffers were modified to contain sodium phosphate instead of Tris-HCl. Furthermore, to optimise stability, NaCl was removed from the final gel filtration buffer.

2.8.3 Purification of adrenodoxin reductase

AdxRed was initially purified in the same way as that for Adx (Section 2.8.2). Following CPM thermostability analysis (Section 4.6.3) Tris-HCl was replaced in all buffers with HEPES. Moreover, a 50 kDa MWCO centricon (Satorious) was used to concentrate the reverse-purified AdxRed before application to the Superose 6 gel filtration column. The concentration of AdxRed was determined using a calculated extinction coefficient of ε_{280}= 4296 $M^{-1}cm^{-1}$.

2.8.4 Attempted nickel-affinity purification of CYP11B2-CLBH

E. coli cell pellets containing CYP11B2-CLBH were resuspended in B2 Buffer A (150 mM NaCl, 5 mM EDTA in 50 mM potassium phosphate pH 7.4). Membranes were isolated (Section 2.7) and resuspended in B2 Buffer B (150 mM NaCl, 20% glycerol, 0.1 mM EDTA in 50 mM potassium phosphate pH 7.4) to a final concentration of 20 mg/ml. Sodium cholate was added to the membranes to a final concentration of 2.5%, and the solution stirred with 1 mM PMSF for 1 h at 4°C. Insoluble material was removed by centrifugation (150,000g, 30 min, 4°C), and the supernatant retained for further purification. Solubilised CYP11B2-CLBH was passed over a 5 ml HisTrap nickel column (GE Healthcare) three times that had been equilibrated in B2 Buffer B containing 0.6% sodium cholate. The column was washed with B2 buffer C (300 mM NaCl, 20% glycerol (v/v), 0.1 mM EDTA, 0.6% sodium cholate in 50 mM potassium phosphate pH 7.4) containing increasing concentrations (25, 50, 75 and 300 mM) imidazole. The aldosterone synthase content of the wash fractions was determined by ELISA according to Section 2.11.2.

Purification of CYP11B2-CLBH in DM was attempted also with the 0.6% sodium cholate in B2 Buffers C and D replaced with 0.15% DM. The 300 mM imidazole elution fraction was desalted into B2 buffer B containing 0.15% DM, and incubated overnight with 20 μg HRV 3C protease per ml of protein. The iLOV fluorescence of Ni^{2+}-enriched CYP11B2-CLBH before and after cleavage was measured using a FLUOstar Optima plate reader (Section 2.10.2).

2.8.5 Purification of aldosterone synthase and 11β-Hydroxylase

E. coli cell pellets containing CYP11B2-His_6 were resuspended in p450 Buffer A (500 mM sodium chloride, 20% (v/v) glycerol, 0.25 mM EDTA in 50 mM potassium phosphate pH 7.4). Cells were homogenised, incubated with lysozyme for 30 min on ice before 1.5% sodium cholate and 1% Tween-20 were added. The cells were ruptured by sonication using a SONIPREP 150 (Sanyo) with three pulses of 15 s duration followed by three that were 8 s in length, all at a power setting of 10 μA. There was an interval of 1 min between pulses. The cell slurry was then centrifuged (90,000g, 15 min, 4°C). The supernatant was retained and mixed with Ni^{2+}-sepharose beads (GE Healthcare) that had been equilibrated in p450 Buffer A for 1 h at 4°C. After loading, the beads were poured into a gravity-feed, disposable column (Clontech) and washed with 10 column volumes of p450 Buffer B (20 mM imidazole, 500 mM NaCl, 20% glycerol, 0.25 mM EDTA, 0.1 mM PMSF and 0.1 mM ATP in 50 mM potassium phosphate pH 7.4, 1% sodium cholate, 1% Tween-20). B2-His_6 was eluted from the beads using p450 Buffer C (200 mM imidazole, 20% glycerol, 0.25 mM EDTA and 0.1 mM PMSF in 50 mM potassium phosphate pH 7.4, 1% sodium cholate, 1% Tween-20). Red fractions containing aldosterone synthase were collected, pooled, diluted 5-fold with p450 Buffer D (20% glycerol, 0.25 mM EDTA and 1% sodium cholate), and then applied to a SP sepharose ion-exchange column (GE Healthcare) using a peristaltic pump. Aldosterone synthase was eluted using an ÄKTA prime plus purification system with a 0-400 mM gradient of sodium acetate in p450 buffer E (50 mM potassium phosphate pH 7.4, 20% glycerol, 1% sodium cholate). Fractions containing aldosterone synthase were pooled and concentrated to a final volume of 500 μl using a 30 kDa MWCO concentrator (Sartorious). The protein sample was then applied to a Superose 6 gel filtration column pre-equilibrated in p450 buffer F (10 mM sodium chloride, 20% glycerol in 50 mM potassium phosphate pH 7.4, 1% sodium cholate). Those fractions containing pure aldosterone synthase were pooled. All purification steps were carried out at 4°C. 11β-Hydroxylase was purified in exactly the same way as described for aldosterone synthase.

2.8.6 Purification of accessory enzymes

2.8.6.1 Human rhinovirus 3C protease

pET15b-HRV3C was a gift from Dr. Alan Riboldi-Tunnicliffe (University of Glasgow). 3C protease expression was carried out according to Section 2.6.1.3. HRV 3C protease was purified in the same way as that for Adx (Section 2.8.1) until the 3C protease had been loaded onto a 5 ml HisTrap Ni^{2+} column (GE Healthcare). Following binding, the Ni^{2+} column was attached to a BioCad 700E where it was washed with 10 column volumes of 25 mM imidazole, 300 mM NaCl in 50 mM Tris-HCl pH 8.0. 3C protease was eluted using a 0-500 mM imidazole gradient in 150 mM NaCl, 50 mM Tris-HCl pH 8.0. 1 mM DTT and 1 mM EDTA were added to all of the elution fractions. Highly-enriched 3C protease was concentrated using a 10 kDa MWCO centricon (Sartorious), and applied to a Superose 6 gel filtration column equilibrated in 150 mM NaCl, 50 mM Tris-HCl pH 8.0. Fractions containing pure HRV 3C protease were collected, snap-frozen with liquid nitrogen and stored at -20°C.

3C protease activity was assessed by FSEC using SI-CLBH as substrate (Section 2.10.1).

2.8.6.2 Biotin ligase

Biotin ligase was expressed as described in Section 2.6.1.3 and purified by Ni^{2+}-affinity chromatography in the same way as for 3C protease (Section 2.8.4.1). However, no DTT or EDTA was added to the elution fractions. After the Ni^{2+}-affinity step, the biotin ligase was pure so no further chromatographic steps were required. Pure biotin ligase was snap-frozen in liquid nitrogen and stored at -20°C.

Recombinant biotin ligase was used to biotinylate SI-CLBH *in vitro*. 1 mg of pure biotin ligase was stirred with SI-CLBH, 50 μM biotin, 20 μM ATP and 10 mM Mg-o-acetate overnight at 4°C. The next morning, the SI-CLBH was doubly desalted into 150 mM NaCl, 50 mM sodium phosphate pH 7.4, 0.15% DM using a PD10 column. Biotinylated protein was added to streptavidin beads, and mixed by rotating on a wheel for 4 h at 4°C. The beads were loaded into a disposable

gravity feed column, and washed extensively with 50 mM sodium phosphate pH 7.4, 0.15% DM. Immobilised SI-CLBH was visualised by placing the column on a UV-light source and observing iLOV fluorescence.

2.8.7 Methods for protein concentration determination

The protein concentration of membrane aliquots was determined by Bicinchoninic Acid (BCA) assay (Pierce) according to the manufacturer's instructions. Bovine serum albumin (BSA) was used as a standard. The concentrations of purified proteins were determined according to the Beer-Lambert law ($A = \varepsilon cl$) using a calculated extinction coefficient at 280 nm for each protein according to their primary amino acid sequence.

2.9 SDS-PAGE

10-15 μg in a volume of 20 μl of each protein sample to be analysed by SDS-PAGE was mixed with 5 μl of NuPage LDS sample buffer (Invitrogen), and then heated at 70°C for 10 min prior to loading onto either a 10 or 12% Bis-Tris pre-cast gel (Invitrogen). 10 μl of SeeBlue2 pre-stained marker (Invitrogen) was loaded into one of the wells on each gel to allow estimation of the MW of the proteins being analysed. Gels were run in 1x MES buffer (Invitrogen) at 200 V for 45 min. Protein bands were visualised by staining with SimplyBlue SafeStain (Invitrogen) according to the manufacturer's instructions.

2.10 Measuring iLOV fluorescence

2.10.1 iLOV excitation and emission spectra

Excitation and emission spectra for pure iLOV (a gift from Dr. John Christie, University of Glasgow) were recorded and compared against those for flavin mononucleotide (FMN). Measurements were made in a quartz cuvette with a 1 cm pathlength using a Perkin-Elmer L550B spectrophotometer. Fluorescence was measured at right angles to the excitation beam. Excitation spectra were recorded between 300 and 460 nm measuring fluorescence emission at 485 nm. Emission spectra were recorded from 470 to 600 nm, exciting the samples at 450 nm.

2.10.2 Measuring iLOV fluorescence in 96 well plates

The iLOV fluorescence of individual samples (e.g. whole cells or FSEC elution fractions) was determined using a FLUOstar OPTIMA plate-reader. 200 µl of each sample was added to a single well in a black 96-well plate (Corning). Samples were excited at 450 nm and iLOV fluorescence emission measured at 520 nm.

2.11 Analytical size exclusion chromatography

2.11.1 Fluorescence size exclusion chromatography

2 ml of yeast membranes (at a concentration of 20 mg/ml) containing SI-CLBH were solubilised with n-dodecyl-β-D-maltoside (DDM). 0.6 ml of a 10% detergent stock solution was added to the membranes and stirred for 1 h at 4°C. The sample was then centrifuged at high-speed (50,000g, 10 min, 4°C) to pellet any unsolubilised material. The supernatant containing SI-CLBH was filtered before a 500 µl aliquot was injected onto a Superose 6 gel-filtration column equilibrated in 50 mM sodium phosphate pH 7.4, 5% glycerol, 0.01% DM. The column was run at a rate of 0.3 ml/min, and 0.6 ml fractions were collected. iLOV fluorescence was measured in all of the elution fractions as detailed in Section 2.10.2. Using this data, a FSEC profile was generated.

HRV 3C activity was investigated by comparing the FSEC profile of SI-CLBH before and after treatment with the protease. Furthermore, the effects of DTT, EDTA, PMSF, benzamidine and the Roche protease inhibitor cocktail on HRV 3C activity were assessed by comparing FSEC profiles of SI-CLBH that had been treated with 3C protease in the presence of one these reagents with a fully-cleaved sample.

2.11.2 ELISA size exclusion chromatography

E. coli membranes (at a concentration of 20 mg/ml) containing B2-CLBH were solubilised using the detergents Fos Choline-9, sodium cholate, CHAPS, decyl-βD-maltoside, octyl-βD-thioglucoside (OTG) and CYMAL-5. 0.3 ml of each detergent from 10% stock solutions was stirred with 1 ml of membranes in the presence of 1 mM benzamidine, 1 mM PMSF and Roche protease inhibitor cocktail for 1 h at

4°C. The samples were prepared for injection onto the Superose 6 column in the same way as detailed for FSEC (Section 2.11.1). The column was equilibrated in 150 mM NaCl, 0.1 mM EDTA, 50 mM potassium phosphate pH 7.4 containing a CMC concentration of detergent (1.2% Fos Choline-9, 0.6% sodium cholate, 0.5% CHAPS, 0.15% DM, 0.3% OTG, 0.12% CYMAL-5) prior to injecting the solubilised sample. The column was run at 0.3 ml/min and 0.6 ml fractions were collected.

For each detergent, 50 µl aliquots of fractions 15-35 were applied in triplicate to a 96-well ELISA plate (Corning). 50 µl of a coating buffer (0.1 M sodium bicarbonate pH 8.4) was also added to each well to promote protein binding to the side of the wells. The plate was incubated at 4°C overnight with gentle shaking. The next day, the wells were washed three times with TBST (150 mM NaCl, 50 mM Tris-HCl pH 7.6, 0.1% Tween 20) before blocking them with TBST-BSA (TBST with 5% BSA) for 30 min at room temperature. Following this, the wells were washed three times with TBST. Primary antibody (anti-aldosterone synthase Ab that had been diluted 1:2000 with TBST) was added to each well, and the plate incubated on ice for 30 min. [Anti-human aldosterone synthase Ab was a gift from Professor Kunai Muniaki, Keio University, Japan]. Following this, the plate was incubated at room temperature for 1 h with gentle shaking. Wells were washed three times with TBST before they were incubated with secondary antibody (goat anti-rabbit (DAKO), 1:1000 dilution) for 1 h at room temperature with gentle shaking. Before developing, wells were washed five times with TBST. 100 µl of developing solution (Sigma-Aldrich) was added to each well to generate an ELISA signal. Plates were incubated for 30-60 min in the dark. The A_{450} intensity in each well was measured using a Fluostar Optima plate reader.

2.12 Thermostability analysis

2.12.1 Thermal denaturation of adrenodoxin

Thermal denaturation of Adx was performed in clear 96-well plates (Corning). In each well, Adx had a final concentration of 13 mg/ml in a total volume of 200 µl. Along with the protein, each well contained 20 µl of a 10x buffer solution and 20 µl of a 10x additive (e.g. salt) solution. The final volume was made up to

200 μl with dH_20. Once a plate had been made up, it was incubated in a spectrophotometric plate-reader (Molecular Devices Spectra Max Plus 384) at 45°C for 4 h. The A_{414} of the sample was measured at 60 s intervals. Measurements were made in triplicate for each condition.

2.12.2 Analysis of adrenodoxin reductase stability by CPM assay

A stock solution of CPM reagent (7-Diethylamino-3-(4-maleimidophenyl)-4-methylcoumarin) (Sigma-Aldrich) was made by first dissolving it in dimethyl sulfoxide (DMSO) to a concentration of 25 mg/ml, and then diluting it with H_20 to a final concentration of 4 mg/ml. CPM dye was stored in the dark to prevent photobleaching.

CPM thermal denaturation assays were performed in black 96-well plates (Corning). For each condition investigated, protein and buffer control measurements were made in triplicate. Each protein well contained 10 μl (5 μg) of pure AdxRed, 20 μl of a 10x buffer solution as well as 20 μl of either a 10x additive (such as a salt) or dH_2O. The buffer controls contained 10 μl of dH_2O instead of protein. All wells were made up to a final volume of 200 μl with dH_20. Plates were incubated at room temperature for 5 min before 10 μl of CPM reagent was added. The plate was then transferred to a fluorescence plate-reader at a temperature of 45°C. Fluorescence intensity readings were taken at regular intervals over a 3 h period. Baseline fluorescence recorded in the buffer controls were subtracted from the values recorded in the protein wells, before the three difference values for each condition were averaged. Curves showing AdxRed denaturation were plotted as an increase in fluorescence over time.

2.13 Circular dichroism

All CD measurements were made by Dr. Sharon Kelly at the Biophysical Characterisation Unit, University of Glasgow. Far- (190-260 nm) and near-UV/visible (250-550 nm) circular dichroism spectra of pure Adx, AdxRed, aldosterone synthase and 11β-Hydroxylase were recorded on a Jasco J-810 spectropolarimeter using quartz cuvettes with 0.02 and 0.5 cm pathlengths, respectively.

2.14 Crystallisation trials of adrenodoxin and adrenodoxin reductase

The commercial sparse-matrix crystallisation screens JCSG, Morpheus (Molecular Dimensions), Peg/Ion 1&2 and Hampton 1&2 (Hampton Research) were used to identify putative crystallisation conditions for Adx and AdxRed. Both proteins were concentrated to *ca*. 20 mg/ml. A Cartesian HoneyBee nanolitre dispensing system (Genomic Solutions Ltd.) was used to form 1 μl crystallisation drops by mixing 500 nl of the concentrated Adx/AdxRed solutions with 500 nl of the reservoir solution in each of the wells. The plates were stored in a Rhombix Crystal Plate Imager (ThermoScientific) at 20°C. Trays were monitored over a 3 month period. Photos of each crystallisation condition were taken at regular intervals. Possible crystal hits were viewed manually under a microscope, and then tested for diffraction using the in-house X-ray facility (consisting of a Rigaku MicroMax 007 rotating anode generator coupled with MarResearch 345 image plate detector).

2.15 Reduced carbonmonoxide difference spectrum

The reduced carbonmonoxide difference spectra of purified aldosterone synthase and 11β-Hydroxylase were obtained using the original method described by Omura and Sato (Omura and Sato, 1964). All measurements were taken using a Shimadzu UV-1700 Pharmaspec spectrophotometer. 1ml of pure protein was divided between two 500 μl quartz cuvettes. Carbon monoxide was bubbled into the sample cuvette at a rate of approximately 1 bubble per second for 1 min. 1 mg of sodium dithionite was added immediately to both sample and reference cuvettes. The cuvettes were inverted repeatedly until the sodium dithionite had dissolved. The spectrum was then recorded from 400 to 600 nm every 30 s until the peak at 450 nm had reached its maximum intensity.

Aldosterone synthase and 11β-Hydroxylase concentrations were calculated by the Beer-Lambert Law measuring absorption at 450 nm and using the known p450 extinction coefficient ε_{450} = 91 $mM^{-1}cm^{-1}$.

Chapter 3 – A tailored system for the recombinant expression, purification and immobilisation of human membrane proteins

3.1 Introduction

The main goal of my Ph.D. was to develop expression and purification systems for the p450 enzymes aldosterone synthase and 11β-Hydroxylase, as well as their electron transfer proteins adrenodoxin and adrenodoxin reductase. Aldosterone synthase and 11β-Hydroxylase are both human membrane proteins (Section 1.8.5), suggesting that their expression in a heterologous host and functional purification might be difficult. To address this issue, my first task was to create an in-house expression system specifically tailored for use with human membrane proteins.

The Fraser group routinely overexpress human membrane proteins in the yeast *P. pastoris* using the commercially-available pPICZ(α)vector series (Invitrogen) (Fraser, 2006). To facilitate processes such as expression screening, FSEC, affinity purification and protein immobilisation, the Fraser group have created an in-house version of the pPICZA expression vector (termed CLBH) for use with human membrane proteins. The in-house vector has a 3C protease cleavage site – iLOV – biotin acceptor domain – His_{10} (CLBH) tag immediately downstream of the *Not*I cloning site (Figure 3.1). When the CLBH tag was conceived, it was envisaged that (i) the 3C protease site could be used for efficient tag removal, (ii) the fluorescent reporter iLOV could be used for tracking the production and purification of recombinant proteins as well as FSEC, (iii) the biotin acceptor domain could be used for immobilising target proteins on surfaces coated with streptavidin, and (iv) the His_{10} tag could be used for high-affinity Ni^{2+} purification. At the start of this project, the *P. pastoris* CLBH vector had been made but not yet used with any human membrane protein. Therefore, a full characterisation of this novel expression system was performed using the cholesterol biosynthetic enzyme sterol isomerase (SI) as a test protein. SI was

chosen for optimisation studies as it has excellent stability for a human integral membrane protein, and is expressed at high levels in *P. pastoris* (Niall Fraser, personal communication). This Chapter describes the properties and applications of the CLBH tag.

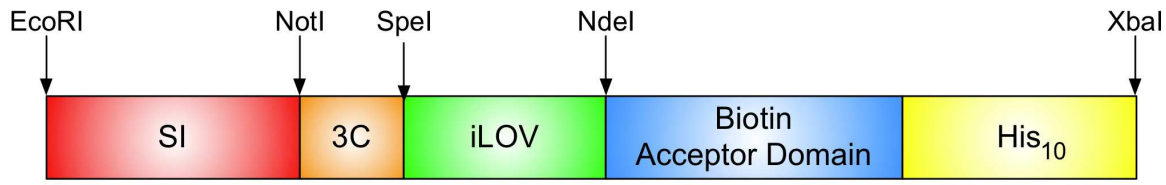

Figure 3.1 Schematic diagram of the SI-CLBH expression construct
The *P. pastoris* expression vector pPICZA (Invitrogen) was modified by the Fraser group to include a novel (CLBH) tag between the *Not*I and *Xba*I cloning sites. The CLBH tag consists of a Human Rhinovirus 3C protease site followed by the improved Light Oxygen Voltage (iLOV) fluorescent reporter, a biotin acceptor domain and a His_{10} tag. A cDNA encoding human sterol isomerase was cloned between the *Eco*RI and *Not*I restriction sites. The SI-CLBH vector was constructed by Dr. Gillian Young.

3.2 iLOV: a novel fluorescent reporter with membrane protein applications

In recent years, it has become common practice to fuse green fluorescent protein (GFP) to the C-terminus of target membrane proteins, facilitating tracking of the recombinant protein through the expression and purification processes (Drew *et al.*, 2008). While GFP has been successfully used as a fluorescence reporter with membrane proteins in both *E. coli* (Drew *et al.*, 2005) and *S. cerevisiae* (Newstead *et al.*, 2007), it is not ideal for use with shake-flask cultures of *P. pastoris* as their oxygen content is essentially zero, hindering GFP chromophore formation. In contrast, as iLOV fluorescence is not dependent upon oxygen availability it would, therefore, be more suited to use in *P. pastoris* than GFP. For this reason, iLOV had been incorporated into pPICZA as part of the CLBH tag.

Here, the absorption and fluorescence properties of iLOV were characterised, and its use as a reporter of membrane protein expression and stabilisation demonstrated.

3.2.1 The spectral properties of iLOV and flavin-mononucleotide

LOV domains fluoresce green upon excitation with UV-A/blue light (Christie *et al.*, 1999; Christie, 2007). LOV fluorescence comes from the flavin mononucleotide (FMN) co-factor, which is bound to the protein scaffold within a central cavity through a combination of hydrogen bonds and van der Waals interactions. FMN and iLOV both have strong absorptions in the region 350-500 nm (Figure 3.2). To identify the optimal wavelength for specifically exciting iLOV over FMN, fluorescence excitation spectra were recorded for both chromophores (Figure 3.3A). Fluorescence emission spectra were also recorded for both iLOV and FMN (Figure 3.3B). The iLOV excitation spectrum has peaks at 350, 370 and 450 nm whereas the FMN spectrum has maxima at 355 and 390 nm only (Figure 3.3A). Thus, it is possible to excite iLOV selectively over FMN by using light with a wavelength of 450 nm. The iLOV emission spectrum has a

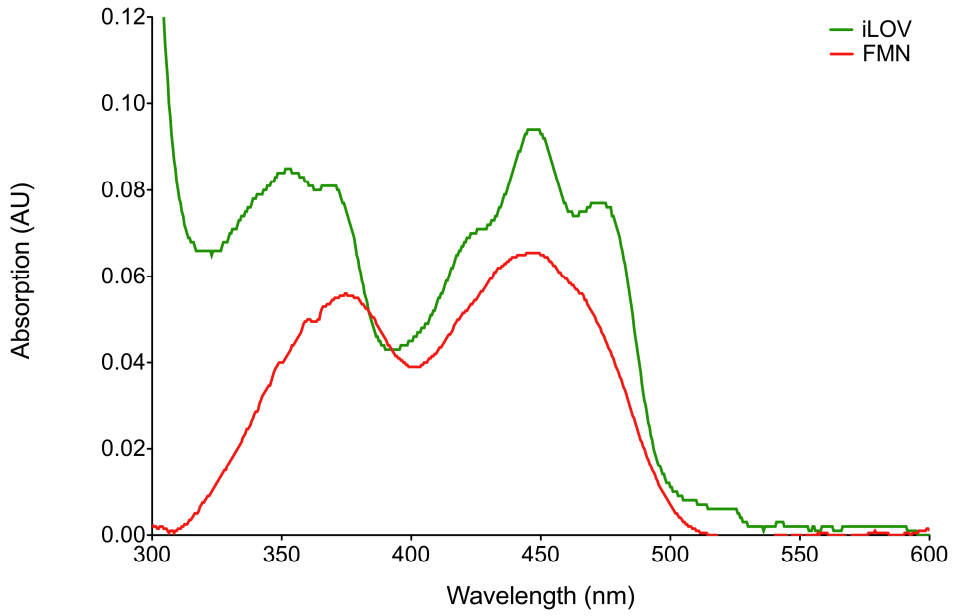

Figure 3.2 The absorption spectra of iLOV and flavin-mononucleotide (FMN)
iLOV has two prominent absorptions in the visible region (a peak at 355 nm with a shoulder at 375 nm, and a second peak at 450 nm with shoulders at 425 and 475 nm). The flavin absorption spectrum consists of two broad absorptions (one in the region 320-390 nm, the other 410-490 nm). For experimental detail, see Section 2.10.1.

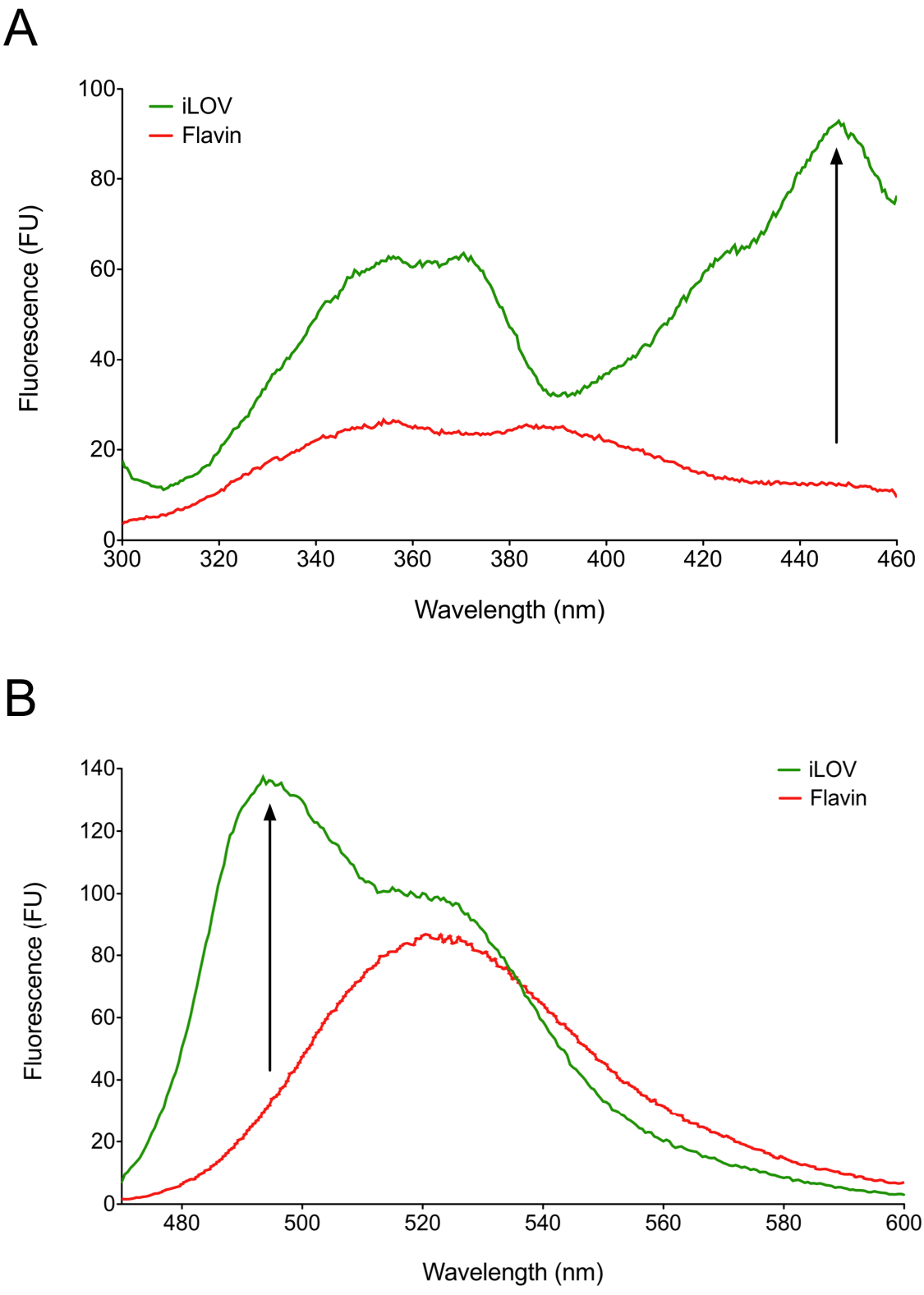

Figure 3.3 The fluorescence properties of iLOV and flavin mononucleotide
(A) Excitation spectra were recorded between 300 and 460 nm measuring fluorescence emission at 485 nm. (B) Following chromophore excitation at 450 nm, emission spectra were recorded in the region 470-600 nm. These experiments showed that the optimal wavelength for exciting iLOV is 450 nm, whereas emission can be effectively measured in the range 485-530 nm. For experimental detail, see Section 2.10.1.

distinctive peak at 485 nm with a pronounced shoulder at 525 nm. In contrast, the emission profile for FMN consists of a single broad peak between 510 and 540 nm (Figure 3.3B). The best wavelength for selectively measuring emission from iLOV but not FMN is 485 nm. However, the shape of its emission spectrum means that iLOV fluorescence can be measured effectively in the range 485 to 530 nm.

3.2.2 Using iLOV to monitor recombinant protein production

In heterologous expression hosts, the production levels of human membrane proteins are often low. To ensure that maximal amounts of proteins of interest are obtained, expression optimisation experiments must be performed. If the production level of a target membrane protein has to be determined by either radioligand binding or Western Blotting, the optimisation process can be unnecessarily time-consuming. However, by fusing the protein of interest to a fluorescent reporter, this potential bottleneck can be overcome. To explore the utility of iLOV as a reporter of membrane protein expression, a time course of SI-CLBH production in a fermenter culture of *P. pastoris* was performed (Figure 3.4).

The yeast culture was grown on glycerol for 30 h to increase cell biomass before the carbon source was changed to methanol, inducing production of SI-CLBH. Samples were taken at regular intervals throughout the fermentation. At each time-point, the level of iLOV fluorescence in intact cells was measured and the wet cell weight per litre of culture determined. From these two values, it was possible to calculate expression levels for SI-CLBH. Using iLOV fluorescence as a measure of the amount of recombinant protein present within the yeast cells, it was possible to determine the expression level of SI-CLBH at each time-point within 30 minutes of taking the sample. This speed of analysis is highly beneficial allowing time courses of recombinant membrane protein production to be followed in real-time. When maximal levels of the target protein have been reached, the fermentation can be stopped and the cells harvested. Furthermore, if expression of a target protein is not successful or unsatisfactorily low, this can be quickly detected and the fermentation aborted. Here, maximal levels of SI-CLBH were obtained by feeding the yeast methanol for *ca*. 50 h (Figure 3.4).

Figure 3.4 Time-course of Sterol Isomerase-CLBH expression in fermenter culture
Yeast were grown on glycerol for 30 h to increase cell biomass, before the carbon source was changed to methanol inducing production of SI-CLBH (Section 2.5.2). Samples were taken at regular intervals throughout the fermentation. At each time point, 1 ml cells was spun down, and the weight of the pellet recorded. From this, the wet cell weight of the culture was calculated (red line). The cells were then washed twice in water (to remove free flavin present in the media), resuspended in water and whole cell iLOV fluorescence measured (Section 2.10.2). The production level of SI-CLBH was expressed as iLOV fluorescence per amount of wet weight of cells (green line).

3.2.3 Assessing membrane protein aggregation status using iLOV

Aggregation is a common problem encountered when working with membrane proteins, and is usually caused by protein instability in the detergent used for solubilisation and purification purposes. Recently, an approach called fluorescence size-exclusion chromatography (FSEC) has been developed which allows the aggregation status of a fluorescently-tagged membrane protein to be monitored throughout the purification process following membrane solubilisation, even in the presence of other proteins (Kawate and Gouaux, 2006). Usually, the membrane protein of interest is tagged with GFP. Here, the utility of iLOV as a fluorescence reporter for FSEC purposes was assessed.

Membranes containing SI-CLBH were solubilised using the detergent decyl-βD-maltoside (DM). Following centrifugation, the supernatant was applied to a Superose 6 gel filtration column. iLOV fluorescence was measured in all of the elution fractions. The elution profile consisted of a single symmetric fluorescent peak showing that SI is monodisperse in DM (Figure 3.5).

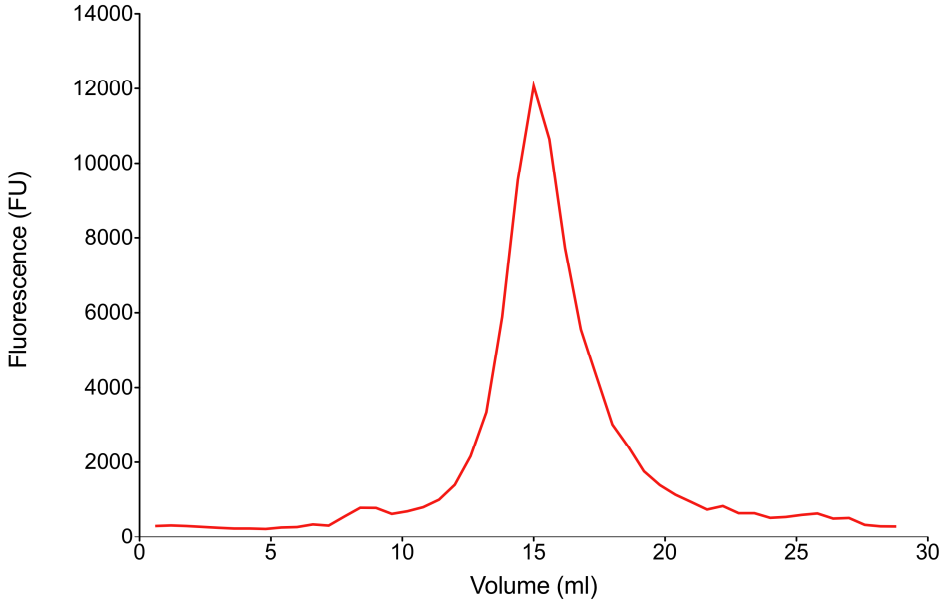

Figure 3.5 FSEC analysis of SI-CLBH solubilised in DM
Membranes containing SI-CLBH were solubilised in 2.5% decyl-βD-maltoside (DM). The sample was centrifuged and the supernatant applied to a Superose 6 gel filtration column (Section 2.11.1). iLOV fluorescence was measured in each of the elution fractions (Section 2.10.2), and a profile generated.

This simple experiment shows that SI is stable in DM. More importantly, it shows that the iLOV fluorescent reporter is compatible with FSEC.

3.3 Removal of the CLBH tag using 3C protease

Site-specific proteases are commonly used to remove tags from recombinant proteins following their purification (Arnau *et al.*, 2006). Frequently used enzymes include thrombin, Factor X and Tobacco Etch Virus (TEV) protease.

In the CLBH vector, a cleavage site (LEVLFQ|GP) for human rhinovirus (HRV) 3C protease is positioned between the recombinant protein and the iLOV domain (Figure 3.1). HRV 3C had been chosen for use with the in-house vector because it has high catalytic power even at low temperatures (4°C), making it compatible for use with membrane proteins with poor stability (Waugh, 2011). Here, a purification protocol for 3C protease was developed, and its requirements for catalytic activity assessed by FSEC.

His-tagged HRV 3C was expressed in *E. coli* and purified by a combination of Ni^{2+}-affinity and size-exclusion chromatography. Large quantities of very pure protein

were obtained (Figure 3.6). Peak fractions from the gel filtration column were analysed by SDS-PAGE (Figure 3.7). A single band with a MW of *ca.* 25 kDa was observed, showing that the 3C protease was indeed pure.

Having successfully purified 3C protease, a simple assay was devised to check the activity of the recombinant protein. SI-CLBH solubilised with dodecyl-βD-maltoside (DDM) was incubated with 3C protease overnight at 4°C in buffer containing 1 mM EDTA and 1 mM DTT. The sample was then applied to a Superose 6 gel filtration column and the fluorescence of the elution fractions measured (Figure 3.8). An elution profile for untreated SI-CLBH was also generated (Figure 3.8). SI-CLBH had an elution volume of 15 ml. Following treatment with 3C protease, however, a single fluorescent peak with an elution volume of 20 ml was observed. This mobility shift on the gel-filtration column was due to cleavage of the CLBH tag by HRV 3C, demonstrating that the recombinant protease was catalytically active.

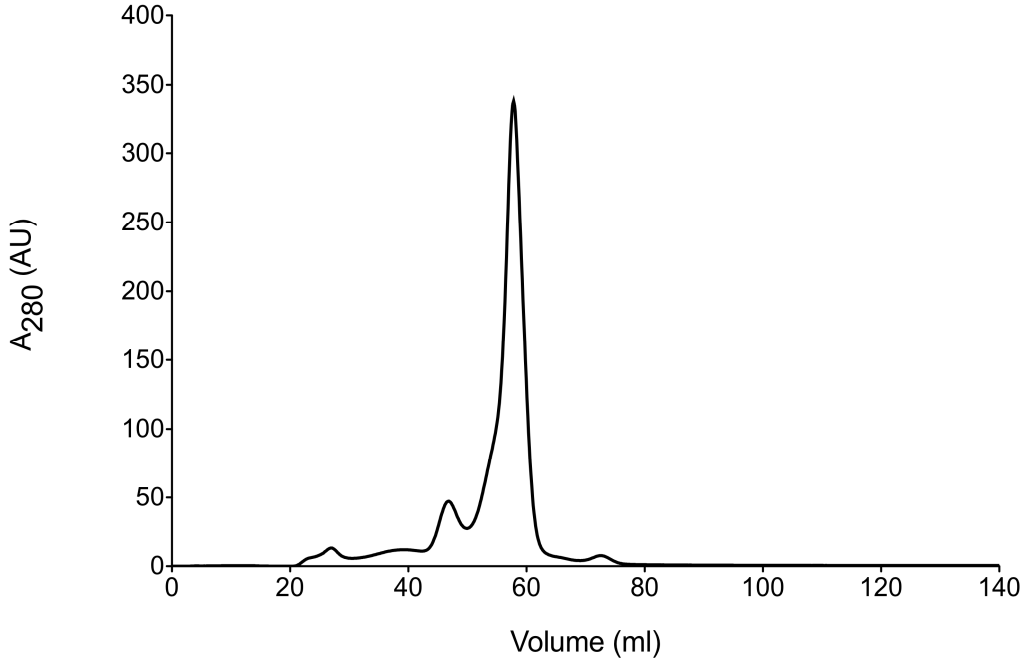

Figure 3.6 Purification of human rhinovirus 3C protease by size exclusion chromatography
A highly-enriched sample of 3C protease purified by Ni^{2+}-affinity chromatography was concentrated and applied to a Superose 6 gel filtration column equilibrated in 1 mM DTT, 1 mM EDTA, 150 mM NaCl in 50 mM Tris HCl pH 7.4. The major elution peak (at *ca.* 60 ml) was 3C protease.

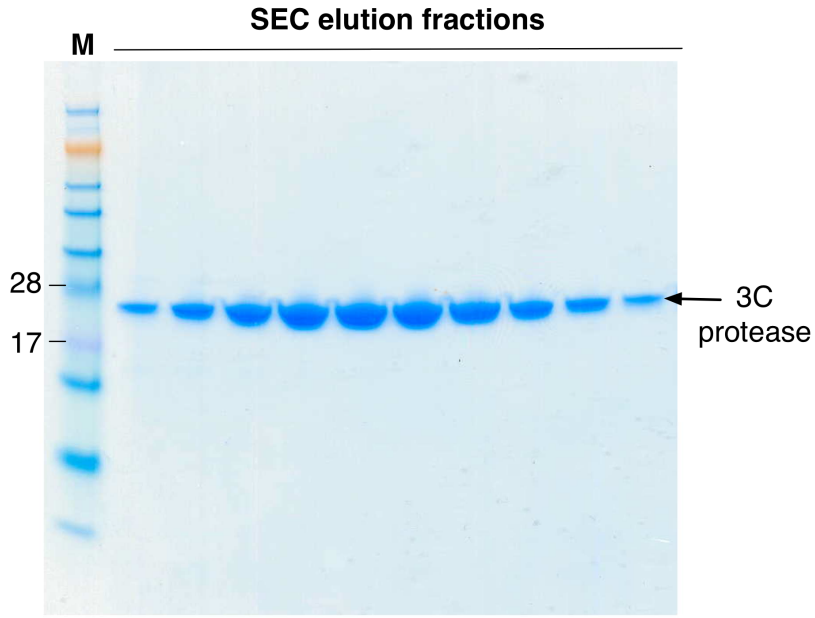

Figure 3.7 SDS-PAGE analysis of pure human rhinovirus 3C protease
The peak fractions eluted from the gel filtration column (Figure 3.6) were analysed by SDS-PAGE (Section 2.9). A single, strong band with a MW of *ca.* 25 kDa corresponding to pure 3C protease (predicted MW 22 kDa) was observed across the elution peak.

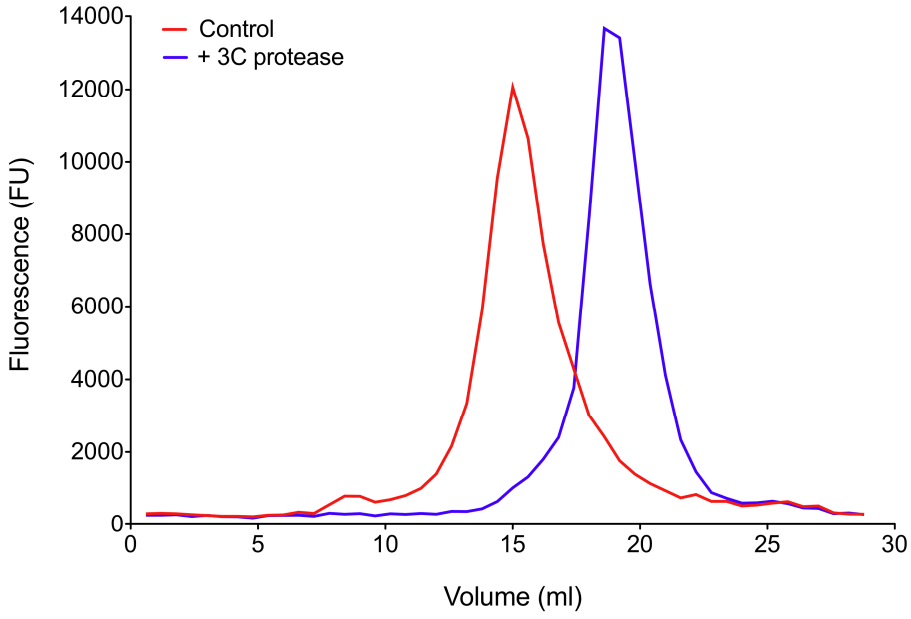

Figure 3.8 Assessing the catalytic activity of recombinant human rhinovirus 3C protease
The catalytic activity of recombinant HRV 3C was assessed by FSEC analysis using SI-CLBH as a substrate for the protease. SI-CLBH was solubilised 2.5% n-dodecyl-β–D-maltoside (DDM) and split into two samples, one of which was incubated with 20 µg/ml 3C protease overnight at 4℃ in 50 mM sodium phosphate, 1mM EDTA, 1 mM DTT, 5% glycerol and 0.01% DDM, pH 7.4. The next day, both samples were applied to a Superose 6 gel filtration column and the fluorescence of the elution fractions measured (Section 2.11.1). The untreated sample (red) eluted at 15 ml whereas the sample treated with 3C protease (blue) eluted at 20 ml.

To optimise the conditions for cleavage by HRV 3C, SI-CLBH solubilised in DDM was incubated with the protease in different buffer conditions. Following treatment with 3C protease, the cleavage mixtures were analysed by FSEC (Figure 3.9). SI-CLBH was only fully-cleaved in the presence of 1 mM DTT. In contrast, EDTA was not required for 3C protease activity (Figure 3.9).

When purifying a recombinant protein, inhibitors must be included in all of the buffers to prevent the target protein from being degraded by proteases endogenous to the heterologous host. There is an obvious risk that these will inhibit HRV 3C also, preventing cleavage of the CLBH tag. Therefore, the effects of three of the most commonly used protease inhibitors, namely phenylmethanesulfonylfluoride (PMSF), benzamidine and the Roche complete protease inhibitor cocktail were tested.

SI-CLBH solubilised in DDM was incubated with 3C protease either alone or with one of the inhibitors. The cleavage mixtures were then analysed by FSEC (Figure 3.10). The presence of PMSF did not inhibit tag removal. However, incomplete cleavage of SI-CLBH by 3C protease was observed in the presence of both the Roche inhibitor cocktail and benzamidine. It was therefore concluded that PMSF but not Roche Complete or benzamidine could be used in conjunction with 3C protease.

3.4 Recombinant protein purification using the CLBH tag

The CLBH vector was designed in a way that would enable purification of recombinant proteins in four simple steps comprising: (i) Ni^{2+}-affinity purification, (ii) cleavage of the CLBH tag using 3C protease, (iii) reverse Ni^{2+}-affinity purification, and (iv) size exclusion chromatography (SEC) (Figure 3.11).

When required, a second affinity purification step could be performed by biotinylating the CLBH tag *in vitro* with biotin ligase and then applying the protein mixture to (strept)avidin resin (Section 3.5).

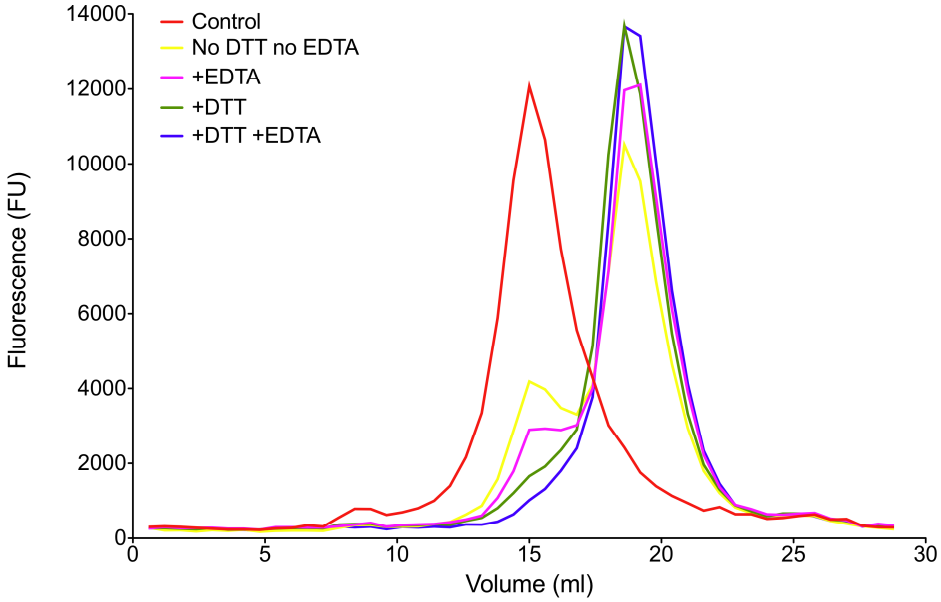

Figure 3.9 Buffer requirements for HRV 3C protease activity
SI-CLBH solubilised in DDM was incubated with 3C protease in a range of buffer conditions. Following this, the cleavage mixtures were analysed by FSEC (Section 2.11.1). In the absence of both 1mM DTT and 1mM EDTA (yellow), incomplete tag cleavage was observed. However, the CLBH tag was fully cleaved when the proteolysis cocktail contained 1 mM DTT (with (blue) or without (green) EDTA). In the presence of 1mM EDTA alone (purple), tag removal was incomplete.

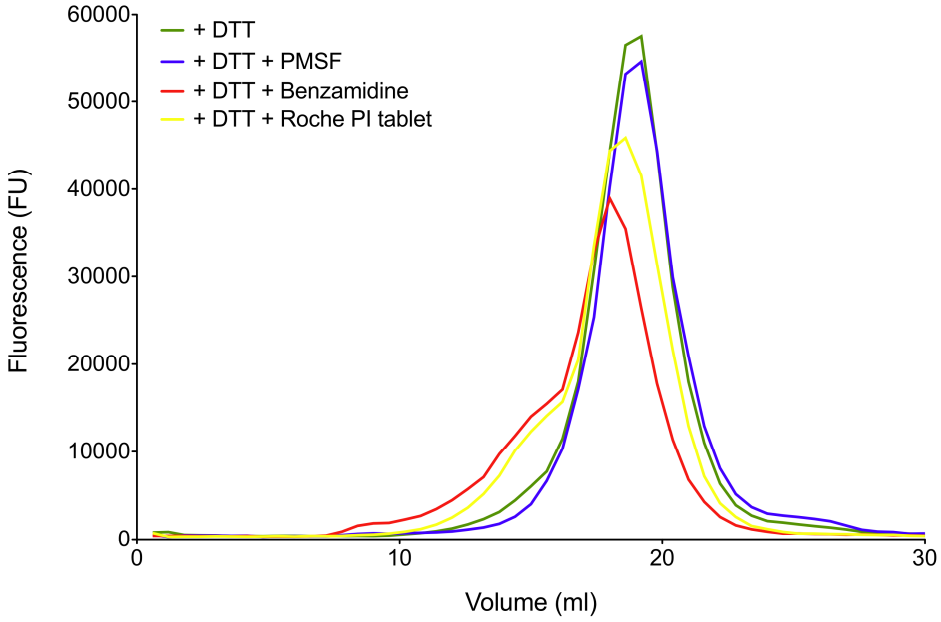

Figure 3.10 The effect of protease inhibitors on HRV 3C protease activity
SI-CLBH solubilised in 2.5% DDM was incubated with 20 µg/ml 3C protease and 1 mM DTT either alone (green) or in the presence of a commonly used protease inhibitor (1mM PMSF (blue), 1mM benzamidine (red) or 1X Roche complete protease inhibitor (PI) tablet (yellow)). The cleavage mixtures were analysed by FSEC (Section 2.11.1). 3C protease activity was not inhibited by PMSF. However, incomplete cleavage of the CLBH tag by HRV 3C was observed in the presence of both Roche complete PI tablet and benzamidine.

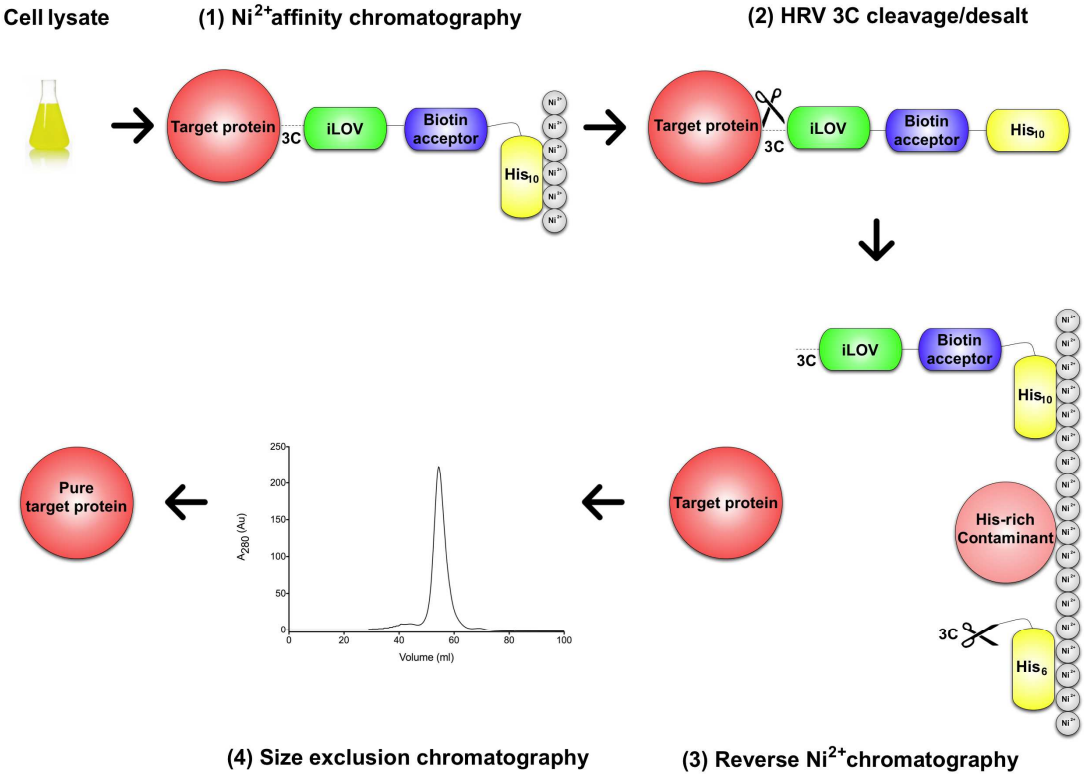

Figure 3.11 Cartoon representation of the strategy used to purify CLBH-tagged proteins
The cell lysate is (1) purified by Ni^{2+}-affinity chromatography through binding of the His_{10} tag to the nickel resin. (2) Fractions from the Ni^{2+} column containing the CLBH-tagged protein are pooled, desalted and then cleaved overnight with 3C protease. (3) The next day, the cleavage mixture is passed over a fresh Ni^{2+} column. This removes cleaved CLBH, His-tagged HRV 3C and His-rich contaminants from the sample. (4) Finally, the reverse-purified protein is concentrated and applied to a gel filtration column, from which fractions containing pure target protein are collected

To test the usefulness of the CLBH tag for obtaining milligram amounts of pure protein, SI was purified from yeast membranes containing SI-CLBH. Previously, FSEC analysis had shown that SI is monodisperse in DM (Figure 3.7), suggesting that SI could be stably purified to homogeneity in this detergent. Membranes containing SI-CLBH (resuspended in SI Buffer B (Section 2.8.1)) were solubilised with DM. Following centrifugation, the supernatant fraction (containing SI-CLBH) was applied to a Ni^{2+} column. The iLOV reporter provided a simple way of tracking the CLBH-tagged fusion protein throughout the purification process. Binding of SI-CLBH to the Ni^{2+}-column could be readily visualised by exposing the column to UV-radiation and observing iLOV fluorescence (Figure 3.12). The efficiency of SI-CLBH binding to the column could also be readily calculated by measuring the fluorescence of the solubilised sample before and after it had been passed over the column. Typically, at least 80% of the SI-CLBH bound to the Ni^{2+}-column (results not shown).

Figure 3.12 Visualisation of SI-CLBH bound to a Ni^{2+} column
The iLOV fluorescence reporter provided a simple way of tracking SI-CLBH over the course of the Ni^{2+}-affinity purification step. Detergent-solubilised material (left, eppendorf) was loaded onto a Ni^{2+} column (right). Successful binding of the recombinant protein to the column was readily visualised by observing fluorescence from iLOV following illumination with UV-light.

The column was washed with buffer containing 500 mM NaCl and 75 mM imidazole (Section 2.8.1) to remove proteins that had bound non-specifically to the column via ionic interactions and His-rich contaminants, respectively. SI-CLBH was then eluted using buffer containing 300 mM imidazole. Fluorescent fractions containing SI-CLBH were pooled, desalted (to remove imidazole) and incubated overnight with HRV 3C protease. The next day, cleaved SI was passed over a fresh Ni^{2+}-column to remove cleaved CLBH, His-tagged 3C protease and His-rich contaminants (that bound to the original Ni^{2+} column) in a reverse affinity-purification step. The flow-through containing highly-enriched SI was collected, concentrated and applied to a Superose 6 gel filtration column (Figure 3.13). The SEC elution profile consisted of a single, large symmetric peak which suggested that SI was both pure and monodisperse. Peak fractions were pooled and analysed by SDS-PAGE, along with fractions from each of the purification stages (Figure 3.14).

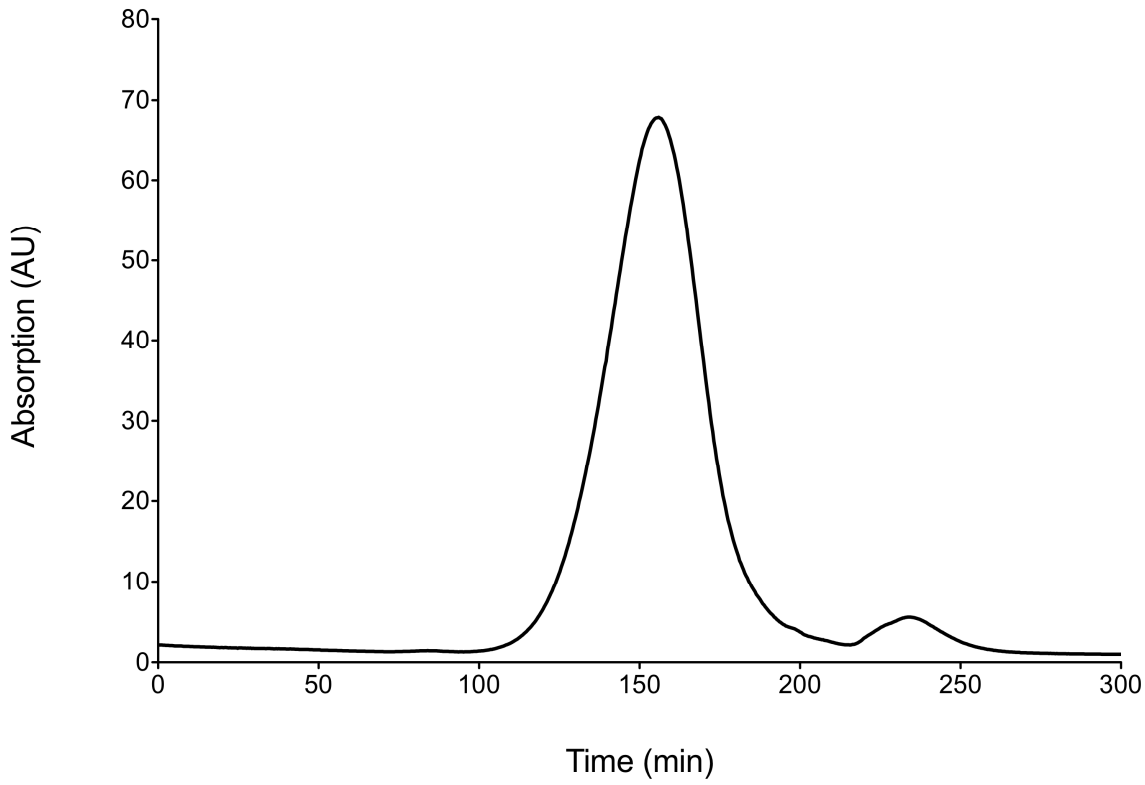

Figure 3.13 Elution of pure sterol isomerase from a Superose 6 gel filtration column
A highly-enriched sample of SI in DM was purified by gel filtration using a Superose 6 column equilibrated in 150 mM NaCl, 0.1 mM EDTA, 10% glycerol, 0.15% DM, 50 mM sodium phosphate pH 7.4 at a flow-rate of 0.3 ml/min. Peak fractions were pooled and analysed by SDS-PAGE (Fig. 3.14).

SDS-PAGE analysis showed that SI-CLBH was largely pure following Ni^{2+}-affinity purification, with a major band visible at *ca.* 45 kDa (Figure 3.14). The purity of the sample at this stage can be explained in terms of the SI-CLBH expression level in yeast membranes. On membrane solubilisation, there was so much SI-CLBH in solution that only a few contaminant proteins were able to bind to the Ni^{2+} column. Thus, the sample was largely pure following a single chromatographic step. Following cleavage with 3C protease, new bands appeared at *ca.* 22 and 23 kDa corresponding to SI and the –CLBH tag, respectively (Figure 3.14). After reverse-purification, the sample was essentially pure with a major band at 22 kDa corresponding to SI (Figure 3.14). The gel-filtration step did not result in any further purification of SI (Figure 3.14). A faint band at *ca.* 42 kDa that was observed in both the reverse-purified and SEC samples was thought to be an SDS-induced dimer of SI.

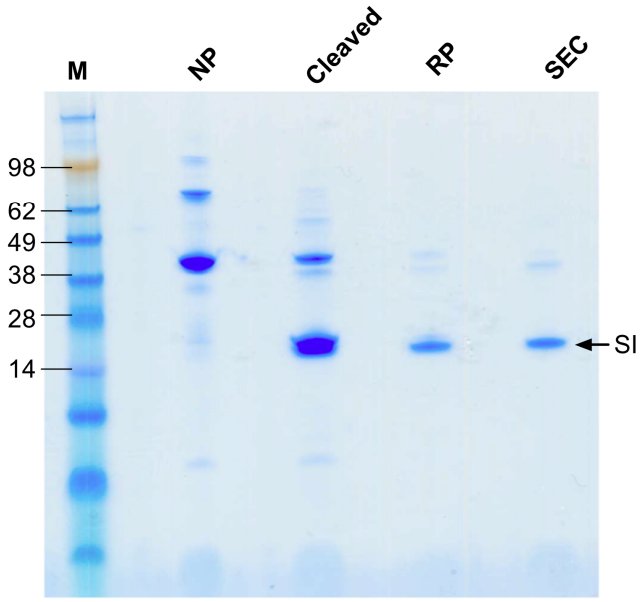

Figure 3.14 SDS-PAGE analysis of samples from different stages of the sterol isomerase purification
The CLBH tag was successfully used to purify SI in four steps: (i) SI-CLBH was solubilised in DM and purified by Ni^{2+}-affinity chromatography (NP), (ii) the fusion protein was cleaved with 3C protease, generating CLBH and SI, (iii) the cleavage mixture was reverse-purified (RP) using a fresh Ni^{2+} column, and (iv) highly-enriched SI was concentrated and applied to a Superose 6 gel filtration column (SEC) (Section 2.8.1). Samples from each stage of the purification process were analysed by SDS-PAGE (Section 2.9). SI-CLBH (the major band at *ca.* 44 kDa) was largely pure after Ni^{2+}-affinity purification (lane 1). Following cleavage with 3C protease, new bands appeared at *ca.* 22 and 23 kDa corresponding to SI and the CLBH tag, respectively (lane 2). After reverse-purification, the SI was essentially pure (lane 3). Application to the gel-filtration column did not result in any further purification of SI (lane 4).

3.5 Immobilising recombinant membrane proteins using the CLBH tag

Fusion of the *P. shermanii* transcarboxylase biotin acceptor domain to the C-terminus of selected GPCRs increases their expression in *P. pastoris* by up to 5-fold (Grünewald *et al.*, 2004; Andre *et al.*, 2006; Lundström *et al.*, 2006). The primary reason for including this domain within the CLBH tag, therefore, was to increase the production levels of target membrane proteins. However, biotinylation of this domain would also enable immobilisation of target proteins on (strept)avidin-coated surfaces, potentially allowing: (i) the purification of low-abundance membrane proteins; and/or (ii) the interaction between small molecules and proteins of interest to be probed using methods such as target immobilised NMR screening (TINS) (Siegal and Hollander, 2009) and surface plasmon resonance (SPR) (Navratilova and Hopkins, 2010).

Biotinylated proteins are rare in nature with only one known in *E. coli* (Fall, 1979), five in S. cerevisiae (Lim *et al.*, 1987) and four in mammalian cells (Robinson *et al.*, 1983; Chandler and Ballard, 1988). Although the *P. shermanii* biotin acceptor domain can be biotinylated endogenously by *S. cerevisiae*, only a small fraction of the available sites were modified (Cronan, 1990). To overcome this problem, a system was developed that allows CLBH-tagged proteins to be biotinylated *in vitro*.

Biotin ligase was amplified from *E. coli* strain 0157 genomic DNA by PCR, cloned into pGEM T-Easy and then transferred to the *E. coli* expression vector pET15b (Figure 3.15).

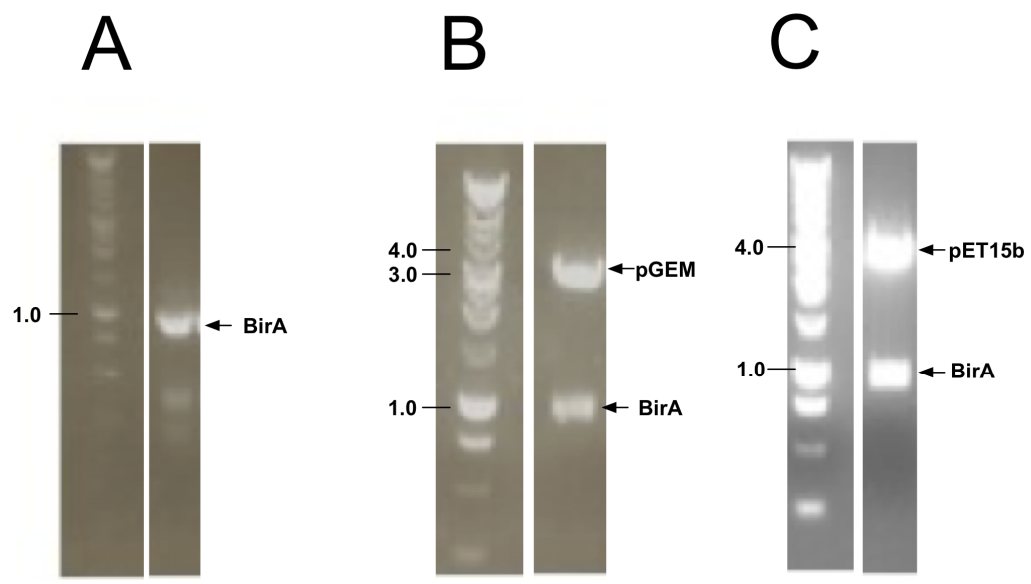

Figure 3.15 PCR amplification of biotin ligase and cloning into pET15b
(A) Biotin ligase (BirA) was amplified by PCR from *E. coli* strain 0157 and (B) sub-cloned into pGEM T-Easy. Recombinant plasmids were identified by digesting with *Eco*RI which yielded fragments of 3.0 (corresponding to pGEM) and 1.0 Kb (BirA). (C) The cDNA encoding biotin ligase was sub-cloned from pGEM T-Easy to pET15b. Recombinant plasmids were identified by restriction digestion with *Pvu*I, yielding fragments of 5.6 (pET15b) and 1.0 Kb (BirA) (Section 2.3.9).

Biotin ligase was expressed in *E. coli*, and purified by Ni^{2+}-affinity chromatography by virtue of a His_6 tag located at the N-terminus of the recombinant protein. Elution fractions from the Ni^{2+} column were analysed by SDS-PAGE. A single band with a MW of 37 kDa was observed, indicating that biotin ligase had been successfully purified in a single step (Figure 3.16).

The activity of recombinant biotin ligase was assessed by biotinylating detergent-solubilised SI-CLBH *in vitro*. Ni^{2+}-affinity purified SI-CLBH (Section 3.4) was incubated with biotin ligase, 50 μM biotin, 20 μM ATP and 10 mM magnesium-o-acetate overnight at 4°C. Following biotinylation, SI-CLBH was desalted twice (to remove the biotin) before mixing with streptavidin beads. Following this, the beads were transferred to a gravity-feed column where they were washed extensively. When the column was viewed under UV light, the streptavidin beads were brightly fluorescent indicating that SI-CLBH had been successfully immobilised. This demonstrated that the recombinant biotin ligase was active.

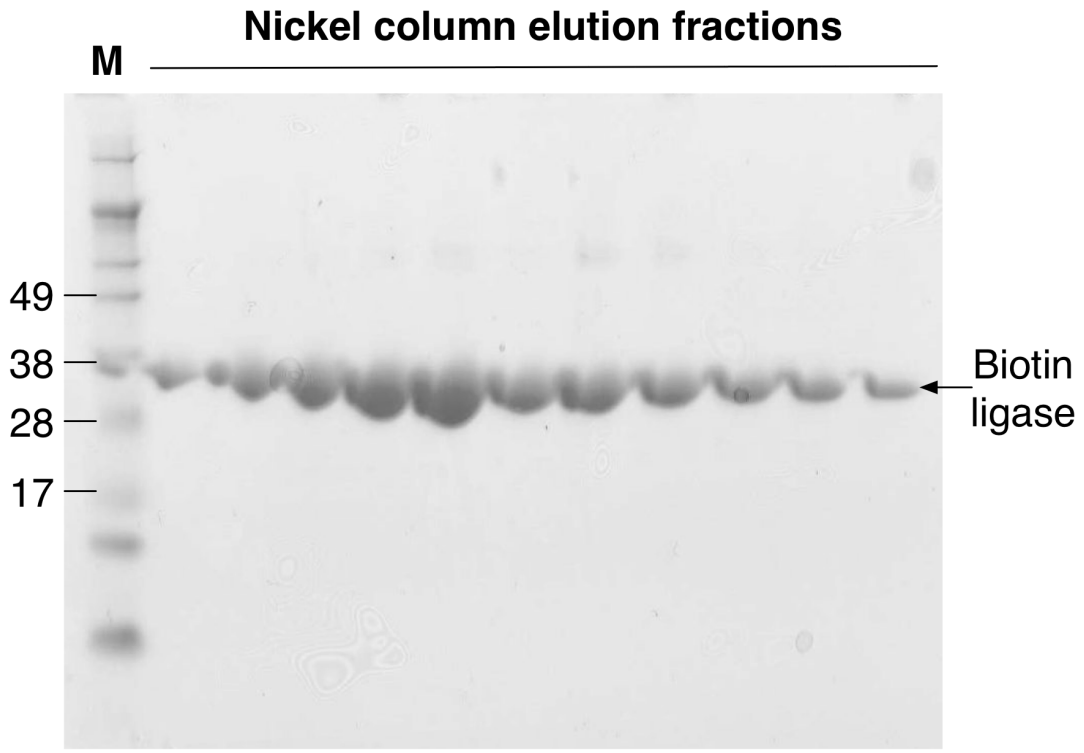

Figure 3.16 SDS-PAGE analysis of pure biotin ligase
Recombinant biotin ligase was expressed in *E. coli* and purified by Ni^{2+}-affinity chromatography (Section 2.8.6.2). Peak elution fractions were analysed by SDS-PAGE. A single band at *ca.* 37 kDa corresponding to pure BirA was observed.

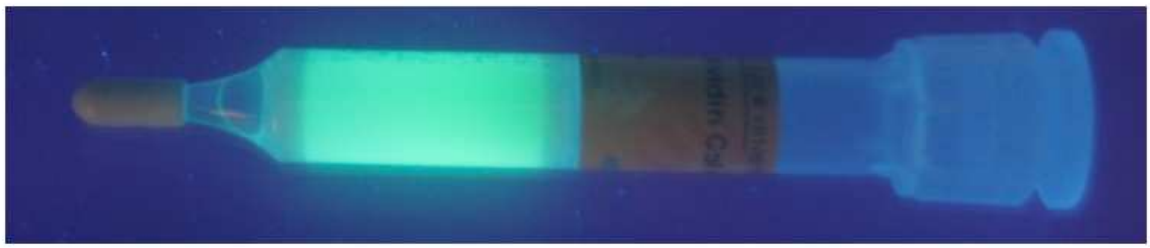

Figure 3.17 Immobilisation of SI-CLBH on streptavidin beads following *in vitro* biotinylation
SI–CLBH was biotinylated *in vitro* using recombinant biotin ligase (Section 2.8.6.2). The sample was desalted and loaded onto a streptavidin column. Following extensive washing, the column was viewed under UV light. The streptavidin beads were brightly fluorescent indicating that SI-CLBH had been successfully immobilised.

3.6 Conclusion

The CLBH tag is an attractive system for the recombinant expression, purification, characterisation and immobilisation of human membrane proteins. In this chapter, the properties and applications of the CLBH tag were investigated.

iLOV is a novel fluorescent reporter derived from the LOV2 domain of *A. thaliana* phototropin 2. Here, the spectral properties of iLOV were characterised, and optimal wavelengths for selective excitation of (λ = 450 nm) as well as measuring fluorescence emission from (λ = 485 nm) iLOV identified. Using these wavelengths, it was possible to monitor CLBH-tagged membrane proteins both *in vivo* and *in vitro*. For example, the expression level of SI-CLBH in fermenter culture could be monitored by measuring iLOV fluorescence, eliminating the need for time-consuming methods such as radioligand binding or Western Blotting to establish the production level of the protein of interest. By measuring whole cell iLOV fluorescence at regular intervals, the expression of CLBH tagged membrane proteins can be readily optimised. *In vitro*, iLOV can be used for determining the aggregation status of CLBH-tagged membrane proteins in detergent solution by FSEC as well as for tracking recombinant proteins throughout their purification.

Using the CLBH tag, human sterol isomerase was purified to homogeneity in four simple steps (Ni^{2+}-affinity purification; cleavage with 3C protease; reverse Ni^{2+}-affinity purification; gel filtration). Allowing for the exceptionally high expression levels observed with SI, it should be possible to purify other CLBH-tagged membrane proteins in the same way. Where necessary, however, a second affinity purification step could be introduced by biotinylating the CLBH tag *in vitro* with biotin ligase, and then applying the protein mixture to (strept)avidin resin.

The ability to immobilise target proteins on (strept)avidin-coated surfaces was particularly exciting as it opens up the possibility of studying the interaction of small molecular fragments and proteins of interest by techniques such as TINS and SPR, an important step in designing highly-specific novel drugs. In relation

to this thesis, if aldosterone synthase and 11β-Hydroxylase could be immobilised on a streptavidin surface, it may be possible to identify molecular fragments which bind to one enzyme and not the other, allowing specific inhibitors to be designed.

Having developed a generic approach for making and purifying recombinant proteins, the CLBH tag was used to obtain pure adrenodoxin and adrenodoxin reductase (Chapter 4), and gave critical insights into the expression and purification of aldosterone synthase and 11β-Hydroxylase (Chapter 5).

Chapter 4 - Expression, purification and characterisation of human adrenodoxin and adrenodoxin reductase

4.1 Introduction

My primary research goal was to purify milligram quantities of functional human 11β-Hydroxylase and aldosterone synthase for structural studies and drug discovery purposes. Before either p450 could be used in crystallisation trials or high-throughput screening assays, however, it was necessary to show that the enzymes were fully functional. P450 activity can be measured in several different ways including determining the rate of substrate consumption, product formation or NADPH oxidation. Irrespective of which approach is chosen, any activity assay developed for use with either 11β-Hydroxylase or aldosterone synthase will require inclusion of their electron donors adrenodoxin (Adx) and adrenodoxin reductase (AdxRed).

In Chapter 3, a generic system for the recombinant expression and purification of human proteins was described. Here, the CLBH tag was used to obtain milligram amounts of pure Adx and AdxRed with a view to developing a reconstituted electron transfer system *in vitro* for use with both 11β-Hydroxylase and aldosterone synthase. Furthermore, initial results from the 1000 genomes project has revealed that there are a large number of non-synonomous SNPs in the coding regions of both Adx and AdxRed in the general population (www.1000genomes.org). As yet, how these SNPs affect the rates of aldosterone and cortisol synthesis *in vivo*, if at all, is not known. As a first step towards understanding the properties of naturally occurring Adx and AdxRed variants *in vitro*, the wild-type proteins have been biophysically characterised and crystallisation efforts attempted.

4.2 PCR amplification of mature human adrenodoxin and adrenodoxin reductase

Although Adx and AdxRed function in the mitochondria, they are both nuclear-encoded and translated in the cytoplasm as pre-proteins with molecular weights (MW) of 19 and 54 kDa, respectively. Following import into mitochondria, their N-terminal targeting sequences are removed to give mature forms of both proteins (Adx, MW 13 kDa; AdxRed, 50 kDa) (Matocha and Waterman, 1984; Vonrhein *et al.*, 1999).

cDNAs encoding the mature forms of Adx (αα 61-184) and AdxRed (□□ 33-491) were generated by PCR and transferred into the cloning vector pGEM T-Easy (Section 2.3.4). Recombinant plasmids containing mature human Adx and AdxRed cDNAs were identified by restriction digestion with *Eco*RI (Figure 4.1), and then sequenced to check that no mutations had been introduced during the PCR step.

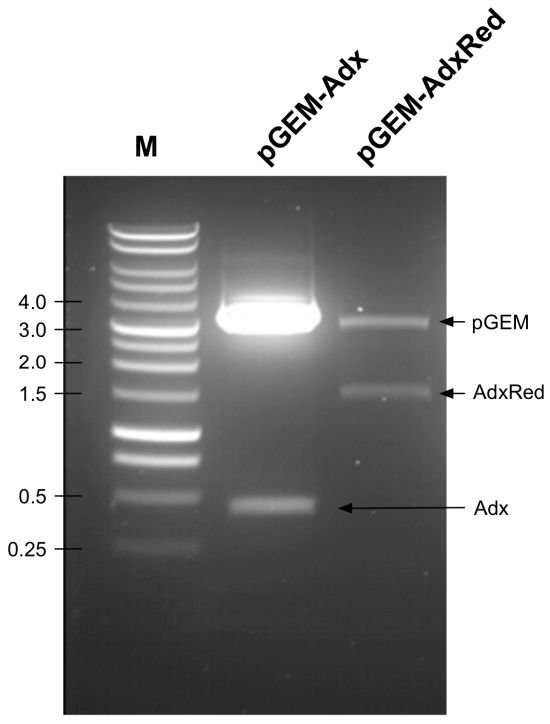

Figure 4.1 Restriction analysis of pGEM plasmids containing human Adx and AdxRed
cDNAs encoding the mature forms of human Adx and AdxRed were generated by PCR (Section 2.3.2) and sub-cloned into pGEM T-Easy (Section 2.3.4). Recombinant plasmids were identified by restriction digestion with *Eco*RI. The digests were resolved on a 1% agarose gel (Section 2.3.1.2). DNA fragments of size 3.0 (pGEM T-Easy), 0.4 (Adx) and 1.5 Kb (AdxRed) were observed.

4.3 Expression and partial purification of adrenodoxin reductase using the *P. pastoris* CLBH system

4.3.1 Vector construction

Initially, the expression of AdxRed was attempted using the *P. pastoris* CLBH expression system described in Chapter 3. The cDNA encoding human AdxRed was excised from pGEM T-Easy by digestion with *Eco*RI and *Not*I, isolated and then transferred into the equivalent cloning sites in the (pPICZ)A-CLBH vector. Recombinant plasmids were identified by restriction digestion with *Eco*RI and *Not*I (Figure 4.2). The AdxRed-CLBH construct was subsequently transformed into *P. pastoris* strain X33 by electroporation (Section 2.4.2.2).

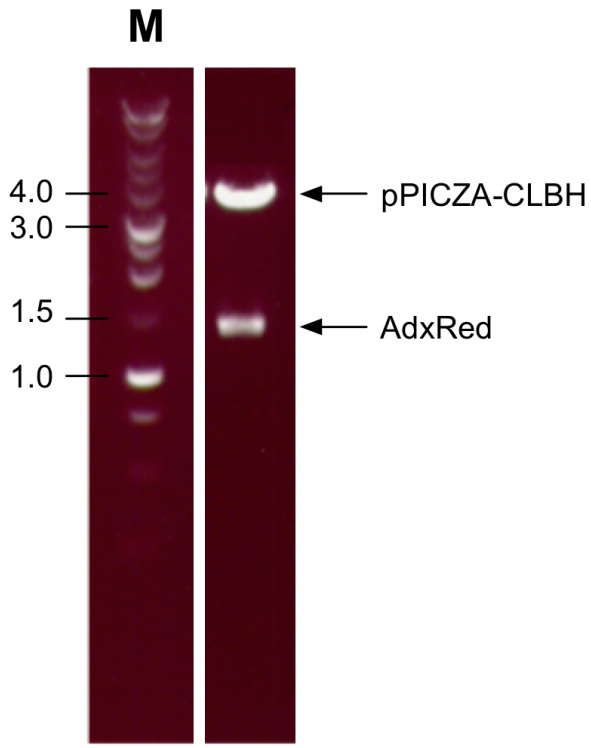

Figure 4.2 Restriction analysis of pPICZA - AdxRed - CLBH
The cDNA encoding mature AdxRed was sub-cloned from pGEM T-Easy to pPICZA-CLBH using the restriction enzymes *Eco*RI and *Not*I (Section 2.3.5). Recombinant expression plasmids containing AdxRed were identified by digesting the yeast vector with *Eco*RI and *Not*I. Fragments were resolved on a 1% agarose gel (Section 2.3.1.2). Bands corresponding to pPICZA-CLBH and AdxRed were observed at *ca.* 4.0 and 1.5 Kb, respectively.

4.3.2 Production of AdxRed-CLBH in *P. pastoris*

Following transformation of an expression plasmid into *P. pastoris*, a range of colonies must be screened to identify the clone expressing the highest levels of recombinant protein (Macauley-Patrick *et al.*, 2005). The expression level of a CLBH-tagged recombinant protein in whole cells can be rapidly determined by measuring fluorescence from the iLOV reporter (Section 3.2.3). Clonal selection was performed on a series of AdxRed-CLBH yeast colonies. Transformants were grown up overnight at 30°C in 1 ml cultures of BMGY (a basal medium) in a 48-well plate. AdxRed-CLBH expression was induced by replacing the BMGY with BMMY (an induction medium), and the yeast incubated for a further 24 h at 22°C. The test expression experiments for each colony were performed in duplicate. Cells were harvested by centrifugation, washed twice and then resuspended in 1 ml of water. The cells were then transferred (in duplicate) to a 96-well plate, where iLOV fluorescence was measured ($\lambda_{excitation}$ = 450 nm, $\lambda_{emission}$ = 520 nm). For each transformant, the quantity of whole cell iLOV per ml of culture was determined (Figure 4.3). Disappointingly, the fluorescence levels in the AdxRed transformants were not much higher than the X33 control, suggesting that *P. pastoris* is a poor host for expressing AdxRed. Despite the production levels of AdxRed-CLBH being low, the transformant that expressed the most recombinant protein was retained for further analysis.

The highest expressing Adx-CLBH yeast transformant was grown in fermenter culture to purify the recombinant protein. In a bioreactor, the yeast's growth environment (including dissolved oxygen content, media pH, growth temperature and carbon source feed rates) can be tightly controlled ensuring that maximal cell densities and recombinant protein expression levels are obtained. AdxRed expression in fermenter culture was carried out as described in Section 2.5.2. In short, the yeast was first grown on glycerol to increase the culture's biomass. After this, the culture was starved (to ensure that all of the added glycerol had been consumed) before the carbon source was switched to methanol. When the induction phase was complete, the cells were harvested.

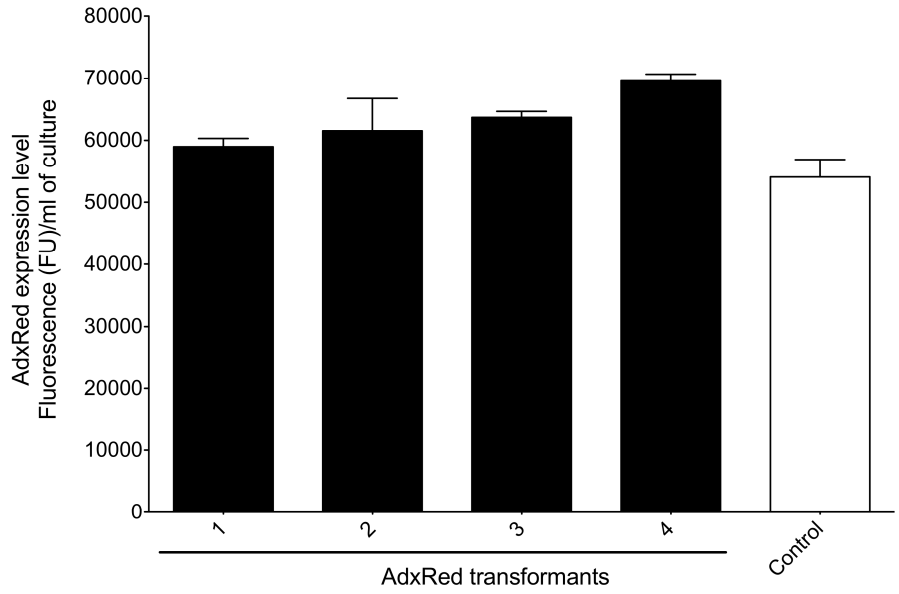

Figure 4.3 Clonal analysis of *P. pastoris* transformants expressing AdxRed-CLBH
AdxRed-CLBH transformants were grown up overnight at 30°C in 1 ml cultures of BMGY. Recombinant protein production was induced by replacing the media with BMMY and then incubating the yeast at 22°C for 24 h. AdxRed production levels were determined by measuring iLOV fluorescence from whole cells (Section 2.5.1).

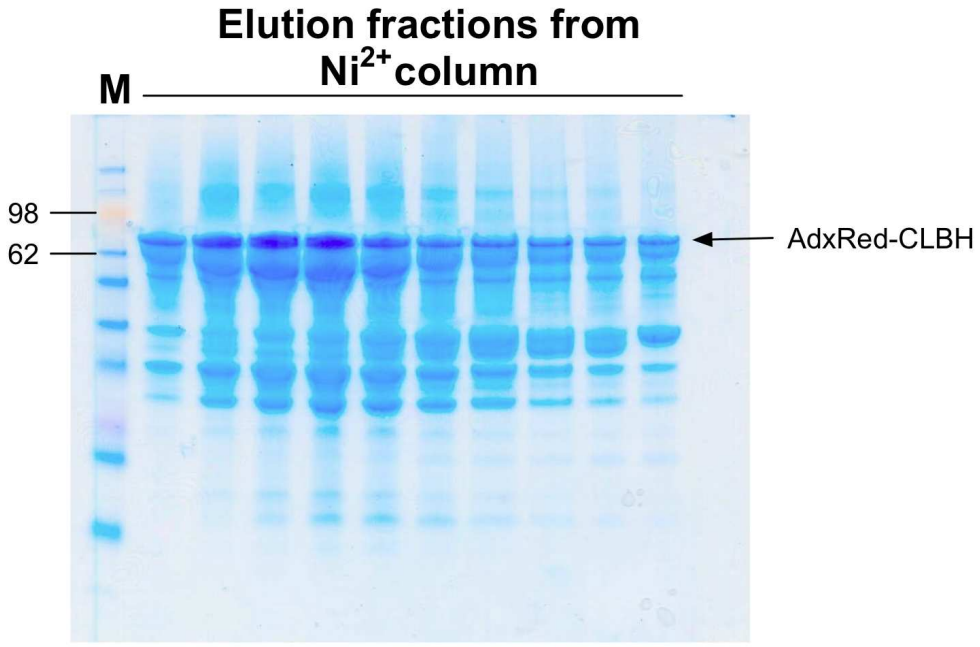

Figure 4.4 SDS-PAGE analysis of Ni^{2+}-enriched AdxRed-CLBH
AdxRed that had been expressed in *P. pastoris* was purified by Ni^{2+}-affinity chromatography. Fluorescent elution fractions containing AdxRed-CLBH were analysed by SDS-PAGE. Samples were resolved on a 10% Bis-Tris gel. A band at *ca*. 75 kDa was tentatively identified as AdxRed-CLBH (actual MW 73 kDa).

Cells were resuspended in buffer A (150 mM NaCl in 50 mM Tris HCl pH7.4), and lysed using a cell disrupter. Cellular debris was removed by centrifugation at low speed (10,000g). The supernatant, which contained the AdxRed-CLBH, was retained. Consistent with the clonal selection results, the iLOV fluorescence in the supernatant was low, indicating that AdxRed-CLBH is expressed at low levels in *P. pastoris* even in fermenter culture.

A purification of AdxRed was attempted from 1.5 kg of yeast cell biomass. Following disruption, the cell lysate volume was so large that, to make the purification manageable, ammonium sulphate precipitation was performed and a series of fractions generated. The fraction that had the highest fluorescence was dialysed overnight at 4°C against buffer B (75 mM imidazole, 150 mM NaCl in 50 mM Tris HCl pH 7.4), before it was applied to a Ni^{2+} column. The column was washed with 10 column volumes of buffer B before AdxRed-CLBH was eluted using buffer C (300 mM imidazole, 150 mM NaCl in 50 mM Tris HCl pH 7.4). Elution fractions which were fluorescent (and therefore expected to contain AdxRed-CLBH) under UV-illumination were analysed by SDS-PAGE (Figure 4.4). A band observed at *ca.* 75 kDa was tentatively identified as AdxRed-CLBH. However, the presence of numerous other contaminant proteins in the elution fractions suggested that further purification steps would be required before pure AdxRed could be obtained.

Ultimately, the expression level of AdxRed in *P. pastoris* was too low for easy purification. It was concluded, therefore, that it would be necessary to use an alternative expression system for AdxRed.

4.4 An *E. coli* CLBH expression vector for expressing adrenodoxin and adrenodoxin reductase

Having encountered difficulties in making AdxRed in *P. pastoris*, expression of Adx and AdxRed in *E. coli* was now explored. Modified pET21a expression vectors containing the –CLBH tag and either the mature Adx or AdxRed cDNA were generated by way of a two-step ligation strategy (Figure 4.5). The –CLBH tag was amplified by PCR using the pPICZA vector as template (Figure 4.6A). The oligonucleotide primers used for PCR amplification contained restriction sites that would allow the CLBH tag to be cloned into pET21a (5'-3' primer, *Not*I; 3'-5', *Bam*HI). In the first instance, however, the CLBH PCR product was transferred into pGEM T-Easy. Recombinant plasmids containing the CLBH cDNA were identified by restriction analysis (Figure 4.6B). The –CLBH tag was released from pGEM T-Easy by digesting with *Not*I and *Bam*HI. The mature human Adx and AdxRed cDNAs, previously amplified and sub-cloned into pGEM T-Easy (Figure 4.1), were released from the vector using *Nde*I (part of the pGEM multi-cloning site) and *Not*I. The Adx and AdxRed cDNAs were ligated to CLBH via their *Not*I overhangs (Figure 4.5A). The Adx(Red)-CLBH fragment was then ligated to pET21a vector that been previously treated with *Nde*I and *Bam*HI (Figure 4.5B). Correctly assembled, recombinant pET21a - Adx(Red) - CLBH vector (Figure 4.5C) was identified by restriction analysis with *Nde*I (Figure 4.7).

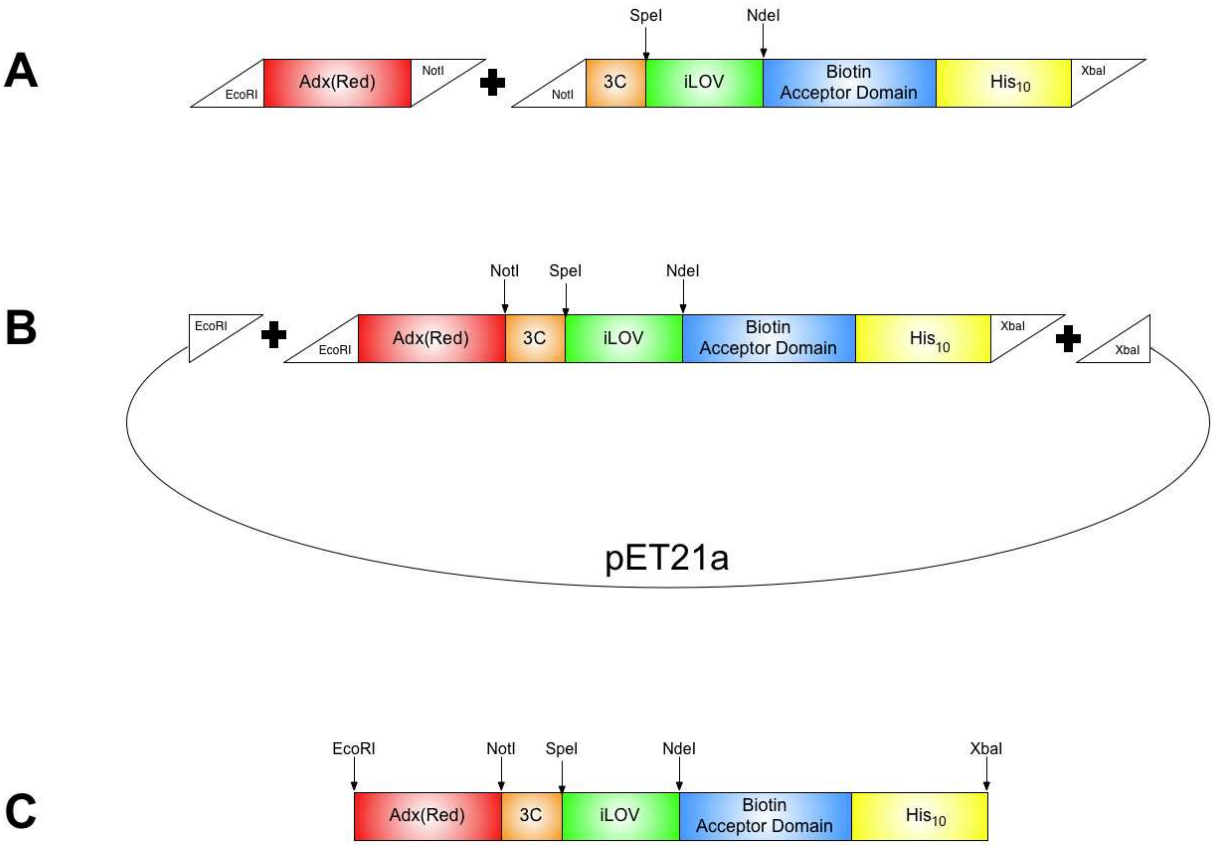

Figure 4.5 Schematic diagram illustrating the two-step ligation strategy used to make the pET21a – Adx(Red) – CLBH *E. coli* expression vectors

(A) Mature Adx and AdxRed cDNAs were ligated first to the CLBH tag, and then (B) to the pET21a vector to create (C) pET21a - Adx(Red) – CLBH.

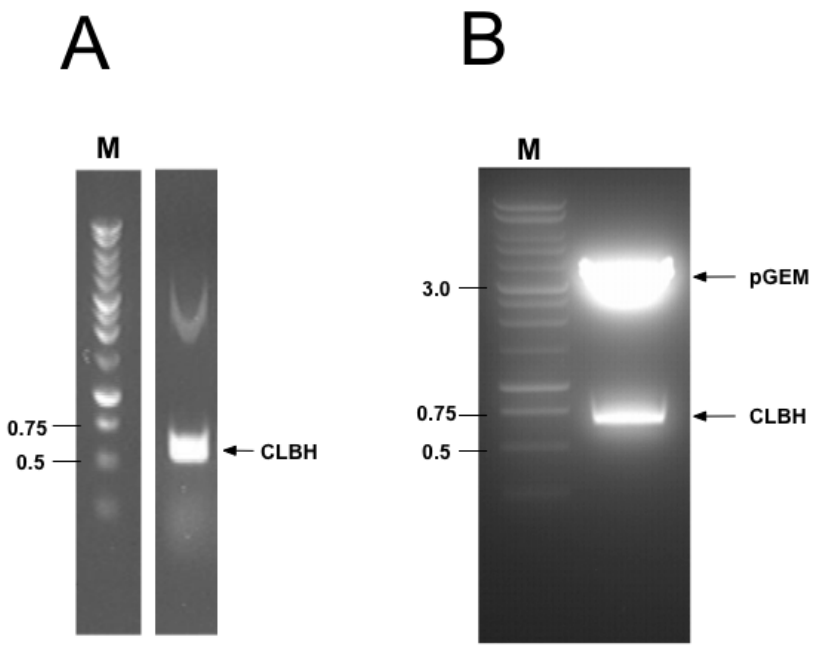

Figure 4.6 PCR amplification of the CLBH tag and restriction analysis of pGEM-CLBH
(A) The -CLBH tag was amplified by PCR using the pPICZA vector as template and sub-cloned into pGEM T-Easy (Section 2.3.3). (B) Recombinant plasmids were identified by restriction analysis with *Eco*RI, yielding fragments of *ca.* 3.0 (vector) and 0.6 Kb (CLBH).

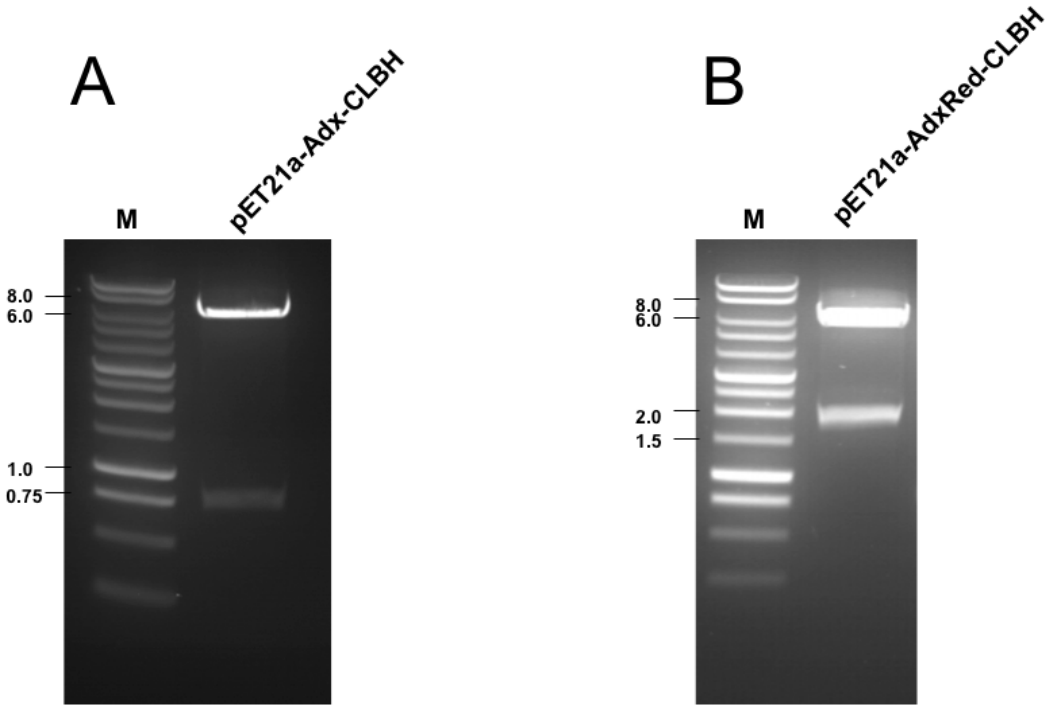

Figure 4.7 Restriction analysis of pET21a – Adx(Red) – CLBH
Recombinant plasmids were identified by restriction analysis with *Nde*I. Digestion of the Adx and AdxRed vectors with *Nde*I gave fragments with sizes (Adx, 5.4 and 0.7; AdxRed, 5.4 and 1.8 Kb) consistent with correct assembly of the recombinant plasmids.

4.5 Purification of adrenodoxin and adrenodoxin reductase from *E. coli*

4.5.1 Expression of adrenodoxin and adrenodoxin reductase in *E. coli*

Adx- and AdxRed-CLBH were expressed in *E. coli* as described in Section 2.6.1, and then harvested by centrifugation. Cell pellets were resuspended in 150 mM NaCl, 0.1 mM EDTA in 50 mM Tris-HCl pH 7.4. Expression of both CLBH-tagged proteins could be easily monitored by illuminating the cells with UV light and observing fluorescence from the iLOV reporter. In contrast to the poor expression levels of AdxRed in *P. pastoris*, substantial whole cell iLOV fluorescence was observed for both Adx and AdxRed following expression in *E. coli*. This allowed quick progression to the development of purification protocols for both electron transfer proteins.

4.5.2 Purification of adrenodoxin

Following expression, the *E. coli* cells were lysed by mechanical rupturing and Adx-CLBH purified by Ni^{2+}-affinity chromatography as described for AdxRed-CLBH expressed in *P. pastoris* (Section 4.3.2). Following elution from the nickel column, fractions containing partially purified Adx-CLBH were brown in colour and fluoresced green when viewed under UV light (Figure 4.8 A, B). When the Ni^{2+}-enriched sample was analysed by SDS-PAGE, a strong band with a molecular weight of *ca.* 38 kDa thought to correspond to Adx-CLBH was observed (Figure 4.8C). The fluorescent fractions were pooled and desalted to remove the imidazole present in the elution buffer. The –CLBH tag was removed from Adx by incubating the sample with 3C protease at 4°C overnight. Adx was then further purified by reverse Ni^{2+}-affinity chromatography. The cleavage mixture was applied to a fresh Ni^{2+} column which bound the –CLBH tag, His-tagged 3C protease as well as contaminant proteins that had non-specifically bound to the original Ni^{2+} column but not Adx. Brown fractions containing Adx were pooled and concentrated before they were applied to a Superose 6 gel filtration column. The SEC elution profile consisted of a single sharp, symmetrical peak (Figure 4.9A), suggesting that Adx was both pure and monodisperse. Peak fractions from the gel filtration step were analysed by SDS-PAGE. A single band

was observed at *ca.* 13 kDa confirming that the Adx was pure (Figure 4.9B). Purified human Adx had a characteristic ferrodoxin absorption spectrum with

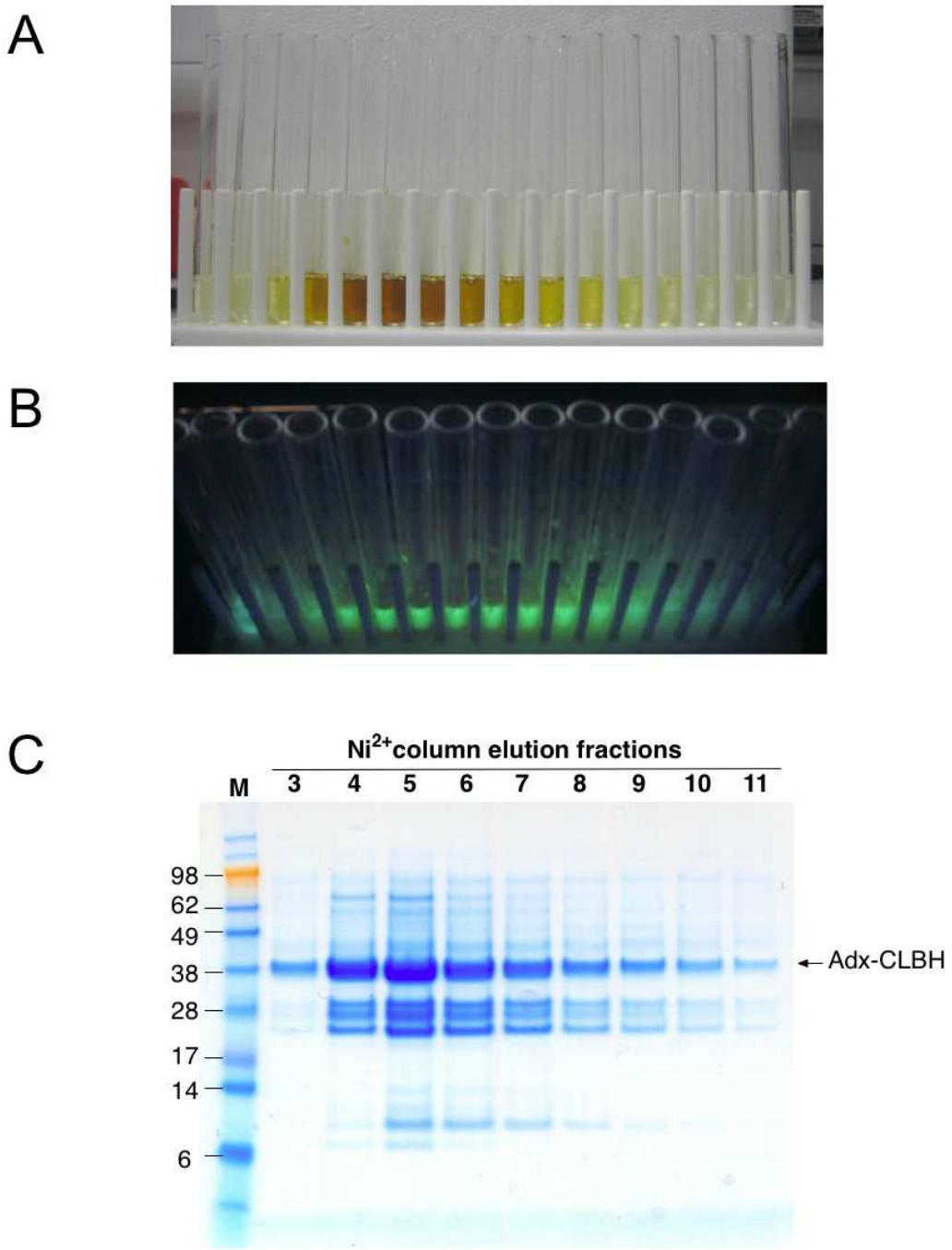

Figure 4.8 Visualisation and SDS-PAGE analysis of Ni^{2+}-affinity purified Adx-CLBH
Fractions containing Ni^{2+}-enriched Adx-CLBH were (A) brown under natural light and (B) fluorescent green following illumination with UV-radiation. (C) The elution fractions from the Ni^{2+} column were analysed by SDS-PAGE. The gel showed a major band clearly visible at *ca.* 38 kDa which was thought to be Adx-CLBH (predicted MW 37 kDa).

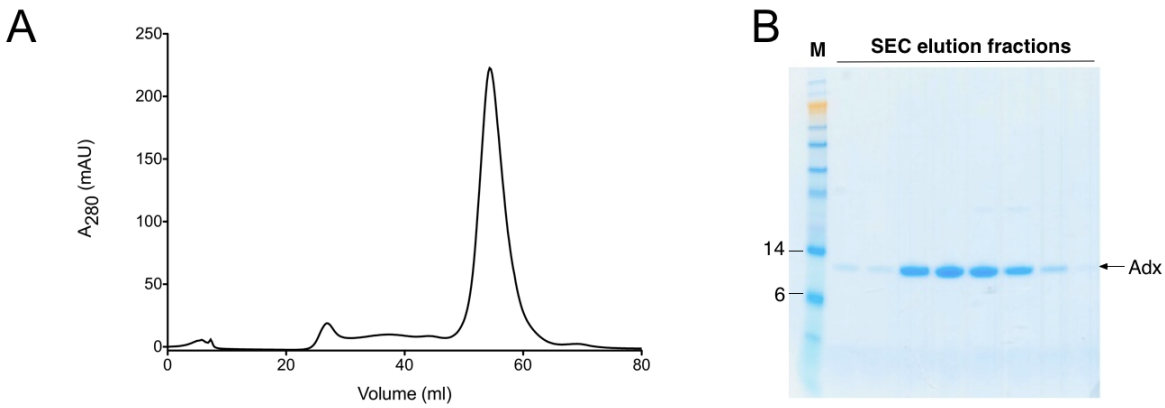

Figure 4.9 Pure Adx
Highly-enriched Adx was applied to a Superose 6 gel filtration column (Section 2.8.2). (A) The SEC elution profile consisted of a single sharp symmetric peak suggesting that Adx was both pure and monodisperse. (B) Peak fractions were analysed by SDS-PAGE (Section 2.9). A single band was observed at *ca.* 13kDa confirming that Adx was pure.

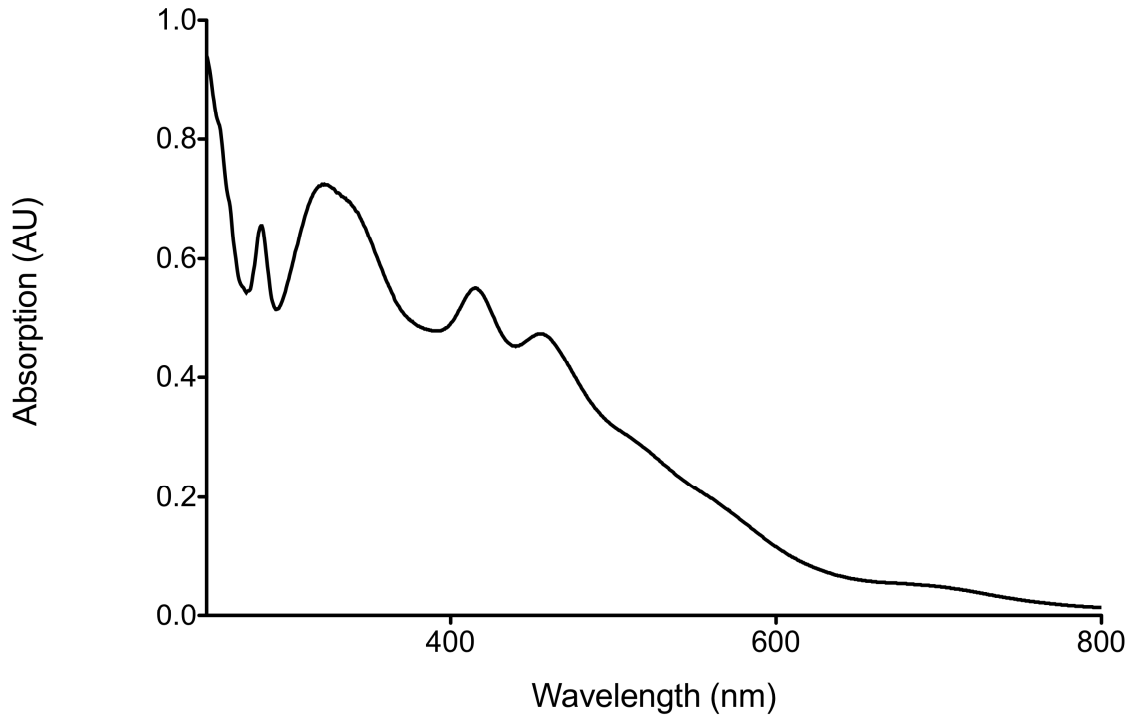

Figure 4.10 Absorption spectrum of pure human Adx
The absorption spectrum of pure human Adx displays a characteristic ferrodoxin absorption spectrum with maxima at 322, 414 and 455 nm.

maxima arising from the iron-sulfur cluster at 322, 414 and 455 nm (Figure 4.10). The concentration of pure Adx was determined using a calculated extinction coefficient based on the amino acid content of the recombinant protein (Adx ε_{280} = 3230 $M^{-1}cm^{-1}$).

4.5.3 Purification of adrenodoxin reductase

AdxRed-CLBH was purified by Ni^{2+}-affinity chromatography in the same way as that for Adx-CLBH (Section 4.5.2). Elution fractions from the Ni^{2+} column were yellow when viewed under natural light (Figure 4.11A), and fluorescent green when illuminated with UV radiation (Figure 4.11B). SDS-PAGE analysis of the Ni^{2+} elution fractions showed that AdxRed-CLBH was only partially pure (Figure 4.11C). A band with a MW of *ca.* 70 kDa was tentatively identified as AdxRed-CLBH. Next, the partially purified AdxRed-CLBH was desalted, cleaved by overnight incubation with 3C protease and reverse-purified using a fresh Ni^{2+} column. The highly-enriched AdxRed sample was applied to a Superose 6 gel-filtration column. The SEC elution profile had a single sharp peak suggesting that AdxRed was both pure and monodisperse (Figure 4.12A). Peak fractions were analysed by SDS-PAGE. A single band with a MW of *ca.* 49 kDa was observed, showing that AdxRed was pure (Figure 4.12B). The absorption spectrum of human AdxRed consists of a broad absorption peak in the region 360-380 nm and a second peak at 450 nm with shoulders at 425 and 475 nm (Figure 4.13).

The concentration of pure AdxRed was determined using a calculated extinction coefficient based on the amino acid content of the recombinant protein (AdxRed ε_{280} = 45295 $M^{-1}cm^{-1}$).

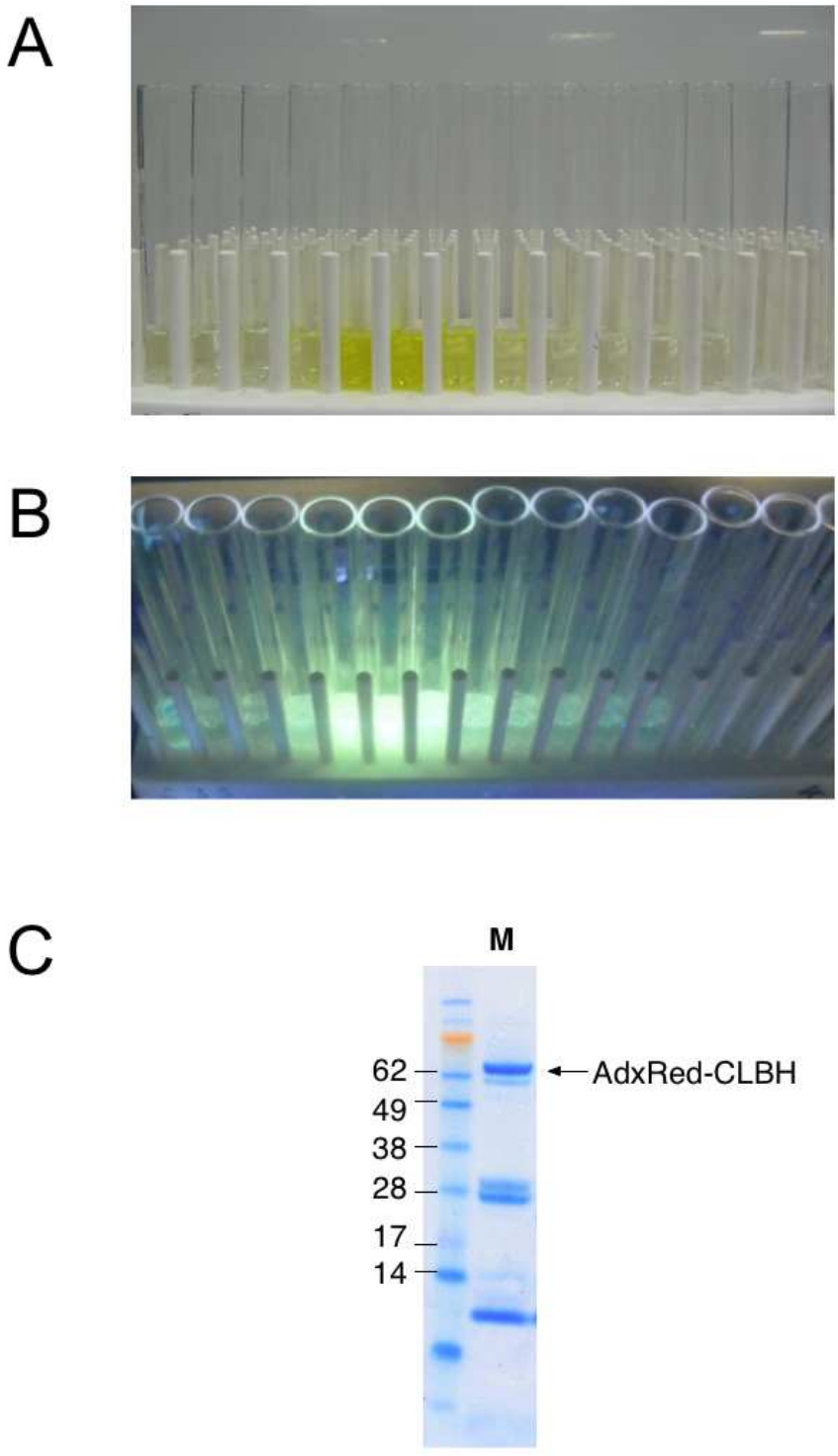

Figure 4.11 Visualisation and SDS-PAGE analysis of Ni^{2+}-affinity purified AdxRed-CLBH
Fractions containing AdxRed-CLBH were (A) yellow under natural light and (B) fluorescent green when illuminated with UV-light. (C) The elution fractions were analysed by SDS-PAGE (Section 2.9). A band at *ca.* 70 kDa was tentatively identified as AdxRed-CLBH.

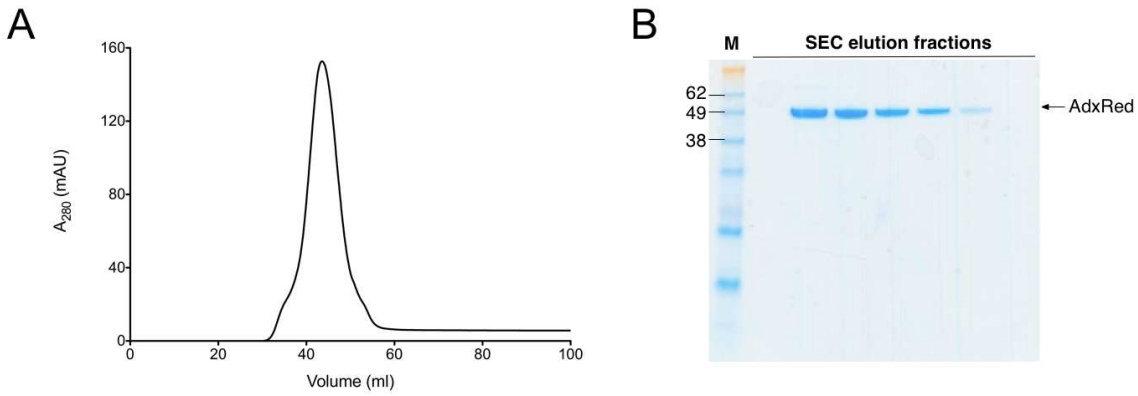

Figure 4.12 Pure AdxRed
A highly-enriched, concentrated AdxRed sample was applied to a Superose 6 gel filtration column (Section 2.8.3). (A) The SEC elution profile consisted of a single sharp symmetric peak suggesting that AdxRed was both pure and monodisperse. (B) Peak fractions were analysed by SDS-PAGE (Section 2.9). A single band was observed at *ca.* 49 kDa confirming that the AdxRed was pure.

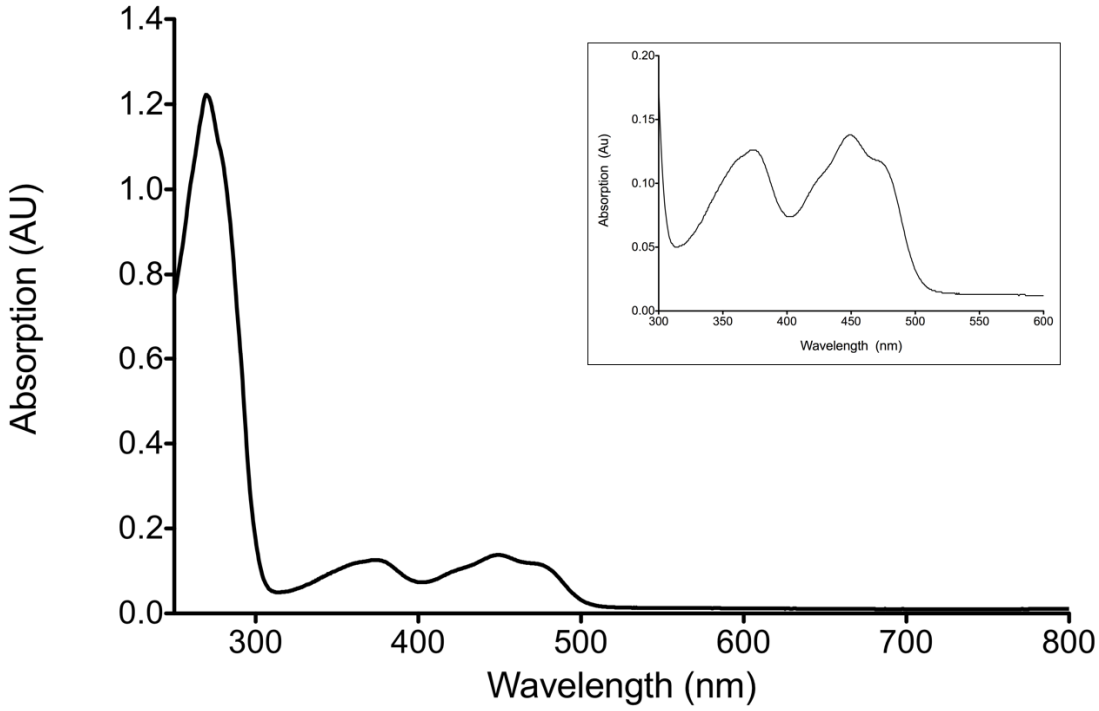

Figure 4.13 Absorption spectrum of pure AdxRed
The absorption spectrum of human AdxRed consists of a broad absorption peak between 360 and 380 nm, with a second maximum at 450 nm flanked by shoulders at 425 and 475 nm. For experimental detail, see Section 2.8.3.

4.6 Biophysical characterisation of adrenodoxin and adrenodoxin reductase

The primary need for purifying human Adx and AdxRed was to develop activity assays for both aldosterone synthase and 11β-Hydroxylase. In recent years, however, it has become apparent that there are a substantial number of natural variants in both Adx and AdxRed that may affect blood pressure in humans. These proteins are, therefore, worthy of further study in their own right.

4.6.1 Natural variants of adrenodoxin and adrenodoxin reductase

The 1000 genomes project[4] is a comprehensive resource on human genetic variation that lists all of the SNPs that have been identified through sequencing the genomes of numerous people. Thus far, 7 non-synonymous (amino-acid changing) SNPs have been identified in the coding regions of Adx (Table 4.1), with a further 41 discovered for AdxRed (Table 4.2). Although certain of the amino acid changes are conservative in nature (e.g. Adx, Asp132Glu and Val85Ala) others are considerably less so (e.g. Adx, His122Tyr; AdxRed, Pro358Ser and Arg139Trp). To assess whether these amino acid sequence variations affect the rate of electron transfer from NADPH to aldosterone synthase and 11β-Hydroxylase *in vivo*, it will be necessary to construct a series of mutants and test them *in vitro*. Unfortunately, due to time restrictions this was beyond the scope of this thesis. However, as a first step towards expressing, purifying and analysing the properties of the naturally-occurring variants *in vitro*, a biophysical characterisation of both wild-type proteins was performed.

[4] www.1000genomes.org

Table 4.1 Non-synonymous SNPs in the coding regions of Adx

Variant	Amino acid change
219 C/A	73 Asn/Lys
254 T/C	85 Val/Ala
364 C/T	122 His/Tyr
388 A/G	130 Ile/Val
396 T/A	132 Asp/Glu
428 G/C	143 Gly/Ala
532 A/G	178 Ile/Val

Table 4.2 Non-synonymous SNPs in the coding regions of AdxRed

Variant	Amino acid change	Variant	Amino acid change
20 G/T	7 Arg/Leu	866 C/T	289 Thr/Met
120 G/T	40 Gln/His	919 C/T	307 Arg/Cys
235 C/T	79 Arg/Cys	979 C/T	327 Arg/Trp
296 C/T	99 Thr/Met	994 G/A	332 Val/Ile
368 G/A	123 Arg/Gln	1052 C/T	351 Thr/Met
415 C/T	139 Arg/Trp	1061 T/A	354 Met/Lys
419 C/T	140 Ala/Val	1072 C/T	358 Pro/Ser
515 C/T	172 Pro/Leu	1102 T/A	368 Tyr/Asn
538 G/A	180 Val/Met	1103 A/G	368 Tyr/Cys
616 C/A	206 Leu/Ile	1111 C/T	371 Arg/Cys
620 T/G	207 Leu/Trp	1133 C/T	378 Pro/Leu
624 C/G	208 Cys/Trp	1145 A/G	382 Lys/Arg
641 C/T	214 Thr/Met	1220 G/A	407 Arg/Lys
656 G/T	219 Gly/Val	1270 G/A	424 Gly/Ser
680 A/C	227 Lys/Thr	1297 G/T	433 Ala/Ser
748 A/T	250 Met/Leu	1349 T/G	450 Leu/Arg
761 C/T	254 Pro/Leu	1369 C/T	457 Arg/Trp
767 C/T	256 Ala/Val	1432 A/G	478 Thr/Ala
769 C/T	257 Arg/Trp	1441 C/T	481 Pro/Ser
827 C/A	276 Pro/His	1477 C/T	493 Arg/Cys
863 G/A	288 Arg/Gln		

4.6.2 Optimising adrenodoxin stability

When a protein of interest is used in activity assays or for characterisation studies (including structure determination), it is essential that the protein is robust and does not denature. A protein's stability can be affected by a variety of factors including the type, pH and ionic content of the buffer in which it resides. Protein stability can be assessed by measuring the rate of protein denaturation upon exposure to high temperature. Unstable proteins denature more rapidly than stable ones. Protein denaturation can be followed in different ways (e.g. changes in the secondary structure composition of a protein can be followed by circular dichroism (CD)). For those proteins that have co-factors which absorb in the visible region, changes in the spectral properties of the bound chromophore can be used as a reporter of protein denaturation.

The absorption spectrum of Adx has maxima at 322, 414 and 455 nm. The effect of prolonged heat treatment on the absorption profile of Adx was assessed by incubating pure Adx (in 150 mM NaCl, 0.1 mM EDTA in 50 mM Tris HCl pH 7.4) at 45°C for 1 h and recording the spectrum every 5 min (Figure 4.14). The absorption maxima decreased steadily in intensity with time. By 45 min, the maxima at 414 and 455 nm could no longer be distinguished (Figure 4.14). It was concluded that the rate of decrease in absorption at 414 nm that occurs on heating at 45°C for 1 h could be used as a measure of Adx thermostability.

The Adx denaturation assay was adapted for use in a 96-well plate format so that several different buffers could be tested simultaneously. For each condition, measurements were made in triplicate and the decrease in A_{414} plotted against time.

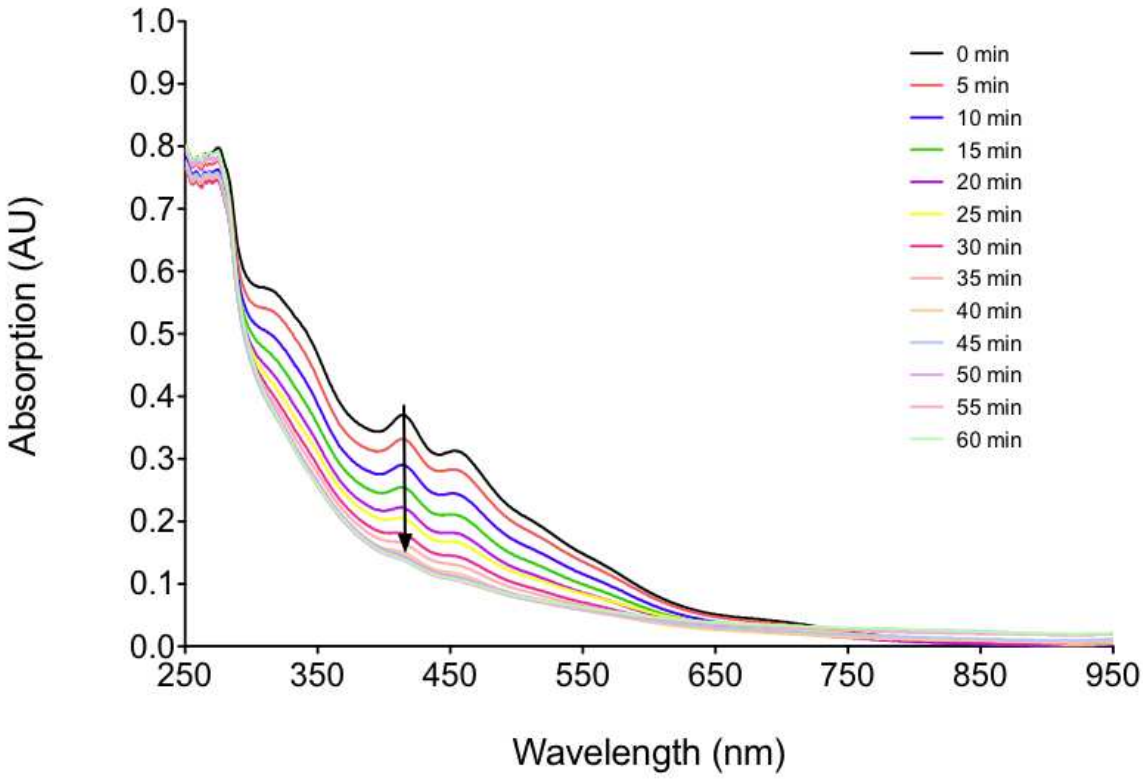

Figure 4.14 Changes in the absorption spectrum of Adx upon prolonged incubation at 45°C
An initial absorption spectrum of Adx was recorded at room temperature (black line) in 50 mM Tris-HCl, 150 mM NaCl, pH 7.4. To monitor the denaturation of Adx over time, the sample was heated at 45℃ for 1 h . Adx spectra were recorded at 5 min intervals.

To identify the optimal buffer for purifying and storing Adx, a series of thermal denaturations were performed in a range of buffers at different pH (MES, pH 5-6; MOPS, 6.5-7.5; HEPES, 6.5-7.5; Tris, 7.5-8.5; sodium phosphate, pH 5-8; CAPS, 9.5-11). Adx used in the thermostability assays had been purified in Tris at pH 7.4. Tris is widely regarded as a harsh buffer and has several drawbacks including a temperature dependent pKa and poor buffering capacity below pH 7.5 (Good *et al.*, 1966; Stoll and Blanchard, 1990). Here, the mildly destabilising tendencies that Tris shows with many proteins was used to identify buffer conditions in which Adx had maximum thermostability.

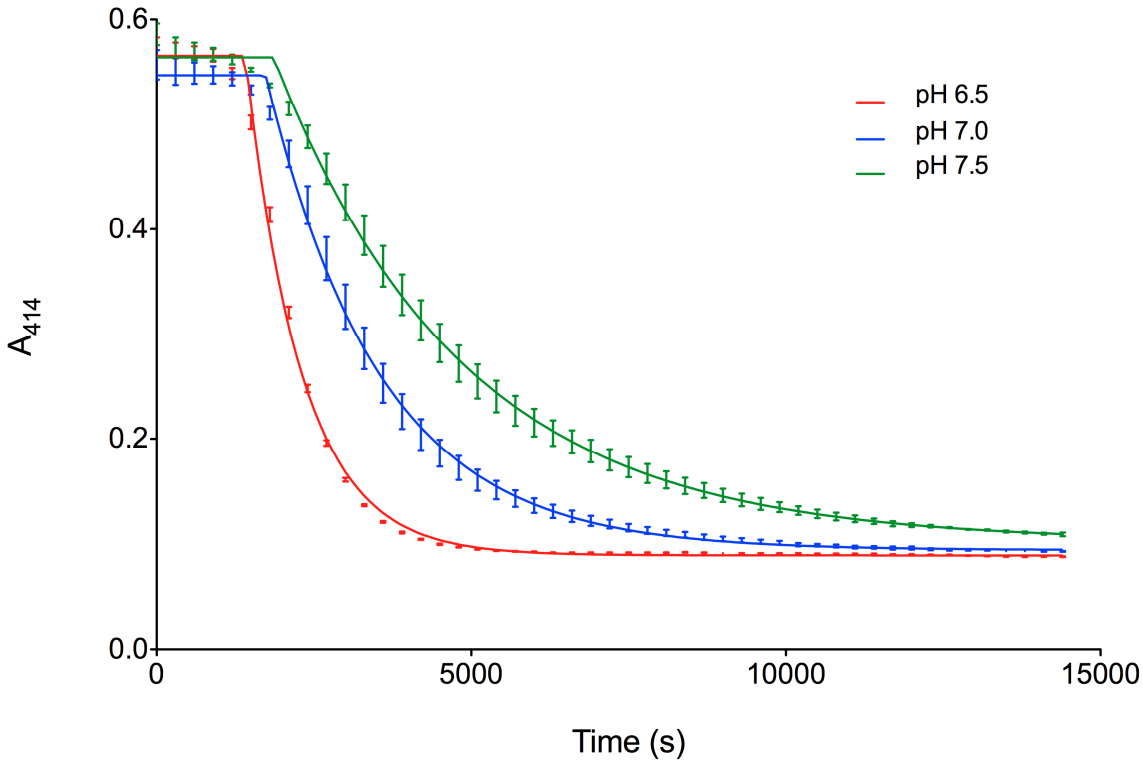

Figure 4.15 Adx stability in MOPS buffer at different pH
Adx was unfolded in the presence of 50 mM MOPS at three different pH values by extended incubation at 45℃. The rate of Adx denaturation was determined by measuring the decrease in A_{414} with time (Section 2.12.1).

Representative data showing Adx denaturation in MOPS buffer at pH 6.5, 7.0 and 7.5 is presented in Figure 4.15. The results clearly showed that the rate of Adx denaturation increased as the pH of the MOPS buffer decreased (Figure 4.15). In MOPS, Adx was most stable at pH 7.5.

To compare Adx stability in different buffers, the percentage of the original A_{414} absorption remaining at 90 min (5400 s) was determined for each condition and plotted as a bar chart (Figure 4.16). This value is a measure of what proportion of Adx had denatured during the course of the assay. The higher the percentage, the more stable Adx was. Adx was most stable in sodium phosphate buffer with a pH value of 8. In this condition, only 15% of the original A_{414} signal had been lost at 5400 s, indicating excellent Adx thermostability. All subsequent Adx purifications were carried out using sodium phosphate buffers at pH 7.4.

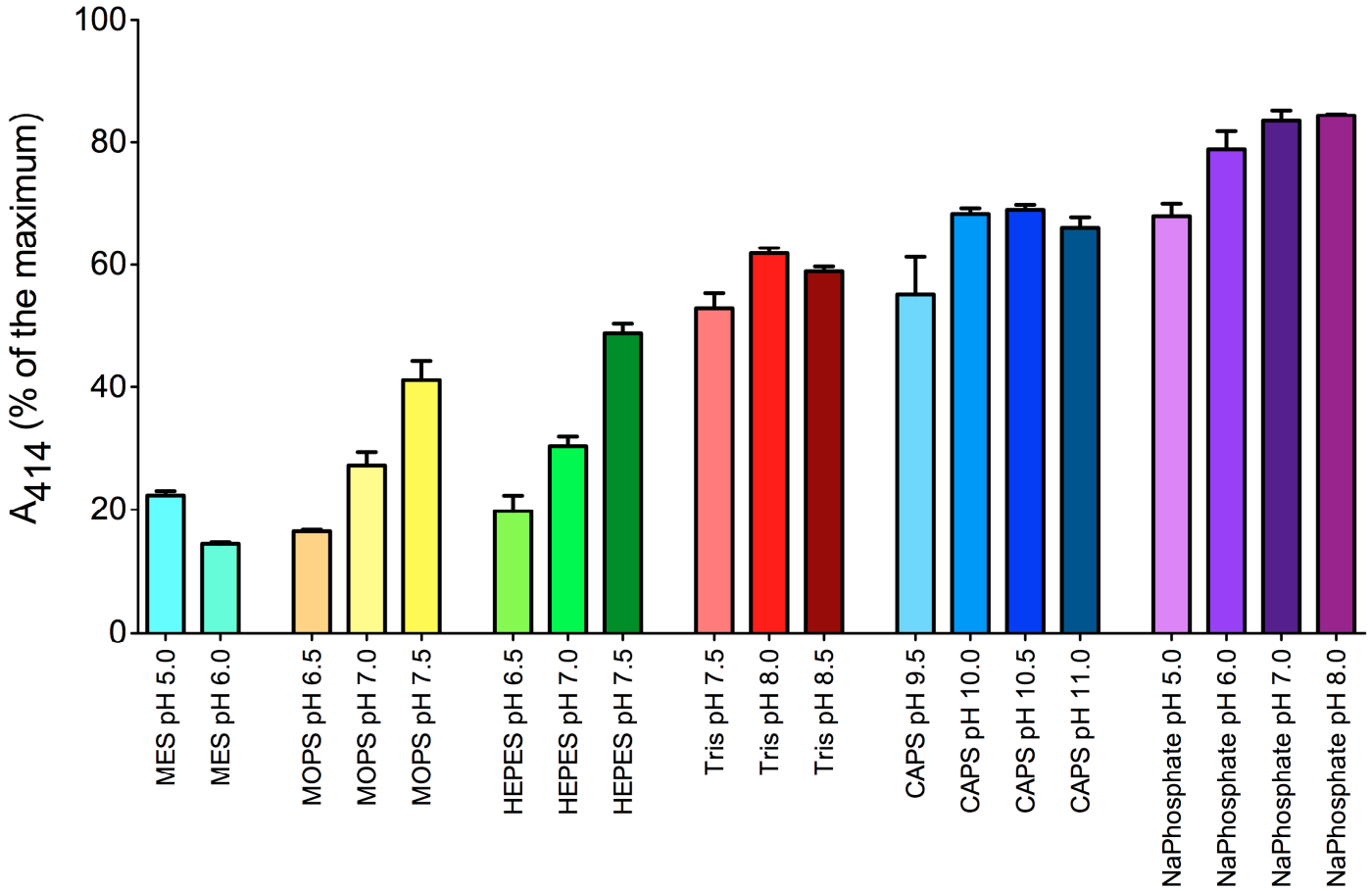

Figure 4.16 Adx stability in different buffer solutions
Adx was unfolded in the presence of a range of buffers with differing pH by extended incubation at 45℃ (Section 2.12.1). The percentage of the original Adx A_{414} absorption remaining at 90 min was determined for each buffer condition and plotted as a bar chart. The higher the percentage, the smaller the amount of Adx that had denatured.

4.6.3 Optimising adrenodoxin reductase stability

AdxRed has a prominent absorption in the region 425 to 475 nm. It was envisaged that a wavelength in this range could be selected for studying the thermal denaturation of AdxRed in a similar way to that used with Adx (Section 4.6.2). An initial experiment was carried out to determine the extent and rate of decrease in A_{450} (wavelength of AdxRed maximum absorption) upon incubating the protein at 45°C. However, it was found that AdxRed was highly unstable; after only five minutes at 45°C the AdxRed had not only fully-denatured but precipitated out of solution also (Figure 4.17).

The extreme instability of AdxRed precluded the option of following a decrease in its absorption by the FAD co-factor with time on heating as an index of stability. Rather, the fluorescence-based CPM assay (Alexandrov *et al.*, 2008) was used to identify buffer conditions in which AdxRed had increased stability as it is sensitive to small changes in protein structure. Mature AdxRed contains 7 Cys residues and is, therefore, suitable for use with the CPM assay. AdxRed was denatured at a fixed temperature of 45°C. Measurements were made on a 96-well plate which allowed several buffer conditions to be screened at once. The amount of fluorescence due to unfolding of AdxRed was determined by subtracting the background fluorescence in a buffer control from that measured in the presence of protein. AdxRed unfolding was studied in the buffers MES, MOPS, HEPES, Tris, CAPS and sodium phosphate over the pH range 5.5-11 (Figure 4.18).

With HEPES, the CPM fluorescence increased with time until a plateau was reached, a typical unfold plot. In certain buffer conditions, however, there was a rapid increase in fluorescence which fell back with time (e.g the unfold experiments in Tris). In these conditions, AdxRed was so unstable that following rapid unfolding the protein precipitated out of solution, explaining the decrease in fluorescence. AdxRed had good stability in MES (pH 5.5, 6), HEPES (6.5, 7., 7.5), MOPS (7.5, 8) and sodium phosphate (4, 5, 6, 7). Of these, HEPES pH 7 was chosen as the optimal buffer for purification purposes.

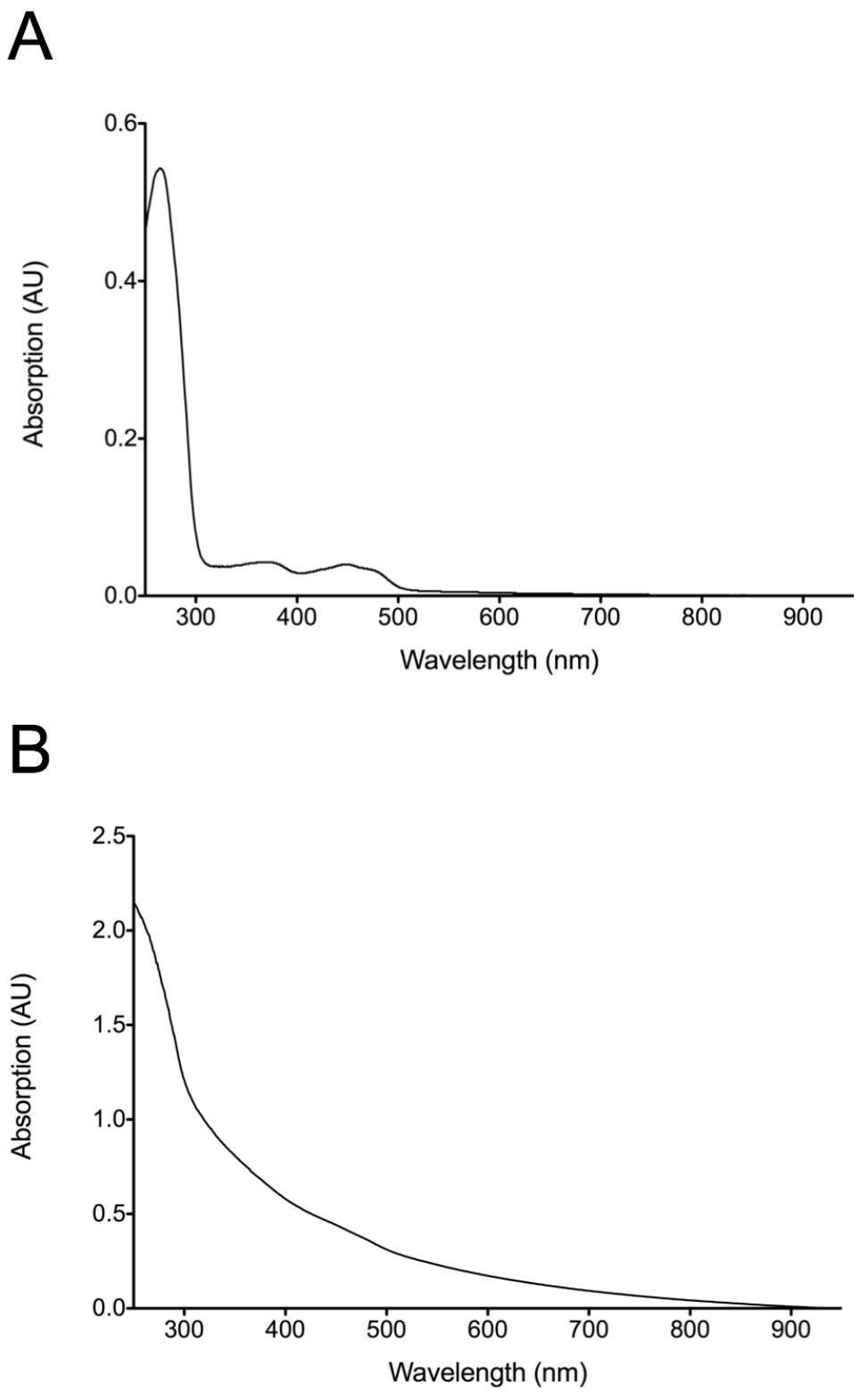

Figure 4.17 Change in AdxRed absorption spectrum upon heat treatment
(A) AdxRed absorption spectrum was measured at room temperature in 50 mM Tris-HCl, 150 mM NaCl. (B) AdxRed was incubated at 45℃ for 5 min and its spectrum was then recorded. The AdxRed was very unstable and precipitated out of solution almost immediately. An increase in sample turbidity caused increased light scattering.

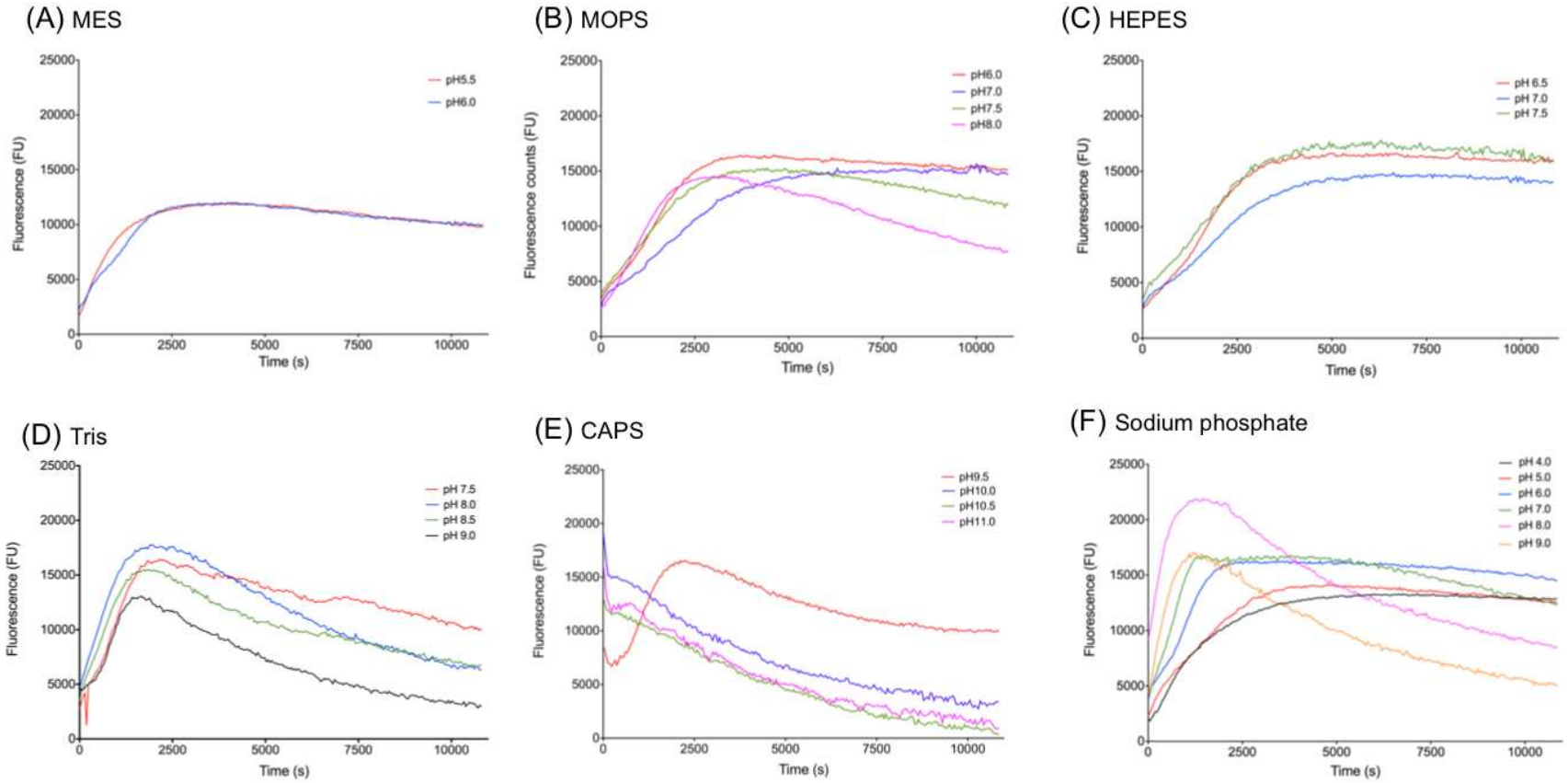

Figure 4.18 AdxRed stability at 45°C in different buffer conditions

The extent of AdxRed denaturation was determined by reaction with CPM reagent (which labels solvent-exposed cysteine residues) (Section 2.12.2). As the protein unfolds, cysteines from the inner core become accessible to the fluorochrome resulting in an increase in fluorescence with time. In certain conditions, AdxRed was so unstable that following rapid unfolding the protein precipitated out of solution causing a decrease in fluorescence (e.g. in Tris). AdxRed had good stability in MES (pH 5.5, 6), HEPES (6.5, 7., 7.5), MOPS (7.5, 8) and sodium phosphate (4, 5, 6, 7). Of these, HEPES pH 7 was chosen as the optimal buffer for purification purposes.

4.6.4 Crystallisation of human adrenodoxin and adrenodoxin reductase

Milligram quantities of stable Adx and AdxRed were purified in sodium phosphate and HEPES buffer, respectively. Pure protein was concentrated to between 20-40 mg/ml, and then used with a series of sparse-matrix crystallisation screens (JCSG+, Morpheus, Peg/Ion 1& 2 and Hampton 1&2). A series of sitting-drop trays were set up in which 0.5 μl of the concentrated protein was added to 0.5 μl of the precipitant solution. Crystallisation trays were incubated at 20°C in a Rhombix plate hotel. Wells were photographed regularly to monitor crystal formation.

With Adx, initial crystallisation attempts resulted in the formation of spherulites (Figure 4.19A) and salt crystals (Figure 4.19B). Subsequent efforts resulted in the formation of small protein crystals (Figure 4.19C). However, these did not diffract in an X-ray beam. No successful crystallisation ‘hits’ were observed with AdxRed. Further work will be required to obtain crystals of human Adx and AdxRed that diffract to high-resolution.

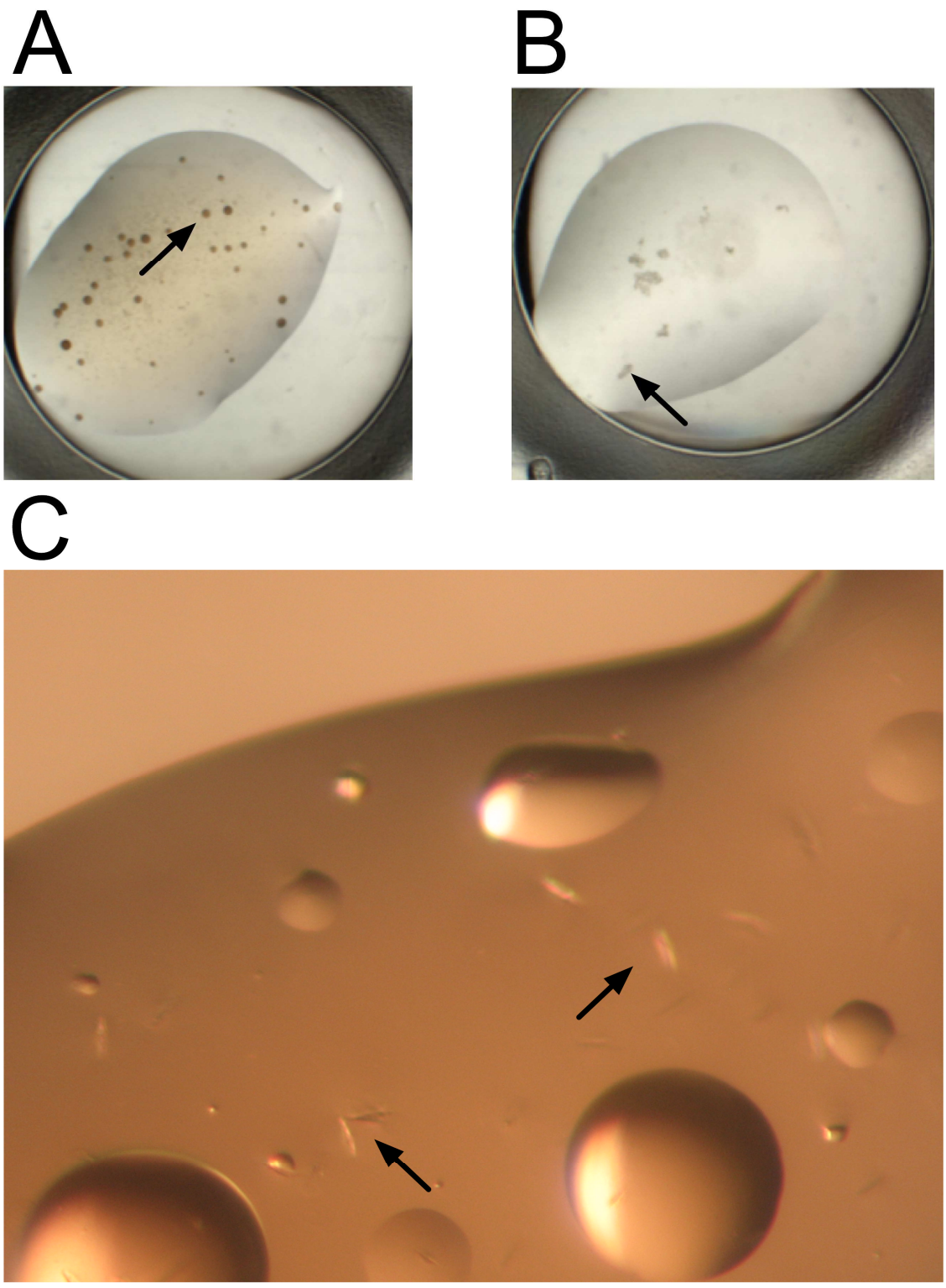

Figure 4.19 Adx crystallisation
Adx, purified in sodium phosphate buffer, was concentrated to between 20-40 mg/ml and used with a series of sparse-matrix crystallisation screens (Section 2.14). Initial attempts resulted in the formation of (A) spherulites and (B) salt crystals. Later efforts resulted in the formation of (C) delicate protein crystals. Unfortunately, these did not diffract on the in-house X-ray beam. Further work will be required to identify diffracting crystals of Adx.

4.6.5 Characterisation of adrenodoxin and adrenodoxin reductase by circular dichroism

Circular dichroism (CD) refers to the differential absorption of left- and right-handed polarised light by chiral molecules. CD signals only occur at those wavelengths where the asymmetric molecule absorbs. Proteins have several chromophores which absorb electromagnetic radiation. These include peptide bonds (which absorb between 180 and 240 nm), aromatic amino acids (260 to 320 nm) and disulphide bonds (260 nm).

The different kinds of secondary structure (e.g. α-helices and β-sheet) that occur in proteins have characteristic CD spectra in the far-UV (which arise from the chiral arrangement of the peptide bonds in each structure). A number of algorithms have been developed that provide an estimate of a protein's secondary structure from its far-UV CD spectrum (Kelly *et al.*, 2005).

Proteins also have measurable CD in the near-UV (region 260 – 320 nm) arising from their constituent aromatic amino acids (Trp, Tyr, Phe). The actual shape and intensity of the CD-signal in the far-UV is different for each type of protein, and depends on the number of each type of aromatic amino acid present, their mobility and their environment (H-bonding, proximity of polar groups and polarisability). The near-UV CD spectrum of a protein provides a valuable fingerprint of its tertiary structure, and can be used to compare, for example, the structural similarity of wild-type and mutant forms of the protein (Kelly *et al.*, 2005).

CD spectra of Adx and AdxRed were recorded both in the far-UV (Figure 4.20) and near-UV/visible regions (Figure 4.21). Measurements were performed in the laboratory of Dr. Sharon Kelly (University of Glasgow). The far-UV spectra were fitted using the CONTIN-LL alogorithm (Provencher and Glockner, 1981; Van Stokkum *et al.*, 1990; Whitmore and Wallace, 2008). The root-mean-squared deviation values of both fits were too high to allow accurate predictions of the secondary structure content of either protein. However, the spectra are still useful because they can be used as references for assessing the structural integrity of Adx and AdxRed mutants. The near-UV/visible CD spectrum for Adx

has a strong CD signal at 440 nm, which is caused by its iron-sulphur cluster (Figure 4.21). Other maxima were observed at 256, 295 and 339 nm. The equivalent spectrum from AdxRed has a sharp peak at 270 nm, associated with absorption by its FAD co-factor. The near-UV/visible CD spectra will also be used as references with Adx and AdxRed natural variants made by recombinant expression prior to their use in activity assays *in vitro*.

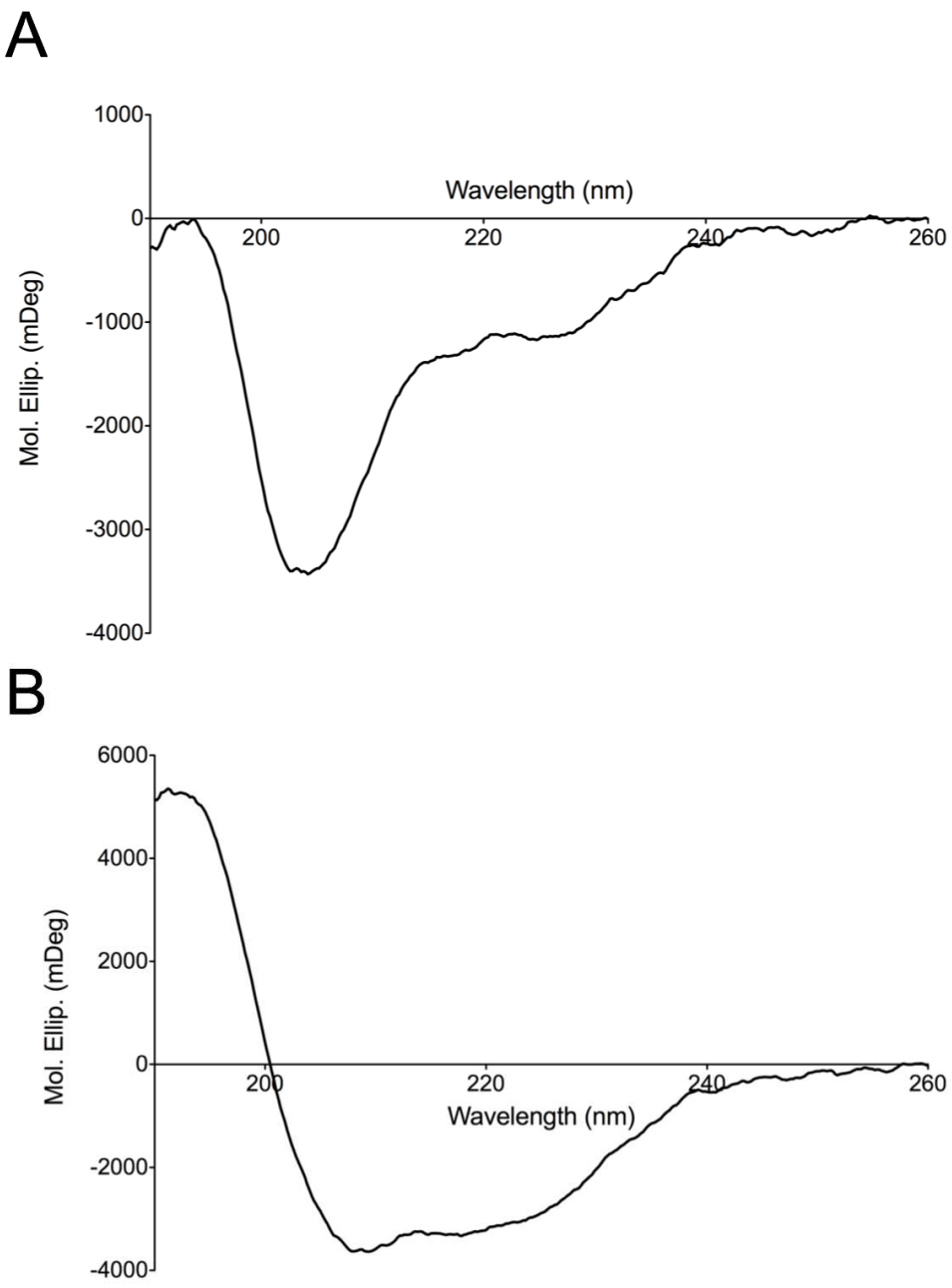

Figure 4.20 Far-UV CD spectra of Adx and AdxRed
The CD spectra of (A) Adx and (B) AdxRed were recorded in the far-UV. Measurements were made using protein with a concentration of 1 mg/ml in a cuvette with a pathlength of 0.5 cm (Section 2.13).

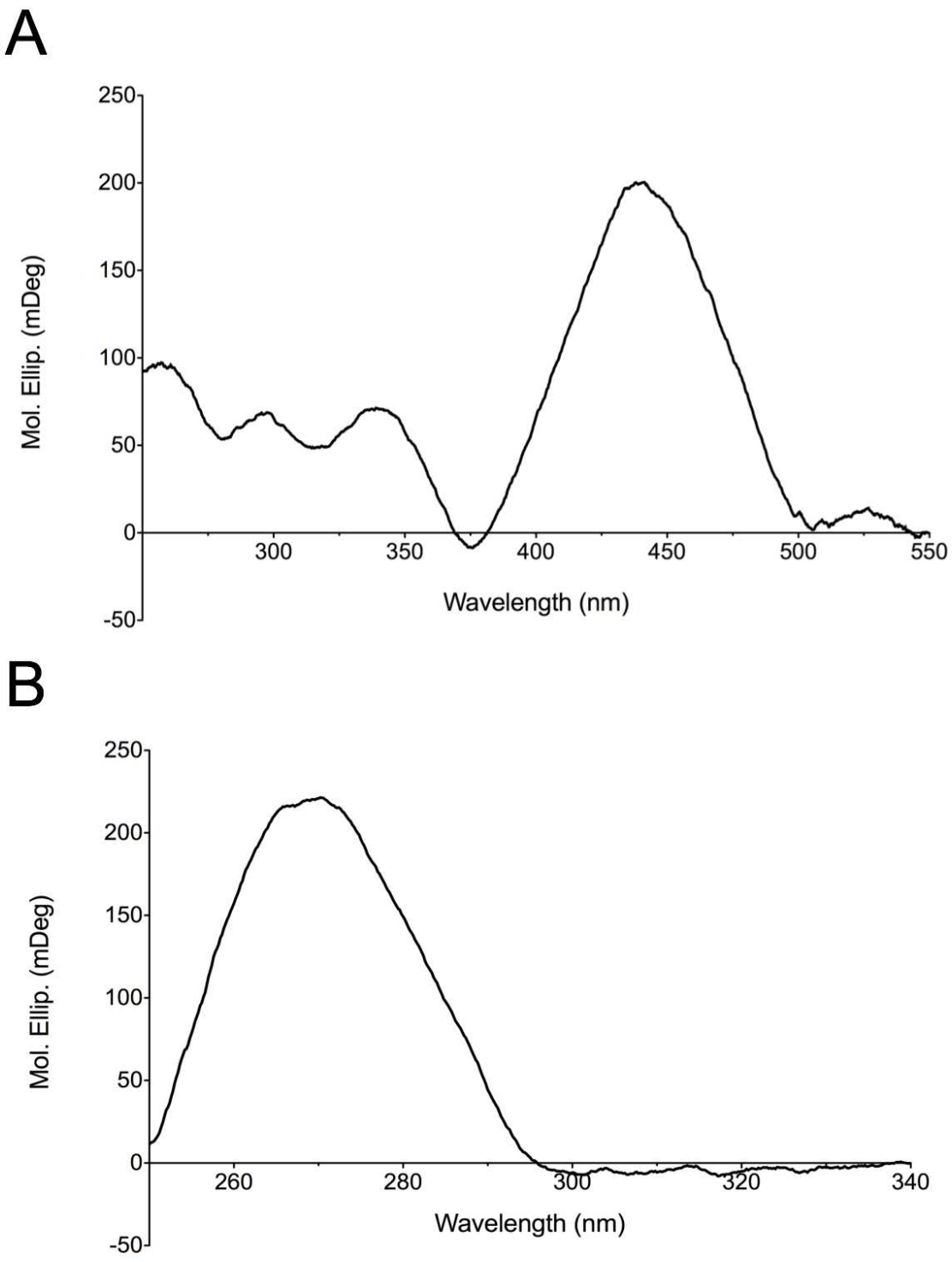

Figure 4.21 Near-UV/visible CD spectra of Adx and AdxRed
(A) The Adx spectrum has a strong CD signal at 440 nm arising from absorption by its iron-sulphur cluster. Other maxima can be observed at 256, 295 and 339 nm. (B) The AdxRed spectrum has a sharp peak at 270 nm, associated with absorption by its FAD co-factor. Measurements were made using protein with a concentration of 1 mg/ml in a cuvette with a pathlength of 0.5 cm (Section 2.13).

4.7 Conclusion

This chapter describes the successful expression and purification of the electron transfer proteins Adx and AdxRed. Initial efforts to make AdxRed in *P. pastoris* were abandoned as the production levels of the recombinant protein were too low to allow its purification on a milligram scale. This necessitated the use of another heterologous host. cDNAs encoding Adx and AdxRed were introduced into the *E. coli* expression vector pET21a along with the CLBH tag. In this system, Adx and AdxRed could be made on a milligram scale and purified to homogeneity in four simple steps (Ni^{2+}-afffinity, 3C cleavage, reverse Ni^{2+}-affinity and gel-filtration).

The primary purpose for obtaining pure Adx and AdxRed was to develop activity assays for both aldosterone synthase and 11β-Hydroxylase. Over the course of the last few years, however, it has become apparent that there are a substantial number of natural variants in both Adx and AdxRed that may affect blood pressure in people. As a first step towards expressing, purifying and analysing the properties of naturally-occurring variants of Adx and AdxRed *in vitro*, a brief biophysical characterisation of the wild-type proteins was performed.

The stability of Adx in a range of buffer conditions was investigated using an absorption-based thermal denaturation assay. Adx was found to have greatest stability in sodium phosphate buffer with a pH between 7 and 8. AdxRed stability was explored using the CPM assay. AdxRed is considerably less stable than Adx. Maximal stability was observed in MOPS buffer closely-followed by HEPES pH 7. All subsequent purifications were performed in the buffers that gave maximal thermostability (Adx, sodium phosphate pH 7.4; AdxRed, HEPES pH 7).

Crystallisation trials were performed for both Adx and AdxRed. As yet, no diffracting crystals have been obtained. CD spectra were recorded for both proteins in the far-UV and near-UV/visible regions. In the future, these spectra will be used as references to assess the structural integrity of any Adx or AdxRed natural variants made by recombinant expression prior to their use in activity assays *in vitro*.

Chapter 5 – Expression and purification of human aldosterone synthase and 11β-Hydroxylase

5.1 Introduction

The primary aim of my Ph.D. was to purify functional human aldosterone synthase and 11β-Hydroxylase for structural studies and drug-screening purposes. As both enzymes are monotopic membrane proteins, they were expected to be challenging to make in a heterologous host on a milligram-scale as well as purify in an active form (Gonzalez and Korzekwa, 1995). Previously, a range of expression systems have been used to make cytochrome p450s including *E. coli* (Sandhu *et al.*, 1994), yeast (Eugster *et al.*, 1990), insect (Aoyama *et al.*, 1990) and mammalian cells (Patten *et al.*, 1992). Initial efforts to express both aldosterone synthase and 11β-Hydroxylase were focused on the *P. pastoris* CLBH expression system detailed in Chapter 3. *P. pastoris* has been successfully used to make a range of cytochrome p450s of varying origins, including spiny dogfish shark CYP17 (Trant, 1996), plant CYP79D1 (Andersen *et al.*, 2000) and human CYP2D6 (Dietrich *et al.*, 2005), suggesting that it may be a good host for the expression of aldosterone synthase and 11β-Hydroxylase also. However, no expression of either aldosterone synthase or 11β-Hydroxylase was observed in *P. pastoris*. An alternative *E. coli*-based expression system was developed that yielded milligram amounts of both aldosterone synthase and 11β-Hydroxylase, from which pure and functional protein was obtained. This Chapter details all efforts to express and purify aldosterone synthase and 11β-Hydroxylase.

5.2 Expression of aldosterone synthase and 11β-Hydroxylase in *P. pastoris*

5.2.1 Vector construction

Aldosterone synthase and 11β-Hydroxylase are synthesised in the cytosol as precursor proteins, and then targeted to mitochondria via N-terminal (αα 1-24) leader sequences. Following their import, mature forms of both enzymes are

generated within the mitochondria by specific cleavage of the targeting sequences. For the purposes of structure determination and drug-screening, it was only necessary to express and purify the mature forms of 11β-Hydroxylase and aldosterone synthase (both αα 25-503). Subtle modifications to the amino acid sequence of the N-terminus of p450 enzymes are necessary for their successful expression in a heterologous host (Barnes *et al.*, 1991). Here, the aldosterone synthase and 11β-Hydroxylase mitochondrial targeting sequences were replaced with a four amino acid sequence (MATK) which has previously been shown to aid recombinant cytochrome p450 production (Figure 5.1A) (Zöllner *et al.*, 2008). cDNAs encoding the modified

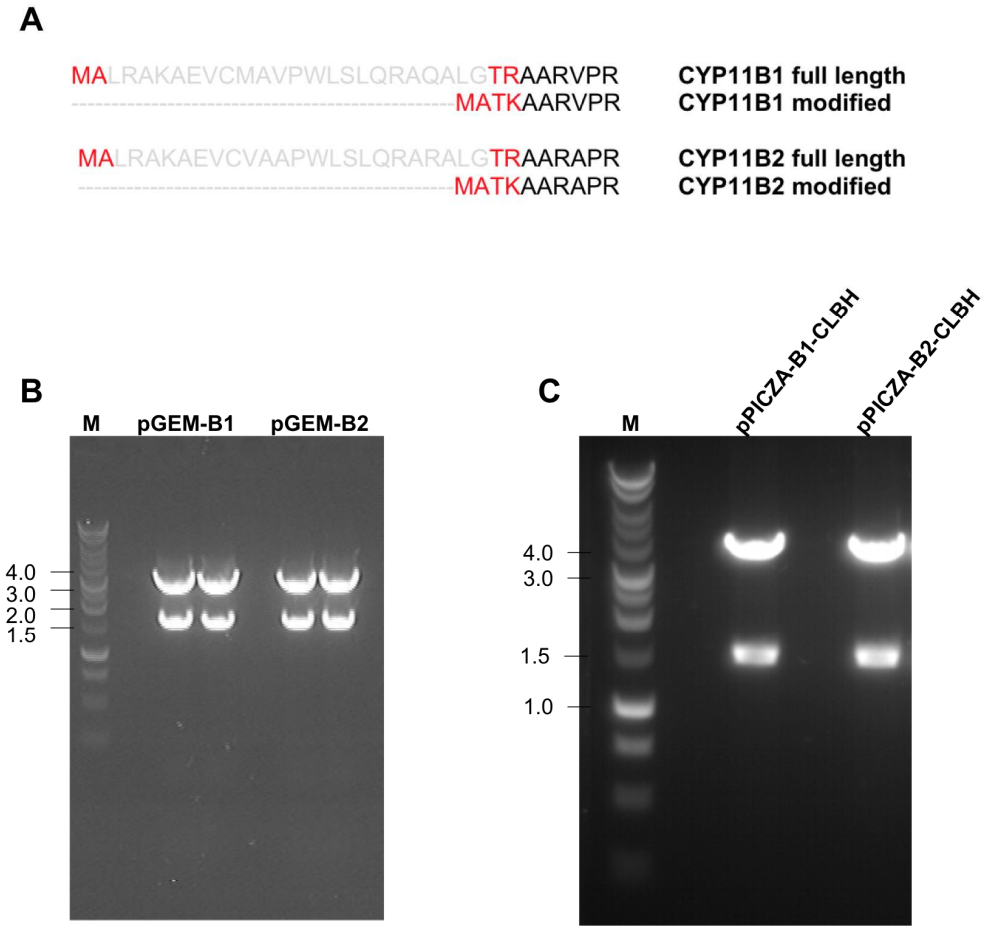

Figure 5.1 Construction of CYP11B1/B2-CLBH *P. pastoris* expression vectors
(A) To facilitate the recombinant production of aldosterone synthase and 11β-Hydroxylase, their N-terminal mitochondrial targeting sequences were removed and replaced with a four amino acid sequence (MATK) previously shown to aid cytochrome p450 expression. (B) cDNAs encoding the modified forms of B1 and B2 were generated by PCR, and cloned into pGEM T-Easy (Section 2.3.2). Recombinant plasmids were identified by restriction digestion with *Eco*RI (vector, 3.0 Kb; B1/B2, 1.5 Kb). (C) The modified B1/B2 cDNAs were sub-cloned from pGEM T-Easy to pPICZA-CLBH using *Eco*RI and *Not*I. Recombinant expression plasmids were identified by digesting the yeast vector with *Eco*RI and *Not*I (vector, 3.9 Kb B1/B2, 1.5 Kb).

forms of aldosterone synthase and 11β-Hydroxlase were generated by PCR, and cloned into pGEM T-Easy (Figure 5.1B). Recombinant plasmids were identified by restriction digestion with *Eco*RI, and then sequenced to ensure that no mutations had been introduced during the PCR step.

The modified aldosterone synthase and 11β-Hydroxylase cDNAs were then sub-cloned from pGEM T-Easy to pPICZA-CLBH. Recombinant expression plasmids were identified by digesting the yeast vector with *Eco*RI and *Not*I (Figure 5.1C).

5.2.2 Production of aldosterone synthase and 11β-Hydroxylase in *P. pastoris*

Both CYP11B1- and B2-CLBH constructs were transformed into the *P. pastoris* strain X33 by electroporation (Section 2.4.2.2). Multi-copy integrants were selected using zeocin. Clonal selection was performed for aldosterone synthase and 11β-Hydroxylase in the same way described for AdxRed (Section 4.3.2). In short, following induction with methanol, the expression levels of 11β-Hydroxylase and aldosterone synthase in the transformants were assessed by measuring the levels of whole cell iLOV fluorescence. Unexpectedly, fluorescence levels in the transformants were essentially the same as the control yeast, suggesting that *P. pastoris* is unable to make either 11β-Hydroxylase or aldosterone synthase (Figure 5.2).

Although the clonal selection results suggested that *P. pastoris* is unable to make aldosterone synthase, an aldosterone synthase transformant was grown and induced in a 7 litre bioreactor to assess whether any aldosterone synthase expression could be detected in fermenter culture. Samples were taken at regular intervals throughout the fermentation. At each time point, the wet cell weight of the culture was determined and the production level of B2-CLBH assessed by measuring whole cell iLOV fluorescence (Figure 5.3). Consistent with the clonal selection results, negligible levels of iLOV fluorescence were observed in fermenter culture, confirming that *P. pastoris* is unable to make aldosterone synthase. It was concluded, therefore, that an alternative expression system would be needed to produce aldosterone synthase.

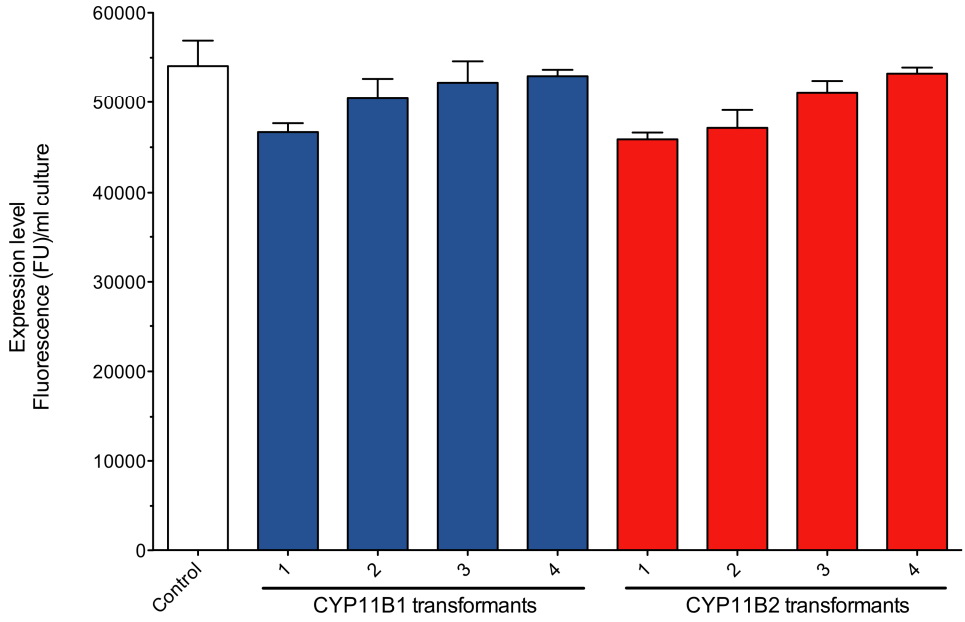

Figure 5.2 Expression analysis of *P. pastoris* colonies transformed with CYP11B1/CYP11B2-CLBH

Transformants were grown up overnight at 30°C in 1 ml cultures of BMGY. Recombinant protein production was induced by growing the yeast in BMMY at 22°C for 24 h. Cytochrome p450 expression levels were determined by measuring iLOV fluorescence in intact yeast cells (Section 2.5.1). The levels of fluorescence observed in the aldosterone synthase and 11β-Hydroxylase transformants were the same as that for the X33 control, suggesting that *P. pastoris* is unable to express either aldosterone synthase or 11β-Hydroxylase.

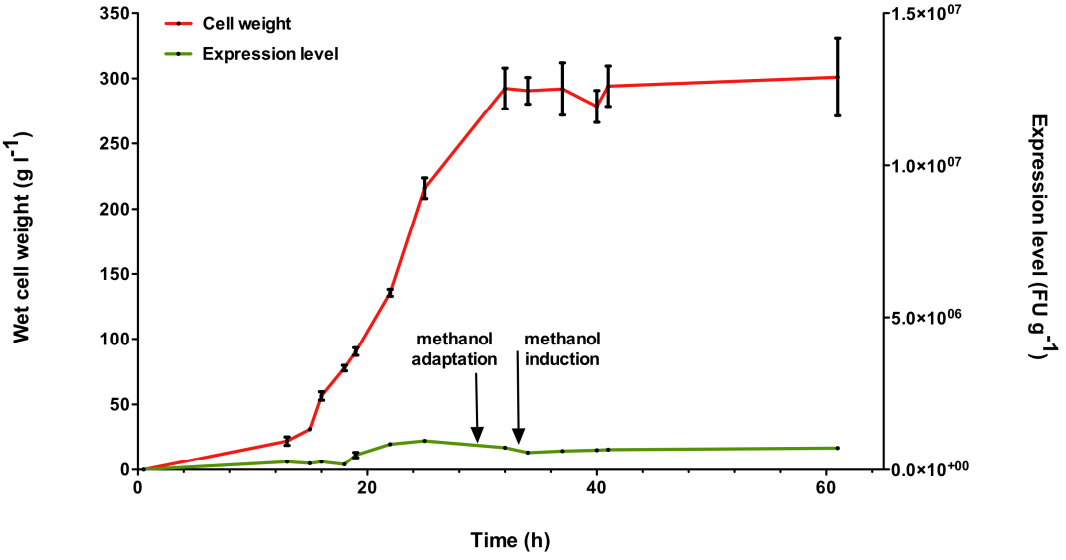

Figure 5.3 Time-course of CYP11B2-CLBH expression in *P. pastoris* fermenter culture

Samples were taken at regular intervals throughout the fermentation of CYP11B2-CLBH (Section 2.5.2). At each time point, the wet cell weight of the culture was determined (red line) and the production level of B2-CLBH calculated (green line).

5.3 11β-Hydroxylase and aldosterone synthase expression in *E. coli*

5.3.1 pET21a-CYP11B1/B2-CLBH vector construction

The most commonly used host for recombinant expression and purification of cytochrome p450 enzymes is *E. coli*. Therefore, the cDNAs encoding the mature, N-terminally modified versions of 11β-Hydroxylase and aldosterone synthase (Section 5.2.1) were sub-cloned from pGEM T-Easy to the pET21a-CLBH expression vector detailed in Section 4.4, with a view to assessing the utility of *E. coli* for expressing aldosterone synthase and 11β-Hydroxylase. Recombinant plasmids were identified by restriction digestion with *Nde*I (Figure 5.4).

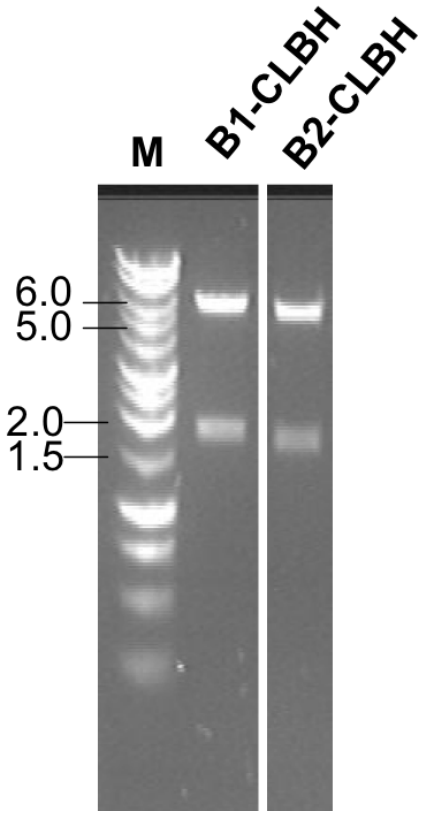

Figure 5.4 Restriction analysis of pET21a-CYP11B1/B2-CLBH
cDNAs encoding the mature, N-terminally modified versions of 11β-Hydroxylase and aldosterone synthase were sub-cloned from pGEM T-Easy to the pET21a-CLBH expression vector (Section 2.4). Recombinant plasmids were identified by restriction digestion with *Nde*I, which yielded two fragments of expected size (1.8, 5.9 Kb).

5.3.2 Optimisation of B2-CLBH expression in *E. coli*

pET21a-CYP11B2-CLBH was transformed into the *E. coli* BL21 expression strain together with pGro7 (a plasmid encoding the bacterial chaperones GroEL and GroES). Cells were grown at 37ºC in LB until the culture had an OD_{600} of 0.6. At this stage, 1 mM IPTG and 1 mM arabinose were added to induce expression of B2-CLBH and GroEL/ES, respectively, and the temperature reduced to 27ºC. Cells were harvested 4, 16, 24 and 48 h post-induction. All of the samples had measurable levels of iLOV fluorescence, suggesting that *E. coli* is able to express aldosterone synthase (Figure 5.5).

B2-CLBH was expected to be membrane-associated. To establish whether or not this was the case, the cells were lysed by mechanical disruption, cytosolic and membrane fractions prepared by centrifugation, and the fluorescence content of the samples measured. Surprisingly, both the cytosolic and membrane fractions of all the time-points were fluorescent. To understand why this was the case, a series of FSEC experiments were performed. Membranes were solubilised using CHAPS (an ionic-detergent that had been successfully used with other mammalian p450s (e.g. Annalora *et al.*, 2010)), and the supernatant applied to a Superose 6 gel-filtration column. Elution profiles were generated for all four time points (Figure 5.5A). The samples harvested at 16 and 24 h both had two major peaks in their elution profiles. The peak at *ca.* 13 ml corresponded to B2-CLBH. A second peak eluting at *ca.* 20 ml was observed. Previous studies with SI showed that cleavage of the CLBH tag with 3C protease yielded a FSEC peak at *ca.* 20 ml also (Figure 3.8). This suggested that there is a proteolytically-sensitive region in aldosterone synthase towards its C-terminus, close to the 3C cleavage site in the fusion protein. The fluorescent peak for the breakdown product was greater in magnitude than that for the intact fusion protein, illustrating how sensitive B2-CLBH is to proteolysis. The optimal induction time for maximal B2-CLBH expression was between 16 and 24 h. Elution profiles were also generated for each of the cytosolic fractions (Figure 5.5B). The samples that been induced for 16 and 24 h had a single major peak at *ca.* 20 ml corresponding to the breakdown product. None of the cytosolic fractions contained intact B2-CLBH (Figure 5.5B).

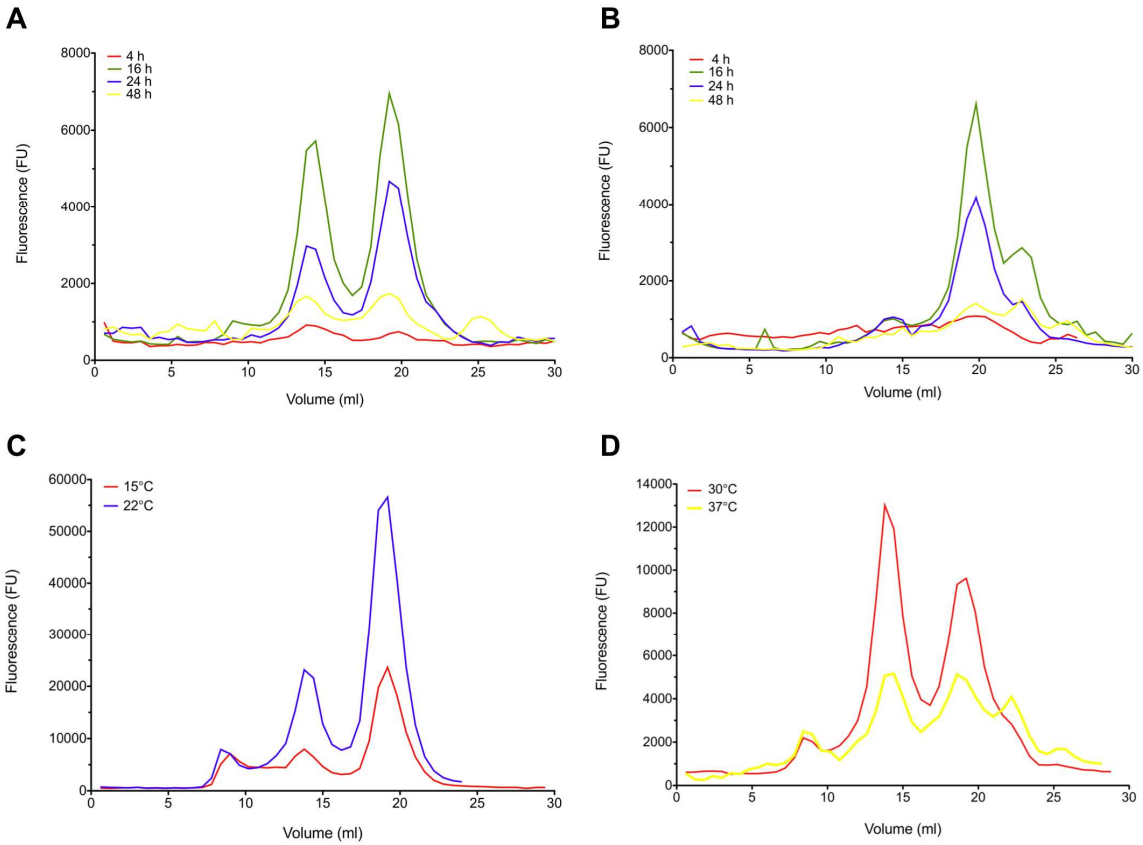

Figure 5.5 Optimisation of CYP11B2-CLBH expression in *E. coli*
E. coli cells expressing CYP11B2-CLBH were cultured at 37ºC in 500 ml LB until the cultures reached an OD_{600} of 0.6. At this stage, protein expression was induced by addition of 1mM IPTG and 1 mg/ml arabinose. Induction was performed for different periods of time (A and B) as well as at different temperatures (C and D). Following induction, cells were harvested, mechanically disrupted, and cytosolic and membrane fractions prepared. Membranes were solubilised using CHAPS and then analysed by FSEC (A, C and D; Section 2.11.1). In these elution profiles, two peaks were clearly visible corresponding to B2-CLBH (elution volume of *ca.* 13 ml) and a breakdown product (20 ml). The cytosolic fractions only contained breakdown product (B). Maximal B2-CLBH expression was obtained by inducing the cells for 16 h at 30℃.

Together, these results suggested that: (i) B2-CLBH localises to the membrane, (ii) the fusion protein is sensitive to proteolytic cleavage in a region of aldosterone synthase towards its C-terminus proximal to the 3C recognition site, and (iii) the breakdown product is water-soluble.

Having determined that an induction period of 16 h yielded the highest levels of recombinant protein, the effects of temperature on the synthesis and proteolysis of B2-CLBH were explored. Expression cultures were induced at four different temperatures (15, 22, 30, 37ºC) for 16 h. Cells were harvested and membranes isolated. Following this, the membranes were solubilised using CHAPS, and the resulting supernatants analysed by FSEC. In all four elution profiles, peaks corresponding to B2-CLBH (elution volume 13 ml) and the breakdown product (20 ml) were observed (Figure 5.5C, D). At low induction temperatures (15 and 22ºC), there was more breakdown product than intact protein (Figure 5.5C), suggesting that the recombinant protein was being cleaved by endogenous proteases faster than it was being made. At 37°C, there was an equal amount of B2-CLBH and breakdown product (Figure 5.5D). Only at an induction temperature of 30°C did more B2-CLBH accumulate than breakdown product (Figure 5.5D). This suggested that the optimal temperature for expressing B2-CLBH in *E. coli* was 30°C.

Cleavage of the B2-CLBH fusion protein by endogenous bacterial proteases was highly undesirable. This problem was overcome by including 5 mM EDTA in the buffer used for cell lysis suggesting that aldosterone synthase was being cleaved by (a) metalloprotease(s).

5.3.3 ELISA-SEC: assessing the polar surface availability of aldosterone synthase in detergent solution

Following on from the successful expression of aldosterone synthase in *E. coli*, it was now necessary to identify a suitable detergent for solubilising, purifying and crystallising the enzyme.

For use with a target membrane protein, a detergent must fulfil three criteria: (i) the detergent must efficiently remove the protein from the membrane, (ii)

the membrane protein must be stable/monodisperse in the chosen detergent, and (iii) for structural studies, it is essential that the detergent-solubilised protein has sufficient polar surface area available for the formation of lattice contacts.

By fusing a fluorescence reporter (such as GFP or iLOV) to the C-terminus of a membrane protein of interest, it is possible to assess the protein's aggregation status by FSEC as well as calculate the efficiency of solubilisation (Kawate and Gouaux, 2006). However, there is not an established technique for assessing the extent of a membrane protein's polar surface exposure in detergent solution. To address this deficiency, a new methodology called ELISA-SEC (ESEC) was devised which allows the aggregation status and polar surface availability of a target membrane protein in detergent solution to be probed at the same time.

ESEC is a simple adaptation of the FSEC technique. A detergent-solubilised sample is applied to a gel filtration column. Elution fractions are collected, and analysed by ELISA using an Ab that binds to the surface of the target protein (Figure 5.6). Similar to FSEC, the aggregation status of a target membrane protein can be evaluated in the presence of other proteins as the ELISA signal comes from an antibody specific to the protein of interest. However, ESEC has notable advantages over FSEC. First, ESEC can be used with any membrane protein where there is an antibody available against an antigenic epitope on the surface of the protein. In contrast, FSEC can only be used with membrane proteins that have been engineered to have a fluorescent reporter attached to either their N- or C-termini. Second, in detergent solution, the antibody will only be able to bind to the target protein if the surface epitope is not covered by detergent. For this reason, the size of the ELISA signal gives insights into the extent of the protein's surface exposure.

Figure 5.6 ELISA-SEC
ELISA-SEC is a simple adaptation of the absorption (A)SEC/FSEC methodologies used to assess membrane protein stability in detergent solution. In ESEC, a detergent-solubilised sample is applied to a gel filtration column, elution fractions collected and then analysed using an antibody that binds to a surface epitope on the target protein by ELISA. Using ESEC, insights into the aggregation status and the polar surface exposure of a target membrane protein in detergent solution can be gained. Figure adapted from Kawate and Gouaux (2006).

Membranes containing B2-CLBH were solubilised in a range of detergents and applied, one at a time, to a Superose 6 gel filtration column equilibrated in buffer containing a CMC concentration of the detergent being investigated. Fractions were collected, and analysed by ELISA using specific anti-aldosterone synthase antibodies (Nishimoto *et al.*, 2010) (Figure 5.7).

When B2-CLBH was solubilised using Fos Choline-9 (FC-9) a sharp monodisperse peak of strong intensity was observed (fractions 25-31) (Figure 5.7A). The presence of an earlier peak (fractions 15-19) suggested that some of the B2-CLBH was aggregated (Figure 5.7A). In OTG, only aggregate was observed (fractions 21-24) (Figure 5.7B). In CYMAL-5, a monodisperse peak was observed (fractions 25-30) with a small amount of aggregate present (fractions 21-24) (Figure 5.7C). In DM and CHAPS, the ESEC profiles each consisted of a solitary broad, bell-shaped peak (DM, fractions 20-30; CHAPS 25-31) (Figure 5.7D, E). The most promising detergent for use with aldosterone synthase identified by ESEC was sodium cholate (Figure 5.7F). In sodium cholate, B2-CLBH had a sharp, symmetric peak with a strong ELISA signal, indicating the recombinant protein was stable and had extensive polar surface exposure.

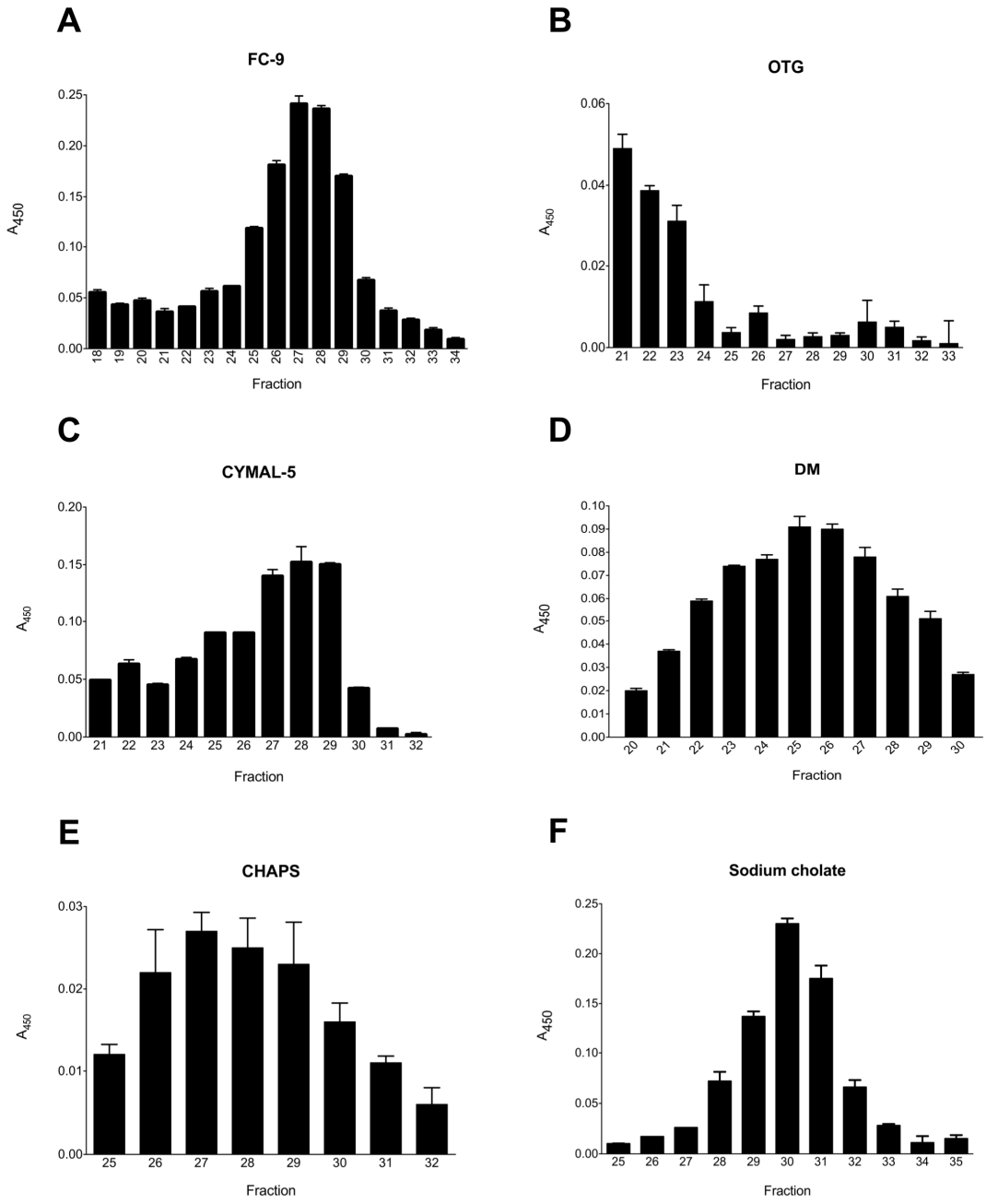

Figure 5.7 ESEC analysis of CYP11B2-CLBH in detergent solution
Membranes containing B2-CLBH were solubilised with detergent and applied to a Superose 6 gel filtration column equilibrated in buffer containing a CMC concentration of that same detergent (FC-9 1.2%; OTG 0.3%; CYMAL-5 0.1%; DM 0.01%; CHAPS 0.5%; Sodium cholate 0.6%). Fractions were collected, and analysed by ELISA using anti-B2 Abs (Section 2.11.2). (A) In FC-9, a sharp monodisperse peak was observed. However, there was some protein aggregate present too. Aggregate was also observed in (B) OTG and (C) CYMAL-5. In (D) DM and (E) CHAPS, the ESEC profiles each consisted of a solitary broad, bell-shaped peak. (F) The optimal detergent for solubilising aldosterone synthase was sodium cholate. In this detergent, the ESEC profile consisted of a sharp, symmetric peak with a strong ELISA signal indicating that the recombinant protein was stable and had extensive polar surface exposure.

5.3.4 Solubilisation and attempted purification of CYP11B2-CLBH using a nickel column

After sodium cholate had been identified as the optimal detergent for solubilising aldosterone synthase, a trial Ni^{2+}-affinity purification of B2-CLBH was attempted. Membranes containing B2-CLBH were solubilised using sodium cholate. Insoluble material was removed by centrifugation, and the absorption profile of the supernatant recorded in the region 350-700 nm (Figure 5.10). The absorption spectrum had a haem Soret peak absorption at 413 nm. This was unexpected. In their low spin state, cytochrome p450s have a Soret peak absorption at ~420 nm. In their high spin state, the p450 Soret absorption band is at ~390 nm. Free haem absorbs maximally at 408 nm. The Soret absorption of the supernatant fraction at 413 nm was, therefore, difficult to interpret. It may have suggested that the supernatant contained some correctly folded aldosterone synthase in its low spin state along with a considerable amount of free haem (released on breakdown of the p450 enzyme). Alternatively, the haem absorption from B2-CLBH may have been so small compared to that from endogenous bacterial haem containing proteins that the aldosterone synthase contribution could not be seen. In short, it was not possible to say anything conclusive about either the abundance or the spin state of B2-CLBH in the detergent-solubilised sample from its absorption spectrum.

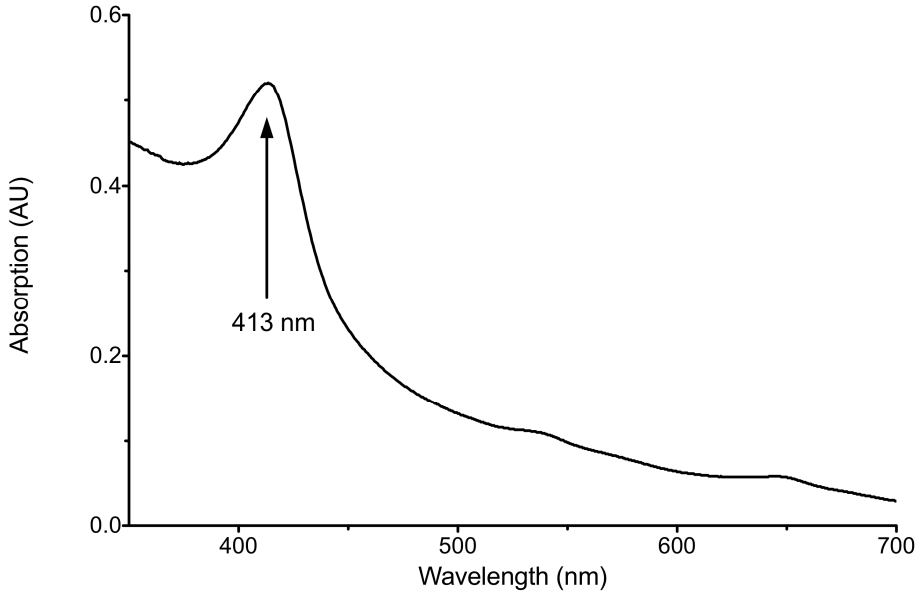

Figure 5.8 Absorption spectrum of solubilised CYP11B2-CLBH
The absorption spectrum of the supernatant fraction obtained following suloubilisation of *E. coli* membranes containing CYP11B2-CLBH was measured. A Soret peak at 413 nm was observed.

Solubilised B2-CLBH was passed over a Ni^{2+} column several times. The column was then washed with buffers containing increasing concentrations of imidazole (25, 50, 75 and 300 mM). Aliquots from the unbound and wash fractions were analysed by ELISA to determine their aldosterone synthase content (Figure 5.9). A very low signal was observed in the detergent-solubilised fraction (Figure 5.9). This was unexpected given the previous ESEC results (Figure 5.7). The most likely explanation for this observation was that the high concentrations of sodium cholate used for solubilising the membranes prevented the majority of B2-CLBH from binding to the Ab on the ELISA plate. However, some B2-CLBH did bind to the Ni^{2+}-column albeit weakly. Most of the recombinant protein was eluted from the column using 75 mM imidazole. The remainder was released using 300 mM imidazole (Figure 5.9). The most striking thing about the ELISA results, however, was the low signal intensity observed in the wash and elution fractions, again suggesting that the vast majority of the B2-CLBH had not bound to the column.

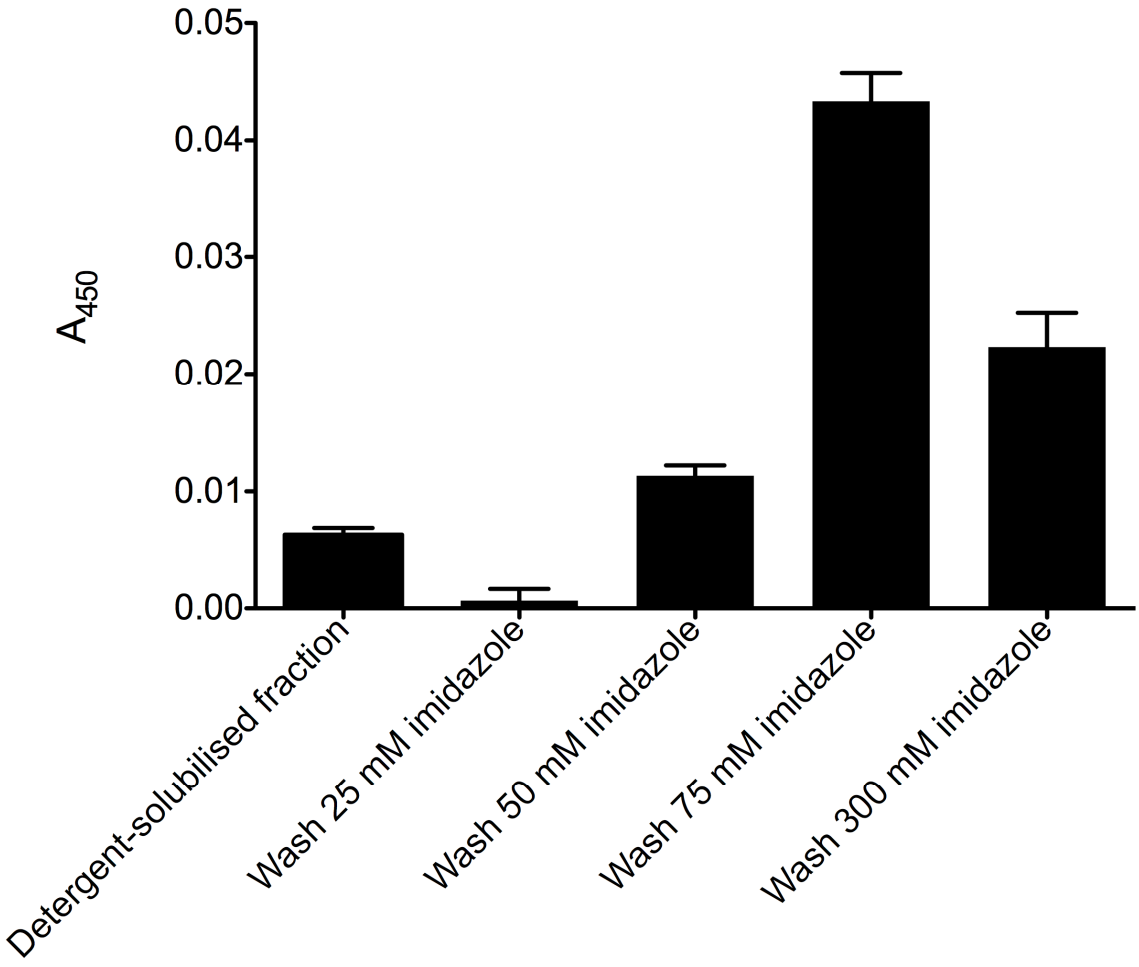

Figure 5.9 ELISA analysis of the wash fractions from an attempted purification of B2-CLBH using a Ni^{2+}-column

B2-CLBH solubilised in sodium cholate was passed over a Ni^{2+} column. The column was then washed with buffers containing increasing concentrations of imidazole (25, 50, 75 and 300 mM). Most of the recombinant protein was eluted from the column using 75 mM imidazole; the remainder with 300 mM. The most striking thing about the ELISA results, however, was the low signal intensity observed in all of the wash fractions, suggesting that the vast majority of the B2-CLBH had not bound to the column.

Although it was thought unlikely, it may have been possible that the sodium cholate was interfering with binding of the B2-CLBH to the Ni^{2+} resin. To explore this possibility, B2-CLBH was solubilised in DM and passed over a fresh Ni^{2+} column. Similar to that which had been observed with sodium cholate, the vast majority of the recombinant protein did not bind to the column, suggesting that the binding problem was not an artefact of using sodium cholate (results not shown). The B2-CLBH elution fractions from the DM purification experiment were pooled and incubated with 3C protease overnight at 4°C. The following day, the levels of iLOV fluorescence had increased by a factor of 8 (Figure 5.10). This

suggested that fusion of the CLBH tag to aldosterone synthase was causing fluorescence from the iLOV reporter to be quenched.

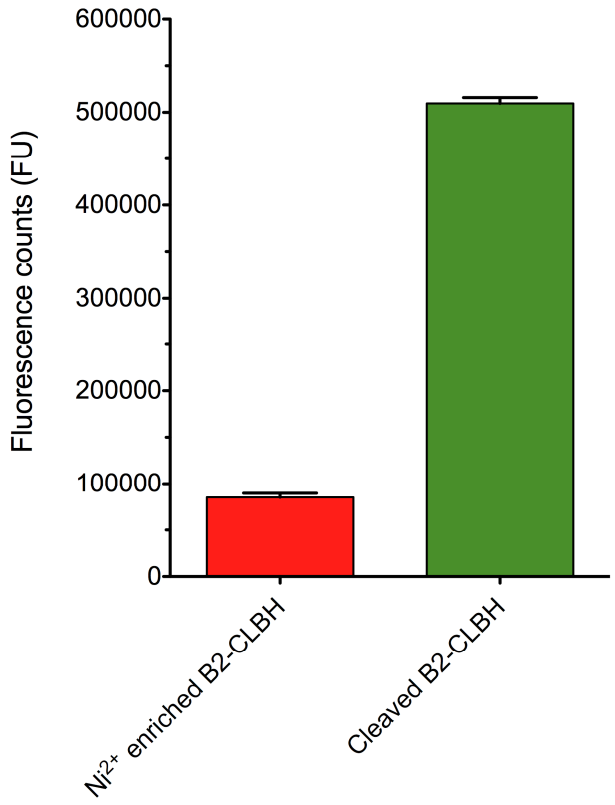

Figure 5.10 Fusion of the CLBH tag to aldosterone synthase quenches iLOV fluorescence Ni^{2+}-enriched B2-CLBH had fluorescence counts of *ca*. 85030 FU. Upon cleavage with HRV 3C protease overnight at 4°C, the fluorescence counts increased to *ca*. 509776. These results indicated that iLOV fluorescence was quenched when placed in proximity to the aldosterone synthase haem.

At this stage, using the CLBH construct, it had been shown that: (i) aldosterone synthase can be made in *E. coli*; (ii) aldosterone synthase is sensitive to proteolysis at its C-terminus; (iii) the optimal expression conditions for aldosterone synthase in *E. coli* are an induction period of 16 h at a temperature of 30°C; and (iv) aldosterone synthase is monodisperse in sodium cholate. However, for reasons that were not understood, the B2-CLBH construct did not bind to pre-packed Ni^{2+} columns in the way that was expected. To address whether or not this problem was being caused by the CLBH tag, the construct was re-engineered to have a simple C-terminal His_6 tag.

5.3.5 CYP11B1/B2-His$_6$

5.3.5.1 Vector construction

The N-terminally modified aldosterone synthase and 11β-Hydroxylase cDNAs were sub-cloned from the original pGEM T-Easy vectors (Section 5.2.1) into pET21a (which has a C-terminal His$_6$ tag) between the *Nde*I and *Not*I cloning sites. Recombinant plasmids were identified by restriction digestion (Figure 5.11). Once isolated, the B1- and B2-His$_6$ constructs were transformed into the *E. coli* expression strain C43 (DE3), in which the chaperone plasmid pGro7 had already been introduced. C43 (DE3) is a modified version of the *E. coli* expression strain BL21 (DE3) which has increased levels of intracellular membranes compared to the parental strain and is, therefore, better suited to the production of membrane proteins (Miroux and Walker, 1996; Arechaga *et al.*, 2000). It was hoped that by using this strain increased levels of aldosterone synthase and 11β-Hydroxylase expression could be obtained.

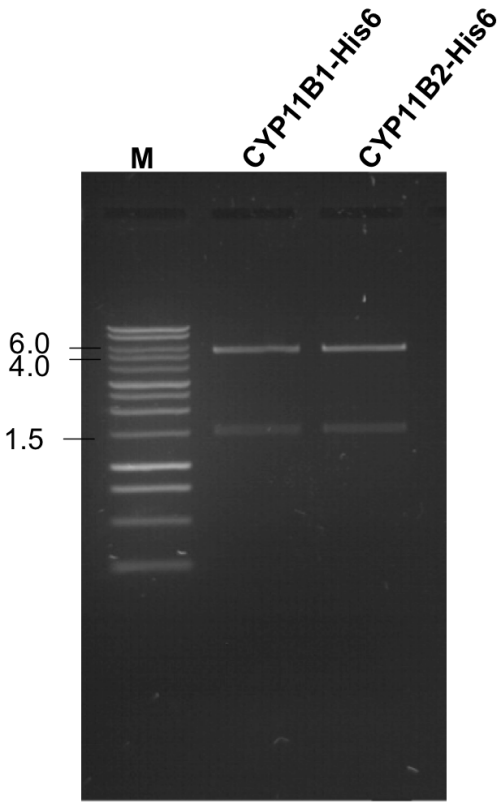

Figure 5.11 Restriction analysis of pET21a-CYP11B1/B2-His$_6$
cDNAs encoding the mature, N-terminally modified versions of 11β-Hydroxylase and aldosterone synthase were sub-cloned from pGEM T-Easy (Section 5.2.1) to pET21a. Recombinant plasmids were identified by restriction digestion with *Nde*I and *Not*I, which gave two fragments of expected size (1.5, 5.3 Kb).

5.3.5.2 ESEC analysis and attempted purification of CYP11B2-His$_6$

B2-His$_6$ was expressed in C43 cells using the optimised induction conditions identified with the CLBH construct. Following this, membranes were isolated and solubilised with sodium cholate. The supernatant was applied to a Superose 6 gel-filtration column. Fractions were collected and their aldosterone synthase content determined by ELISA. The ESEC profile consisted of a single, sharp peak showing that B2-His$_6$ is monodisperse in sodium cholate (Figure 5.12), similar to that which had been observed with the B2-CLBH construct (Figure 5.7F). As expected, B2-His$_6$ eluted from the gel-filtration column later than B2-CLBH (Fraction 35-36 v Fraction 30) consistent with it having a smaller size (MW 50 v 73 kDa).

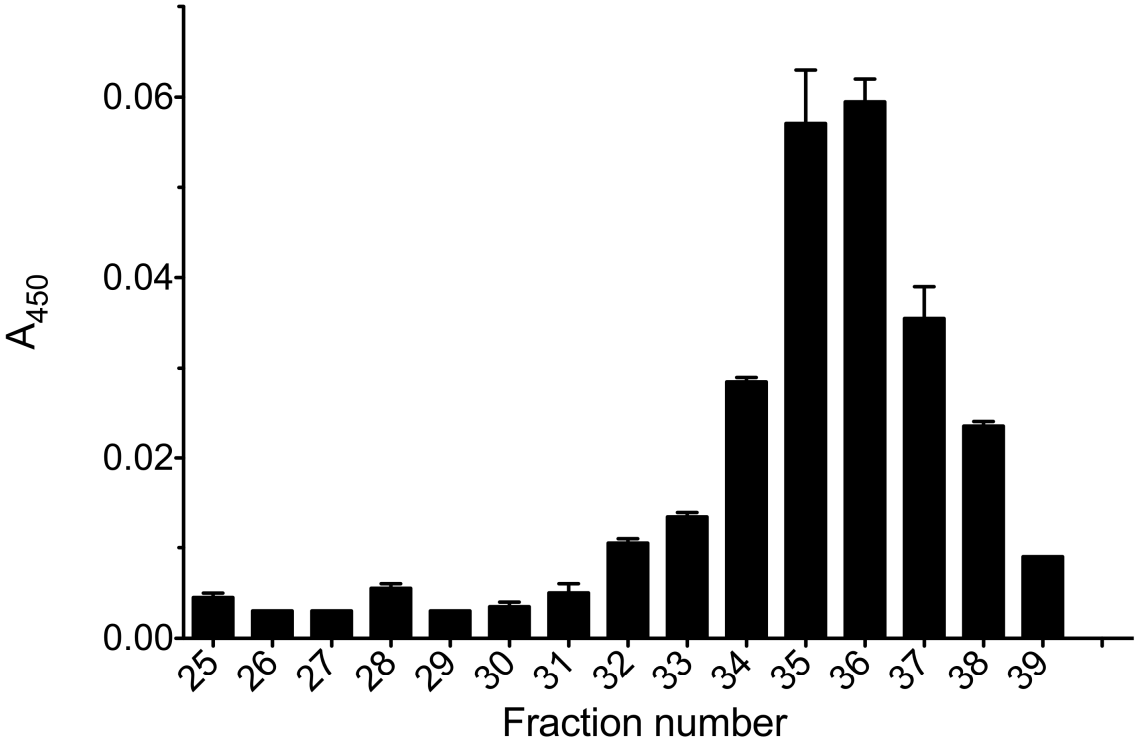

Figure 5.12 ESEC analysis of CYP11B2-His$_6$ solubilised in sodium cholate
Membranes containing B2-His$_6$ were solubilised with sodium cholate and applied to a Superose 6 gel-filtration column. Fractions were collected and analysed by ELISA using anti-B2 antibodies. A single, sharp peak was observed showing that B2-His$_6$ is monodisperse in sodium cholate.

After showing that B2-His_6 was stable in sodium cholate, a Ni^{2+}-affinity purification was attempted. Membranes containing B2-His_6 were treated with sodium cholate, and an absorption spectrum of the supernatant fraction recorded. Similar to that which had been observed with B2-CLBH, the Soret maximum of the haem absorption was at 413 nm (results not shown). The solubilised material was passed over a fresh Ni^{2+} column, which, following loading, was washed with buffers containing first 20 and then 40 mM imidazole. Material that had specifically bound to the column was eluted using 300 mM imidazole. The B2 content of the wash and elution fractions were determined by ELISA (Figure 5.13). The fraction containing the most aldosterone synthase was the 300 mM imidazole elution. Similar to that observed with the B2-CLBH construct, however, the intensity of the ELISA signal in the wash and elution fractions was low, suggesting that the vast majority of the recombinant protein had not bound to the column.

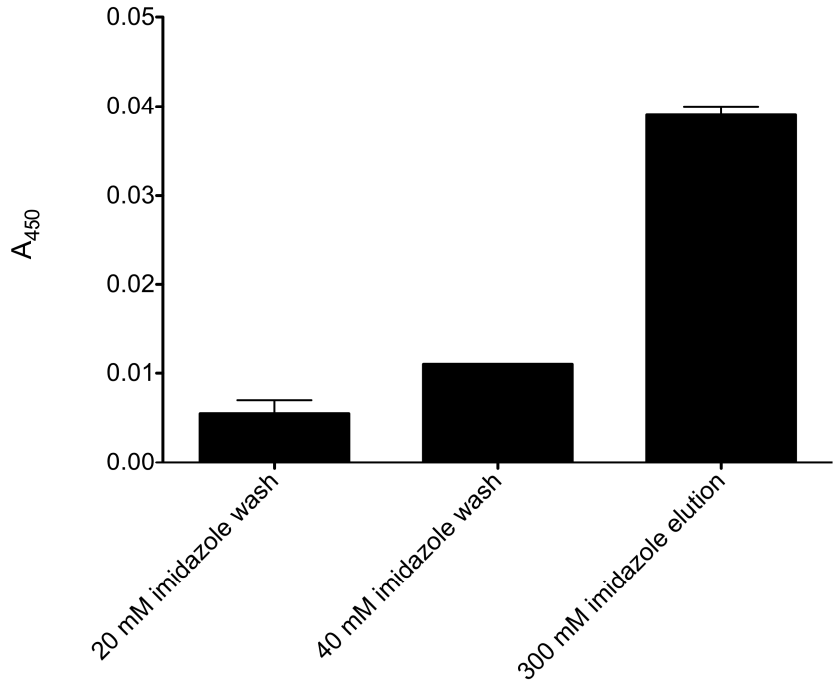

Figure 5.13 ELISA analysis of wash and elution fractions from attempted Ni^{2+}-affinity purification of B2-His_6

B2-His_6 solubilised in sodium cholate was passed over a Ni^{2+} column. Following loading, the column was washed with buffers containing 20 and 40 mM imidazole. Proteins specifically bound to the column were eluted using 300 mM imidazole. The B2 content of the purification fractions were determined by ELISA. As expected, the fraction containing the most aldosterone synthase was the 300 mM imidazole elution fraction. Similar to that observed with the B2-CLBH construct, however, the ELISA signal in the wash and elution fractions was rather low, suggesting that the vast majority of the recombinant protein had not bound to the column.

5.3.5.3 Purification of 11β-Hydroxylase and aldosterone synthase

Towards the end of my Ph.D., a paper was published by Rita Bernhardt's lab reporting the purification and characterisation of aldosterone synthase (Hobler *et al.*, 2012). Having read the details of the paper, it became apparent that there was substantial overlap between what I had been doing and what had been accomplished by Bernhardt and her team. In particular, the expression construct used, the induction conditions as well as the detergent used for solubilisation and purification purposes (sodium cholate) were largely similar.

However, three subtle but significant differences were noted between my protocol and that of Bernhardt, which turned out to be essential for functional purification of both aldosterone synthase and 11β-Hydroxylase. First, I used a mechanical cell disruptor to break open the bacteria. Following this, I isolated membranes and solubilised them with detergent. In contrast, Bernhardt's group lysed the cells by sonication in the presence of detergent. Second, Bernhardt's team used the gentle detergent Tween-20 along with sodium cholate for solubilising aldosterone synthase. Third, Bernhardt and co-workers used Ni^{2+}-sepharose beads rather than a fixed Ni^{2+}-column for the IMAC step. These small differences between protocols turned out to be the difference between success and failure in purifying both aldosterone synthase and 11β-Hydroxylase.

5.3.5.4 Cell lysis and aldosterone synthase functional integrity

Following expression in a heterologous host, cells must be lysed to release the recombinant protein for purification purposes. There are many different methods for breaking open cells. These include enzymatic digestion of cell walls (e.g. with lysozyme), permeabilisation of the cell membrane with detergent as well as using mechanical force (e.g. using a French Press). In the Fraser lab, all cells are routinely broken open using a Constant Systems Cell Disruptor. Following this, membranes are isolated and later solubilised with detergent immediately prior to starting a purification experiment. When this strategy was applied to B2-His_6 made in *E. coli*, the detergent-solubilised material always had a prominent absorption in the visible region at 413 nm, irrespective of what detergent was used to break-up the membranes even when a combination of sodium cholate and Tween-20 was used (Figure 5.14). However, when the same

cells were treated with lysozyme, and sonicated in the presence of sodium cholate and Tween-20, the haem Soret band absorption had a maximum at 423 nm (Figure 5.14), corresponding to aldosterone synthase in its low spin state. It was clear, therefore, that mechanical breakage of the *E. coli* cells using the Cell Disruptor was damaging the recombinant protein but why this was happening was not understood.

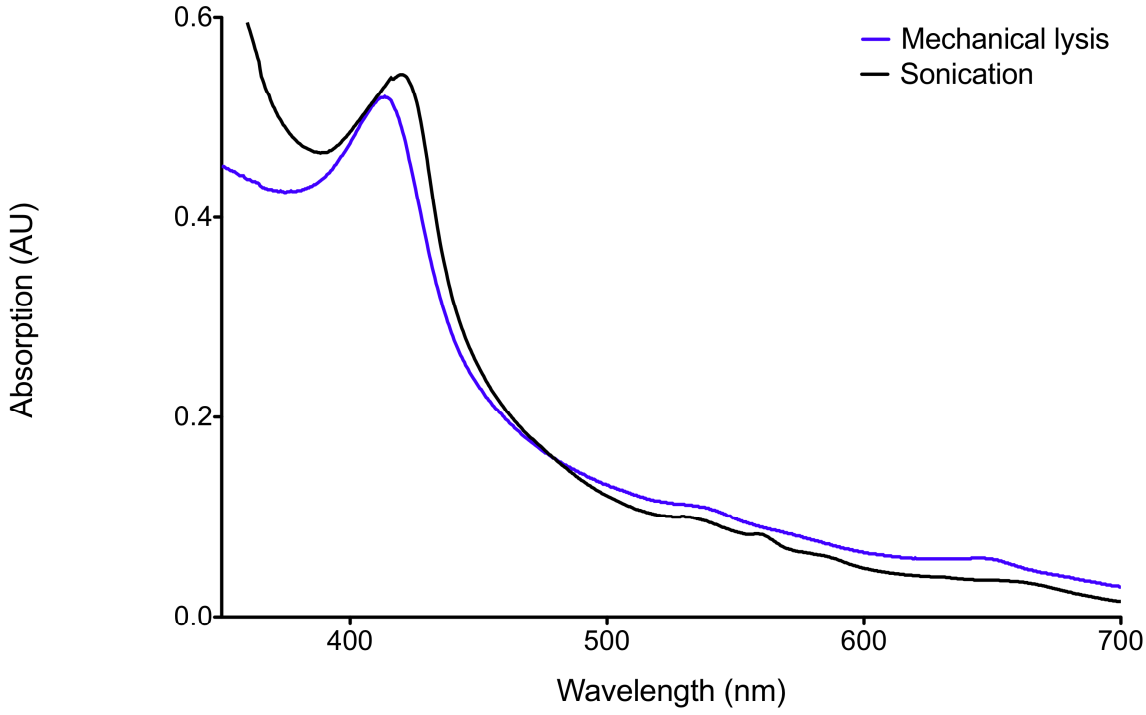

Figure 5.14 The effect of the method of cell disruption on the absorption spectrum of an *E. coli* cell lysate containing B2-His_6

E. coli cells containing B2-His_6 were lysed in two different ways: (i) the cells were broken open with mechanical force using a Constant Systems cell disruptor. Following this, membranes were isolated and then solubilised using a combination of sodium cholate and Tween-20; (ii) the cells were treated with lysozyme prior to disruption by sonication in the presence of the same detergents. The absorption spectra of the resulting lysates were subtly but significantly different. The cells lysed mechanically had a haem Soret absorption maximum at 413 nm (blue line) whereas cells lysed by sonication had a main peak at 423 nm (black). As sonication unequivocally yielded aldosterone synthase in its low-spin state, this method was chosen for all subsequent cell disruptions.

5.3.5.5 Partial purification of CYP11B2-His$_6$ using nickel sepharose beads

Having successfully expressed aldosterone synthase and found a way to lyse the cells keeping the enzyme in its low-spin state, efforts were focused on purifying the recombinant protein. Up until this point, all Ni^{2+}-affinity purifications had been carried out using pre-packed Ni^{2+} columns (GE Healthcare). In the Bernhardt protocol, however, Ni^{2+}-sepharose beads were used. Here, *E. coli* cells expressing B2-His$_6$ were disrupted by sonication in the presence of sodium cholate and Tween-20. The cell lysate was centrifuged, and the supernatant containing detergent-solubilised aldosterone synthase mixed with Ni^{2+} beads. Following loading, the beads were transferred to a gravity-feed column and washed with a buffer containing 20 mM imidazole, 1% sodium cholate and 1% Tween-20. Bound protein was eluted in buffer containing 300 mM imidazole, 1% sodium cholate and 1% Tween-20 (Figure 5.15A). A series of red-coloured fractions were collected (Figure 5.15B), and then pooled together. The combined eluate had a strong absorption band at 423 nm with maxima at 536 and 560 nm, typical of a p450 enzyme in its low-spin state (Figure 5.15C). The Ni^{2+}-purified sample was analysed by SDS-PAGE (Figure 5.15D). A band at *ca.* 49 kDa was tentatively identified as aldosterone synthase. Last, some of the pooled eluate was applied to a Superose 6 gel-filtration column for ESEC analysis. A single, sharp peak was observed which showed that the partially-purified B2-His$_6$ was monodisperse (Figure 5.15E). Of note, however, the elution fraction which contained most aldosterone synthase was number 31. Previously, ESEC analysis of B2-His$_6$ solubilised with sodium cholate alone peaked around fractions 35 and 36 (Figure 5.12). This suggested that the aldosterone synthase had bound a significant amount of Tween-20 giving the recombinant protein a significantly higher apparent MW than in the presence of sodium cholate alone, explaining its early exit from the gel-filtration column.

For reasons not well understood, B2-His$_6$ bound well to loose Ni^{2+}-sepharose beads but not to a pre-packed Ni^{2+} column. All subsequent purifications were performed using Ni^{2+} beads.

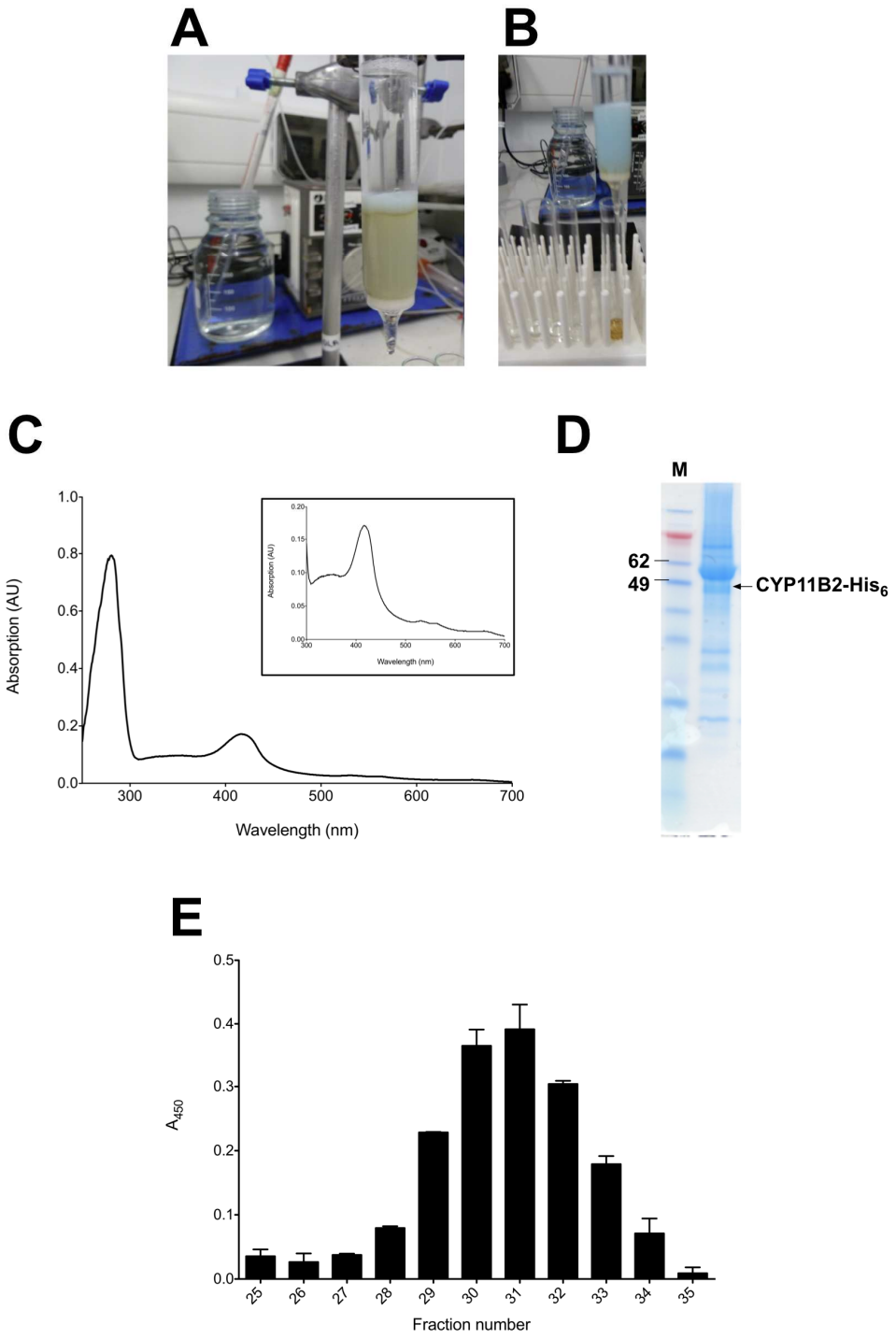

Figure 5.15 Partial purification of aldosterone synthase
B2-His_6 was partially-purified from an *E. coli* cell lysate by Ni^{2+}-affinity chromatography using sepharose beads. (A) The recombinant protein was eluted from the Ni^{2+} beads in 50 mM potassium phosphate, pH 7.4 containing 300 mM imidazole, 1% sodium cholate and 1% Tween-20. (B) A series of red-coloured fractions containing aldosterone synthase were collected. (C) B2-His_6 had a strong absorption band at 423 nm with maxima at 536 and 560 nm, typical of a p450 enzyme in its low-spin state. (D) The Ni^{2+}-enriched sample was analysed by SDS-PAGE. A band at *ca.* 49 kDa was tentatively identified as aldosterone synthase. (E) An aliquot of the partially-purified sample was applied to a Superose 6 gel-filtration column for ESEC analysis The elution profile consisted of a single, sharp peak showing that Ni^{2+}-enriched aldosterone synthase was monodisperse.

5.3.5.6 Purifying aldosterone synthase and 11β-Hydroxylase

Following Ni^{2+}-affinity purification, although highly-enriched, the aldosterone synthase sample was not pure. To achieve a homogenous sample, further purification steps were required. In the Bernhardt protocol, Ni^{2+}-enriched aldosterone synthase was passed over an anion-exchange column and the flow-through collected. Next, the sample was applied to a cation-exchange column on which the aldosterone synthase bound. The column was washed extensively, and the recombinant protein eluted using a sodium acetate salt gradient. The buffers used for the ion-exchange step contained sodium cholate but not Tween-20. Fractions containing aldosterone synthase were pooled, and exchanged into a final purification buffer containing both sodium cholate and Tween-20 by repeatedly concentrating the sample and diluting it with the new buffer.

Bernhardt's protocol was unnecessarily complicated, and the opportunity existed to develop a methodology that was substantially easier to use. First, the anion-exchange purification was dispensed with, as one ion-exchange step was deemed sufficient. Second, to check the aggregation status of the purified protein, a size-exclusion purification step was included following the ion-exchange process.

Last, the purification buffers used for ion-exchange and size-exclusion chromatographies contained only sodium cholate. Tween-20 was omitted as it is a large, heterogenous detergent incompatible with protein crystallisation. It was hoped that by using sodium cholate alone, pure protein could be obtained that would be useful for structural studies.

Both aldosterone synthase and 11β-Hydroxylase were purified using a 3-step protocol consisting of: (i) Ni^{2+}-affinity chromatography using Ni^{2+} sepharose beads, (ii) ion-exchange using a negatively charged SP-sepharose column, and (iii) gel-filtration using a Superose 6 column (Figure 5.16).

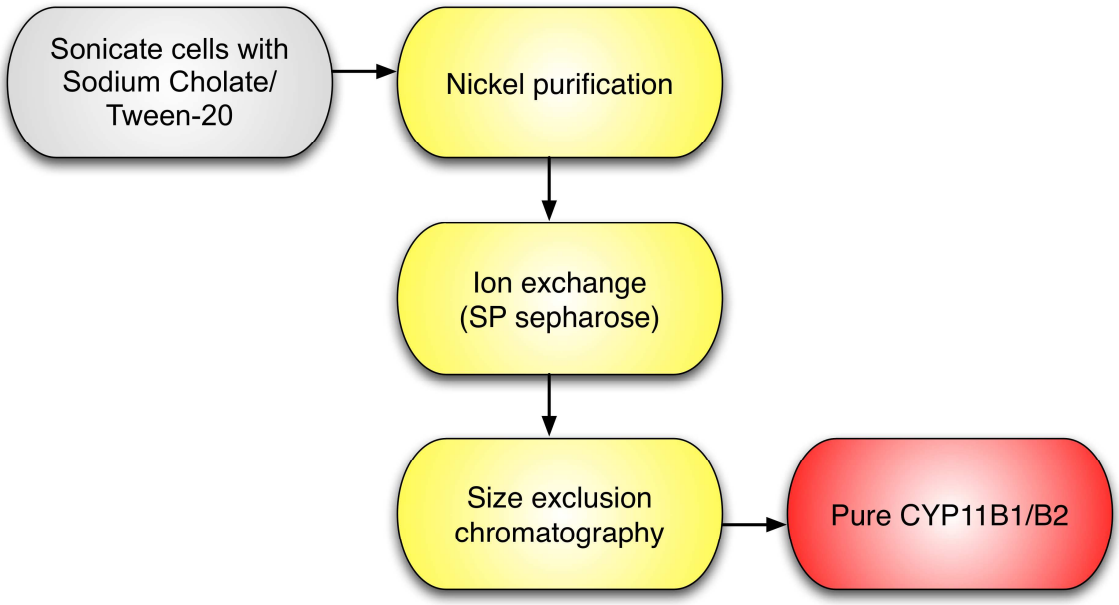

Figure 5.16 A three-step protocol for purifying aldosterone synthase and 11β-Hydroxylase
His-tagged human aldosterone synthase and 11β-Hydroxylase were expressed in *E. coli*. Cells were harvested and then sonicated in the presence of sodium cholate and Tween-20. The cell lysate was centrifuged, and the supernatant fraction mixed with nickel beads. Following extensive washing, aldosterone synthase or 11β-Hydroxylase was eluted from the beads using 300 mM imidazole. The eluate was diluted and then purified by ion-exchange chromatography using a SP-sepharose column. Last, the highly-enriched aldosterone synthase or 11β-Hydroxylase sample was concentrated and applied to a gel-filtration column, from which pure protein was obtained (Section 2.8.5).

In more detail, *E. coli* cells expressing aldosterone synthase or 11β-Hydroxylase were lysed by sonication in the presence of sodium cholate and Tween-20. Insoluble material was removed by centrifugation and the supernatant containing the enzyme was mixed with nickel-beads. Non-specifically bound proteins were removed by washing the beads with buffer containing 20 mM imidazole, 500 mM sodium chloride, 1% sodium cholate and 1% Tween-20. Mg-ATP was also included in the wash buffer to remove any residual GroEL. Aldosterone synthase/11β-Hydroxylase was released using buffer containing 200 mM imidazole, 1% sodium cholate and 1% Tween-20. The eluant fractions containing aldosterone synthase/11β-Hydroxylase were loaded onto a pre-packed SP sepharose ion-exchange column using a peristaltic pump. Binding of the recombinant protein to the SP column was readily visualised as the white column turned brown. Once loading was complete, the column was attached to an ÄKTA system where it was washed extensively. Aldosterone synthase/11β-

Hydroxylase was eluted using a 0-400 mM sodium acetate gradient. Ion-exchange buffers contained 1% sodium cholate but not Tween-20.

The fractions containing aldosterone synthase/11β-Hydroxylase were pooled and concentrated before application to a Superose 6 column. The recombinant protein could be satisfactorily concentrated to *ca.* 1 mg/ml. Of critical importance, it was noted that above this concentration both p450 enzymes precipitated out of solution. The elution profile from the gel-filtration column typically showed a single, sharp peak suggesting that the recombinant protein was both pure and monodisperse (Figure 5.17A). Peak gel-filtration fractions from purifications of aldosterone synthase and 11β-Hydroxylase were analysed by SDS-PAGE. In both cases, a dominant band was observed at *ca.* 49 kDa, suggesting that the recombinant proteins had been successfully purified (Figure 5.17B, C). In order to confirm their identity, the protein bands were excised and sent for analysis by tandem mass spectrometry at the University of Dundee Proteomics Facility. For both bands, numerous peptides were identified that mapped to the primary acid sequences of the modified aldosterone synthase and 11β-Hydroxylase constructs, thus confirming that human 11β-Hydroxylase and aldosterone synthase had been successfully purified (Figure 5.18).

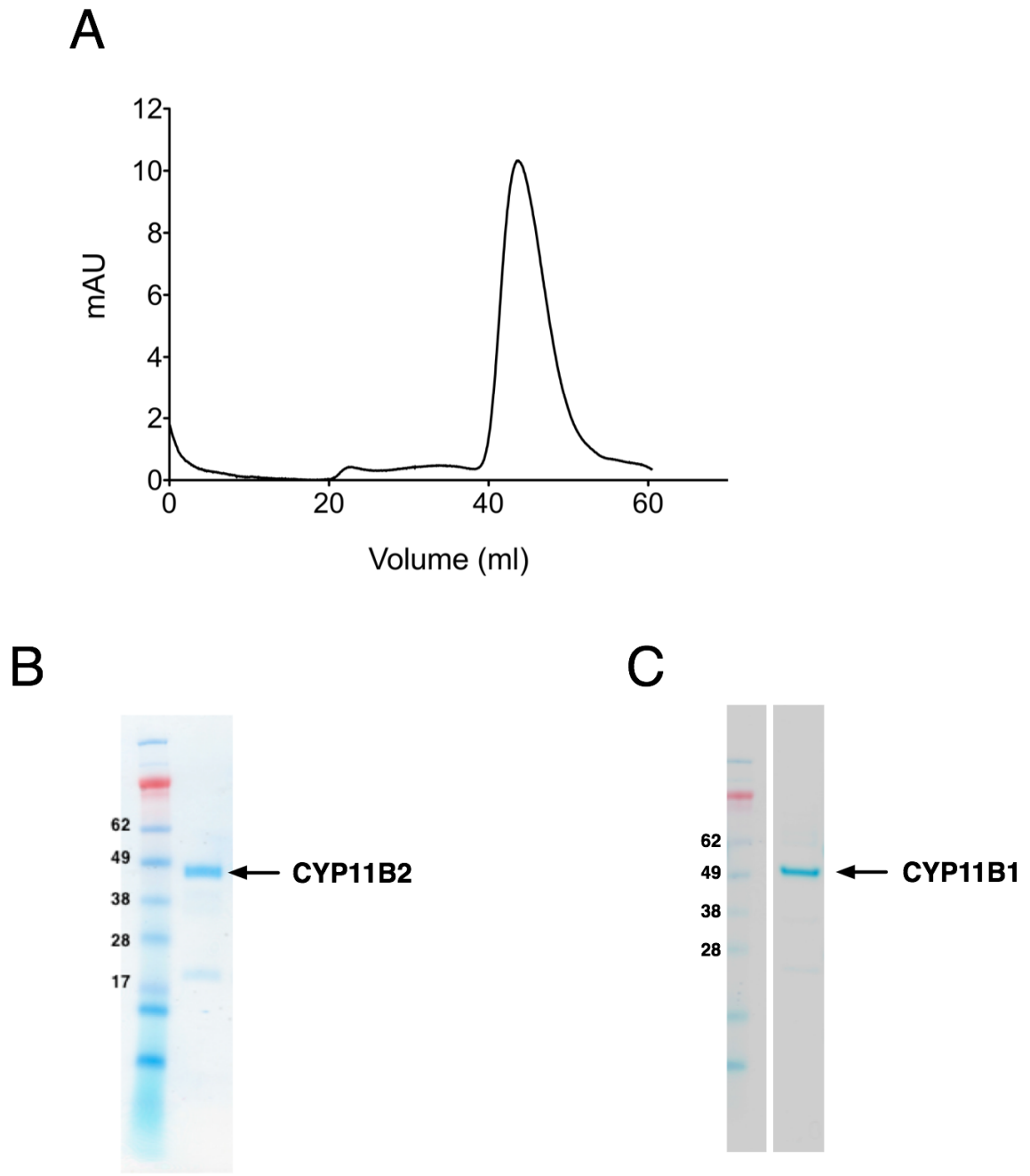

Figure 5.17 Purified aldosterone synthase and 11β-Hydroxylase
(A) Highly-enriched aldosterone synthase was concentrated and applied to a Superose 6 gel-filtration column. The elution profile contained a single, sharp peak suggesting that the aldosterone synthase was both pure and monodisperse. (B) The peak SEC elution fraction was analysed by SDS-PAGE. A dominant band at *ca.* 49 kDa was observed suggesting that the aldosterone synthase was largely pure. (C) 11β-Hydroxylase was purified in a similar way to that for aldosterone synthase. SDS-PAGE analysis of the peak gel-filtration fraction showed a single band with a MW of *ca.* 49 kDa, suggesting that the 11β-Hydroxylase was pure.

A

```
1    MATKAARVPR TVLPFEAMPR RPGNRWLRLL QIWREQGYED LHLEVHQTFQ
51   ELGPIFRYDL GGAGMVCVML PEDVEKLQQV DSLHPHRMSL EPWVAYRQHR
101  GHKCGVFLLN GPEWRFNRLR LNPEVLSPNA VQRFLPMVDA VARDFSQALK
151  KKVLQNARGS LTLDVQPSIF HYTIEASNLA LFGERLGLVG HSPSSASLNF
201  LHALEVMFKS TVQLMFMPRS LSRWTSPKVW KEHFEAWDCI FQYGDNCIQK
251  IYQELAFSRP QQYTSIVAEL LLNAELSPDA IKANSMELTA GSVDTTVFPL
301  LMTLFELARN PNVQQALRQE SLAAAASISE HPQKATTELP LLRAALKETL
351  RLYPVGLFLE RVASSDLVLQ NYHIPAGTLV RVFLYSLGRN PALFPRPERY
401  NPQRWLDIRG SGRNFYHVPF GFGMRQCLGR RLAEAEMLLL LHHVLKHLQV
451  ETLTQEDIKM VYSFILRPSM FPLLTFRAIN
```

B

```
1    MATKAARAPR TVLPFEAMPQ HPGNRWLRLL QIWREQGYEH LHLEMHQTFQ
51   ELGPIFRYNL GGPRMVCVML PEDVEKLQQV DSLHPCRMIL EPWVAYRQHR
101  GHKCGVFLLN GPEWRFNRLR LNPDVLSPKA VQRFLPMVDA VARDFSQALK
151  KKVLQNARGS LTLDVQPSIF HYTIEASNLA LFGERLGLVG HSPSSASLNF
201  LHALEVMFKS TVQLMFMPRS LSRWISPKVW KEHFEAWDCI FQYGDNCIQK
251  IYQELAFNRP QHYTGIVAEL LLKAELSLEA IKANSMELTA GSVDTTAFPL
301  LMTLFELARN PDVQQILRQE SLAAAASISE HPQKATTELP LLRAALKETL
351  RLYPVGLFLE RVVSSDLVLQ NYHIPAGTLV QVFLYSLGRN AALFPRPERY
401  NPQRWLDIRG SGRNFHHVPF GFGMRQCLGR RLAEAEMLLL LHHVLKHFLV
451  ETLTQEDIKM VYSFILRPGT SPLLTFRAIN
```

Figure 5.18 Analysis of purified aldosterone synthase and 11β-Hydroxylase by tandem mass spectrometry

SDS-PAGE analysis of pure aldosterone synthase and 11β-Hydroxylase both showed a single band at *ca.* 49 kDa (Figure 5.17). To identify unequivocally the proteins on the gel, the bands were excised and sent for analysis by tandem mass spectrometry. For both bands, numerous peptides were identified which mapped to the primary acid sequences of the modified (A) 11β-Hydroxylase and (B) aldosterone synthase constructs, thus confirming that human 11β-Hydroxylase and aldosterone synthase had been successfully purified. Regions of the protein for which there was at least one peptide fragment were highlighted in red.

5.4 Biophysical characterisation of aldosterone synthase and 11β-Hydroxylase

5.4.1 UV/Vis absorption spectroscopy

Cytochrome p450 enzymes have characteristic absorption spectra. They can exist in either a high- or a low-spin form, depending on the spin-state of the haem-iron. In the low-spin form, the haem Soret absorption maximum is at *ca.* 420 nm whereas the Soret peak in the high-spin form is around 390 nm. On binding substrate, p450s enzymes are shifted from their low- to high-spin states.

Both aldosterone synthase and 11β-Hydroxylase were purified in their low-spin state with Soret maxima at 418 nm (Figure 5.19A, B). Addition of 50 μM 11-deoxycorticosterone to aldosterone synthase shifted it to its high-spin form with the haem Soret maximum now at 392 nm (Figure 5.19A). 11β-Hydroxylase could be shifted to a high-spin form through adding a high concentration (200 μM) of 11-deoxycorticosterone but not by adding 11-deoxycortisol (its natural substrate) (Figure 5.19B). This result was unexpected.

Cytochrome p450s are so-called as they have a strong characteristic absorption at 450 nm when the enzyme is reacted with carbon monoxide under reducing conditions. Here, reduced carbon monoxide difference spectra were obtained for both aldosterone synthase and 11β-Hydroxylase. The p450 enzymes were split in two, one of which was bubbled with carbon monoxide gas. Following this, both samples were reduced by adding sodium dithionite.

Reduced carbon monoxide difference spectra were obtained by recording the absorption spectra of the reduced samples treated with carbon monoxide using the untreated reduced samples as a reference (Omura and Sato, 1964). A defined peak at 448 nm was clearly visible in the difference spectrum for both aldosterone synthase and 11β-Hydroxylase, demonstrating that the recombinant proteins had retained some of their functionality throughout the purification process (Figure 5.19C, D; Figure 5.20). Protein concentration was estimated using an extinction coefficient of 91 mM^{-1} cm^{-1} at 448 nm.

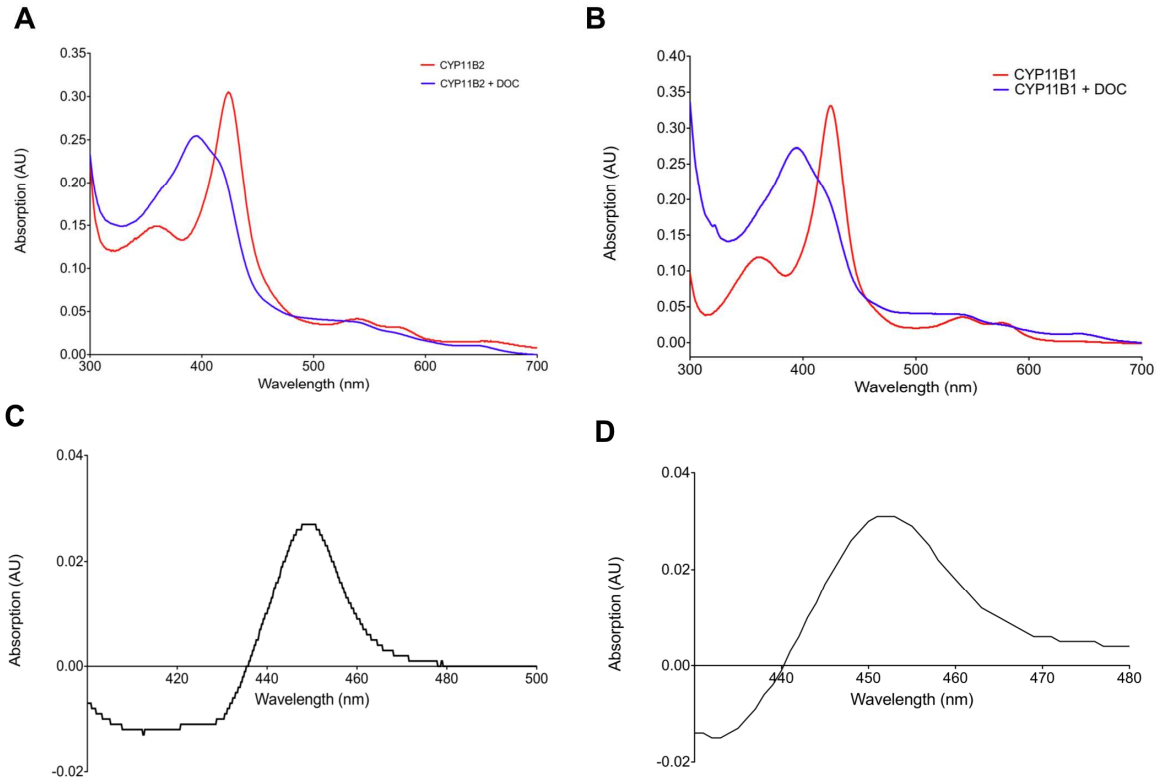

Figure 5.19 Spectral characterisation of pure aldosterone synthase and 11β-Hydroxylase
(A) Aldosterone synthase has a Soret absorption maximum at 418 nm (red) in its low-spin state, which could be shifted to 393 nm (high-spin state (blue)) upon addition of 50 μM 11-deoxycorticosterone (DOC). (B) A similar Soret peak shift (low spin, 418 nm, blue; high spin, 393 nm, red) was observed upon addition of 200 μM DOC to purified 11β-Hydroxylase. Reduced CO spectra for (C) aldosterone synthase and (D) 11β-Hydroxylase were obtained (Section 2.15). Defined peaks at 448 nm were clearly visible in both spectra, demonstrating that both 11β-Hydroxylase and aldosterone synthase had retained their activity throughout the purification process.

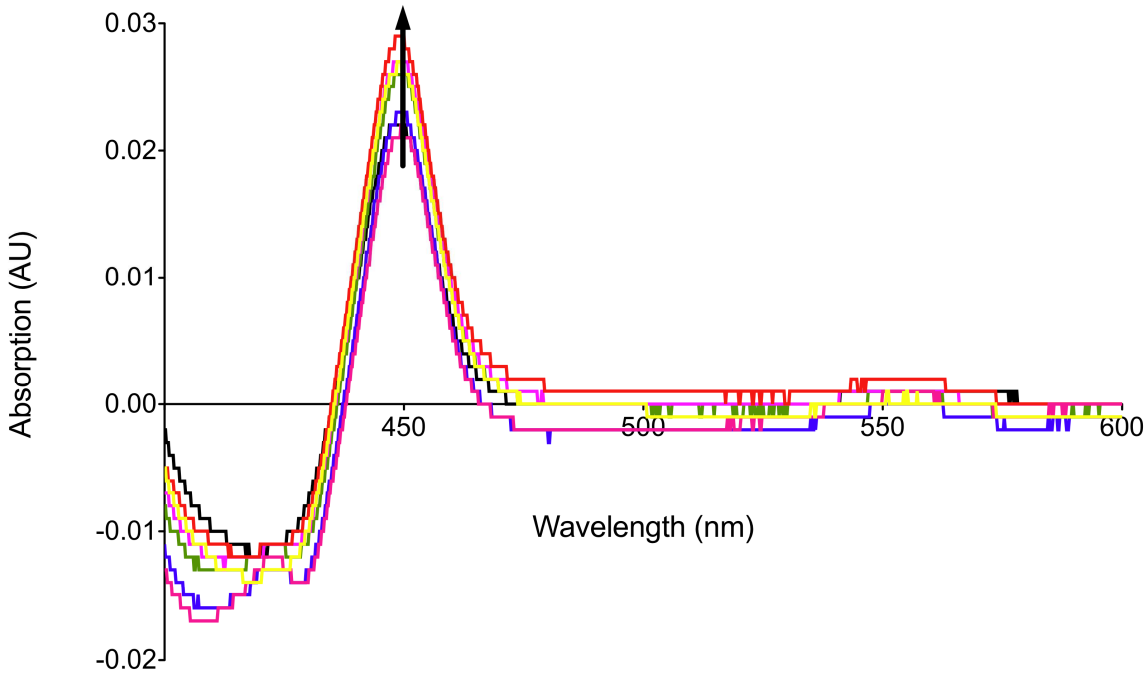

Figure 5.20 Reduced CO spectrum for aldosterone synthase
Pure aldosterone synthase was split in two. One of the aliquots was bubbled with carbon monoxide gas. Both samples were then reduced by adding sodium dithionite. Reduced carbon monoxide difference spectra were obtained at regular time intervals by recording the absorption spectra of the reduced sample bubbled with carbon monoxide using the untreated reduced sample as a reference. A defined absorption peak at 448 nm was clearly visible in the difference spectrum that increased in magnitude with time.

5.5 Conclusion

Here, a system for the recombinant expression and purification of human 11β-Hydroxylase and aldosterone synthase has been developed.

Initial efforts to express aldosterone synthase in *P. pastoris* were abandoned as the yeast was unable to make the recombinant protein. However, successful expression of both aldosterone synthase and 11β-Hydroxylase was achieved in *E. coli*. Using the pET21a-CLBH vector, optimal induction conditions for aldosterone synthase and 11β-Hydroxylase production were identified. Furthermore, using the CLBH vector, it became apparent that aldosterone synthase has a region towards its C-terminus that is sensitive to cleavage by bacterial metalloproteases.

A novel technique (called ESEC) was developed which allowed the simultaneous assessment of the aggregation state and the polar surface exposure of aldosterone synthase in a range of different detergents. Using ESEC, sodium cholate was identified as the optimal detergent for solubilising and purifying aldosterone synthase.

Using CYP11B1/B2-His_6 constructs, both aldosterone synthase and 11β-Hydroxylase were purified in a partially functional form using a simple three step protocol consisting of Ni^{2+}-affinity, ion-exchange and size-exclusion chromatographies. For success, it was essential to break the cells open by sonication in the presence of sodium cholate and Tween-20. Furthermore, the Ni^{2+}-affinity step had to be performed using Ni^{2+} sepharose beads and not a pre-packed column to ensure efficient binding of the recombinant protein.

Tween-20 was not required for functional purification of aldosterone synthase. However, in sodium cholate alone, when aldosterone synthase was concentrated to >1 mg/ml, aldosterone synthase precipitated out of solution. This suggested that when aldosterone synthase is in sodium cholate there are still hydrophobic patches on the surface of the protein not covered with detergent, which gives the protein a propensity to aggregate at high concentration. Presumably, Tween-20 stabilises aldosterone synthase and 11β-Hydroxylase by covering over these hydrophobic patches. However, as Tween-20 is a large, heterogenous detergent, it is not useful for crystallisation purposes. This means that an alternative additive will have to be found that prevents the p450 enzymes from aggregating at high concentration and yet can be used in crystallisation trials. Once this issue has been addressed, it will be possible to solve the structures of both proteins. Additionally, as aldosterone synthase and 11β-Hydroxylase can be purified in an active form, it will be possible to use the pure protein in drug-screening experiments to identify small molecules that specifically inhibit aldosterone synthase.

Chapter 6 - General discussion and future perspectives

Aldosterone plays a key role in regulating body fluid balance in people, stimulating sodium uptake, potassium excretion and water retention in the distal tubules and collecting ducts of the kidney nephron. Considering the physiological function of aldosterone, it is not surprising that many patients with essential hypertension have relative aldosterone excess too (Connell *et al.*, 2008). Drugs that block aldosterone action through antagonising mineralocorticoid receptor function significantly reduce blood pressure *in vivo* (Pitt *et al.*, 1999; Pitt *et al.*, 2003). To circumvent side-effects commonly observed with mineralocorticoid receptor antagonists, considerable research effort is currently being invested in trying to discover specific inhibitors of aldosterone synthase that reduce plasma aldosterone levels in people. Identifying molecules that selectively interact with aldosterone synthase but not 11β-Hydroxylase is extremely challenging as the two enzymes have 93% sequence identity. However, by solving the 3-dimensional structures of both p450s, it should be possible to design small molecules that bind with high-affinity to aldosterone synthase but not 11β-Hydroxylase. Sustained crystallisation trials require milligram quantities of pure, functional protein. The primary aim of my Ph.D. was to develop a system for expressing and purifying aldosterone synthase and 11β-Hydroxylase for structural studies. With a view to creating activity assays for both aldosterone synthase and 11β-Hydroxylase *in vitro*, protocols for making and purifying the electron transfer proteins adrenodoxin (Adx) and adrenodoxin reductase (AdxRed) were established.

At the outset of this thesis, it was expected that a eukaryotic cell type would be required for producing the proteins of interest as they were all of human origin. For this reason, the "CLBH" expression and purification system was developed in *Pichia pastoris* with sterol isomerase (SI) as a test protein, fully expecting to use the modified yeast vector at a later stage with aldosterone synthase, 11β-Hydroxylase, Adx and AdxRed. Although SI could be made in *P. pastoris* on a

milligram scale, this was not the case for aldosterone synthase, 11β-Hydroxylase or AdxRed. Although unexpected, these results help to show that the usefulness, or otherwise, of a particular heterologous host cell for making a specific target protein can only be determined by experiment. In general, this means that several different expression systems may have to be tried before one is found that is suitable for making the protein of interest. To enhance the rate of expression screening, it is now common to fuse a fluorescent reporter (typically GFP) to either the N- or C-terminus of a target protein. Here, the production of several different CLBH-tagged proteins in both *P. pastoris* and *E. coli* was monitored by measuring iLOV fluorescence. It was found that aldosterone synthase, 11β-Hydroxylase, Adx and AdxRed could all be successfully made in *E. coli* on a milligram scale.

The CLBH tag enabled purification of SI, Adx and AdxRed using a generic approach consisting of four simple steps (Ni^{2+}-affinity, cleavage with 3C protease, reverse Ni^{2+}-affinity, gel-filtration). The purification process could be simplified further by performing the 3C cleavage step on the first Ni^{2+} column when the recombinant protein is bound to it, eliminating the need for a reverse-purification step. With hindsight, the problems encountered trying to purify B2-CLBH by Ni^{2+}-affinity chromatography were not caused by the CLBH tag. Rather, it was subsequently discovered that His-tagged aldosterone synthase and 11β-Hydroxylase would only bind to Ni^{2+}-sepharose beads but not to a pre-packed Ni^{2+} column. This means that, at least in principle, it should be possible to purify both aldosterone synthase and 11β-Hydroxylase using the CLBH constructs. In general, the CLBH tag can be used for purifying both soluble and membrane proteins to homogeneity. Indeed, since its inception, the CLBH tag has been used in the Fraser lab to purify a diverse range of proteins including PscD and PscB (subunits of the photosynthetic reaction centre from green bacteria), the EGF-binding domains of uromodulin as well as several different G-protein coupled receptors (Niall Fraser, personal communication).

The CLBH tag can be biotinylated *in vitro* using recombinant biotin ligase, which allows proteins of interest to be immobilised on (strept)avidin coated surfaces. This is an elegant feature of the CLBH system, and is compatible with drug-

design techniques such as target immobilised NMR screening (TINS) (Siegal and Hollander, 2009) and surface plasmon resonance (SPR) (Navratilova and Hopkins, 2010) where the target protein has to be immobilised on a surface prior to screening molecular and/or fragment libraries. If time had allowed, it would have been interesting to have immobilised aldosterone synthase and 11β-Hydroxylase on an appropriate surface and screened both enzymes against a fragment library by SPR to identify small molecules that bind to aldosterone synthase but not 11β-Hydroxylase. Aldosterone synthase and 11β-Hydroxylase could be immobilised using the CLBH tag. However, the structures of several steroidogenic p450s have shown that the enzyme's C-terminus is located in/near the membrane, with its active site facing the membrane (Mast *et al.*, 2011; Strushkevich *et al.*, 2011; DeVore and Scott, 2012). This may suggest, therefore, that a C-terminal tag is not ideal for immobilising aldosterone synthase or 11β-Hydroxylase for drug screening by SPR as it would position the active site of the enzyme towards the immobilisation surface away from the flow of molecular fragments. Alternatively, the p450 enzymes could be immobilised using antibodies. The anti-B2 Abs used in the ESEC experiments recognise an epitope on the surface of aldosterone synthase in a region equivalent to the β-strands 1 and 2 of the side-chain cleavage enzyme structure (Strushkevich *et al.*, 2011). If these antibodies were used to immobilise aldosterone synthase, the enzyme active site would be correctly orientated (pointing towards the flow of molecular fragments) for drug-screening experiments.

Fusion of the iLOV fluorescence reporter to the C-terminus of aldosterone synthase, 11β-Hydroxylase, Adx and AdxRed gave critical insights into their expression, purification, stability and integrity. In particular, the protease-sensitive region towards the C-terminus of aldosterone synthase would not have been identified if the enzyme had been expressed with a His_6 rather than a CLBH tag. Arguably the most intriguing result from my thesis was the dramatic increase in iLOV fluorescence that was observed when partially-purified B2-CLBH was cleaved with 3C protease. The putative quenching of iLOV fluorescence by the p450 haem group is an unusual phenomenon, and one that I would liked to have explored given more time. Potentially, the B2-iLOV fusion could be used as a reporter of protease activity both *in vitro* and *in vivo*, taking advantage of the

8-fold increase in iLOV fluorescence that occurs when the reporter is cleaved from the C-terminus of the p450. By introducing different protease recognition sites between aldosterone synthase and iLOV, the biosensor could be readily adapted for use with any protease from any organism. Potentially, the B2-iLOV biosensor has several advantages over existing technologies aimed at measuring protease activity. First, as the B2-iLOV fusion relies on flavin and haem co-factors (which are ubiquitous in nature), it is likely that the biosensor could be used in most, if not all, cell types. Second, as the biosensor is a protein it can be readily made and purified for use in high-throughput screening studies to identify novel inhibitors of protease activity *in vitro*. Third, as the B2-iLOV fusion can be expressed *in vivo*, it can be used to assess the biological activity of cell permeable protease inhibitors in living cells. Furthermore, as iLOV has a strong fluorescence in the absence of oxygen, the B2 fusion protein could be used to monitor protease activity in hypoxic conditions (e.g. such as in solid tumours). However, before the B2-iLOV fusion could be used as a biosensor, it would have to be engineered to make the protein water-soluble (rather than membrane associated).

A novel technique called ELISA size-exclusion chromatography (ESEC) was developed which allowed the simultaneous assessment of the aggregation state and the polar surface exposure of aldosterone synthase in a range of different detergents. ESEC is a simple adaptation of FSEC (the current method of choice for determining the optimal detergent for solubilising and purifying target membrane proteins with). Similar to FSEC, the aggregation status of a target membrane protein can be evaluated in the presence of other proteins as the ELISA signal is generated via an antibody specific to the protein of interest. However, ESEC has a couple of notable advantages over FSEC. First, ESEC can be used with any membrane protein where there is an antibody available against an antigenic epitope on the surface of the protein. In contrast, FSEC can only be used with membrane proteins that have been engineered to have a fluorescent reporter attached to either their N- or C-termini. Second, the antibody will not be able to bind to the target protein if the surface epitope is covered by detergent. For this reason, the size of the ELISA signal gives insights into how much of the protein's surface is exposed to the aqueous environment. Using

ESEC, sodium cholate was identified as the optimal detergent for solubilising and purifying aldosterone synthase.

After considerable effort, protocols were obtained that allowed functional aldosterone synthase and 11β-Hydroxylase to be purified. En route, two unusual preparative problems were discovered. First, it was found that mechanical disruption of *E. coli* cells expressing aldosterone synthase rendered the recombinant protein inactive. This was observed as a prominent absorption in the visible region at 413 nm following solubilisation of membranes containing aldosterone synthase with detergent. However, when the same cells were treated with lysozyme, and sonicated in the presence of sodium cholate and Tween-20, the haem Soret band absorption had a maximum at 423 nm, indicating the presence of aldosterone synthase in its low spin state. Although it is not understood why mechanical disruption should affect the spectral properties of aldosterone synthase in the way that was observed, it suggests that aldosterone synthase is sensitive to high-pressure forces. Second, it was found that CYP11B2-His_6 bound with high-efficiency to Ni^{2+}-sepharose beads but not to pre-packed Ni^{2+} columns. This observation is hard to rationalise. It is possible that when the recombinant protein was passed over the column the His_6 tag was masked by detergent prevent binding to the immobilised Ni^{2+} ions. When the cell lysate was mixed by rotation with Ni^{2+} beads, however, the dynamic loading environment may have resulted in exposure of the His_6 tag allowing capture of the recombinant protein on the Ni^{2+} beads.

The detergent Tween-20 was included in the buffers used for breaking open *E. coli* cells expressing CYP11B1/B2-His_6 as well as those for Ni^{2+}-affinity purification in accordance with the aldosterone synthase purification protocol published recently by Rita Bernhardt's group (Hobler *et al.*, 2012). Tween-20 is an extremely mild detergent, traditionally used as a washing agent in Western Blots where it helps to prevent non-specific Ab binding. Although Tween-20 can be used to solubilise membrane proteins, it is not compatible with crystallisation trials as it is a large, heterogenous detergent. Therefore, ion-exchange and gel-filtration purification steps with nickel-affinity enriched aldosterone synthase and 11β-Hydroxylase were performed in the presence of sodium cholate alone. It

was found that functional purification of aldosterone synthase does not require Tween-20. However, in sodium cholate alone, when purified aldosterone synthase was concentrated to >1 mg/ml, the p450 enzyme precipitated out of solution. This suggested that in sodium cholate there must be hydrophobic patches on the surface of aldosterone synthase not covered with detergent that drive enzyme aggregation at high protein concentrations. As Tween-20 can not be used for structural biology purposes, an alternative additive/detergent will have to be found that prevents the p450 enzymes from aggregating at high concentration and yet can be used in crystallisation trials. One possibility are the facial amphiphiles (Zhang *et al.*, 2007) which have been used by others to obtain high-resolution structures of selected mammalian p450 enzymes including CYP24A1 (Annalora et al., 2010), CYP2B6 (Gay et al., 2010) and CYP2B4 (Gay et al., 2011). Furthermore, prior to starting crystallisation trials, thermostability assays need to be performed to identify the optimal buffer conditions for use with aldosterone synthase and 11β-Hydroxylase. One these issues have been addressed, it should be possible to obtain crystals of both aldosterone synthase and 11β-Hydroxylase that diffract to high-resolution.

In the next phase of the work, the electron transfer proteins (Adx, AdxRed) will be reconstituted *in vitro* with both aldosterone synthase and 11β-Hydroxylase to determine whether or not the p450 enzymes are catalytically active. Enzyme activity could be assessed by measuring the rate of substrate consumption (11-Hydroxylase, deoxycortisol; aldosterone synthase, 11-deoxycorticosterone) or production (11-Hydroxylase, cortisol; aldosterone synthase, aldosterone) formation. However, it will likely be easier to monitor the rate of NADPH oxidation by AdxRed through measuring changes in A_{340}. Once assays have been developed for both aldosterone synthase and 11β-Hydroxylase, they can be used to determine IC_{50} values for any molecular 'hits' identified in drug-screening experiments. Additionally, once activity assays have been established, the effect of non-synonymous mutations in Adx or AdxRed on the rate of aldosterone or cortisol production can be investigated. If any of the non-synonymous polymorphisms affect steroid biosynthesis *in vitro*, it would be very interesting to look at the prevalence of the SNPs in a hypertensive population cohort compared to matched control patients.

In conclusion, this thesis describes the successful expression, purification and characterisation of the human cytochrome p450 enzymes aldosterone synthase and 11β-Hydroxylase, as well as their associated electron transfer proteins, Adx and AdxRed. This work provides a solid foundation for future efforts to solve the structures of aldosterone synthase and 11β-Hydroxylase to atomic resolution. In addition, the purified proteins can be used in drug-screening experiments to identify novel specific inhibitors of aldosterone synthase for the treatment of hypertension.

Bibliography

Alexandrov, A.I., Mileni, M., Chien, E.Y.T., Hanson, M.A. and Stevens, R.C. (2008). Microscale fluorescent thermal stability assay for membrane proteins. *Structure* **16**(3): 351-359.

Alisio, A. and Mueckler, M. (2010). Purification and characterization of mammalian glucose transporters expressed in *Pichia pastoris*. *Protein Expression and Purification* **70**(1): 81-87.

Andersen, M.D., Busk, P.K., Svendsen, I. and Møller, B.L. (2000). Cytochromes p450 from cassava (Manihot esculenta Crantz) catalyzing the first steps in the biosynthesis of the cyanogenic glucosides linamarin and lotaustralin - Cloning, functional expression in Pichia pastoris, and substrate specificity of the isolated recombinant enzymes. *Journal of Biological Chemistry* **275**(3): 1966-1975.

Andre, N., Cherouati, N., Prual, C., Steffan, T., Zeder-Lutz, G., Magnin, T., Pattus, F., Michel, H., Wagner, R. and Reinhart, C. (2006). Enhancing functional production of G protein-coupled receptors in *Pichia pastoris* to levels required for structural studies via a single expression screen. *Protein Science* **15**(5): 1115-1126.

Annalora, A., Bobrovnikova-Marjon, E., Serda, R., Lansing, L., Chiu, M.L., Pastuszyn, A., Iyer, S., Marcus, C.B. and Omdahl, J.L. (2004). Rat cytochrome P450C24 (CYP24A1) and the role of F249 in substrate binding and catalytic activity. *Archives of Biochemistry and Biophysics* **425**(2): 133-146.

Annalora, A.J., Goodin, D.B., Hong, W.-X., Zhang, Q., Johnson, E.F. and Stout, C.D. (2010). Crystal structure of CYP24A1, a mitochondrial cytochrome p450 involved in vitamin D metabolism. *Journal of Molecular Biology* **396**(2): 441-451.

Aoyama, T., Nagata, K., Yamazoe, Y., Kato, R., Matsunaga, E., Gelboin, H.V. and Gonzalez, F.J. (1990). Cytochrome b5 potentiation of cytochrome p450 catalytic activity demonstrated by a vaccinia virus-mediated *in situ*

reconstitution system. *Proceedings of the National Academy of Sciences of the United States of America* **87**(14): 5425-5429.

Arechaga, I., Miroux, B., Karrasch, S., Huijbregts, R., de Kruijff, B., Runswick, M.J. and Walker, J.E. (2000). Characterisation of new intracellular membranes in *Escherichia coli* accompanying large scale over-production of the b subunit of F1Fo ATP synthase. *FEBS Letters* **482**(3): 215-219.

Arnau, J., Lauritzen, C., Petersen, G.E. and Pedersen, J. (2006). Current strategies for the use of affinity tags and tag removal for the purification of recombinant proteins. *Protein Expression and Purification* **48**(1): 1-13.

Barnes, H.J., Arlotto, M.P. and Waterman, M.R. (1991). Expression and enzymatic activity of recombinant cytochrome p450 17-α-hydroxylase in *Escherichia coli Proceedings of the National Academy of Sciences of the United States of America* **88**(13): 5597-5601.

Barr, M., MacKenzie, S.M., Friel, E.C., Holloway, C.D., Wilkinson, D.M., Brain, N.J.R., Ingram, M.C., Fraser, R., Brown, M., Samani, N.J., Caulfield, M., Munroe, P.B., Farrall, M., Webster, J., Clayton, D., Dominiczak, A.F., Connell, J.M.C. and Davies, E. (2007). Polymorphic variation in the 11ß-hydroxylase gene associates with reduced 11-hydroxylase efficiency. *Hypertension* **49**(1): 113-119.

Bassett, M.H., White, P.C. and Rainey, W.E. (2004). The regulation of aldosterone synthase expression. *Molecular and Cellular Endocrinology* **217**(1-2): 67-74.

Bassett, M.H., Zhang, Y., Clyne, C., White, P.C. and Rainey, W.E. (2002). Differential regulation of aldosterone synthase and 11ß-hydroxylase transcription by steroidogenic factor-1. *Journal of Molecular Endocrinology* **28**(2): 125-135.

Bernhardt, R. (2006). Cytochromes p450 as versatile biocatalysts. *Journal of Biotechnology* **124**(1): 128-145.

Betancourt-Calle, S., Calle, R.A., Isales, C.M., White, S., Rasmussen, H. and Bollag, W.B. (2001). Differential effects of agonists of aldosterone

secretion on steroidogenic acute regulatory phosphorylation. *Molecular and Cellular Endocrinology* **173**(1-2): 87-94.

Bhalla, V., Soundararajan, R., Pao, A.C., Li, H. and Pearce, D. (2006). Disinhibitory pathways for control of sodium transport: regulation of ENaC by SGK1 and GILZ. *American Journal of Physiology-Renal Physiology* **291**(4): 714-721.

Bill, R.M., Henderson, P.J.F., Iwata, S., Kunji, E.R.S., Michel, H., Neutze, R., Newstead, S., Poolman, B., Tate, C.G. and Vogel, H. (2011). Overcoming barriers to membrane protein structure determination. *Nature Biotechnology* **29**(4): 335-340.

Blumenfeld, J.D., Sealey, J.E., Schlussel, Y., Vaughan, E.D., Sos, T.A., Atlas, S.A., Muller, F.B., Acevedo, R., Ulick, S. and Laragh, J.H. (1994). Diagnosis and treatment of hyperaldosteronism. *Annals of Internal Medicine* **121**(11): 877-885.

Brand, E., Chatelain, N., Mulatero, P., Fery, I., Curnow, K., Jeunemaitre, X., Corvol, P., Pascoe, L. and Soubrier, F. (1998). Structural analysis and evaluation of the aldosterone synthase gene in hypertension. *Hypertension* **32**(2): 198-204.

Brilla, C.G., Matsubara, L.S. and Weber, K.T. (1993). Anti-aldosterone treatment and the prevention of myocardial fibrosis in primary and secondary hyperaldosteronism. *Journal of Molecular and Cellular Cardiology* **25**(5): 563-575.

Brilla, C.G. and Weber, K.T. (1992). Mineralocorticoid excess, dietary sodium and myocardial fibrosis. *Journal of Laboratory and Clinical Medicine* **120**(6): 893-901.

Brohawn, S.G., del Marmól, J. and MacKinnon, R. (2012). Crystal Structure of the Human K2P TRAAK, a Lipid- and Mechano-Sensitive K^+ Ion Channel. *Science* **335**(6067): 436-441.

Butterworth, M.B., Edinger, R.S., Frizzell, R.A. and Johnson, J.P. (2009). Regulation of the epithelial sodium channel by membrane trafficking. *American Journal of Physiology-Renal Physiology* **296**(1): F10-F24.

Caffrey, M. (2003). Membrane protein crystallization. *Journal of Structural Biology* **142**(1): 108-132.

Calhoun, D.A., White, W.B., Krum, H., Guo, W., Bermann, G., Trapani, A., Lefkowitz, M.P. and Ménard, J. (2011). Effects of a novel aldosterone synthase inhibitor for treatment of primary hypertension results of a randomized, double-blind, placebo- and active-controlled phase 2 trial. *Circulation* **124**(18): 1945-U1124.

Carpenter, E.P., Beis, K., Cameron, A.D. and Iwata, S. (2008). Overcoming the challenges of membrane protein crystallography. *Current Opinion in Structural Biology* **18**(5): 581-586.

Cereghino, G.P.L., Cereghino, J.L., Ilgen, C. and Cregg, J.M. (2002). Production of recombinant proteins in fermenter cultures of the yeast *Pichia pastoris*. *Current Opinion in Biotechnology* **13**(4): 329-332.

Chalfie, M., Tu, Y., Euskirchen, G., Ward, W.W. and Prasher, D.C. (1994). Green fluorescent protein as a marker for gene-expression. *Science* **263**(5148): 802-805.

Chandler, C.S. and Ballard, F.J. (1988). Regulation of the breakdown rates of biotin-containing proteins in Swiss 3T3-L1 cells *Biochemical Journal* **251**(3): 749-755.

Chapman, N., Dobson, J., Wilson, S., Dahlöf, B., Sever, P.S., Wedel, H. and Poulter, N.R. (2007). Effect of spironolactone on blood pressure in subjects with resistant hypertension. Hypertension. **49:** 839-845.

Chapman, S., Faulkner, C., Kaiserli, E., Garcia-Mata, C., Savenkov, E.I., Roberts, A.G., Oparka, K.J. and Christie, J.M. (2008). The photoreversible fluorescent protein iLOV outperforms GFP as a reporter of plant virus infection. *Proceedings of the National Academy of Sciences of the United States of America* **105**(50): 20038-20043.

Che, Q., Schreiber, M.J., Jr. and Rafey, M.A. (2009). Beta-blockers for hypertension: Are they going out of style? *Cleveland Clinic Journal of Medicine* **76**(9): 533-542.

Cherezov, V., Rosenbaum, D.M., Hanson, M.A., Rasmussen, S.G.F., Thian, F.S., Kobilka, T.S., Choi, H.-J., Kuhn, P., Weis, W.I., Kobilka, B.K. and Stevens, R.C. (2007). High-resolution crystal structure of an engineered human beta(2)-adrenergic G protein-coupled receptor. *Science* **318**(5854): 1258-1265.

Chloupkova, M., Pickert, A., Lee, J.-Y., Souza, S., Trinh, Y.T., Connelly, S.M., Dumont, M.E., Dean, M. and Urbatsch, I.L. (2007). Expression of 25 human ABC transporters in the yeast *Pichia pastoris* and characterization of the purified ABCC3 ATPase activity. *Biochemistry* **46**(27): 7992-8003.

Chobanian, A.V., Bakris, G.L., Black, H.R., Cushman, W.C., Green, L.A., Izzo, J.L., Jones, D.W., Materson, B.J., Oparil, S., Wright, J.T. and Roccella, E.J. (2003). The seventh report of the Joint National Committee on prevention, detection, evaluation, and treatment of high blood pressure - The JNC 7 Report. *Jama-Journal of the American Medical Association* **289**(19): 2560-2572.

Christie, J.M. (2007). Phototropin blue-light receptors. Annual Review of Plant Biology. **58:** 21-45.

Christie, J.M., Reymond, P., Powell, G.K., Bernasconi, P., Raibekas, A.A., Liscum, E. and Briggs, W.R. (1998). Arabidopsis NPH1: A flavoprotein with the properties of a photoreceptor for phototropism. *Science* **282**(5394): 1698-1701.

Christie, J.M., Salomon, M., Nozue, K., Wada, M. and Briggs, W.R. (1999). LOV (light, oxygen, or voltage) domains of the blue-light photoreceptor phototropin (nph1): Binding sites for the chromophore flavin mononucleotide. *Proceedings of the National Academy of Sciences of the United States of America* **96**(15): 8779-8783.

Conn, J.W. (1955). Primary aldosteronism. *Journal of Laboratory and Clinical Medicine* **45**(4): 661-664.

Connell, J.M.C., Fraser, R. and Davies, E. (2001). Disorders of mineralocorticoid synthesis. *Best Practice & Research Clinical Endocrinology & Metabolism* **15**(1): 43-60.

Connell, J.M.C., MacKenzie, S.M., Freel, E.M., Fraser, R. and Davies, E. (2008). A lifetime of aldosterone excess: Long-term consequences of altered regulation of aldosterone production for cardiovascular function. *Endocrine Reviews* **29**(2): 133-154.

Cosme, J. and Johnson, E.F. (2000). Engineering microsomal cytochrome p450 2C5 to be a soluble, monomeric enzyme - Mutations that alter aggregation, phospholipid dependence of catalysis, and membrane binding. *Journal of Biological Chemistry* **275**(4): 2545-2553.

Cowley, A.W., Jr. (2006). The genetic dissection of essential hypertension. *Nature Reviews Genetics* **7**(11): 829-840.

Cranston, W.I. and Jueljensen, B.E. (1962). Effects of spironolactone and chlorthalidone on arterial pressure. *Lancet* **1**(7240): 1161-&.

Cronan, J.E. (1990). Biotinylation of proteins *in vivo* - a post-translational modification to label, purify and study proteins *Journal of Biological Chemistry* **265**(18): 10327-10333.

Crosson, S. and Moffat, K. (2001). Structure of a flavin-binding plant photoreceptor domain: Insights into light-mediated signal transduction. *Proceedings of the National Academy of Sciences of the United States of America* **98**(6): 2995-3000.

Dahlöf, B., Devereux, R.B., Kjeldsen, S.E., Julius, S., Beevers, G., de Faire, U., Fyhrquist, F., Ibsen, H., Kristiansson, K., Lederballe-Pedersen, O., Lindholm, L.H., Nieminen, M.S., Omvik, P., Oparil, S. and Wedel, H. (2002). Cardiovascular morbidity and mortality in the Losartan Intervention For Endpoint reduction in hypertension study (LIFE): a randomised trial against atenolol. *Lancet* **359**(9311): 995-1003.

Davies, E., Holloway, C.D., Ingram, M.C., Friel, E.C., Inglis, G.C., Swan, L., Hillis, W.S., Fraser, R. and Connell, J.M.C. (2001). An influence of variation in the aldosterone synthase gene (*CYP11B2*) on corticosteroid responses to ACTH in normal human subjects. *Clinical Endocrinology* **54**(6): 813-817.

Davies, E., Holloway, C.D., Ingram, M.C., Inglis, G.C., Friel, E.C., Morrison, C., Anderson, N.H., Fraser, R. and Connell, J.M.C. (1999). Aldosterone excretion rate and blood pressure in essential hypertension are related to polymorphic differences in the aldosterone synthase gene *CYP11B2*. *Hypertension* **33**(2): 703-707.

Debonneville, C., Flores, S.Y., Kamynina, E., Plant, P.J., Tauxe, C., Thomas, M.A., Münster, C., Chraïbi, A., Pratt, J.H., Horisberger, J.D., Pearce, D., Loffing, J. and Staub, O. (2001). Phosphorylation of Nedd4-2 by Sgk1 regulates epithelial Na^+ channel cell surface expression. *Embo Journal* **20**(24): 7052-7059.

Deisenhofer, J., Epp, O., Miki, K., Huber, R. and Michel, H. (1985). Structure of the protein subunits in the photosynthetic reaction centre of rhodopseudomonas-viridis at 3Å resolution. *Nature* **318**(6047): 618-624.

Denisov, I.G., Makris, T.M., Sligar, S.G. and Schlichting, I. (2005). Structure and chemistry of cytochrome p450. *Chemical Reviews* **105**(6): 2253-2278.

DeVore, N.M. and Scott, E.E. (2012). Structures of cytochrome p450 17A1 with prostate cancer drugs abiraterone and TOK-001. *Nature* **482**(7383): 116-U149.

Dietrich, M., Grundmann, L., Kurr, K., Valinotto, L., Saussele, T., Schmid, R.D. and Lange, S. (2005). Recombinant production of human microsomal cytochrome p450 2D6 in the methylotrophic yeast *Pichia pastoris*. *Chembiochem* **6**(11): 2014-2022.

Dooley, R., Harvey, B.J. and Thomas, W. (2012). Non-genomic actions of aldosterone: From receptors and signals to membrane targets. *Molecular and Cellular Endocrinology* **350**(2): 223-234.

Drepper, T., Eggert, T., Circolone, F., Heck, A., Krauss, U., Guterl, J.K., Wendorff, M., Losi, A., Gartner, W. and Jaeger, K.E. (2007). Reporter proteins for in vivo fluorescence without oxygen. *Nat Biotechnol* **25**(4): 443-445.

Drew, D., Newstead, S., Sonoda, Y., Kim, H., von Heijne, G. and Iwata, S. (2008). GFP-based optimization scheme for the overexpression and

purification of eukaryotic membrane proteins in *Saccharomyces cerevisiae*. *Nature Protocols* **3**(5): 784-798.

Drew, D., Slotboom, D.J., Friso, G., Reda, T., Genevaux, P., Rapp, M., Meindl-Beinker, N.M., Lambert, W., Lerch, M., Daley, D.O., Van Wijk, K.J., Hirst, J., Kunji, E. and De Gier, J.W. (2005). A scalable, GFP-based pipeline for membrane protein overexpression screening and purification. *Protein Science* **14**(8): 2011-2017.

Drew, D.E., von Heijne, G., Nordlund, P. and de Gier, J.W.L. (2001). Green fluorescent protein as an indicator to monitor membrane protein overexpression in *Escherichia coli*. *FEBS Letters* **507**(2): 220-224.

Edwards, C.R.W., Burt, D., McIntyre, M.A., Dekloet, E.R., Stewart, P.M., Brett, L., Sutanto, W.S. and Monder, C. (1988). Localisation of 11ß-hydroxysteroid dehydrogenase tissue specific protector of the mineralocorticoid receptor. *Lancet* **2**(8618): 986-989.

Eisenberg, M.J., Brox, A. and Bestawros, A.N. (2004). Calcium channel blockers: an update. *The American Journal of Medicine* **116**(1): 35-43.

Eugster, H.P., Sengstag, C., Meyer, U.A., Hinnen, A. and Wurgler, F.E. (1990). Constitutive and inducible expression of human cytochrome p450IA1 in yeast *Saccharomyces Cerevisiae* - an alternative enzyme source for *in vitro* studies *Biochemical and Biophysical Research Communications* **172**(2): 737-744.

Ewen, K.M., Kleser, M. and Bernhardt, R. (2011). Adrenodoxin: The archetype of vertebrate-type 2Fe-2S cluster ferredoxins. *Biochimica Et Biophysica Acta-Proteins and Proteomics* **1814**(1): 111-125.

Fall, R.R. (1979). Analysis of microbial biotin proteins. *Methods in Enzymology* **62**: 390-398.

Fraser, N.J. (2006). Expression and functional purification of a glycosylation deficient version of the human adenosine 2a receptor for structural studies. *Protein Expression and Purification* **49**(1): 129-137.

Funder, J.W. (1997). Glucocorticoid and mineralocorticoid receptors: Biology and clinical relevance. *Annual Review of Medicine* **48**: 231-240.

Gay, S.C., Shah, M.B., Talakad, J.C., Maekawa, K., Roberts, A.G., Wilderman, P.R., Sun, L., Yang, J.Y., Huelga, S.C., Hong, W.-X., Zhang, Q., Stout, C.D. and Halpert, J.R. (2010). Crystal structure of a cytochrome p450 2B6 genetic variant in complex with the inhibitor 4-(4-Chlorophenyl)imidazole at 2.0-Å Resolution. *Molecular Pharmacology* **77**(4): 529-538.

Gay, S.C., Zhang, H., Wilderman, P.R., Roberts, A.G., Liu, T., Li, S., Lin, H.-l., Zhang, Q., Woods, V.L., Jr., Stout, C.D., Hollenberg, P.F. and Halpert, J.R. (2011). Structural analysis of mammalian cytochrome p450 2B4 covalently bound to the mechanism-based inactivator tert-butylphenylacetylene: Insight into partial enzymatic acivity. *Biochemistry* **50**(22): 4903-4911.

Ghosh, D., Griswold, J., Erman, M. and Pangborn, W. (2009). Structural basis for androgen specificity and oestrogen synthesis in human aromatase. *Nature* **457**(7226): 219-U119.

Gonzalez, F.J. and Korzekwa, K.R. (1995). Cytochrome p450 expression systems. *Annual Review of Pharmacology and Toxicology* **35**: 369-390.

Good, N.E., Winget, G.D., Winter, W., Connolly, T.N., Izawa, S. and Singh, R.M.M. (1966). Hydrogen ion buffers for biological research. *Biochemistry* **5**(2): 467-&.

Gotoh, O. (1992). Substrate recognition sites in cytochrome-p450 family-2 (CYP2) proteins inferred from comparative analyses of amino-acid and coding nucleotide-sequences. *Journal of Biological Chemistry* **267**(1): 83-90.

Grünewald, S., Haase, W., Molsberger, E., Michel, H. and Reilander, H. (2004). Production of the human D-2S receptor in the methylotrophic yeast P-pastoris. *Receptors & Channels* **10**(1): 37-50.

Guengerich, F.P. (2004). Cytochrome p450: What have we learned and what are the future issues? *Drug Metabolism Reviews* **36**(2): 159-197.

Guyton, A.C. (1991). Blood-pressure control - special role of the kidneys and body-fluids. *Science* **252**(5014): 1813-1816.

Hanahan, D. (1983). Studies on transformation of *Escherichia coli* with plasmids. *Journal of Molecular Biology* **166**(4): 557-580.

Hannemann, F., Bichet, A., Ewen, K.M. and Bernhardt, R. (2007). Cytochrome p450 systems - biological variations of electron transport chains. *Biochimica et Biophysica Acta (BBA) - General Subjects* **1770**(3): 330-344.

Hattangady, N.G., Olala, L.O., Bollag, W.B. and **Rainey**, W.E. (2012). Acute and chronic regulation of aldosterone production. *Molecular and Cellular Endocrinology* **350**(2): 151-162.

Hobler, A., Kagawa, N., Hutter, M.C., Hartmann, M.F., Wudy, S.A., Hannemann, F. and Bernhardt, R. (2012). Human aldosterone synthase: Recombinant expression in *E. coli* and purification enables a detailed biochemical analysis of the protein on the molecular level. *Journal of Steroid Biochemistry and Molecular Biology* **132**(1-2): 57-65.

Hochuli, E., Bannwarth, W., Dobeli, H., Gentz, R. and Stuber, D. (1988). Genetic approach to facilitate purification of recombinant proteins with a novel metal chelate adsorbent. *Bio-Technology* **6**(11): 1321-1325.

HOPE study investigators (2000). Effects on an Angiotensin-Converting-Enzyme Inhibitor, Ramipril, on Cardiovascular Events in High-Risk Patients. *New England Journal of Medicine* **342**(2): 145-153

Horisberger, J.D. (1998). Amiloride-sensitive Na channels. *Current Opinion in Cell Biology* **10**(4): 443-449.

Huang, J.R., Craggs, T.D., Christodoulou, J. and Jackson, S.E. (2007). Stable intermediate states and high energy barriers in the unfolding of GFP. *Journal of Molecular Biology* **370**(2): 356-371.

Hunte, C., Koepke, J., Lange, C., Rossmanith, T. and Michel, H. (2000). Structure at 2.3 angstrom resolution of the cytochrome bc_1 complex from the yeast Saccharomyces cerevisiae co-crystallized with an antibody Fv fragment. *Structure with Folding & Design* **8**(6): 669-684.

Ikonen, E. (2008). Cellular cholesterol trafficking and compartmentalization. *Nature Reviews Molecular Cell Biology* **9**(2): 125-138.

Inglis, G.C., Plouin, P.F., Friel, E.C., Davies, E., Fraser, R. and Connell, J.M.C. (2001). Polymorphic differences from normal in the aldosterone synthase gene (*CYP11B2*) in patients with primary hyperaldosteronism and adrenal tumour (Conn's syndrome). *Clinical Endocrinology* **54**(6): 725-730.

Jo, Y., King, S.R., Khan, S.A. and Stocco, D.M. (2005). Involvement of protein kinase C and cyclic adenosine 3 ',5 '-monophosphate-dependent kinase in steroidogenic acute regulatory protein expression and steroid biosynthesis in Leydig cells. *Biology of Reproduction* **73**(2): 244-255.

Julius, S., Nesbitt, S.D., Egan, B.M., Weber, M.A., Michelson, E.L., Kaciroti, N., Black, H.R., Grimm, R.H., Messerli, F.H., Oparil, S. and Schork, M.A. (2006). Feasibility of treating prehypertension with an angiotensin-receptor blocker. *New England Journal of Medicine* **354**(16): 1685-1697.

Kaplan, N.M. and Opie, L.H. (2006). Controversies in cardiology 2 - Controversies in hypertension. *Lancet* **367**(9505): 168-176.

Kawate, T. and Gouaux, E. (2006). Fluorescence-detection size-exclusion chromatography for precrystallization screening of integral membrane proteins. *Structure* **14**(4): 673-681.

Kearney, P.M., Whelton, M., Reynolds, K., Muntner, P., Whelton, P.K. and He, J. (2004). Global burden of hypertension: analysis of worldwide data. *Lancet* **365**(9455): 217-223.

Kelly, S.M., Jess, T.J. and Price, N.C. (2005). How to study proteins by circular dichroism. *Biochimica Et Biophysica Acta-Proteins and Proteomics* **1751**(2): 119-139.

Kobilka, B. and Schertler, G.F. (2008). New G-protein-coupled receptor crystal structures: insights and limitations. *Trends in Pharmacological Sciences* **29**:79-83

Lawes, C.M.M., Vander Hoorn, S. and Rodgers, A. (2008). Global burden of blood-pressure-related disease, 2001. *Lancet* **371**(9623): 1513-1518.

Lee, S.-Y., Letts, J.A. and MacKinnon, R. (2009). Functional reconstitution of purified human Hv1 H^+ channels. *Journal of Molecular Biology* **387**(5): 1055-1060.

Lichty, J.J., Malecki, J.L., Agnew, H.D., Michelson-Horowitz, D.J. and Tan, S. (2005). Comparison of affinity tags for protein purification. *Protein Expression and Purification* **41**(1): 98-105.

Lifton, R.P., Dluhy, R.G., Powers, M., Rich, G.M., Cook, S., Ulick, S. and Lalouel, J.M. (1992). A chimaeric 11ß-hydroxylase aldosterone synthase gene causes glucocorticoid-remediable aldosteronism and human hypertension. *Nature* **355**(6357): 262-265.

Lim, F., Rohde, M., Morris, C.P. and Wallace, J.C. (1987). Pyruvate carboxylase in the yeast pyc mutant *Archives of Biochemistry and Biophysics* **258**(1): 259-264.

Lucas, S., Heim, R., Negri, M., Antes, I., Ries, C., Schewe, K.E., Bisi, A., Gobbi, S. and Hartmann, R.W. (2008). Novel aldosterone synthase inhibitors with extended carbocyclic skeleton by a combined ligand-based and structure-based drug design approach. *Journal of Medicinal Chemistry* **51**(19): 6138-6149.

Lucas, S., Negri, M., Heim, R., Zimmer, C. and Hartmann, R.W. (2011). Fine-tuning the selectivity of aldosterone synthase inhibitors: Structure-activity and structure-selectivity insights from studies of heteroaryl substituted 1,2,5,6-tetrahydropyrrolo 3,2,1-ij quinolin-4-one derivatives. *Journal of Medicinal Chemistry* **54**(7): 2307-2319.

Lundström, K., Wagner, R., Reinhart, C., Desmyter, A., Cherouati, N., Magnin, T., Zeder-Lutz, G., Courtot, M., Prual, C., Andre, N., Hassaine, G., Michel, H., Cambillau, C. and Pattus, F. (2006). Structural genomics on membrane proteins: comparison of more than 100 GPCRs in 3 expression systems. *Journal of Structural and Functional Genomics* **7**(2): 77-91.

Macauley-Patrick, S., Fazenda, M.L., McNeil, B. and Harvey, L.M. (2005). Heterologous protein production using the *Pichia pastoris* expression system. *Yeast* **22**(4): 249-270.

Malo, G.D., Pouwels, L.J., Wang, M., Weichsel, A., Montfort, W.R., Rizzo, M.A., Piston, D.W. and Wachter, R.M. (2007). X-ray structure of Cerulean GFP: a tryptophan-based chromophore useful for fluorescence lifetime imaging. *Biochemistry* **46**(35): 9865-9873.

Mast, N., Annalora, A.J., Lodowski, D.T., Palczewski, K., Stout, C.D. and Pikuleva, I.A. (2011). Structural basis for three-step sequential catalysis by the cholesterol side chain cleavage enzyme CYP11A1. *Journal of Biological Chemistry* **286**(7): 5607-5613.

Matocha, M.F. and Waterman, M.R. (1984). Discriminatory processing of the precursor forms of cytochrome $p450_{scc}$ and adrenodoxin by adrenocortical and heart-mitochondria *Journal of Biological Chemistry* **259**(13): 8672-8678.

Miller, W.L. and Auchus, R.J. (2011). The molecular biology, biochemistry, and physiology of human steroidogenesis and its disorders. *Endocrine Reviews* **32**(1): 81-151.

Milliez, P., Girerd, X., Plouin, P.F., Blacher, J., Safar, M.E. and Mourad, J.J. (2005). Evidence for an increased rate of cardiovascular events in patients with primary aldosteronism. *Journal of the American College of Cardiology* **45**(8): 1243-1248.

Miroux, B. and Walker, J.E. (1996). Over-production of proteins in *Escherichia coli*: Mutant hosts that allow synthesis of some membrane proteins and globular proteins at high levels. *Journal of Molecular Biology* **260**(3): 289-298.

Mohanty, A.K., Simmons, C.R. and Wiener, M.C. (2003). Inhibition of tobacco etch virus protease activity by detergents. *Protein Expression and Purification* **27**(1): 109-114.

Mountjoy, K.G., Robbins, L.S., Mortrud, M.T. and Cone, R.D. (1992). The cloning of a family of genes that encode the melanocortin receptors. *Science* **257**(5074): 1248-1251.

Müller, J.J., Lapko, A., Bourenkov, G., Ruckpaul, K. and Heinemann, U. (2001). Adrenodoxin reductase-adrenodoxin complex structure suggests electron

transfer path in steroid biosynthesis. *Journal of Biological Chemistry* **276**(4): 2786-2789.

Mune, T., Rogerson, F.M., Nikkila, H., Agarwal, A.K. and White, P.C. (1995). Human hypertension caused by mutations in the kidney isozyme of 11ß-hydroxysteroid dehydrogenase. *Nature Genetics* **10**(4): 394-399.

Narasaka, T., Suzuki, T., Moriya, T. and Sasano, H. (2001). Temporal and spatial distribution of corticosteroidogenic enzymes immunoreactivity in developing human adrenal. *Molecular and Cellular Endocrinology* **174**(1-2): 111-120.

Navratilova, I. and Hopkins, A.L. (2010). Fragment screening by surface plasmon resonance. *Acs Medicinal Chemistry Letters* **1**(1): 44-48.

Neves, S.R., Ram, P.T. and Iyengar, R. (2002). G-protein pathways. *Science* **296**(5573): 1636-1639.

Newstead, S., Kim, H., von Heijne, G., Iwata, S. and Drew, D. (2007). High-throughput fluorescent-based optimization of eukaryotic membrane protein overexpression and purification in *Saccharomyces cerevisiae*. *Proceedings of the National Academy of Sciences of the United States of America* **104**(35): 13936-13941.

Newton-Vinson, P., Hubalek, F. and Edmondson, D.E. (2000). High-level expression of human liver monoamine oxidase B in *Pichia pastoris*. *Protein Expression and Purification* **20**(2): 334-345.

Nishimoto, K., Nakagawa, K., Li, D., Kosaka, T., Oya, M., Mikami, S., Shibata, H., Itoh, H., Mitani, F., Yamazaki, T., Ogishima, T., Suematsu, M. and Mukai, K. (2010). Adrenocortical zonation in humans under normal and pathological conditions. *Journal of Clinical Endocrinology & Metabolism* **95**(5): 2296-2305.

Nishizaka, M.K., Zaman, M.A. and Calhoun, D.A. (2003). Efficacy of low-dose spironolactone in subjects with resistant hypertension. *American Journal of Hypertension* **16**(11): 925-930.

Nogueira, E.F. and Rainey, W.E. (2010). Regulation of aldosterone synthase by activator transcription factor/cAMP response element-binding protein family members. *Endocrinology* **151**(3): 1060-1070.

Nollert, P. (2005). Membrane protein crystallization in amphiphile phases: practical and theoretical considerations. *Progress in biophysics and molecular biology* **88**(3): 339-357.

Nyblom, M., Öberg, F., Lindkvist-Petersson, K., Hallgren, K., Findlay, H., Wikström, J., Karlsson, A., Hansson, O., Booth, P.J., Bill, R.M., Neutze, R. and Hedfalk, K. (2007). Exceptional overproduction of a functional human membrane protein. *Protein Expression and Purification* **56**(1): 110-120.

Odermatt, A. and Atanasov, A.G. (2009). Mineralocorticoid receptors: Emerging complexity and functional diversity. *Steroids* **74**(2): 163-171.

Okada, T., Takeda, K. and Kouyama, T. (1998). Highly selective separation of rhodopsin from bovine rod outer segment membranes using combination of bivalent cation and alkyl(thio)glucoside. *Photochemistry and Photobiology* **67**(5): 495-499.

Omdahl, J.L., Swamy, N., Serda, R., Annalora, A., Berne, M. and Rayb, R. (2004). Affinity labeling of rat cytochrome p450 C24 (CYP24) and identification of Ser57 as an active site residue. *Journal of Steroid Biochemistry and Molecular Biology* **89-90**(1-5): 159-162.

Omura, T. and Sato, R. (1964). Carbon monoxide-binding pigment of liver microsomes. I. Evidence for its hemoprotein nature. *Journal of Biological Chemistry* **239**(7): 2370-&.

Ondetti, M.A. and Cushman, D.W. (1977). Design of specific inhibitors of angiotensin-converting enzyme - new class of orally active antihypertensive agents. *Science* **196**(4288): 441-444.

Ormö, M., Cubitt, A.B., Kallio, K., Gross, L.A., Tsien, R.Y. and Remington, S.J. (1996). Crystal structure of the *Aequorea victoria* green fluorescent protein. *Science* **273**(5280): 1392-1395.

Otyepka, M., Skopalik, J., Anzenbacherova, E. and Anzenbacher, P. (2007). What common structural features and variations of mammalian p450s are known to date? *Biochimica Et Biophysica Acta-General Subjects* **1770**(3): 376-389.

Patten, C.J., Ishizaki, H., Aoyama, T., Lee, M.J., Ning, S.M., Huang, W., Gonzalez, F.J. and Yang, C.S. (1992). Catalytic properties of the human cytochrome p450 2E1 produced by cDNA expression in mammalian cells. *Archives of Biochemistry and Biophysics* **299**(1): 163-171.

Paulis, L., Steckelings, U.M. and Unger, T. (2012). Key advances in antihypertensive treatment. *Nature Reviews Cardiology* **9**(5): 276-285.

Paulis, L. and Unger, T. (2010). Novel therapeutic targets for hypertension. *Nature Reviews Cardiology* **7**(8): 431-441.

Payne, A.H. and Hales, D.B. (2004). Overview of steroidogenic enzymes in the pathway from cholesterol to active steroid hormones. *Endocrine Reviews* **25**(6): 947-970.

Pearce, D. and Kleyman, T.R. (2007). Salt, sodium channels, and SGK1. *Journal of Clinical Investigation* **117**(3): 592-595.

Penning, T.M. (1997). Molecular endocrinology of hydroxysteroid dehydrogenases. *Endocrine Reviews* **18**(3): 281-305.

Pitt, B., Remme, W., Zannad, F., Neaton, J., Martinez, F., Roniker, B., Bittman, R., Hurley, S., Kleiman, J. and Gatlin, M. (2003). Eplerenone, a selective aldosterone blocker, in patients with left ventricular dysfunction after myocardial infarction. *New England Journal of Medicine* **348**(14): 1309-1321.

Pitt, B., Zannad, F., Remme, W.J., Cody, R., Castaigne, A., Perez, A., Palensky, J. and Wittes, J. (1999). The effect of spironolactone on morbidity and mortality in patients with severe heart failure. *New England Journal of Medicine* **341**(10): 709-717.

Pojoga, L., Gautier, S., Blanc, H., Guyene, T.T., Poirier, O., Cambien, F. and Benetos, A. (1998). Genetic determination of plasma aldosterone levels in essential hypertension. *American Journal of Hypertension* **11**(7): 856-860.

Poulos, T.L., Finzel, B.C., Gunsalus, I.C., Wagner, G.C. and Kraut, J. (1985). The 2.6-Å crystal structure of pseudomonas-putida cytochrome p450. *Journal of Biological Chemistry* **260**(30): 6122-6130.

Poulos, T.L., Finzel, B.C. and Howard, A.J. (1987). High-resolution structure of p450cam. *Journal of Molecular Biology* **195**(3): 687-700.

Provencher, S.W. and Glockner, J. (1981). Estimation of globular protein secondary structure from circular dichroism. *Biochemistry* **20**(1): 33-37.

Puddey, I.B., Beilin, L.J. and Vandongen, R. (1987). Regular alcohol use raises blood-pressure in treated hypertensive subjects - a randomized controlled trial. *Lancet* **1**(8534): 647-651.

Rasmussen, S.G.F., Choi, H.-J., Rosenbaum, D.M., Kobilka, T.S., Thian, F.S., Edwards, P.C., Burghammer, M., Ratnala, V.R.P., Sanishvili, R., Fischetti, R.F., Schertler, G.F.X., Weis, W.I. and Kobilka, B.K. (2007). Crystal structure of the human beta(2) adrenergic G-protein-coupled receptor. *Nature* **450**(7168): 383-U384.

Remington, S.J. (2006). Fluorescent proteins: maturation, photochemistry and photophysics. *Current opinion in structural biology* **16**(6): 714-721.

Robinson, B.H., Oei, J., Saunders, M. and Gravel, R. (1983). [^{3}H] biotin-labeled proteins in cultured human skin fibroblasts from patients with pyruvate-carboxylase deficiency. *Journal of Biological Chemistry* **258**(10): 6660-6664.

Rocha, R., Chander, P.N., Khanna, K., Zuckerman, A. and Stier, C.T. (1998). Mineralocorticoid blockade reduces vascular injury in stroke prone hypertensive rats. *Hypertension* **31**(1): 451-458.

Ruilope, L.M. (2012). Current challenges in the clinical management of hypertension. *Nature Reviews Cardiology* **9**(5): 267-275.

Sambrook, J., Fritsch, E.F. and Maniatis, T. (1989). Molecular cloning: a laboratory manual.

Sandhu, P., Guo, Z.Y., Baba, T., Martin, M.V., Tukey, R.H. and Guengerich, F.P. (1994). Expression of modified human cytochrome p450 1A2 in *Escherichia Coli* - stabilisation, purification, spectral characterisation and catalytic activities of the enzyme. *Archives of Biochemistry and Biophysics* **309**(1): 168-177.

Siegal, G. and Hollander, J.G. (2009). Target Immobilization and NMR Screening of Fragments in Early Drug Discovery. *Current Topics in Medicinal Chemistry* **9**(18): 1736-1745.

Simard, J., Ricketts, M.L., Gingras, B., Soucy, P., Feltus, F.A. and Melner, M.H. (2005). Molecular biology of the 3ß-hydroxysteroid dehydrogenase/Delta(5)-Delta(4) isomerase gene family. *Endocrine Reviews* **26**(4): 525-582.

Sono, M., Roach, M.P., Coulter, E.D. and Dawson, J.H. (1996). Heme-containing oxygenases. *Chemical Reviews* **96**(7): 2841-2887.

Sonoda, Y., Cameron, A., Newstead, S., Omote, H., Moriyama, Y., Kasahara, M., Iwata, S. and Drew, D. (2010). Tricks of the trade used to accelerate high-resolution structure determination of membrane proteins. *FEBS Letters* **584**(12): 2539-2547.

Sookoian, S., Gianotti, T.F., Gonzalez, C.D. and Pirola, C.J. (2007). Association of the C-344T aldosterone synthase gene variant with essential hypertension: a meta-analysis. *Journal of Hypertension* **25**(1): 5-13.

Spät, A. (2004). Glomerulosa cell - a unique sensor of extracellular K+ concentration. *Molecular and Cellular Endocrinology* **217**(1-2): 23-26.

Spät, A. and Hunyady, L. (2004). Control of aldosterone secretion: A model for convergence in cellular signaling pathways. *Physiological Reviews* **84**(2): 489-539.

Speiser, P.W. and White, P.C. (2003). Congenital adrenal hyperplasia. *New England Journal of Medicine* **349**(8): 776-788.

Stamler, J., Rose, G., Stamler, R., Elliott, P., Dyer, A. and Marmot, M. (1989). INTERSALT study findings - public-health and medical-care implications. *Hypertension* **14**(5): 570-577.

Stewart, P.M., Gupta, A., Sheppard, M.C., Whorwood, C.B., Howie, A.J., Milford, D.V. and Krozowski, Z.S. (1996). Hypertension in the syndrome of apparent mineralocorticoid excess due to mutation of the 11ß-hydroxysteroid dehydrogenase type 2 gene. *The Lancet* **347**(8994): 88-91.

Stocco, D.M. and Clark, B.J. (1996). Regulation of the acute production of steroids in steroidogenic cells. *Endocrine Reviews* **17**(3): 221-244.

Stockand, J.D. (2002). New ideas about aldosterone signaling in epithelia. *American Journal of Physiology-Renal Physiology* **282**(4): F559-F576.

Stoll, V.S. and Blanchard, J.S. (1990). Buffers - principles and practice. *Methods in Enzymology* **182**: 24-38.

Strushkevich, N., MacKenzie, F., Cherkesova, T., Grabovec, I., Usanov, S. and Park, H.-W. (2011). Structural basis for pregnenolone biosynthesis by the mitochondrial monooxygenase system. *Proceedings of the National Academy of Sciences of the United States of America* **108**(25): 10139-10143.

Terpe, K. (2003). Overview of tag protein fusions: from molecular and biochemical fundamentals to commercial systems. *Applied Microbiology and Biotechnology* **60**(5): 523-533.

Timmermans, P., Wong, P.C., Chiu, A.T., Herblin, W.F., Benfield, P., Carini, D.J., Lee, R.J., Wexler, R.R., Saye, J.A.M. and Smith, R.D. (1993). Angiotensin-II receptors and angiotensin-II receptor antagonists. *Pharmacological Reviews* **45**(2): 205-251.

Toddturla, K.M., Schnermann, J., Fejestoth, G., Narayfejestoth, A., Smart, A., Killen, P.D. and Briggs, J.P. (1993). Distribution of mineralocorticoid and glucocorticoid receptor messenger-RNA along the nephron. *American Journal of Physiology* **264**(5): F781-F791.

Tomaschitz, A., Pilz, S., Ritz, E., Obermayer-Pietsch, B. and Pieber, T.R. (2010). Aldosterone and arterial hypertension. *Nature Reviews Endocrinology* **6**(2): 83-93.

Trant, J.M. (1996). Functional expression of recombinant spiny dogfish shark (Squalus acanthias) cytochrome p450c17 (17 alpha-hydroxylase/C-17,C-20-lyase) in yeast (*Pichia pastoris*). *Archives of Biochemistry and Biophysics* **326**(1): 8-14.

Tsujita, Y., Iwai, N., Katsuya, T., Higaki, J., Ogihara, T., Tamaki, S., Kinoshita, M., Mannami, T., Ogata, J. and Baba, S. (2001). Lack of association between genetic polymorphism of *CYP11B2* and hypertension in Japanese: The Suita Study. *Hypertension Research* **24**(2): 105-109.

Ulick, S., Levine, L.S., Gunczler, P., Zanconato, G., Ramirez, L.C., Rauh, W., Rösler, A., Bradlow, H.L. and New, M.I. (1979). Syndrome of apparent mineralocorticoid excess associated with defects in the peripheral metabolism of cortisol. *Journal of Clinical Endocrinology & Metabolism* **49**(5): 757-766.

Ulick, S., Wang, J.Z. and Morton, D.H. (1992). The biochemical phenotypes of two inborn-errors in the biosynthesis of aldosterone. *Journal of Clinical Endocrinology & Metabolism* **74**(6): 1415-1420.

Van Stokkum, I.H.M., Spoelder, H.J.W., Bloemendal, M., Van Grondelle, R. and Groen, F.C.A. (1990). Estimation of protein secondary structure and error analysis from circular dichroism spectra *Analytical Biochemistry* **191**(1): 110-118.

Vasan, R.S., Evans, J.C., Larson, M.G., Wilson, P.W.F., Meigs, J.B., Rifai, N., Benjamin, E.J. and Levy, D. (2004). Serum aldosterone and the incidence of hypertension in nonhypertensive persons. *New England Journal of Medicine* **351**(1): 33-41.

Vonrhein, C., Schmidt, U., Ziegler, G.A., Schweiger, S., Hanukoglu, I. and Schulz, G.E. (1999). Chaperone-assisted expression of authentic bovine adrenodoxin reductase in *Escherichia coli*. *FEBS Letters* **443**(2): 167-169.

Walker, B.R. (2007). Glucocorticoids and cardiovascular disease. *European Journal of Endocrinology* **157**(5): 545-559.

Wang, M., Roberts, D.L., Paschke, R., Shea, T.M., Masters, B.S.S. and Kim, J.J.P. (1997). Three-dimensional structure of NADPH-cytochrome p450 reductase: Prototype for FMN- and FAD-containing enzymes. *Proceedings of the National Academy of Sciences of the United States of America* **94**(16): 8411-8416.

Waterman, M.R. and Bischof, L.J. (1996). Mechanisms of ACTH(cAMP)-dependent transcription of adrenal steroid hydroxylases. *Endocrine Research* **22**(4): 615-620.

Waugh, D.S. (2005). Making the most of affinity tags. *Trends in Biotechnology* **23**(6): 316-320.

Waugh, D.S. (2011). An overview of enzymatic reagents for the removal of affinity tags. *Protein Expression and Purification* **80**(2): 283-293.

Wehling, M. (1994). Nongenomic actions of steroid-hormones. *Trends in Endocrinology and Metabolism* **5**(8): 347-353.

Weinberger, M.H., Roniker, B., Krause, S.L. and Weiss, R.J. (2002). Eplerenone, a selective aldosterone blocker, in mild-to-moderate hypertension. *American Journal of Hypertension* **15**(8): 709-716.

Weiss, H.M. and Grisshammer, R. (2002). Purification and characterization of the human adenosine A(2a) receptor functionally expressed in *Escherichia coli*. *European Journal of Biochemistry* **269**(1): 82-92.

Weiss, H.M., Haase, W., Michel, H. and Reilander, H. (1998). Comparative biochemical and pharmacological characterization of the mouse 5HT(5A) 5-hydroxytryptamine receptor and the human beta(2)-adrenergic receptor produced in the methylotrophic yeast *Pichia pastoris*. *Biochemical Journal* **330**: 1137-1147.

Werck-Reichhart, D. and Feyereisen, R. (2000). Cytochromes p450: a success story. *Genome biology* **1**(6): REVIEWS3003.

Whelton, P.K., He, J., Cutler, J.A., Brancati, F.L., Appel, L.J., Follmann, D. and Klag, M.J. (1997). Effects of oral potassium on blood pressure - Meta-analysis of randomized controlled clinical trials. *Jama-Journal of the American Medical Association* **277**(20): 1624-1632.

White, P.C., Curnow, K.M. and Pascoe, L. (1994). Disorders of steroid 11ß-hydroxylase isozymes. *Endocrine Reviews* **15**(4): 421-438.

White, P.C., New, M.I. and Dupont, B. (1987). Congenital adrenal hyperplasia. *New England Journal of Medicine* **316**(24): 1519-1524.

White, P.C. and Slutsker, L. (1995). Haplotype analysis of *CYP11B2*. *Endocrine Research* **21**(1-2): 437-442.

White, S.H. (2009). Biophysical dissection of membrane proteins. *Nature* **459**(7245): 344-346.

Whitmore, L. and Wallace, B.A. (2008). Protein secondary structure analyses from circular dichroism spectroscopy: Methods and reference databases. *Biopolymers* **89**(5): 392-400.

Williams, P.A., Cosme, J., Sridhar, V., Johnson, E.F. and McRee, D.E. (2000). Mammalian microsomal cytochrome p450 monooxygenase: Structural adaptations for membrane binding and functional diversity. *Molecular Cell* **5**(1): 121-131.

Yang, F., Moss, L.G. and Phillips, G.N. (1996). The molecular structure of green fluorescent protein. *Nature Biotechnology* **14**(10): 1246-1251.

Young, W.F. (2007). Primary aldosteronism: renaissance of a syndrome. *Clinical Endocrinology* **66**(5): 607-618.

Zaman, M.A., Oparil, S. and Calhoun, D.A. (2002). Drugs targeting the renin-angiotensin-aldosterone system. *Nat Rev Drug Discov* **1**(8): 621-636.

Zhang, Q., Ma, X., Ward, A., Hong, W.-X., Jaakola, V.-P., Stevens, R.C., Finn, M.G. and Chang, G. (2007). Designing facial amphiphiles for the stabilization of integral membrane proteins. *Angewandte Chemie-International Edition* **46**(37): 7023-7025.

Zhao, B., Lei, L., Kagawa, N., Sundaramoorthy, M., Banerjee, S., Nagy, L.D., Guengerich, F.P. and Waterman, M.R. (2012). Three-dimensional structure of steroid 21-hydroxylase (cytochrome p450 21A2) with two substrates reveals locations of disease-associated variants. *Journal of Biological Chemistry* **287**(13): 10613-10622.

Zhou, Y.F., Morais-Cabral, J.H., Kaufman, A. and MacKinnon, R. (2001). Chemistry of ion coordination and hydration revealed by a K^+ channel-Fab complex at 2.0 angstrom resolution. *Nature* **414**(6859): 43-48.

Zöllner, A., Kagawa, N., Waterman, M.R., Nonaka, Y., Takio, K., Shiro, Y., Hannemann, F. and Bernhardt, R. (2008). Purification and functional characterization of human 11ß hydroxylase expressed in *Escherichia coli*. *Febs Journal* **275**(4): 799-810.